IntechOpen

Trace Elements

Human Health and Environment

Edited by Hosam El-Din M. Saleh and Eithar El-Adham

TRACE ELEMENTS - HUMAN HEALTH AND ENVIRONMENT

Edited by **Hosam El-Din M. Saleh**
and **Eithar El-Adham**

Trace Elements - Human Health and Environment
http://dx.doi.org/10.5772/intechopen.72339
Edited by Hosam El-Din M. Saleh and Eithar El-Adham

Contributors

Periyadan K Krishnakumar, Mohammed Qurban, Geetha Sasikumar, Mehmet S Dogan, Agostinho Almeida, M. De Rezende Pinto, Jun-ichi Chikawa, M. S. El-Shahawi, D. A. Al-Eryani, W. Ahmad, Z.M. Saigl, H. Alwael, S.O. Bahaffi, Y.M. Moustafa, Georgy Nevinsky, Natalia Zaksas, Sofia Koukina, Nikolay Lobus, Hosam Saleh

Notice

First published in London, United Kingdom, 2018 by IntechOpen
eBook (PDF) Published by IntechOpen, 2019
IntechOpen is the global imprint of INTECHOPEN LIMITED, registered in England and Wales, registration number: 11086078, The Shard, 25th floor, 32 London Bridge Street
London, SE19SG – United Kingdom
Printed in Croatia

British Library Cataloguing-in-Publication Data
A catalogue record for this book is available from the British Library

Additional hard and PDF copies can be obtained from orders@intechopen.com

Trace Elements - Human Health and Environment
Edited by Hosam El-Din M. Saleh and Eithar El-Adham

p. cm.

Print ISBN 978-1-78923-670-5

Online ISBN 978-1-78923-671-2

eBook (PDF) ISBN 978-1-83881-677-3

Meet the editors

Hosam Saleh is Professor of Radioactive Waste Management in the Radioisotope Department, Atomic Energy Authority, Egypt. He was awarded MSc and PhD degrees in Physical Chemistry from Cairo University. His interest lies in the study of innovative economic and environment-friendly techniques for the management of hazardous and radioactive wastes. He has authored many peer-reviewed scientific papers and book chapters, and is the editor of several books from renowned international publishers.

Eithar El-Adham is Associate Professor of Pediatrics in the Radioisotope Department, Atomic Energy Authority, Egypt. She was awarded an MSc from Cairo University and a PhD from the Institute of Postgraduate Childhood Studies. She has authored many peer-reviewed medical papers. Her interests lie in the diagnosis and therapy of pediatric diseases and common pediatric health problems, and experimental trials to find a safe natural alternative to lifelong iron chelation in thalassemics.

Contents

Preface

Trace elements, including metals, play an important role in many biological systems, both in normal or pathological processes. For the human metabolism, chromium, arsenic, cadmium, mercury, and lead are considered to be the notorious "top five" toxins among all trace elements. Hexavalent chromium, for example, is highly toxic and carcinogenic; the same is valid for mercury vapor and various bivalent mercury compounds. To understand the expedient toxicity of these five heavy metals mechanistically, one has to take into account that these metals exert outstanding affinity for strongly binding with sulfur; if present in the human body, they can easily bind to the thiol (–SH) groups of the amino acid cysteine in enzymes, thus inhibiting or even stopping important metabolic reactions, which deteriorates the health status of the affected person, and often ends in death.

Trace elements are resistant towards biodegradation; therefore, they undergo environmental accumulation, which enables their entrance into the food chain. Prior to mitigating trace element pollution, it is of importance to develop enhanced analytical systems to reliably and precisely determine the level of trace element contamination of soil, water, and air. Migration of trace elements into areas originally not polluted by them typically occurs as dust, by leaching through soil, or by dispersing heavy metals containing sewage sludge.

We are tremendously optimistic that the exploratory and scientific attempts collected and summarized in this book will encourage researchers all over the globe to deepen their activities in this field, and to attract the interest of undergraduates as well as of progressive representatives from relevant various sectors. Primarily, these activities will boost the impatiently desired breakthrough of advanced "trace element" identification and application processes.

Particular acknowledgment goes to the publishing process manager, Ms. Dajana Pemac, for her cooperation, exceptional efforts, and prompt response to my requests. Again, we would like to thank cordially all contributors to this issue for their supreme work.

Hosam El-Din M. Saleh, Ph.D.
Atomic Energy Authority
Radioisotope Department
Nuclear Research Center
Giza, Egypt

Section 1

Introduction to Trace Elements

Chapter 1

Introductory Chapter: An Introduction to Trace Elements

Martin Koller and Hosam M. Saleh

Additional information is available at the end of the chapter

http://dx.doi.org/10.5772/intechopen.75010

1. Introduction

"Trace elements" are such building blocks of our planet and all living organisms, which, although occurring in rather modest concentration levels, are indispensable for a plethora of metabolic processes. Especially since the last decades, we observe enormously increasing efforts devoted by the scientific community to investigate, characterize and quantify trace elements. So-called "essential trace elements" are important constituents of human food, animal fodder, plant fertilizers, or cultivation media to form biotechnologically relevant microbes. Trace elements travel from the soil through the food chain, starting from phytoplankton until reaching our dinner tables; apart from food, drinking water is another important source for trace element uptake by all organisms. This makes trace elements interesting for diverse scientists such as analytical chemists, biochemists, geologists, physiologists, zoologists, and botanists [1].

In dependence on the scientific realm, different definitions for the terminus "trace elements" are found. An analytical chemist considers an element in a given sample with an average concentration of less than 100 ppm on an atomic counting basis or less than 100 μg/g on a mass basis, a "trace element". In contrast, biochemists define "trace elements" as those elements, which, although present only in tiny amounts, are needed to maintain the physiological balance of an organism, often acting as cofactors in enzymatic reactions; this biochemical definition encompasses various heavy metals (iron, copper, nickel, vanadium, cobalt, manganese, molybdenum, chromium, and zinc), some nonmetals (boron and iodine), and certain metalloids (selenium, silicon, and arsenic). This definition implies a daily requirement for "essential trace elements" by humans in amounts between 50 μg and 18 mg/day [2]. To become susceptible toward metabolizing by animals and humans, some trace elements need to undergo transformation by microbes into complex bioavailable forms, as observed in the case of cobalt, which is utilized mainly as cyanocobalamin (vitamin B_{12}) [3, 4]. Moreover,

geologists define trace elements by concentrations not surmounting 1 pro mille of a rock or mineral. In addition, the term "trace element" is frequently used when analyzing the elemental composition of igneous rocks, hence those rocks formed by magma. In mineralogy, trace elements can substitute network-forming ions in mineral crystal structures; here, trace elements are not vital to a mineral's defined composition and do not appear in the mineral's chemical formula. However, as well known in the case of quartz, those metals occurring in trace quantities result in characteristic coloration of the minerals; for example, the substitution of silicon by iron in traces gives the quartz amethysts its famous purple coloration [5].

Keeping with trace elements playing a role in human metabolism, we find at least two of them as so-called "vital poisons" in the periodic system of elements, namely chromium and arsenic, well-known toxins, which, nevertheless, are essential for the functioning of our metabolism. Apart from the 14 undisputed essential trace elements mentioned in the above paragraphs, others, such as fluorine, strontium, or lithium, are suggested to also display biological functions in humans, which, although not clearly elucidated yet mechanistically, are evidenced by element deprivation effects in diverse metabolic studies [1, 6]. In addition, limited circumstantial evidence for certain benefits or biological function in mammals is reported in the case of the metals aluminum, rubidium, cadmium, germanium, tin, and lead, the so-called "ultra-trace elements" [7]. Only for prokaryotes, a physiological role of tungsten [8] and lanthanum [9] is generally accepted. What is not included in this list are all those elements which are present in significant amounts in our body, such as the four biological basic elements hydrogen, oxygen, carbon, and nitrogen and the macroelements sulfur, chlorine, phosphorus, magnesium, sodium, potassium, and calcium.

2. Determination of trace elements

However, trace elements are not only blessing but also curse by generating environmental and health-related concerns when exceeding certain concentration levels. In the context of environmentally sensitive trace elements, it is often not easy to draw a clear line between the desired concentration range of a trace element and the range in which it already exerts toxicity [10]. Aquatic environments, soil, organisms, food, fodder, energy carriers like coal, and airborne particles are targets, which are potentially contaminated with trace elements; this, in turn, provokes the need for modern, reliable, and fast tools for determination of trace element in diverse matrices. Although many problems caused by trace elements are already well managed in the meanwhile, constant vigilance in environmental exposure, application, and nutritional supply of trace elements still displays the *conditio sine qua non*, and calls for intensified research in trace element determination. For example, during mining, beneficiation, and combustion of coal as well as during metal mining and follow-up treatments, a total of about 26 trace elements, among them toxic heavy metals like mercury, need to be considered and quantified [6]. In the biological field, many plants are described to heavily accumulate trace elements from soil (metal "hyperaccumulator"

plants); to understand these uptake mechanism and how the plants develop the required resistance factors needed to withstand the high concentration of trace elements, which often are highly toxic heavy metals, needs highly precise detection devices [11, 12]. The determination of type and concentration of trace elements in nutrition, body tissue and liquids, coal, water, soil, and so on is regarded as the first and most important step to follow the mechanisms controlling the dispersal and accumulation of trace elements. Element speciation in different media (water, soil, food, plants tissue, coal, biological matter, food and fodder, minerals, etc.) is pivotal to assess an element's toxicity, bioavailability, environmental mobility, and biogeochemical performance. Classical methods for elemental analysis, such as gravimetric, titrimetric, calorimetric, and so on, do not sufficiently address the precision requirements when analyzing elements in trace concentrations. Therefore, new analytical techniques have been developed, which greatly simplified the quantitation of many trace elements and considerably extended their detection range. In this context, the development of reproducible and accurate techniques for trace element analysis in different media using spectroscopic instrumentation is continuously advanced. Here, inductively coupled plasma mass spectroscopy (ICP-MS) analysis of trace elements is of increasing importance; among the different ICP-MS techniques, modern developments like dynamic reaction cell inductively coupled plasma mass spectrometry (DRC-ICP-MS) was successfully used to simultaneously determine 17 trace elements in blood samples [13]. Similar techniques encompass sector field inductively coupled plasma mass spectrometry (SF-ICP-MS), which was successfully used for determination of aluminum, beryllium, cadmium, cobalt, chromium, mercury, manganese, nickel, lead, and vanadium in urine, serum, blood, and cerebrospinal fluid [14]. Moreover, laser ablation inductively coupled plasma mass spectrometry (LA-ICP-MS) constitutes a quantitative microbeam technique for rapid and accurate determinations of trace element concentrations in the sub-ppm range in various target materials [15]. A classical method, atom absorption spectroscopy (AAS), is still widely used to quantify various trace elements [16, 17], for example, the well-known graphite furnace atomic absorption spectrometry, which was, *inter alia*, successfully used for trace element determination in fish samples [18]. Prior to AAS measurement, biological samples to be investigated for trace elements need to be solubilized by different ashing techniques; here, a multitude of methods exists, with the use of nitric acid for "wet ashing" often being the method of choice [19]. Decades ago, X-ray fluorescence analysis was recognized as a viable tool to determine trace elements in geological samples [20–22]; in this context, a study reported by Leoni and Saitta in 1976 illustrated the viability of this technique to determine a total of 29 metals in rock and mineral samples in an astonishingly broad concentration range between 1 and 5000 ppm [20]. This AAS technique was later advanced to make it more custom-oriented and better applicable to different types of samples. Moreover, radiochemical trace element analysis is also widely used, mainly using radiochemical neutron activation analysis [23, 24]. By resorting to this method, trace elements were accurately determined in various samples, which are as diverse as human tissue [23], food products [16], and also in terrestrial, lunar, and meteoritic rock samples [24].

Author details

Martin Koller[1] and Hosam M. Saleh[2]*

*Address all correspondence to: hosamsaleh70@yahoo.com

1 Office of Research Management and Service, c/o Institute of Chemistry, University of Graz, Graz, Austria

2 Radioisotope Department, Nuclear Research Center, Atomic Energy Authority, Cairo, Egypt

References

[1] Prashanth L, Kattapagari KK, Chitturi RT, Baddam VRR, Prasad LK. A review on role of essential trace elements in health and disease. Journal of Dr. NTR University of Health Sciences. 2015;**4**(2):75

[2] Mertz W. The essential trace elements. Science. 1981;**213**(4514):1332-1338

[3] Fairweather-Tait SJ. Bioavailability of trace elements. Food Chemistry. 1992;**43**(3):213-217

[4] Rickes EL, Brink NG, Koniuszy PR, Wood TR, Folkers K. Vitamin B12, a cobalt complex. Science (Washington). 1948;**108**(2797):134

[5] Lameiras FS, Nunes EHM, Vasconcelos WL. Infrared and chemical characterization of natural amethysts and prasiolites colored by irradiation. Materials Research. 2009;**12**(3):315-320

[6] Swaine DJ. Why trace elements are important. Fuel Processing Technology. 2000;**65**:21-33

[7] Nielsen FH. Ultratrace minerals. In: Shils ME et al. USDA, ARS Source: Modern nutrition in health and disease. Baltimore: Williams & Wilkins; 1999. pp. 283-303

[8] Andreesen JR, Makdessi K. Tungsten, the surprisingly positively acting heavy metal element for prokaryotes. Annals of the New York Academy of Sciences. 2008;**1125**(1):215-229

[9] Campbell AK, Naseem R, Wann K, Holland IB, Matthews SB. Fermentation product butane 2, 3-diol induces Ca^{2+} transients in *E. coli* through activation of lanthanum-sensitive Ca^{2+} channels. Cell Calcium. 2007;**41**(2):97-106

[10] Wang J, Liu G, Liu H, Lam PK. Multivariate statistical evaluation of dissolved trace elements and a water quality assessment in the middle reaches of Huaihe River, Anhui, China. Science of the Total Environment. 2017;**583**:421-431

[11] Tangahu BV, Sheikh Abdullah SR, Basri H, Idris M, Anuar N, Mukhlisin M. A review on heavy metals (As, Pb, and Hg) uptake by plants through phytoremediation. International Journal of Chemical Engineering. 2011;**2011**. Article ID 939161

[12] Chandra S, Gusain YS, Bhatt A. Metal hyperaccumulator plants and environmental pollution. In: Microbial Biotechnology in Environmental Monitoring and Cleanup. PA, USA: Hershey, IGI Global; 2018. pp. 305-317

[13] D'Ilio S, Violante N, Di Gregorio M, Senofonte O, Petrucci F. Simultaneous quantification of 17 trace elements in blood by dynamic reaction cell inductively coupled plasma mass spectrometry (DRC-ICP-MS) equipped with a high-efficiency sample introduction system. Analytica Chimica Acta. 2006;**579**(2):202-208

[14] Bocca B, Alimonti A, Petrucci F, Violante N, Sancesario G, Forte G, Senofonte O. Quantification of trace elements by sector field inductively coupled plasma mass spectrometry in urine, serum, blood and cerebrospinal fluid of patients with Parkinson's disease. Spectrochimica Acta Part B: Atomic Spectroscopy. 2004;**59**(4):559-566

[15] Liu Y, Hu Z, Gao S, Günther D, Xu J, Gao C, Chen H. *In situ* analysis of major and trace elements of anhydrous minerals by LA-ICP-MS without applying an internal standard. Chemical Geology. 2008;**257**(1-2):34-43

[16] Bermudez GM, Jasan R, Plá R, Pignata ML. Heavy metal and trace element concentrations in wheat grains: Assessment of potential non-carcinogenic health hazard through their consumption. Journal of Hazardous Materials. 2011;**193**:264-271

[17] Singh M, Yadav P, Garg VK, Sharma A, Singh B, Sharma H. Quantification of minerals and trace elements in raw caprine milk using flame atomic absorption spectrophotometry and flame photometry. Journal of Food Science and Technology. 2015;**52**(8):5299-5304

[18] Tüzen M. Determination of heavy metals in fish samples of the middle Black Sea (Turkey) by graphite furnace atomic absorption spectrometry. Food Chemistry. 2003;**80**(1):119-123

[19] Clegg MS, Keen CL, Lönnerdal B, Hurley LS. Influence of ashing techniques on the analysis of trace elements in animal tissue. Biological Trace Element Research. 1981;**3**(2):107-115

[20] Leoni L, Saitta M. X-ray fluorescence analysis of 29 trace elements in rock and mineral standards. Rendiconti della Societa Italiana di Mineralogia e Petrologia. 1976;**32**(2): 497-510

[21] Rowe H, Hughes N, Robinson K. The quantification and application of handheld energy-dispersive X-ray fluorescence (ED-XRF) in mudrock chemostratigraphy and geochemistry. Chemical Geology. 2012;**324**:122-131

[22] Margui E, Zawisza B, Sitko R. Trace and ultratrace analysis of liquid samples by X-ray fluorescence spectrometry. TrAC Trends in Analytical Chemistry. 2014;**53**:73-83

[23] Lievens P, Versieck J, Cornelis R, Hoste J. The distribution of trace elements in normal human liver determined by semi-automated radiochemical neutron activation analysis. Journal of Radioanalytical and Nuclear Chemistry. 1977;**37**(1):483-496

[24] Keays RR, Ganapathy R, Laul JC, Krähenbühl U, Morgan JW. The simultaneous determination of 20 trace elements in terrestrial, lunar and meteoritic material by radiochemical neutron activation analysis. Analytica Chimica Acta. 1974;**72**(1):1-29

Section 2

Trace Elements in the Human Body

Chapter 2

Minor and Trace Elements in Whole Blood, Tissues, Proteins and Immunoglobulins of Mammals

Natalia P. Zaksas and Georgy A. Nevinsky

Additional information is available at the end of the chapter

http://dx.doi.org/10.5772/intechopen.75939

Abstract

Microelements play different important roles in many physiological processes in all biological systems in both normal physiological and pathological conditions. They take part in the transport of nutrients and gases, support temperature, acid-base balance, homeostasis of the human organisms, maternal and child mental health, the functioning of enzymes, protein and DNA syntheses, cytoskeleton activation, etc. We have performed simultaneous determination of a number of minor and trace elements in whole blood and tissues of mammals by two-jet plasma atomic emission spectrometry (TJP-AES). TJP-AES allows direct analysis of powders without wet acid digestion and can be used for analysis of both large and small amount of the sample, which is important for biomedical investigations with humans and experimental animals. In addition, a content of different elements in preparations of human immunoglobulins was estimated by TJP-AES as well as using different physicochemical methods, the functional role of metal ions in antibodies functioning was analyzed. The analysis of the relative activity of antibodies with catalytic activity (abzymes) in the hydrolysis of DNA, RNA, proteins, peptides and oxidation-reduction reactions and the role of metal ions in the catalysis of these reactions by abzymes were carried out.

Keywords: two-jet plasma atomic emission spectrometry analysis, minor and trace elements, functional role of metals

1. Introduction

Minor and trace elements including metals play important roles in many systems, normal and pathologic processes. Nowadays, there are many methods for elemental analysis of different biological samples. Atomic absorption spectrometry (AAS), inductively coupled plasma atomic

emission spectrometry (ICP-AES) and mass spectrometry (ICP-MS) are usually used for analysis of blood and animal tissues [1, 2]. Generally, these methods require matrix destruction with concentrated acids. Using microwave-assisted wet acid digestion with temperature control and elevated pressure allows reducing the time of sample digestion and risk of element losses. For direct ICP-MS analysis of whole blood and serum, dilution with alkaline solutions containing EDTA, ammonia and Triton X-100 was also employed to lyse the blood cells and prevent blood clotting [3, 4]. To improve the analytical capabilities of the methods applied, the new analytical techniques and reagents are being developed. A collision/reaction cell technology allowed the removal of polyatomic interferences and extended the capabilities of ICP-MS for trace element determination [5]. To decrease limits of detection (LODs) of trace elements, different ways of their preconcentration were offered. For determining the low concentration of Pb in blood serum by flame AAS, Barbosa with coauthors [6] used oxidized carbon nanotubes covered with bovine serum albumin layers; preconcentration was performed in untreated blood serum and allowed getting LOD of Pb at the level of 2 μg/L. Mortada with coauthors [7] suggested hydroxyapatite nanorods prepared from recycled eggshell for solid phase extraction of Pb, Cu and Zn from solutions of different biological samples followed by AAS analysis. In spite of undeniable progress in developing the above-mentioned methods, the analysis of biological samples using solid sampling is very attractive as the analytical procedure is simple and risk of contamination and analyte losses is improbable. To adapt the above methods for direct analysis of solid biological samples, laser ablation (LA) and electrothermal vaporization (ETV) were applied. LA-ICP-MS has got significant attention over the last decade for the analysis of biological samples [8]. It has been mainly applied to produce images of element distributions in human and animal tissues, which is of great scientific interest [9]. The main challenge of facing the LA-ICP-MS application is fully quantitative analysis requiring complex strategies for producing reliable calibrating materials. Lack of certified reference materials (CRMs) with different biological matrices and complications of preparing matrix-matched calibration samples [10] often make it difficult to carry out quantitative multi-elemental analysis of different biological tissues. This problem is well known for ETV-ICP-AES, X-ray fluorescence and laser-induced breakdown spectrometry (LIBS).

In recent times, LIBS has been applied as a screening tool for trace element bio-imaging in human and animal organs. To detect Wilson's disease, the study of Cu distribution in human liver was carried out [11]. A low-cost approach allows the quick detection of pathological accumulation of Cu in the affected organs. The LIBS mapping of the mice kidney slices after injection of a solution containing Gd-based nanoparticles was performed [12]. Each of the above methods has both advantages and disadvantages, and the choice of the analytical method depends on the sample nature, analytical tasks and availability of appropriate device and calibration samples. In the present work, two-jet plasma atomic emission spectrometry (TJP-AES) was used for analysis of different biological samples.

2. Two-jet plasma atomic emission spectrometry

2.1. A two-jet plasmatron

The TJP was developed by Zheenbaev and Engel'sht in the USSR (Kyrgyzstan Institute of Physics) in the mid-1970s [13]. It is a direct current (dc) plasma that differs from dc plasmas described [14, 15]

http://dx.doi.org/10.5772/intechopen.75939

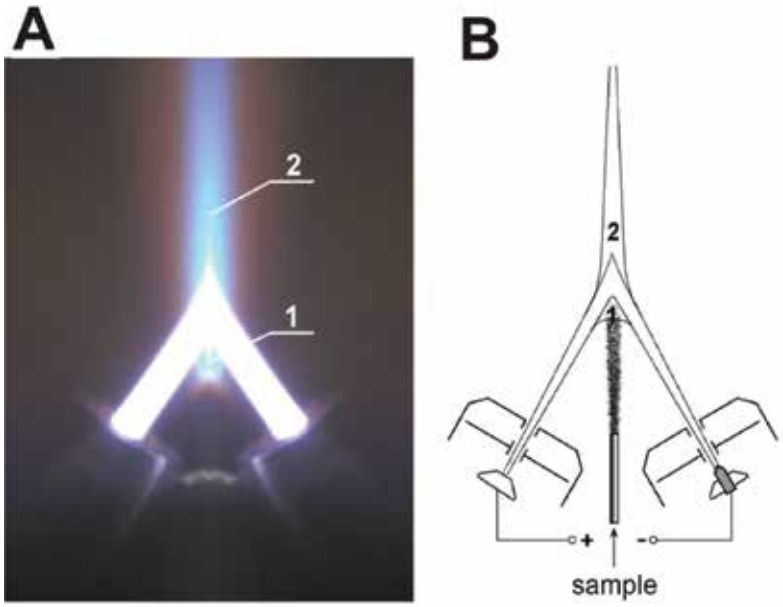

Figure 1. (A) Plasma torch; (B) electrode unit and analytical regions of the plasma flow: 1, before the jet confluence; 2, after the jet confluence.

and an ICP by a high power, which allows analysis of powdered samples without sample dissolution. Although the TJP appeared approximately at the same time as an ICP, TJP-AES was not generally recognized since only a few copies of the plasmatron were produced; it has not been modernized for decades. Nowadays, TJP-AES is experiencing a new stage in its development because a new modern plasmatron was designed at "VMK-Optoelektronika" (Russia). A photograph of the plasma torch and scheme of electrode unit are presented in **Figure 1**.

Argon plasma jets are generated in non-consumable electrodes (copper anode and tungsten cathode); they join at the output to form plasma discharge. The argon consumption does not usually exceed 5 l/min. The power supply of the plasma generator, gas flow and automatic sample introduction systems are computer controlled. A TJP power can be fixed from 5 to 12 kW by varying the current strength in the range of 40–100 A. Current fluctuation does not exceed 1%. A new plasmatron is equipped with a concave diffraction grating (2400 lines/mm) and two multicrystal photodiode arrays allowing spectra to be measured in two spectral ranges: 190–350 and 390–450 nm.

To transfer powders into the plasma, a powder introduction device was developed. The sample is placed in a Plexiglas beaker, inserted into the device and roiled with blast waves produced by a spark between zirconium electrodes over the surface of the powder. An aerosol obtained is delivered into the plasma with a carrier gas. The device allows the introduction of both small and large amount of the samples (5–500 mg).

2.2. Analytical regions

There are two analytical regions in the TJP – before and after the jet confluence (**Figure 1**). The region of the confluence is not used for analysis due to high background emission. A study of behavior of a wide range of elements in the plasma has shown that the highest ratio of the

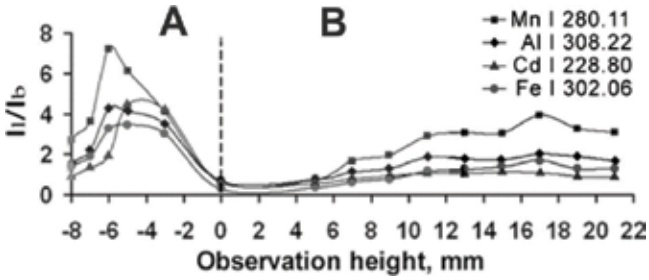

Figure 2. I_i/I_b distribution along the plasma flow for Mn I 280.11, Al I 308.22; Cd I 228.80 and Fe I 302.06 lines: region (A) before the jet confluence, (B) after the jet confluence; 0 – point in the region of the confluence.

analytical line intensity to the background one (I_i/I_b) realizes in the region before the jet confluence both for atomic and ionic lines. As an example, the distribution of I_i/I_b for analytical lines Mn I 280.11, Al I 308.22; Cd I 228.80 and Fe I 302.06 along the plasma flow is shown in **Figure 2**.

Analytical lines of Ag and Zn registered in the region before and after the jet confluence are shown in **Figure 3**.

As it is seen, the analytical signals are at the level of background fluctuations in the region after the jet confluence, but they are considerably higher than background in the region before one, which testifies to better LODs of elements in this region. One of the problems arising in the TJP-AES analysis of powdered samples is their incomplete evaporation which can lead to a systematic underestimation of the analysis results. The short residence time of the sample in the plasma is one of the reasons for the partial sample evaporation. In addition, evaporation efficiency depends on chemical composition, structure and particle size of powdered samples [17]. To demonstrate evaporation efficiency in the analytical zones of the TJP, silicon carbide (SiC) powders with an average particle size of 1, 3, 7.5, 17, 22 and 36 μm were used. SiC is a heat-resistant material having a high hardness close to the hardness of diamond. SiC evaporation was controlled by the intensity of weak Si I 212.30 line. To avoid signal self-absorption, the powders were diluted with graphite 100 times. The dependence of Si I 212.30 line intensity on the particle size is given in **Figure 4**.

The different behavior of silicon line is observed in the regions investigated. In the region before the jet confluence, there is an increase in the silicon line intensity along with a decrease in the particle size, the smaller particle size and the better evaporation efficiency. However, the complete sample evaporation does not occur even at a particle size of 3 μm. In the region after the jet confluence, the maximum intensity is achieved even at a particle size of 17 μm. The decrease in intensity at smaller particles seems to occur due to the introduction of light particles into the region after the confluence is complicated by a resistance of the consistent plasma jets. Nevertheless, the effect of particle size on evaporation efficiency is considerably weaker in the region after the jet confluence. Thus, the region before the jet confluence provides lower detection limits of elements than the region after one, but evaporation efficiency is better in the region after the jet confluence. Therefore, the choice of the analytical region depends on an analytical task and sample nature.

http://dx.doi.org/10.5772/intechopen.75939

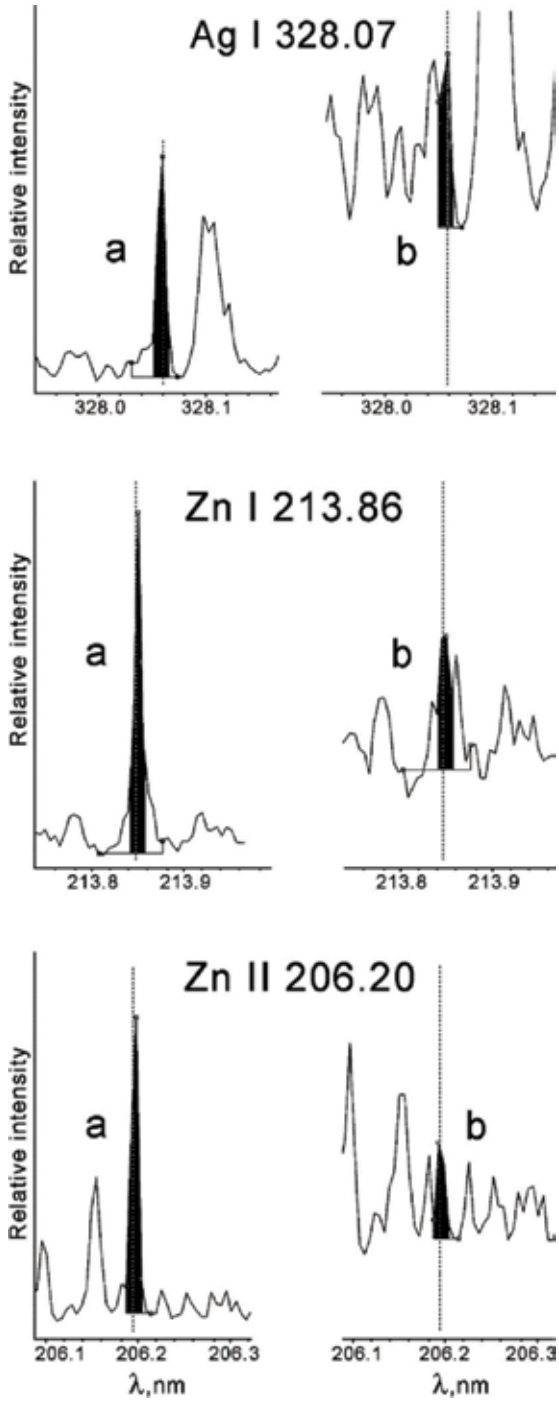

Figure 3. Analytical lines Ag I 328.07 (0.05 μg/g), Zn I 213.86 (0.5 μg/g) and Zn II 206.20 (1 μg/g) registered in the region (a) before the jet confluence and (b) after the jet confluence [16].

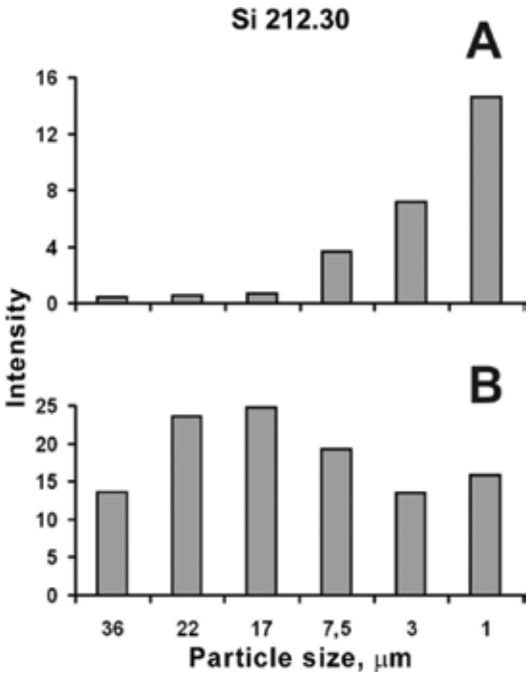

Figure 4. Dependence of Si I 212.30 line intensity on the particle size of SiC in the region (A) before the jet confluence (B) after the jet confluence.

2.3. Excitation mechanisms

To solve the problems appearing in the analysis, it is important to have an idea about the processes occurring in the plasma. The probable mechanisms of an atom and ion excitation in the TJP were investigated [16, 18]. The Boltzmann distribution of excited energy levels for Fe atoms and singly ionized ions was found to take place in both analytical regions, which indicates the predominant excitation of atoms and ions by electron impact. Excitation temperature of Fe atoms and ions, T_{atom} and T_{ion}, respectively, was measured along the plasma flow. In the optimal observation zone of the region before the jet confluence T_{atom} = 6000 K and T_{ion} = 7900 K, and in the observation zone of the region after one T_{atom} = 7060 K and T_{ion} = 8050 K. For atomic and ionic lines, the temperature deviation did not exceed 100 K in the optimal observation zones and was about 250 K near the jet confluence. The considerable difference in T_{atom} and T_{ion} points at the departure from local thermodynamic equilibrium (LTE) in the plasma. The difference is 1900 K for the region before the jet confluence and 990 K for the region after one, which indicates that the region before the jet confluence is more non-equilibrium than the region after one. The disturbance of LTE in the plasma was shown to be due to metastable argon participation in atom ionization.

3. Application of TJP-AES

Originally, the TJP was intended for direct analysis of sparingly soluble geological samples [19], which considerably reduced the analysis time and element losses as compared with wet acid digestion. The spectra were registered in the analytical region after the jet confluence

(**Figure 1**), and calibration samples similar to the analyzed ones were used. The region before the jet confluence was not practically used for analysis.

3.1. Analysis of high purity substances

The region before the jet confluence turned out to be suitable for analysis of high purity substances both by direct technique and after matrix separation. The TJP-AES techniques for analysis of gallium [20], indium and indium oxide [21] and tellurium dioxide [22] were developed. The direct techniques allow determination of about 30 elements using appropriate dilution of the sample with a spectroscopic buffer (graphite powder containing 15 wt.% NaCl) and unified calibration samples based on graphite powder with addition of 15 wt.% NaCl. As it was shown earlier, NaCl addition increases analytical line intensities and suppresses effects of a mineral matrix [23]. CRMs of graphite powder with different combinations of impurities are commercially available (Ural Federal University, Russia); in addition, preparing the reference sample with given element concentration in graphite is not a difficult task. Analysis of the above substances was carried out at the optimal conditions chosen for multi-elemental analysis of graphite powder (**Table 1**). Calibration curves (lgI-lgC) obtained for Cd and Hg in graphite powder are presented in **Figure 5**.

A degree of sample dilution depends on the sample nature; a fourfold dilution is needed for analysis of indium oxide and gallium, and a twofold dilution is quite enough for analysis of tellurium dioxide. The preconcentration of impurities in gallium and indium was accomplished by matrix separation in the form of chlorides; tellurium dioxide was previously reduced by hydrogen to metal, and the preconcentration was performed by vacuum distillation of tellurium. The impurity concentrates contained a high concentration of matrix elements since incomplete matrix separation was applied to avoid the loss of a number of important impurities; they were analyzed by the same way as in the direct techniques. LODs of elements were at the level of 0.01–1 and 0.001–0.1 μg/g for direct analysis and after matrix separation, respectively. The possibility of analysis of such a different substances using unified calibration samples points at comparatively weak matrix affects this excitation source. For comparison, using such an approach for a dc arc with sample evaporation from a crater of graphite electrode requires a 100-, 50-, and 25-fold dilution of gallium, indium and tellurium oxides, respectively, which lead to worsening LODs of elements by more than an order of magnitude. Recently, the similar approach was used for analysis of different soils [24]. In spite of their complex and variable matrix composition, TJP-AES allowed direct determination of

Parameter	Value
Current strength	85 A
Voltage	120 V
Plasma gas flow	4 l/min
Carrier gas flow	0.85 l/min
Angle between the jets	60°
Observation zone	4–5 mm lower than the point of the confluence

Table 1. Working conditions of the two-jet plasma.

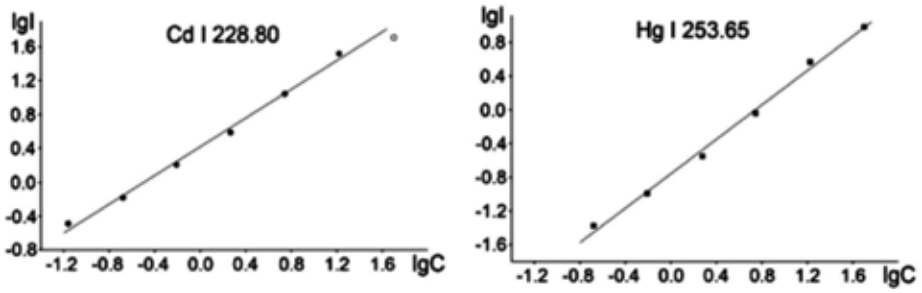

Figure 5. Calibration curves for analytical lines Cd I 228.80 and Hg I 253.65 (C μg/g) [24].

As, B, Cd, Cu, Hg and P after a twofold and Be, Co, Cr, Ga, Nb, Pb and Zn after a 10-fold dilution with a spectroscopic buffer.

3.2. Analysis of biological samples

Solid sampling, with little or no chemical pretreatment, in the analysis of biological samples seems very attractive. The possibility of TJP-AES for direct analysis of biological samples using the same unified approach as for inorganic materials was investigated. First, starch was used to study the organic matrix influence on analytical signals of elements in the TJP [25]. It was found that the presence of 10 wt.% starch in graphite powder with introduced impurities did not affect analytical line intensities of elements while the decrease in intensities by a factor 2–5 was observed in a graphite dc arc. In the TJP, the effect was not observed even in the presence of 20 wt.% starch for many atomic lines of elements. The considerable decrease in intensities in a dc arc is due to a vigorous reaction of starch with air oxygen in an arc discharge with the release of gaseous products, which results in decreasing the residence time of the sample in the plasma. Although the TJP is an open system too, the oxidative reaction occurs less violently than in a dc arc since carrier argon partially displaces air from the excitation zone, and the sample is gradually introduced into the plasma. In addition, gaseous products seem to be retained in the excitation zone by argon flows. The experiments with starch gave hope to get positive results for more complex organic matrices.

3.2.1. Analysis of animal organs

The unified approach mentioned above was tested for animal organs, dried and finely powdered. Dry animal organs contain more than 50 wt.% proteins as well as fats, carbohydrates and others. The effect of such a complex matrix on the analytical signal of elements was studied by the analysis of a spiked sample based on graphite with the addition of 15 wt.% NaCl and 10 wt.% rat liver; concentration of elements introduced was 2.5 μg/g [26]. The analysis was carried out using calibration samples based on graphite powder with addition 15 wt.% NaCl; the spectra were observed in the region before the jet confluence. The analysis results are given in **Table 2**; the satisfactory recoveries were obtained for all investigated elements. Since the liver contained Co, Mn, Mo and Zn, the blank sample was prepared to estimate correctly the recovery of these elements. On the basis of the results obtained, a 10-fold dilution

Element	λ (nm)	Concentrations of elements		Recovery (%)
		Added (μg/g)	Found (μg/g)[a]	
Ag	338.29	2.5	2.4 ± 0.6	96
Ba	233.53	2.5	2.5 ± 1.0	100
Be	265.06	2.5	2.3 ± 0.8	92
Bi	306.77	2.5	2.6 ± 0.8	104
Cd	228.80	2.5	2.5 ± 0.3	100
Co	345.35	–	0.26 ± 0.8[b]	–
		2.5	2.8 ± 0.6	102
Cr	283.56	2.5	2.8 ± 1.4	112
Ga	294.36	2.5	2.4 ± 0.4	96
Hg	253.65	2.5	2.6 ± 0.6	104
Mn	280.11	–	0.80 ± 0.15[b]	–
		2.5	3.5 ± 0.6	108
Mo	317.03	–	0.27 ± 0.10[b]	–
		2.5	2.5 ± 0.3	89
Ni	305.08	2.5	2.3 ± 0.7	92
Pb	283.31	2.5	2.5 ± 0.4	100
Sb	231.15	2.5	2.5 ± 0.7	100
Sn	284.00	2.5	2.3 ± 0.5	92
Zn	213.85	–	6.8 ± 1.7[b]	100
		2.5	9.3 ± 2.0	

[a]Mean ± (95% confidence interval), n = 4.
[b]Value obtained without spike addition.

Table 2. Determination of elements in a spiked graphite powder containing 10% rat liver [26].

of powdered animal organs with buffer and calibration based on graphite powder were suggested for direct analysis of animal organs. To validate the technique, the results of direct analysis of bovine liver were compared with the results obtained after sample carbonization (500°C, 5 min) and autoclave digestion in a mixture of nitric acid and hydrogen peroxide [25]. The carbonized sample was analyzed at the conditions chosen for direct analysis. The solution obtained after acid digestion evaporated on graphite powder, diluted with buffer and analyzed by the same way. As it is seen from **Table 3**, the results of Al, Ca, Cu, Fe, Mg, Mn, Mo, P, Si and Zn satisfactory agree with each other. Only for Fe, Mn and Mo, the results obtained after autoclave digestion are lower than the results of the direct technique, which is likely to be due to their partial loss. The LODs of elements provided by the direct technique are at the level 0.1–10 μg/g, and they are lower by approximately one order of magnitude after carbonization. The use of the carbonization procedure allowed determining the low concentrations of Ag, Cd, Co, Cr, Pb and Ni in the liver.

B	249.77	6.2 ± 2.0	2.7 ± 0.5	5.5 ± 1.0
Ca	317.93	130 ± 20	110 ± 30	130 ± 40
Cd	228.80	<0.4	0.17 ± 0.03	0.25 ± 0.10
Co	345.35	<1	0.31 ± 0.05	—
Cu	324.75	12 ± 2	12 ± 4	10 ± 0.2
Cr	283.56	<1	0.2 ± 0.04	0.24 ± 0.06
Fe	302.06	250 ± 40	210 ± 70	150 ± 30
Mg	277.98	470 ± 80	460 ± 120	420 ± 90
Mn	279.83	16 ± 2	13 ± 3	9.5 ± 2.4
Mo	317.03	18 ± 3	20 ± 5	9.0 ± 2.3
Ni	305.08	<1	0.6 ± 0.1	0.77 ± 0.25
P, wt.%	214.91	0.99 ± 0.08	0.85 ± 0.25	0.76 ± 0.11
Pb	283.31	<1	0.40 ± 0.07	0.40 ±0.11
Si	288.16	22 ± 8	31 ± 14	22 ± 11
Zn	213.86	62 ± 15	55 ± 10	60 ± 8

[a]95% confidence interval.

Table 3. Results of the TJP-AES analysis of bovine liver (μg/g) [25].

The technique suggested is very suitable for analysis of dry internals such as liver, kidney and spleen which are easily ground in a Plexiglas mortar to a powder with the particle size of 20–30 μm. However, the direct analysis of bovine and pork muscle CRMs and rat brain was found to provide the understated results [26]. These tissues are more thermostable than liver and have the particles of more than 100 μm. Flexible fibers of muscles and plastic consistence of brain make it difficult to obtain a powder with small particles. Incomplete evaporation of the samples is the most probable reason for the result underestimations. This problem was overcome by decreasing the consumption of a carrier gas, which increases the residence time of the sample in the excitation zone and concentration of air oxygen participating in organic matrix decomposition. It should be noted that the carbonization conditions are not all-purpose and depend on a kind of tissues. For brain and muscle tissues, the time of carbonization was increased up to 30 min. Thus, in spite of the unified approach to the analysis of organs, peculiarities of different tissues should be taken into account. For direct analysis, 5–10 mg of powdered sample is quite enough; for carbonization procedure, 50–100 mg of the sample is needed. Note that the ICP-AES and ICP-MS techniques with wet acid digestion of organs usually require 100–250 mg of the sample which is not always available. The relative standard deviation of the analysis results of animal organs usually is in the range of 3–12%.

3.2.2. Analysis of whole blood

The problem of availability of biological samples in ample quantity is particularly acute in experiments with living experimental animals (such as mice or rats). Blood is the main subject

Element	λ (nm)	Human blood			Rat blood		
		Direct analysis	Carbonizing	Autoclave digestion	Direct analysis	Carbonizing	Autoclave digestion
Fe	296.67	2300 ± 200[a]	2200 ± 160	2200 ± 200	2600 ± 200	2400 ± 170	2500 ± 200
P	214.91	1700 ± 130	1600 ± 120	1500 ± 110	1400 ± 200	1400 ± 100	1300 ± 150
Ca	317.93	320 ± 20	340 ± 30	300 ± 20	240 ± 30	250 ± 20	280 ± 30
Mg	277.98	130 ± 15	150 ± 20	130 ± 10	120 ± 15	140 ± 15	150 ± 20
Zn	213.86	28 ± 1.6	26 ± 1.4	29 ± 1.7	29 ± 2.0	32 ± 1.5	32 ± 1.4
Cu	324.75	6.6 ± 0.5	6.2 ± 0.4	5.8 ± 0.4	3.6 ± 0.3	3.5 ± 0.3	3.3 ± 0.2

[a]95% confidence interval, n = 4.

Table 4. Concentration of elements in the freeze-dried blood samples (μg/g) [27].

of investigation for living organisms. Whole blood quickly changes over time due to fast clotting, which troubles the sample cutting. The effect of anticoagulants also lasts a limited time. Therefore, for continuous biomedical experiments, freeze-dried whole blood which can be kept for a long time at normal conditions is very convenient. For determining the main essential elements (Fe, P, Ca, Mg, Zn and Cu) in freeze-dried whole blood, the direct technique developed for animal organs was applied [27]. To confirm the possibility of such an approach for blood analysis, the direct analysis of CRM of freeze-dried bovine blood (IAEA A-13) was carried out, and good agreement of the results with the certified values was obtained. In addition, the results of analysis of human and rat freeze-dried whole blood obtained using the different sample preparation procedures were compared (**Table 4**). The direct technique results satisfactory agreed with the results obtained after carbonization (400°C, 15 min) and autoclave digestion, which confirms the possibility of the unified approach for blood analysis. Simple sample preparation (dilution with buffer) and the possibility of analysis of small amount samples, 5–10 mg of blood powder (approximately 20–50 μL liquid blood), are of practical importance. For analysis of whole liquid blood, blood aliquots evaporated on graphite powder under an IR lamp and then carbonized at 400°C for 15 min. The remainder was ground in a mortar and analyzed as in the direct analysis. The techniques suggested were validated for analysis of both freeze-dried and liquid blood serum and plasma.

3.2.3. Analysis of bone

Bone is a highly mineralized mobile tissue which accumulates inorganic substances and diffuses them as the need arises. It contains 25 and 65 wt.% organic and inorganic substances, respectively, and 10 wt.% water. Collagen and calcium hydroxyapatite $Ca_{10}(PO4)_6(OH)_2$ are the main components of bone. Some elements are predominantly in the organic phase, and others are in the mineral phase of bone. It was found that a fourfold dilution of dry powdered bone was quite enough for element determination by the unified direct technique [28]. The results of "added-found" experiment and comparison of the direct technique results with the results of ICP-AES after wet acid digestion of the sample validated the technique. However, underestimating the Ba, Mg, and Sr concentration was obtained. These elements are strongly

Element	λ (nm)	LOD (μg/g)
Ag	328.07	0.1
Bi	306.77	1.2
Cd	228.80	0.5
Co	345.35	1.2
Cr	283.56	0.3
Cu	324.75	0.2
Fe	296.68	2.0
Ga	294.36	0.3
Mn	260.57	0.5
Mo	313.26	0.7
Ni	305.08	0.6
Pb	283.31	1.1
Sn	284.00	0.8
Zn	213.86	1.0

Table 5. Limits of detection (LOD) of elements in bone [28].

bound with calcium hydroxyapatite, and its incomplete evaporation may lead to their understated concentrations. This effect took place even at a mean particle size of 30 μm. The strongest decrease in concentration was observed for Sr replacing Ca in hydroxyapatite. It is well known that strontium rachitis develops in the regions with a high content of radioactive Sr due to the formation of high concentration of strontium hydroxyapatite in bone, which results in the fragility of people and animal teeth and bones. Pretreatment of the samples with nitric acid followed by heating at 300°C or decrease of the consumption of carrier argon as in the case of brain and muscle tissues allowed getting valid results for Ba, Mg, and Sr. The satisfactory results obtained for other elements by direct technique point at their fractional volatilization from the particles in the plasma. These elements seem to be bound with the organic portion of bone or weakly bound with calcium hydroxyapatite. LODs of a number of elements in bone are given in **Table 5**.

Thus, on the example of different animal organs, whole blood and bone the possibility of TJP-AES for realizing the simple analytical techniques was shown. Solid sampling, unified calibration samples, the possibility of analysis of small amount samples are of great interest for experiments with different biological tissues.

4. Analysis of trace element changes in mice treated with $CoCl_2$

Transition-metal cobalt is an essential trace element required for vitamin B_{12} biosynthesis, enzyme activation, etc., but is toxic in high concentrations. We estimated the effect of cobalt

chloride ($CoCl_2$) on relative content of different metal ions in mouse plasma using TJP-AES and on the total protein content [29, 30]. Freeze-dried plasma (2–3 mg) was available for the TJP-AES analysis. On average the relative content of different elements in the plasma of 2-month-old mice balb/c (control group) decreased in the order: Ca > Mg > Si > Fe > Zn > C u ≥ Al ≥ B. The 60 days treatment of mice with $CoCl_2$ (daily dose 125 mg/kg) did not change appreciably the relative content (ReCo) Ca, Cu and Zn, while a 2.3-fold significant decrease in the ReCo of B and a significant increase in the content of Si (3.4-fold), Fe and Al (2.1-fold) and Mg (1.5-fold) was found (**Table 6**). The ReCo of Mo and Co for untreated mice was lower than test sensitivity. Mo in a detectable amount was determined only for two mice in the control group, but the plasmas of 9 out of 16 mice of analyzed group contained this metal. Cobalt treatment resulted in a 2.2-fold decrease in the concentration of total plasma protein and in 1.7-fold immunoglobulins. Clarification of the complex effects of Co^{2+} on its interactions *in vivo* with other trace elements is important for the explanation of cobalt toxicity and disturbances in homeostasis and physiological processes such as development, growth, weight gain, immunity, reproduction, etc. [29].

Homogeneous IgGs purified from sera of mice treated (t-IgGs) and non-treated (nt-IgGs) with $CoCl_2$ containing intrinsically bound metal ions hydrolyze DNA with very low activity and lose this activity in the presence of EDTA [30]. The average relative DNase activity (RAs) of nt-IgGs increased after addition of external metal ions in the following order: $Zn^{2+} < Ca^{2+} < Cu$

Chemical element	Control untreated mice (n = 19)		Mice treated with $CoCl_2$ (n = 16)		Ratio of (2) and (1)*	Significance (*P*)
	Range of values (μg/g)	Average value (μg/g) (value 1)	Range of values (μg/g)	Average value (μg/g) (value 2)		
Ca	540–1670	1099 ± 239	510–1670	1169 ± 288	1.17	0.53
Cu	6.0–20.5	10.1 ± 2.6	5.2–26.5	9.1 ± 2.7	0.99	0.46
Zn	14–53	24.2 ± 6.8	15–49	25.9 ± 5.9	1.18	0.56
B	1.2–6.7	5.8 ± 2.5	1.1–5.6	2.5 ± 0.79	0.47	3×10^{-4}
Mg	190–590	423 ± 102	610–850	625 ± 75	1.76	1.2×10^{-7}
Al	4–13	6.5 ± 2.9	8–25	13.8 ± 3.4	2.53	2.5×10^{-7}
Fe	40–130	69 ± 17.0	72–270	147 ± 50	2.53	2.0×10^{-7}
Si	50–190	101 ± 38	200–520	342 ± 92	4.07	1.0×10^{-9}
Mo	~0	~0	0–9	2.3 ± 2.2		—
Co	~0	~0	7.2–37	16.8 ± 6.5		—
Total protein, mg protein/ml of plasma						
Protein	9.0–16.6	13.7 ± 1.9	2.0–7.7	6.2 ± 1.9		

*For each mouse, the mean of three repeats is used.

Table 6. Relative content of different chemical elements and total protein in the freeze-dried blood plasma of control mice and animals treated with $CoCl_2$ [29].

$^{2+}$ < Fe^{2+} < Mn^{2+} < Mg^{2+} < Co^{2+} < Ni^{2+}. Interestingly, t-IgGs showed lower activity than nt-IgGs in the absence of external metal ions (2.7-fold) as well as in the presence of Cu^{2+} (9.5-fold), Co^{2+} (5.6-fold), Zn^{2+} (5.1-fold), Mg^{2+} (4.1-fold), Ca^{2+} (3.0-fold) and Fe^{2+} (1.3-fold). But t-IgGs were more active than nt-IgGs in the presence of Ni^{2+} (1.4-fold) and especially Mn^{2+} (2.2-fold), which are the best activators of t-IgGs. These data may be useful for an understanding of Co^{2+} toxicity, its effect on a change of metal-dependent specificity of mouse abzymes [30].

5. Abzymes with oxidation-reduction activities

First, we have estimated the content of metals in the lyophilized plasmas of healthy Wistar rats (**Table 7**) by the TJP-AES method [31]. The relative amount of metals in the rat plasma decreased in the order: Ca > Mg > Fe > Cu ≥ Zn > Al ≥ Sr. > Ti ≥ Mo ≥ Mn (**Table 7**).

Metal	**Relative content (μg/g)***									**Average value (μg/g)**
	Rat number									
	1	**2**	**3**	**4**	**5**	**6**	**7**	**8**	**9**	
Ca	1700	1700	**1200**	1500	1700	1300	1200	1700	**2000**	1556 ± 274***
Mg	440	420	280	380	360	310	300	360	410	362 ± 56
Fe	**14****	120	90	110	80	110	**80**	100	110	104 ± 19
Cu	29	25	**22**	24	34	22	25	**39**	33	28.1 ± 6.0
Zn	26	44	**22**	25	**28**	25	26	25	26	27.4 ± 6.4
Al	6.0	**15**	7.0	13	6.0	5.0	5.0	**4.0**	7.0	7.6 ± 3.8
Sr	5.5	6.2	5.3	6.2	8.4	**5.0**	6.2	6.5	**8.4**	6.4 ± 1.2
Ti	**5.0**	3.0	3.0	3.0	3.0	4.0	**3.0**	4.0	4.0	3.6 ± 0.7
Mo	2.3	1.5	**1.1**	1.8	3.3	2.0	2.0	**3.4**	2.7	2.2 ± 0.8
Mn	1.2	**1.6**	1.1	**1.1**	1.3	1.4	1.2	1.4	1.3	1.3 ± 0.2
Pb	<2.0	<2.0	<2.0	<2.0	<2.0	<2.0	<2.0	<2.0	<2.0	<2.0
Cr	1.0	≤1.0[Ω1]	≤1.0	≤1.0	≤1.0	**≤1.0**	≤1.0	≤2.0	**≤6.0**	≤1.7 ± 1.6
Ni	≤1.0-	≤1.0	≤1.0	≤1.0	≤1.0	≤1.0	≤1.0	≤1.0	≤1.0	≤1.0
Co	<1.0	<1.0	<1.0	<1.0	<1.0	<1.0	<1.0	<1.0	<1.0	<0.1
Ag	<0.1	<0.1	<0.1	<0.1	<0.1	<0.1	<0.1	<0.1	<0.1	<0.1

*The content was determined by TJP-AES method; the relative standard deviation of the results from two experiments were within 5–7%.

**The maximal and minimal values for each metal are marked in bold.

***Mean ± S.D.

[Ω1]Sign ≤ in all cases means that the presence of metal in the samples is reliable, but its exact concentration cannot be determined; it can be in the range 0.1–1 μg/g.

Table 7. The relative content of different trace elements and metals in the lyophilized blood plasmas from nine rats.

http://dx.doi.org/10.5772/intechopen.75939

Metal	Relative content (μg/g)	
	sle-IgG_{mix}	ms-IgG_{mix}
Al	7.0	8.0
Ca	10	120
Cu	8.0	4.0
Fe	4.0	9.0
Mg	4.0	17.0
Mn	0.2	~0
Ni	6.5	0.7
Ti	2.0	27.0
Zn	37.0	11.0

*Preparations sle-IgG_{mix} and ms-IgG_{mix} are mixtures of equal amounts of electrophoretically homogeneous IgGs from the sera of 12 SLE (sle-IgG_{mix}) and 12 MS (ms-IgG_{mix}) patients.

**The content was determined by TJP-AES method; the errors of the values from two experiments were within 5–7%.

Table 8. The relative content of metal ions in the lyophilized sle-IgG_{mix} and MS-IgG_{mix} samples from the sera of patients with SLE and MS, respectively*.

Nine plasmas of healthy Wistar rat's sera were used for purification of electrophoretically and immunologically homogeneous IgGs according to [31–35]. Homogeneous IgGs according to data of the TJP-AES method did not contain a detectable amount of Sr and Mo (**Table 8**) [31]. The relative amount of different metals bound to IgGs of SLE and MS patients in average decreased in the following order: Ca ≥ Zn ≥ Ti ≥ Mg ≥ Al ≥ Fe ≥ Cu ≥ Ni > Mn (**Table 8**). Thus, IgGs of individual rats can interact with metal ions showing a significant difference (**Table 8**) in spite of their comparable concentrations in the plasmas (**Table 7**).

We have shown that rat IgGs lose most bound metal ions during the purification [31, 33]. From 26 to 39% of rat IgGs can interact with less or more efficiently with different metals ions. Interestingly, chromatography of IgGs from human plasmas on Chelex non-charged with metal ions led to the binding of a small amount of IgGs (~ 5%) bound with metal ions [36]. Chelex charged with Cu^{2+} ions additionally adsorbed ~ 38% of the total IgGs. In a number of publications, it was shown that all many catalytic activities are the intrinsic properties of mammalian antibodies and are not caused by impurities of any canonical enzymes [37–46]. For this purpose, in all cases, we have checked several previously developed strict criteria proving that all activities of Abs from blood sera and healthy donors and autoimmune patients belong to the Abs [37–46].

All higher organisms generate energy due to aerobic respiration, the process including a four-electron stepwise reduction to water of molecular oxygen [47–51]. The partially reduced species include $OH^{\bullet}$, H_2O_2 and $O_2^{\bullet-}$, are typical oxidants attacking proteins, lipids, DNA and other components of different cells. Oxidative damage of cells components was regarded as the significant factor of carcinogenesis and aging [47, 49, 51].

Antioxidant enzymes (catalases, superoxide dismutases and glutathione peroxidases) are very important for preventing oxidative stress [52–56]. However, these enzymes are located inside of cells, and they undergo rapid inactivation in the blood [54]. Immunoglobulins (Igs) are significantly more stable molecules of blood. Therefore, it was interesting how metal ions can activate oxidation-reduction reactions catalyzed by antibodies. The catalysis of such reactions by the majority of canonical enzymes is dependent on metal ions with variable valence [50, 52–55]. First, we have shown that IgGs of healthy Wistar rats oxidize 3,3′-diaminobenzidine through a peroxidase activity in the presence of H_2O_2 and due to an oxidoreductase activity in the absence of H_2O_2 [31–35]. In the external metal ions absence, the specific peroxidase activity of IgGs of rats varied in the range 1.6–26% comparing with horseradish peroxidase (HRP, taken for 100%). The dialysis of IgGs against EDTA completely lost these activities. External metal ions activated significantly both activities of non-dialyzed (ND) and dialyzed (D) IgGs. The relative activities (RAs) in the presence of external Fe^{2+} or Cu^{2+} ions were increased up to 13–198% compared with that for HRP [31]. Cu^{2+} ions alone stimulated significantly both the oxidoreductase and peroxidase activities of dialyzed D-IgGs, but only at high concentration (≥2 mM) [31]. Mn^{2+} ions were weakly activated peroxidase activity but at >3 mM Mn^{2+} was good cofactor of the oxidoreductase activity at a low concentration (<1 mM). Fe^{2+}-dependent peroxidase activity of D-IgGs was revealed at 0.1–5 mM, but Fe^{2+} cannot activate their oxidoreductase activity. Al^{3+}, Mg^{2+}, Zn^{2+}, Ca^{2+}, and especially Ni^{2+} and Co^{2+} were not able to activate D-IgGs, but slightly activated ND-IgGs containing different intrinsic metal ions. Some metal ions activated IgGs especially ND-Abs in accordance with biphasic curves, which were specific for every individual Ab preparation [31]. The combinations of Fe^{2+} + Zn^{2+}, Fe^{2+} + Mn^{2+}, Cu^{2+} + Mn^{2+} and Cu^{2+} + Zn^{2+} and other metal ions led to the oxidation of substrates mainly with single-phase curves. In parallel to a significant increase of the activities comparing with Fe^{2+}, Cu^{2+} or Mn^{2+} taken separately, the RAs of the oxidation reactions catalyzing by non-dialyzed and dialyzed IgGs, became to be comparable. Ni^{2+}, Mg^{2+} and Co^{2+} sufficiently activated the Cu^{2+}-dependent oxidation of substrates catalyzed by D-IgGs, while Ca^{2+} inhibited these reactions [31].

As mentioned above, the dependencies of the oxidoreductase and peroxidase activities of the ND-IgGs and D-IgGs on the concentrations of Fe^{2+}, Cu^{2+} and Mn^{2+} were biphasic. This indicates that two different metal ions are likely to participate in the catalysis of these reactions. The canonical Cu, Zn superoxide dismutases usually use a Cu^{2+} ion together with a Zn^{2+} ion [53–55]. However, the only Cu^{2+} with variable valency participates in the oxidation of substrates, while Zn^{2+} serves as a second electrophilic metal cofactor of this enzyme [53–55]. The biphasic dependences can show for a similar function of the same second or another second metal ion. Since D-IgGs and ND-IgGs demonstrate a significantly higher activity in the presence of Cu^{2+} ions together with Mn^{2+} or Zn^{2+} ions, some fractions of IgGs can be Cu/Cu, Cu/Mn or Cu/Zn peroxidases or oxidoreductases. A remarkable increase in the IgGs activity by Cu^{2+} ions together with Co^{2+}, Mg^{2+} or Ni^{2+} can speak in favor that these metal ions can also increase the oxidative function of Cu^{2+} to some extent as the second ions [31]. Only Fe^{2+} taken separately was activated the peroxidase activity of D-IgGs at low concentrations (<1 mM). However, $FeCl_2$ was completely unable to activate the oxidoreductase activity of D-IgGs. Most probably, Cu^{2+} + Mn^{2+} is an optimal pair for both the peroxidase and oxidoreductase reactions. It seems more likely that the activation of

http://dx.doi.org/10.5772/intechopen.75939

IgGs by two metal ions with variable oxidation state proceeds either using the second metal as an electrophilic cofactor.

It was demonstrated that small fractions of IgGs from the sera of healthy humans as well as their Fab and $F(ab)_2$ fragments oxidize DAB through peroxidase and oxidoreductase activities [36]. In contrast to rat antibodies, IgGs from human blood have both the dependent and independent on metal ions activities. After dialysis of human IgGs against EDTA and EGTA, the relative peroxidase and oxidoreductase activity dependently of IgG preparation decreased from 100 to ~10–85 and 14–83%, respectively. Addition of external metal ions to D-IgGs and ND-IgGs results in a significant increase in their activities. Separation of IgGs on Chelex results in Abs separation to many different subfractions with different affinities to the chelating resin. In the presence of Cu^{2+} external ions, the specific peroxidase RA of several human IgG subfractions after chromatography achieves 20–27% comparing with horseradish peroxidase (HRP, taken for 100%). The oxidoreductase activity of many IgG subfractions is ~ 4–6-fold higher than that for HRP [36].

It was shown, that IgGs of rats and humans effectively oxidize not only DAB but also many other toxic, carcinogenic and mutagenic compounds such as phenol, *o*-phenylenediamine, α-naphthol, p-hydroquinone, etc. [34]. However, overall, the relative peroxidase and oxidoreductase activities of polyclonal rat IgGs in the presence of different metal ions is ~ 10–100-fold higher than those of polyclonal human IgGs. Interestingly, rats are known as the most resistant mammals to all harmful factors of an environment including carcinogens, mutagens and radiation. One cannot exclude that this is due to better protection of rats compared to peoples from harmful factors due to more active metal-dependent Abs with peroxidase and oxidoreductase activities.

6. Dependence of DNA-hydrolyzing abzymes on metal ions

It was shown in many articles that electrophoretically and immunologically homogeneous polyclonal IgGs from sera of healthy volunteers and experimental mice are not active in the hydrolysis of DNA and RNA (for review see [37–46]). The occurrence of auto-Abs with catalytic activities is a distinctive feature of mammalian autoimmune diseases (reviewed in [37–46]). IgGs and/or IgMs abzymes hydrolyzing DNA and RNA were revealed in the sera of patients with several autoimmune and viral pathologies: SLE [57–61], multiple sclerosis [62–64], Hashimoto's thyroiditis and polyarthritis [65, 66], schizophrenia [67] and with three viral diseases viral hepatitis [68], acquired immunodeficiency syndrome [69] and tick-borne encephalitis [70]), as well as human milk [71–73], SLE mice [74, 75] and experimental autoimmune encephalomyelitis(EAE) mice [76, 77]. Antibodies with DNase activity from the blood of patients and mice with various diseases were dependent on different metal ions [57–70, 74–77], while human milk contains metal-dependent and independent DNase sIgAs and IgGs [71–73]. The RAs of IgGs from the sera of patients (and mice) with different AIDs vary significantly from patient to patient [57–70, 74–77]. **Figure 6** shows the cleavage of plasmid supercoiled (sc)DNA by 10 various IgGs bound with internal metal ions from the sera of patients with various autoimmune diseases.

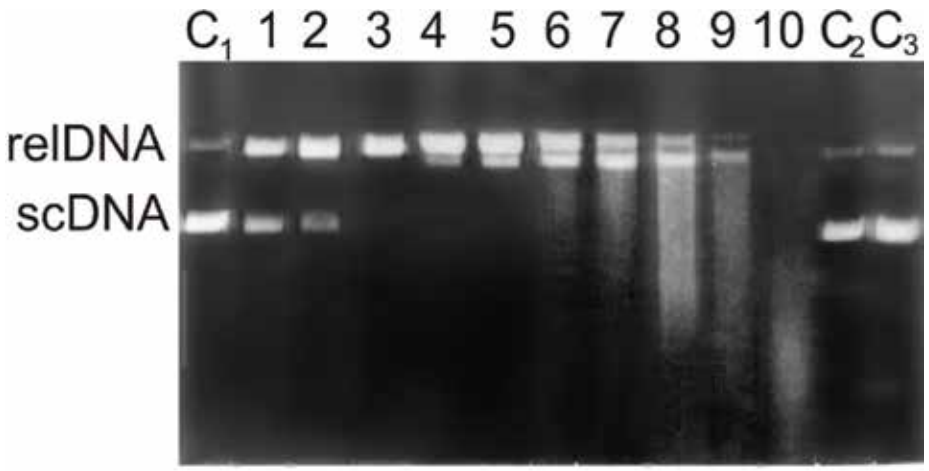

Figure 6. Relative DNase activities of catalytic IgG-abzymes from sera of 10 different patients with various diseases in the hydrolysis of scDNA. Lanes 1–10 correspond to IgGs of 10 different patients; C_1, DNA incubated alone; C_2 and C_3, DNA incubated with Abs of two healthy donors.

During this time, some IgGs cause only single breaks in one strand of scDNA converting it to the relaxed form (lanes 1–3), when others make multiple breaks forming DNA linearization (lanes 4–6). The most active IgGs hydrolyze scDNA into medium- and short-length oligonucleotides (lanes 7–10). Polyclonal DNase IgGs from the sera of autoimmune-prone MRL mice were not after Abs dialysis against EDTA, but were activated by different externally added metal (Me^{2+}) ions: $Mn^{2+} \geq Mg^{2+} > Ca^{2+} \geq Cu^{2+} > Co^{2+} \geq Ni^{2+} \geq Zn^{2+}$ [74, 75]. Fe^{2+} ions could not stimulate the hydrolysis of scDNA by the Abs. The initial rate dependencies on the concentration of different Me^{2+} ions were mostly bell-shaped, having from one to four maxima at different concentrations of Me^{2+} ions. Mn^{2+}, Ni^{2+} and Co^{2+} activated DNA hydrolysis. The Mn^{2+}-dependent scDNA hydrolysis was activated by Ni^{2+}, Ca^{2+}, Co^{2+} and Mg^{2+}, but was inhibited by Zn^{2+} and Cu^{2+}. Only in the case of $Mg^{2+}$and Mg^{2+} or Ca^{2+} as the second metal ions, an accumulation of linear DNA was observed. Affinity chromatography on DNA-cellulose separated DNase mouse IgGs to many subfractions having different affinities for DNA and varying levels of the relative activity (0–100%) in the presence of Mn^{2+}, Ca^{2+} and Mg^{2+} ions. In contrast to all human DNases having 1 pH optimum, mouse IgGs hydrolyzing DNA showed several pronounced pH optima from 4.5 and 9.5; in the presence of Ca^{2+}, Mn^{2+} and Mg^{2+} ions, these dependencies were different. These findings show the extreme diversity of the ability of metal-dependent mouse IgGs functioning at different pHs and to be activated by various optimal metal cofactors. At the same time, a similar situation on an extreme diversity of Me^{2+}-dependent Abs was observed for DNase abzymes from sera of the patient with different autoimmune and viral diseases [70] including monoclonal light chains of human IgGs [78] (e.g., **Figure 7**).

Dependently on patient demonstrated different substrate specificity [63]. All the data obtained showed that polyclonal MS IgGs could contain different combinations of sequence-independent and sequence-dependent endo- and exonuclease activities [63]. The enzymatic properties of the DNA- and RNA-hydrolyzing IgGs of patients with various AIDs [37–46] distinguished them from all known canonical DNases and RNases [79–81].

http://dx.doi.org/10.5772/intechopen.75939

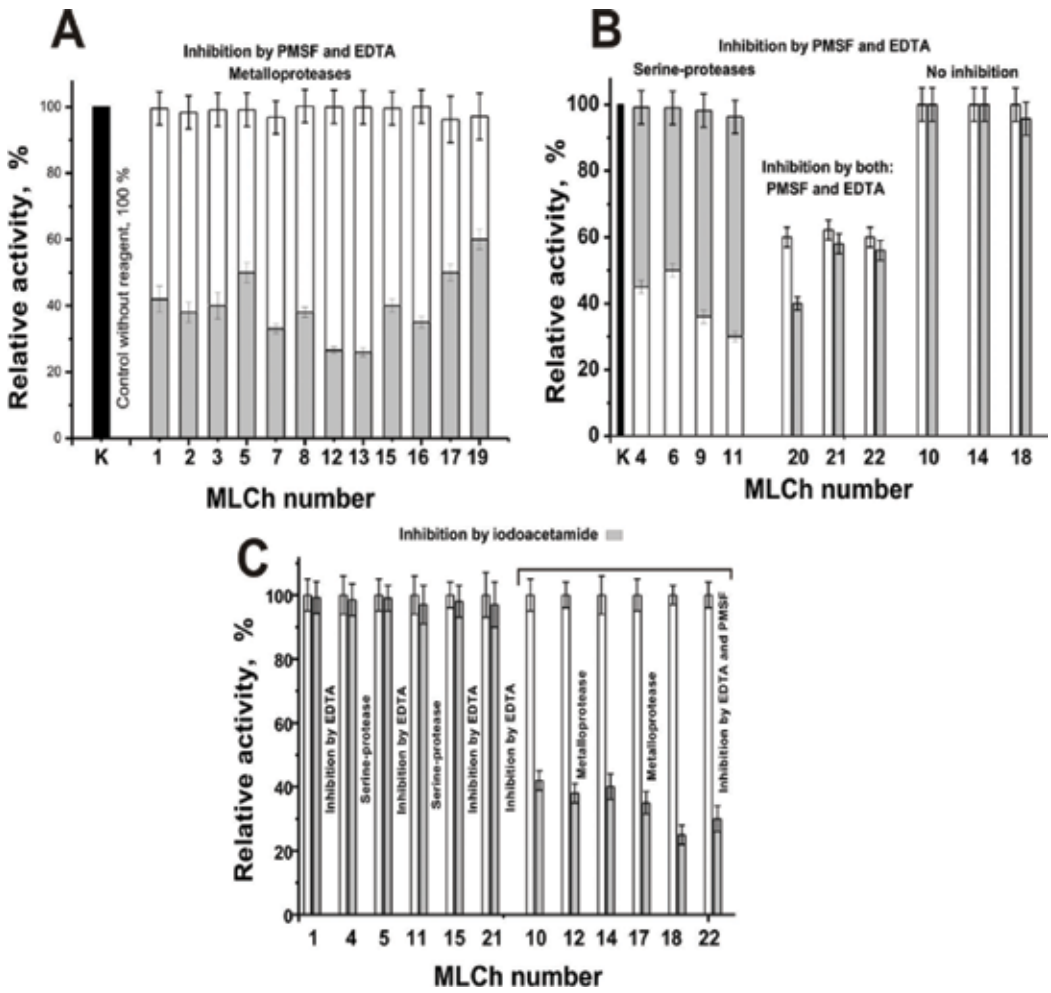

Figure 7. The RAs of MBP-hydrolyzing activity of twenty-two MLChs after their treatment with specific inhibitors of various type proteases. Different MLChs were preincubated in the absence of inhibitors (black bars, control-C), with 50 mM EDTA (gray bars) or 1.0 mM PMSF (white bars) before addition to the standard reaction mixture (A and B). Panel C demonstrates several examples of the RAs of MLChs with metal-dependent (1, 5, 12, 15, and 21) and serine-like activity (4 and 11), which no changing their activity after treatment with iodoacetamide; three MLChs (10, 14, and 18) showing negative response to EDTA and PMSF as well as MLCh-22 having positive answer to PMSF and EDTA after their preincubation with iodoacetamide resulting a significant decrease in the protease activity. Gray and white bars (panel C) correspond respectively to the activity after and before (control) these preparation treatment with iodoacetamide. The Ras of all MLChs before their treatment with different specific inhibitors was taken for 100 %.

Polyclonal DNase IgGs from sera of autoimmune patients, SLE mice, rabbits immunized with DNA and human milk are usually very heterogeneous in their affinity for DNA and can be separated into many subfractions by chromatography on DNA-cellulose [78, 82, 83]. An immunoglobulin light chain phagemid library was prepared using peripheral blood lymphocytes of patients with SLE [78, 82, 83]. Phage particles displaying light chains interacting with DNA were isolated by chromatography on DNA-cellulose; the fraction eluted by 0.5 M NaCl and acidic buffer (pH 2.6) were used for obtaining of individual monoclonal light chains (MLChs, 27–28 kDa) [78, 82, 83].

About 45 of 451 and 33 of 687 individual colonies corresponding to peaks eluted with 0.5 M NaCl and acidic buffer, respectively, were randomly chosen for a study of MLChs with DNase activity. About 15 of 45 (K_m = 260–320 nM) and 19 of 33 (K_m = 3–9 nM) MLChs in the first and second case efficiently hydrolyzed DNA. All 34 MLChs demonstrated different optimal concentrations of KCl or NaCl and pH optima. All MLChs were metal-dependent DNases. The ratio of relative DNA-hydrolyzing activity in the presence of different metal ions was individual for each MLCh. For example, for monoclonal kappa light chain NGK-1 in optimal conditions the RAs decreased in the following order (%): Mn^{2+} (26.3) ≥ Ca^{2+} (23.0) ≥ Mg^{2+} (21.0) > Ni^{2+} (15.0) > Zn^{2+} (11.4) > Cu^{2+} (2.9) > Co^{2+} (0.0) [83]. But in average, the activity in DNA hydrolysis for all MLChs decreased in the following order: $Mn^{2+} > Co^{2+} > Mg^{2+} > Ni^{2+} \approx Ca^{2+} > Cu^{2+} > Zn^{2+}$ [78, 82, 83].

It is known, that Co^{2+}, Mn^{2+}, Ca^{2+} and Ni^{2+} activate mammalian DNase I in much lesser degree than Mg^{2+} ions [80, 81]. Interestingly, human milk polyclonal sIgA DNase abzymes mainly Me^{2+}-independent and they were only slightly activated by Mg^{2+}, Mn^{2+} or Zn^{2+}, and the cleavage of DNA substrates was inhibited by Ca^{2+} and Cu^{2+} [73]. The effect of metal ions on DNase activity of intact Abs from sera of MS patients decreased in the order: $Mn^{2+} > Mg^{2+} > Zn^{2+} > Ca^{2+}$ [84]. The DNA-hydrolyzing activity of tick-borne encephalitis IgGs decreased in the following order: $Mn^{2+} \geq Co^{2+} \geq Mg^{2+} > Ca^{2+}$, while Zn^{2+}, Ni^{2+} and Cu^{2+} did not stimulate DNA hydrolysis [70]. Polyclonal intact IgGs from MRL mice following specific order of DNase activity activation by different metal ions: $Mn^{2+} \geq Mg^{2+} > Ca^{2+} \geq Cu^{2+} > Co^{2+} \geq Ni^{2+} \geq Zn^{2+}$ [74]. Thus, the relative activity of metal-dependent abzymes hydrolyzing DNA depends on the type and timing of the disease as well as can be specific for every individual patient (or animal). On overall, relative metal-dependent DNase activity in blood of patients with different autoimmune and viral diseases increases in the following order: Diabetes < Viral hepatitis ≈ Tick-borne encephalitis < Polyarthritis ≤ Hashimoto's thyroiditis < Schizophrenia < AIDS ≤ Multiple sclerosis < SLE [85].

7. Dependence of RNA-hydrolyzing abzymes on metal ions

First, it was shown that mouse SLE monoclonal IgGs directed against different DNA could effectively hydrolyze both DNA and RNA and cleavage of RNAs is 30–100-fold faster than DNA [86]. Later we have shown that immunization of rabbits with DNA, RNA, RNase A, DNase I or DNase II leads to the formation of abzymes that hydrolyze both DNA and RNA [85]. Interestingly, the substrate specificities of RNase IgGs from patients with autoimmune thyroiditis and polyarthritis [65], SLE [58], MS [62] and hepatitis [68] for different classic homopolynucleotides, cCMP and $tRNA^{Phe}$ with a stable compact structure [39, 59] were different and correlated with the type of disease and were well distinguishable from those of canonical RNases. The activity was strongly dependent on the patient and its disease, but in average increased in the order: hepatitis < polyarthritis < autoimmune thyroiditis < SLE ≤ MS. Abzymes of patients of SLE and MS patients demonstrate new RNase activity stimulated by Mg^{2+} ions [39, 59, 65, 87]. In the presence of Mg^{2+} ions, the abzymes produced products corresponding to new cleavage sites of mutant $tRNA^{Lys}$, indicating its local structural or conformational changes compared to $tRNA^{Lys}$ from mitochondria. Thus, different metal ions play a very important role in the functioning of abzymes with DNase and RNase activities.

http://dx.doi.org/10.5772/intechopen.75939

8. Dependence of protein-hydrolyzing abzymes on metal ions

For the first time, elevated levels of polyclonal antibodies to myelin basic protein (MBP) and abzymes hydrolyzing MBP were detected in the blood of MS [88–91] and then of SLE [92–95] patients. In the blood of healthy donors, no such abzymes have been detected [88–95]. It is believed that the mechanism of the pathogenesis of MS is associated with the destruction of myelin (including MBP), leading to inflammation processes associated with autoimmune reactions [96]. Some immunological and biochemical indicators of patients with MS and SLE are very similar [45]. First, we have shown that polyclonal IgG_{mix} (a mixture of equimolar IgGs from 10 MS patients) can hydrolyze MBP in the presence better, than in the absence of different metal ions [88–91]. According to TJP-AES data, homogeneous IgG preparations of MS patients contained several intrinsic metal ions; Fe ≥ Ca > C u ≥ Zn ≥ Mg ≥ Mn ≥ Pb ≥ Co ≥ Ni [90]. Then, a minor Me^{2+}-dependent fraction was obtained by chromatography of one IgG preparation on Chelex-100. This IgG fraction could not hydrolyze MBP in the absence of metal ions but was activated after addition of external $Mg^{2+} > Mn^{2+} > Cu^{2+} > Ca^{2+}$ [90]. Proteolytic activities of individual IgGs from other MS patients were also activated by Fe^{2+}, Ni^{2+}, Zn^{2+}, Co^{2+} and Pb^{2+}, and especially Ni^{2+}. Interestingly, specific proteolytic metal-dependent and independent activities of IgMs and IgAs from sera of MS patient were usually higher than those of IgGs [89]. A significant diversity of different fractions of polyclonal MS IgGs in their affinity for MBP and the hydrolysis of MBP at different optimal pHs (3–10.5) was demonstrating [91]. IgGs containing kappa- and lambda-light chains showed comparable RAs in the hydrolysis of MBP. IgGs of all four sub-classes were active, with their different average contribution to the total activity of abzymes in the hydrolysis of MBP: IgG1 (1.5–2.1%) < IgG2 (4.9–12.8%) < IgG3 (14.7–25.0%) < IgG4 (71–78%) [91]. The properties of MS abzymes demonstrating their significant catalytic diversity distinguish them from all known mammalian proteases including metal-dependent ones. These abzymes can attack MBP of the myelin-proteolipid shell of axons and play an important role in MS pathogenesis [88–91].

At the initial stage of SLE development antibodies against DNA, as well as DNA- and RNA-hydrolyzing antibodies are mostly developed [37–46]. A little later, however, similar to MS pathology in the case of SLE patients the production of Abs against MBP and abzymes hydrolyzing this protein is happening [92–95]. The relative content of different metal ions in the preparations of lyophilized sle-IgG_{mix} and ms-IgG_{mix} from sera of patients with MS and SLE estimated by TJP-AES method to some extent comparable (**Table 8**). Ca^{2+} was the best activator of SLE-IgG_{mix} and its activity increased in the order: $Ca^{2+} > Mg^{2+} \geq Co^{2+} \geq Fe^{2+} \geq Ni^{2+} \geq Cu^{2+} \geq Mn^{2+}$. Zn^{2+} inhibits the activity, while Fe^{2+} cannot activate sle-IgG_{mix}. Ms-IgG_{mix} before dialysis against EDTA showed another order of the activity: $Mg^{2+} > Mn^{2+} \geq Cu^{2+} \geq Ni^{2+} \geq Co^{2+} \geq Ca^{2+}$, while Fe^{2+} and Zn^{2+} slightly inhibit its activity. Thus, on average, patients with MS and SLE develop abzymes hydrolyzing MBP with different dependence on various metal ions. Combinations of Ca^{2+} + Co^{2} and Ca^{2+} + Mg^{2+} results in a significant increase in the MBP-hydrolyzing activity comparing to Ca^{2+}, Mg^{2+} and Co^{2+} or ions taken separately [92]. Lambda-IgGs demonstrated higher RAs in the hydrolysis of MBP than kappa-IgGs [93]. The pH profiles of IgG4, IgG3, IgG2, IgG1 of SLE patients were unique; their RAs increased in the order: IgG4 < IgG2 < IgG3 < IgG1. Thus, the immune systems of SLE similarly to MS patients produce a variety of metal-dependent anti-MBP abzymes, which can hydrolyze MBP of the myelin-proteolipid shell of axons and can play important role in the pathogenesis of MS and SLE patients [45, 46].

Phagemid library derived from lymphocytes of peripheral blood of patients with SLE was used for obtaining of MLChs hydrolyzing MBP [97–100]. About 22 of 72 MLChs hydrolyzing only MBP (not other control proteins) having various pH optima in a 5.7–9.0 range and different specificity in the hydrolysis of four various MBP oligopeptides [97]. Eleven MLChs were metalloproteases, while four and three MLChs showed serine-like and thiol-like proteolytic activities, respectively. The activity of three MLChs was suppressed by both PMSF and EDTA, while the other two by EDTA and iodoacetamide and one by EDTA, PMSF and iodoacetamide. The ratio of RAs in the presence of Mg^{2+}, Ca^{2+}, Mn^{2+}, Zn^{2+}, Cu^{2+}, Ni^{2+} and Co^{2+} was very specific for all metal-dependent MLChs. For the total preparation of MLChs, the activity decreased in the order: $Ca^{2+} \geq Co^{2+} \approx Mg^{2++} \geq Mn^{2+} \geq Ni^{2} \approx Cu^{2+} \approx Zn^{2+}$ [97].

In addition to these 22, were isolated other 3 MLChs, which were analyzed in more detailed. NGTA1-Me-pro (MLCh-23) was a typical metalloprotease inhibited only by EDTA [98]. The activity of MLCh-23 in the hydrolysis of MBP was reduced in the presence of ions of seven different metals in the following order: $Ca^{2+} > Mg^{2+} > Ni^{2+} \geq Zn^{2+} \geq Co^{2+} \geq Mn^{2+} > Cu^{2+}$. MLCh-23 has two active sites into the light chain with very distinct pH optima: pH 6.0 and 8.5 and different affinity for MBP [98]. Specific inhibitors of NGTA2-Me-pro-Tr (MLCh-24) were PMSF (42%) and EDTA (58%): it exhibits properties of a chimeric protease with serine and metal-dependent activities [99]. The addition of ions of different metals led to a decrease in the activity of MLCh-24 in the following order: $Ca^{2+} \geq Mn^{2+} \geq Mg^{2+} \approx Co^{2+} \approx Ni^{2+} \geq Cu^{2+} \geq Zn^{2}$. NGTA2-Me-pro-Tr is the first example of an MLCh-23 having two combined centers with serine and metalloprotease activities.

It should be noted that all recombinant MLChs were obtained by affinity chromatography of phage particles on MBP-Sepharose. Taking this into account, a very unexpected result was obtained from analysis of NGTA3-pro-DNase (MLCh-25) [100]. Only 1 MLCh-25 of 25 recombinant MLChs effectively hydrolyzed not only MBP but also DNA. Preincubation of MLCh-25 with both PMSF (67%) and EDTA (36%) resulted in suppression of its protease activity. Ions of different metals activated MLCh-25 in the following order: $Ca^{2+} \geq Ni^{2+} > Co^{2+} \approx Mn^{2+} \geq Cu^{2+} \approx Zn^{2+} \geq Mg^{2+}$ [100]. The affinity of MLCh-25 metal-dependent and serine-like active centers for BMP was different. The DNase activity of MLCh-25 decreases in the following order: $Mn^{2+} \approx Co^{2+} \geq Mn^{2+} > Cu^{2+} \approx Ni^{2+} \geq Ca^{2+} > Zn^{2+}$, which completely distinguishes MLCh-25 from canonical DNases [72]. Metal-dependent casein hydrolyzing sIgA antibodies from human milk were described [101]. The RA of sIgAs after removal of intrinsic metal ions increase their activity in the presence of external $Fe^{2+} > Ca^{2+} > Co^{2+} \geq Ni^{2+}$ and especially combinations of metals: $Co^{2+}+Ca^{2+} < Mg^{2+} + Ca^{2+} < Ca^{2+} + Zn^{2+} < Fe^{2+} + Zn^{2+} < Fe^{2+} + Co^{2+} < Fe^{2+} + Ca^{2+}$ [101].

9. Catalytic activities of antibodies of HIV-infected patients

Metal-dependent IgGs and/or IgMs from the blood of HIV-infected patients hydrolyzing DNA [69], viral reverse transcriptase [102] and integrase [103–105], and all histones [106] were described. Average activities of anti-IN IgGs in the hydrolysis of IN decreased in the order $Mn^{2+} > Mg^{2+} \approx Cu^{2+} > Co^{2+}$ while for IgMs in another order $Cu^{2+} > Mn^{2+} > Co^{2+} \gg Mg^{2+}$. Our findings show that active centers of anti-IN polyclonal abzymes of AIDS patients can contain

amino acid residues providing thiol, serine, acidic and metal-dependent proteases. But the ratio of these abzymes activities may be individual for every HIV-infected patient.

In addition, IgGs from sera of HIV-infected patients hydrolyze all human histones [106]. The RAs of IgGs in the hydrolysis of histones (H4, H3, H2a, H2b and H1) varied significantly for Abs of different patients. The effects of different external metal ions on the dialyzed polyclonal IgGs in the hydrolysis of five individual histones were very different. For example, maximal activation of one IgG preparation was observed in the hydrolysis of H4 by Zn^{2+} and Ni^{2+}, H3 by Cu^{2+} and Ni^{2+}, H2a by Cu^{2+}, H2b by Co^{2+} and Ni^{2+}, H1 by Cu^{2+} and Mn^{2+}. Such an exceptional diversity in activation by different metals ions was observed for all 32 IgGs [106]. Importantly, mammalian immune system theoretically can produce up to 10^6 variants of Abs against one antigenic determinant and all of these Abs may be different.

10. Conclusion

Using the TJP-AES method, we have estimated the relative contents of various trace elements, including metals in various organs, tissues and biological fluids of humans and animals, as well as in immunoglobulins from these sources., the maximal RAs of abzymes with different catalytic activities are most often achieved not in the presence of metal ions, which are contained in biological sources and antibodies in maximum quantities. Some specific abzymes show maximum activity in the presence of metal ions, which are minor elements of different organs and biological fluids. The question is why there are so many abzymes with very different properties including metal-dependent ones against the same protein. First, mammalian immune system theoretically can produce up to 10^6 variants of Abs against one antigenic determinant and all of these Abs may be different. In addition, proteins and nucleic acids can adsorb ions of various metals including traces elements on their surfaces. Therefore, some specific antibodies (and abzymes) can be against fragments (antigenic determinants) of DNA and proteins containing no metal ions. Some other specific metal-dependent abzymes with nuclease and protease activities can be antibodies against sequences associated with one or more metal ions. In addition, not only antibodies against substrates imitating transition states of chemical reactions can possess catalytic activities, but also anti-idiotypic Abs against active centers of various enzymes. The activity of many various enzymes depends on the ions of different metals. Since secondary—anti-idiotypic antibodies against such active sites should contain all the structural components of an enzyme active center including amino acid residues for binding metal ions, they can be metal-dependent abzymes. In this chapter, we have analyzed not only the relative content of different metal ions in various biological substances but also analyzed a possible function of metal ions in the catalysis by autoantibodies of different chemical reactions.

Acknowledgements

This research was possible due to grant from the Russian Science Foundation (No. 16-15-10,103) to G.A. Nevinsky).

Author details

Natalia P. Zaksas[1] and Georgy A. Nevinsky[2]*

*Address all correspondence to: nevinky@niboch.nsc.ru

1 Nikolaev Institute of Inorganic Chemistry, Siberian Division, Russian Academy of Sciences, Novosibirsk, Russia

2 Institute of Chemical Biology and Fundamental Medicine, Siberian Division, Russian Academy of Sciences, Novosibirsk, Russia

References

[1] Taylor A, Day MP, Hill S, Marshall J, Patriarca M, White M. Atomic spectrometry update: Review of advances in the analysis of clinical and biological materials, foods and beverages. Journal of Analytical Atomic Spectrometry. 2015;**30**:542-579. DOI: 10.1039/c5ja90001h

[2] Taylor A, Barlow N, Day MP, Hill S, Patriarca M, White M. Atomic spectrometry update: Review of advances in the analysis of clinical and biological materials, foods and beverages. Journal of Analytical Atomic Spectrometry. 2017;**32**:432-476. DOI: 10.1039/c7ja90005h

[3] Barany E, Bergdahl IA, Schьtz A, Skerfving S, Oskarsson A. Inductively coupled mass spectrometry for direct multi-element analysis of diluted whole blood and serum. Journal of Analytical Atomic Spectrometry. 1997;**12**:1005-1009. DOI: 10.1039/A700904F

[4] Krachler M, Heisel C, Kretzer JP. Validation of ultratrace analysis of Co, Cr, Mo and Ni in whole blood, serum and urine using ICP-SMS. Journal of Analytical Atomic Spectrometry. 2009;**24**:605-610. DOI: 10.1039/b821913c

[5] Kerger BD, Gerads R, Gurleyuk H, Urban A, Paustenbach DJ. Total cobalt determination in human blood and synovial fluid using inductively coupled plasma-mass spectrometry: Method validation and evaluation of performance variables affecting metal hip implant patient samples. Toxicological and Environmental Chemistry. 2015;**97**:1145-1163. DOI: 10.1080/02772248.2015.1092735

[6] Barbosa VMP, Barbosa AF, Bettini J, Luccas PO, Figueiredo EC. Direct extraction of lead (II) from untreated human blood serum using restricted access carbon nanotubes and its determination by atomic absorption spectrometry. Talanta. 2016;**147**:478-484. DOI: 10.1016/j.talanta.2015.10.023

[7] Mortada WI, Kenawy IMM, Abdelghany AM, Ismal AM, Donia AF, Nabieh KA. Determination of Cu^{2+}, Zn^{2+} and Pb^{2+} in biological and food samples by FAAS after preconcentration with hydroxyapatite nanorods originated from eggshell. Materials Science and Engineering: C. 2015;**52**:288-296. DOI: 10.1016/j.msec.2015.03.061

[8] Pozebon D, Scheffler GL, Dressler VL, Nunes MAG. Review of the applications of laser ablation inductively coupled plasma mass spectrometry. Journal of Analytical Atomic Spectrometry. 2014;**29**:2204-2228. DOI: 10.1039/c4ja00250d

[9] Becker JS, Matusch A, Wu B. Bioimaging mass spectrometry of trace elements – Recent advance and applications of LA-ICP-MS. Analytica Chimica Acta. 2014;**835**:1-18. DOI: 10.1016/j.aca.2014.04.048

[10] Becker JS, Salber D. New mass spectrometric tools in brain research. Trends in Analytical Chemistry. 2010;**29**:966-979. DOI: 10.1016/j.trac.2010.06.009

[11] Grolmusová Z, Horňáčková M, Plavčan J, Kopáni M, Babál P, Veis P. Laser induced breakdown spectroscopy of human liver samples with Wilson's disease. European Physical Journal Applied Physics. 2013;**63**:208-301. DOI: 10.1051/epjap/2013130030

[12] Motto-Ros V, Sancey L, Wang XC, Ma QL, Lux F, Bai XS, Panczer G, Tillement O, Yu J. Mapping nanoparticles injected into a biological tissue using laser-induced breakdown spectroscopy. Spectrochim Acta Part B. 2013;**87**:168-174. DOI: 10.1016/j.sab.2013.05.020

[13] Zheenbaev ZZ, Engelsht VS. Dvukhstruinyi Plazmatron (Two-Jet Plasmatron). Frunze: Ilim (Russian); 1983. 200 p

[14] Schramel P. ICP and DCP emission spectrometry for trace element analysis in biomedical and environmental samples. Spectrochim Acta Part B. 1988;**43**:881-896. DOI: 10.1016/0584-8547(88)80194-0

[15] Meyer GA. Conical three-electrode d.c. plasma for spectrochemical analysis. Spectrochimica Acta, Part B: Atomic Spectroscopy. 1987;**42**:333-339. DOI: 10.1016/0584-8547(87)80074-5

[16] Zaksas NP. Comparison of excitation mechanisms in the analytical regions of a high-power two-jet plasma. Spectrochimica Acta, Part B: Atomic Spectroscopy. 2015;**109**:39-43. DOI: 10.1016/j.sab.2015.04.012

[17] Cherevko AS. Mechanism of the evaporation of particles of powder test materials in the discharge of a two-jet argon arc plasmatron. Journal of Analytical Chemistry. 2011;**66**:610-619. DOI: 10.1134/S1061934811050042

[18] Zaksas NP, Gerasimov VA. Consideration on excitation mechanisms in a high-power two-jet plasma. Spectrochimica Acta, Part B: Atomic Spectroscopy. 2013;**88**:174-179. DOI: 10.1016/j.sab.2013.06.013

[19] Yudelevich IG, Cherevko AS, Engelsht VS, Pikalov VV, Tagiltsev AP, Zheenbaev ZZ. A two-jet plasmatron for the spectrochemical analysis of geological samples. Spectrochim Acta, Part B. 1984;**39**:777-785. DOI: 1016/0584-8547(84)80086-5

[20] Shelpakova IR, Zaksas NP, Komissarova LN, Kovalevskij SV. Spectral methods for analysis of high-purity gallium with excitation of spectra in the two-jet arc plasmatron. Journal of Analytical Atomic Spectrometry. 2002;**17**:270-273. DOI: 10.1039/B109229B

[21] Zaksas NP, Komissarova LN, Shelpakova IR. Analysis of indium and indium oxide using a two-jet arc plasmatron. Industrial Laboratory. Diagnostics of Materials (Russian). 2007:**73**:89-92. ISSN: 1028-6861

[22] Zaksas NP, Komissarova LN, Shelpakova IR. Atomic-emission spectral analysis of high purity tellurium dioxide with spectral excitation in a two jet arc plasmatron. Analytics and Control. (Russian) 2005;**9**:240-244. ISSN: 2073-1442 (Print). ISSN: 2073-1450 (Online)

[23] Zaksas NP, Shelpakova IR, Gerasimov VA. Determination of trace elements in different powdered samples by atomic emission spectrometrywith spectral excitation in a two-jet arc plasmatron. Journal of Analytical Chemistry. 2004;**59**:222-228. DOI: 10.1023/B:JANC.0000018963.03529.e0

[24] Zaksas NP, Veryaskin AF. Solid sampling in analysis of by soils two-jet plasma atomic emission spectrometry. Analytical Sciences. 2017;**33**:605-609. DOI: 10.2116/analsci.33.605

[25] Zaksas NP, Sultangazieva TT, Korda TM. Using a two-jet arc plasmatron for determining the trace element composition of powdered biological samples. Journal of Analytical Chemistry. 2006;**61**:632-637. DOI: 10.1134/S1061934806060128

[26] Zaksas NP, Nevinsky GA. Solid sampling in analysis of animal organs by two-jet plasma atomic emission spectrometry. Spectrochimica Acta, Part B: Atomic Spectroscopy. 2011;**66**: 861-865. DOI: 10.1016/j.sab.2011.11.001

[27] Zaksas NP, Gerasimov VA, Nevinsky GA. Simultaneous determination of Fe, P, Ca, Mg, Zn and Cu in whole blood by two-jet plasma atomic emission spectrometry. Talanta. 2010;**80**:2187-2190. DOI: 10.1016/j.talanta.2009.10.046

[28] Zaksas NP, Sultangazieva TT, Gerasimov VA. Determination of trace elements in bone by two-jet plasma atomic emission spectrometry. Analytical and Bioanalytical Chemistry. 2008;**391**:687-693. DOI: 10.1007/s00216-008-2050-8

[29] Zaksas N, Gluhcheva Y, Sedykh S, Madzharova M, Atanassova N, Nevinsky G. Effect of $CoCl_2$ treatment on major and trace elements metabolism and protein concentration in mice. Journal of Trace Elements in Medicine and Biology. 2013;**27**:27-30. DOI: 10.1016/j.jtemb.2012.07.005

[30] Legostaeva GA, Zaksas NP, Gluhcheva YG, Sedykh SE, Madzharova ME, Atanassova NN, Buneva VN, Nevinsky GA. Effect of $CoCl_2$ on the content of different metals and a relative activity of DNA-hydrolyzing abzymes in the blood plasma of mice. Journal of Molecular Recognition 2013;**26**:10-22. DOI: 10.1002/jmr.2217. PMID: 23280613

[31] Tolmacheva AS, Zaksas NP, Buneva VN, Vasilenko NL, Nevinsky GA. Oxidoreductase activities of polyclonal IgGs from the sera of Wistar rats are better activated by combinations of different metal ions. Journal of Molecular Recognition. 2009;**22**:26-37. DOI: 10.1002/jmr.923

[32] Ikhmyangan EN, Vasilenko NL, Buneva VN, Nevinsky GA. IgG antibodies with peroxidase-like activity from the sera of healthy Wistar rats. FEBS Letters. 2005;**579**:3960-3964. PMID: 15993881

[33] Ikhmyangan EN, Vasilenko NL, Buneva VN, Nevinsky GA. Metal ions-dependent peroxidase and oxidoreductase activities of polyclonal IgGs from the sera of Wistar rats. Journal of Molecular Recognition. 2006;**19**:91-105. PMID: 16416456

[34] Ikhmyangan EN, Vasilenko NL, Sinitsina OI, Buneva VN, Nevinsky GA. Substrate specificity of rat sera IgG antibodies with peroxidase and oxidoreductase activities. Journal of Molecular Recognition. 2006;**19**:432-440. PMID: 16835846

[35] Ikhmyangan EN, Vasilenko NL, Sinitsyna OI, Buneva VN, Nevinsky GA. The catalytic heterogeneity of G immunoglobulins with peroxidase activity from the blood of healthy Wistar rats. Immunopathology. Allergology and Infectology (Russian). 2006;**2**:32-48

[36] Tolmacheva AS, Blinova EA, Ermakov EA, Buneva VN, Vasilenko NL, Nevinsky GA. IgG abzymes with peroxidase and oxidoreductase activities from the sera of healthy humans. Journal of Molecular Recognition. 2015;**28**:565-580. DOI: 10.1002/jmr.2474

[37] Keinan E, editor. Catalytic Antibodies. Weinheim, Germany: Wiley-VCH Verlag GmbH and Co; 2005. 586 p

[38] Nevinsky GA, Kanyshkova TG, Buneva VN. Natural catalytic antibodies (abzymes) in normalcy and pathology. Biochemistry (Moscow). 2000;**65**:1245-1255

[39] Nevinsky GA, Buneva VN. Human catalytic RNA- and DNA-hydrolyzing antibodies. Journal of Immunology. 2002;**269**:235-249

[40] Nevinsky GA, Favorova OO, Buneva VN. Natural catalytic antibodies – New characters in the protein repertoire. In: Golemis E, editor. Protein-Protein Interactions; A Molecular Cloning Manual. New York, Cold Spring Harbor: Spring Harbor Lab. Press; 2002. pp. 532-534

[41] Nevinsky GA, Buneva VN. Catalytic antibodies in healthy humans and patients with autoimmune and viral diseases. Journal of Cellular and Molecular Medicine. 2003;**7**:265-276. DOI: 10.1111/j.1582-4934.2003.tb00227.x

[42] Nevinsky GA, Buneva VN. Natural catalytic antibodies-abzymes. In: Keinan E, editor. Catalytic Antibodies. Weinheim, Germany: Wiley-VCH Verlag GmbH and Co; 2005. pp. 505-569. DOI: 10.1002/3527603662.ch19

[43] Nevinsky GA. Natural catalytic antibodies in norm and in autoimmune diseases. In: Brenner KJ, editor. Autoimmune Diseases: Symptoms, Diagnosis and Treatment. New York, USA: Nova Science Publishers; 2010. pp. 1-107

[44] Nevinsky GA. Natural catalytic antibodies in norm and in HIV-infected patients. In: Kasenga FH, editor. Understanding HIV/AIDS Management and Care—Pandemic Approaches the 21st Century. Rijeka, Croatia: InTech; 2011. pp. 151-192

[45] Nevinsky GA. Autoimmune processes in multiple sclerosis: Production of harmful catalytic antibodies associated with significant changes in the hematopoietic stem cell differentiation and proliferation. In: Conzalez-Quevedo A, editor. Multiple Sclerosis. Rijeka, Croatia: InTech; 2016. pp. 100-147

[46] Nevinsky GA. Catalytic antibodies in norm and systemic lupus erythematosus. In: Khan WA, editor. Lupus. Rijeka, Croatia: InTech; 2017. pp. 41-101. DOI: 10.5772/67790

[47] Ames BN. Dietary carcinogens and anticarcinogens. Oxygen radicals and degenerative diseases. Science. 1983;**221**:1256-1264. PMID: 6351251

[48] Cutler RG. Antioxidants and aging. The American Journal of Clinical Nutrition. 1991;**53**:373S-3379. PMID: 1985414

[49] Beckman KB, Ames BN. The free radical theory of aging matures. Physiological Reviews. 1998;**78**:547-581. PMID: 9562038

[50] Feuers RJ, Weindruch R, Hart RW. Caloric restriction, aging, and antioxidant enzymes. Mutation Research. 1993;**295**:191-200. PMID: 7507557

[51] Allen RG. Free Radicals in Aging. Boca Raton, FL: CPC Press; 1993. pp. 12-23

[52] Mates JM, Perez-Gomez C, Nunez de Castro I. Antioxidant enzymes and human diseases. Clinical Biochemistry. 1999;**32**:595-603. PMID: 10638941

[53] Mates JM, Sanchez-Jimenez F. Antioxidant enzymes and their implications in pathophysiologic processes. Frontiers in Bioscience. 1999;**4**:D339-D345. PMID: 10077544

[54] Zenkov NK, Lankin VZ, Men'shikova EB. Oxidative Stress. Biochemical and Pathophysiological Aspects. Moscow: MAIK, Nauka/Interperiodica; 2001. pp. 3-343

[55] Dhaunsi GS, Gulati S, Singh AK, Orak JK, Asayama K, Singh I. Demonstration of Cu-Zn superoxide dismutase in rat liver peroxisomes. Biochemical and immunochemical evidence. The Journal of Biological Chemistry. 1992;**267**:6870-6873. PMID: 1551895

[56] Kirkman HN, Gaetani GF. Catalase: A tetrameric enzyme with four tightly bound molecules of NADPH. In: Proceedings of the National Academy of Sciences of the United States of America. 1984;**81**:4343-4347. PMID: 6589599

[57] Shuster AM, Gololobov GV, Kvashuk OA, Bogomolova AE, Smirnov IV, Gabibov AG. DNA hydrolyzing autoantibodies. Science. 1992;**256**:665-667. PMID: 1585181

[58] Buneva VN, Andrievskaia OA, Romannikova IV, Gololobov GV, Iadav RP, Iamkovoĭ VI, Nevinskii GA. Interaction of catalytically active antibodies with oligoribonucleotides. Molecular Biology (Moscow). 1994;**28**:738-743. PMID: 7990801

[59] Vlassov A, Florentz C, Helm M, Naumov V, Buneva V, Nevinsky G, Giegé R. Characterization and selectivity of catalytic antibodies from human serum with RNase activity. Nucleic Acids Research. 1998;**26**:5243-5250. PMID: 9826744

[60] Andrievskaya OA, Buneva VN, Naumov VA, Nevinsky GA. Catalytic heterogeneity of polyclonal RNA-hydrolyzing IgM from sera of patients with lupus erythematosus. Medical Science Monitor. 2000;**6**:460-470. PMID: 11208354

[61] Andrievskaya OA, Buneva VN, Baranovskii AG, Gal'vita AV, Benzo ES, Naumov VA, Nevinsky GA. Catalytic diversity of polyclonal RNA-hydrolyzing IgG antibodies from the sera of patients with lupus erythematosus. Immunology Letters. 2002;**81**:191-198. PMID: 11947924

[62] Baranovskii AG, Kanyshkova TG, Mogelnitskii AS, Naumov VA, Buneva VN, Gusev EI, Boiko AN, Zargarova TA, Favorova OO, Nevinsky GA. Polyclonal antibodies from

blood and cerebrospinal fluid of patients with multiple sclerosis effectively hydrolyze DNA and RNA. Biochemistry (Moscow). 1998;**63**:1239-1248. PMID: 9864461/

[63] Baranovskii AG, Ershova NA, Buneva VN, Kanyshkova TG, Mogelnitskii AS, Doronin BM, Boiko AN, Gusev EI, Favorova OO, Nevinsky GA. Catalytic heterogeneity of polyclonal DNA-hydrolyzing antibodies from the sera of patients with multiple sclerosis. Immunology Letters. 2001;**76**:163-167. PMID: 11306143

[64] Parkhomenko TA, Doronin VB, Castellazzi M, Padroni M, Pastore M, Buneva VN, Granieri E, Nevinsky GA. Comparison of DNA-hydrolyzing antibodies from the cerebrospinal fluid and serum of patients with multiple sclerosis. PLoS One. 2014;**9**:e93001. DOI: 10.1371/journal.pone.0093001

[65] Vlasov AV, Baranovskiĭ AG, Kanyshkova TG, Prints AV, Zabara VG, Naumov VA, Breusov AA, Giege R, Buneva VN, Nevinskiĭ GA. Substrate specificity of DNA- and RNA-hydrolyzing antibodies from blood of patients with polyarthritis and Hashimoto's thyroiditis. Molekulyarnaya Biologiya (Moscow). 1998;**32**:559-569. PMID: 9720080

[66] Nevinsky GA, Breusov AA, Baranovskii AG, Prints AV, Kanyshkova TG, Galvita AV, Naumov VA, Buneva VN. Effect of different drugs on the level of DNA-hydrolyzing polyclonal IgG antibodies in sera of patients with Hashimoto's thyroiditis and nontoxic nodal goiter. Medical Science Monitor. 2001;**7**:201-211. PMID: 11257722

[67] Ermakov EA, Smirnova LP, Parkhomenko TA, Dmitrenok PS, Krotenko NM, Fattakhov NS, Bokhan NA, Semke AV, Ivanova SA, Buneva VN, Nevinsky GA. DNA-hydrolysing activity of IgG antibodies from the sera of patients with schizophrenia. Open Biology. 2015;**5**:150064. DOI: 10.1098/rsob.150064

[68] Baranovsky AG, Matushin VG, Vlassov AV, Zabara VG, Naumov VA, Giege R, Buneva VN, Nevinsky GA. DNA- and RNA-hydrolyzing antibodies from the blood of patients with various forms of viral hepatitis. Biochemistry (Moscow). 1997;**62**:1358-1366. PMID: 9369225

[69] Odintsova ES, Kharitonova MA, Baranovskiĭ AG, Siziakina LP, Buneva VN, Nevinskiĭ GA. DNA-hydrolyzing IgG antibodies from the blood of patients with acquired immunodeficiency syndrome. Molecular Biology (Moscow). 2006;**40**:857-864. PMID: 17086987

[70] Parkhomenko TA, Buneva VN, Tyshkevich OB, Generalov II, Doronin BM, Nevinsky GA. DNA-hydrolyzing activity of IgG antibodies from the sera of patients with tick-borne encephalitis. Biochimie. 2010;**92**:545-554. DOI: 10.1016/j.biochi.2010.01.022

[71] Kanyshkova TG, Semenov DV, Khlimankov DY, Buneva VN, Nevinsky GA. DNA-hydrolyzing activity of the light chain of IgG antibodies from milk of healthy human mothers. FEBS Letters. 1997;**416**:23-26. PMID: 9369225

[72] Buneva VN, Kanyshkova TG, Vlassov AV, Semenov DV, Khlimankov DYu, Breusova LR, Nevinsky GA. Catalytic DNA- and RNA-hydrolyzing antibodies from milk of healthy human mothers. Applied Biochemistry and Biotechnology. 1998;**75**:63-76. PMID: 10214697

[73] Nevinsky GA, Kanyshkova TG, Semenov DV, Vlassov AV, Gal'vita AV, Buneva VN. Secretory immunoglobulin a from healthy human mothers' milk catalyzes nucleic

acid hydrolysis. Applied Biochemistry and Biotechnology. 2000;**83**:115-129. PMID: 10826954

[74] Kuznetsova IA, Orlovskaya IA, Buneva VN, Nevinsky GA. Activation of DNA-hydrolyzing antibodies from the sera of autoimmune-prone MRL-lpr/lpr mice by different metal ions. Biochimica et Biophysica Acta 2007;**1774**:884-896. PMID: 17561457

[75] Kostrikina IA, Kolesova ME, Orlovskaya IA, Buneva VN, Nevinsky GA. Diversity of DNA-hydrolyzing antibodies from the sera of autoimmune-prone MRL/MpJ-lpr mice. Journal of Molecular Recognition. 2011;**24**:557-569. DOI: 10.1002/jmr.1067

[76] Doronin VB, Parkhomenko TA, Korablev A, Toporkova LB, Lopatnikova JA, Alshevskaja AA, Sennikov SV, Buneva VN, Budde T, Meuth SG, Orlovskaya IA, Popova NA, Nevinsky GA. Changes in different parameters, lymphocyte proliferation and hematopoietic progenitor colony formation in EAE mice treated with myelin oligodendrocyte glycoprotein. Journal of Cellular and Molecular Medicine. 2016;**20**:81-94. DOI: 10.1111/jcmm.12704

[77] Aulova KS, Toporkova LB, Lopatnikova JA, Alshevskaya AA, Sennikov SV, Buneva VN, Budde T, Meuth SG, Popova NA, Orlovskaya IA, Nevinsky GA. Changes in haematopoietic progenitor colony differentiation and proliferation and the production of different abzymes in EAE mice treated with DNA. Journal of Cellular and Molecular Medicine. 2017;**21**:3795-3809. DOI: 10.1111/jcmm.13289

[78] Kostrikina IA, Buneva VN, Nevinsky GA. Systemic lupus erythematosus: Molecular cloning of fourteen recombinant DNase monoclonal kappa light chains with different catalytic properties. Biochimica et Biophysica Acta. 2014;**1840**:1725-1737. DOI: 10.1016/j.bbagen.2014.01.027

[79] Shapot VS. Nucleases. Moscow: Medicine Press; 1968. pp. 1-162

[80] Suck D. DNA recognition by DNase I. Journal of Molecular Recognition. 1994;**7**:65-70. PMID: 7826675

[81] Bernardi G. Spleen aciddeoxyribonuclease. In: Boyer PD, editor. The enzymes, 3rd ed., New York: Academic Press; 1971;**4**:271-287

[82] Botvinovskaya AV, Kostrikina IA, Buneva VN, Nevinsky GA. Systemic lupus erythematosus: Molecular cloning of several recombinant DNase monoclonal kappa light chains with different catalytic properties. Journal of Molecular Recognition. 2013;**26**:450-460. DOI: 10.1002/jmr.2286

[83] Kostrikina IA, Odintsova ES, Buneva VN, Nevinsky GA. Systemic lupus erythematosus: Molecular cloning and analysis of recombinant DNase monoclonal κ light chain NGK-1. International Immunology. 2014;**26**:439-450. DOI: 10.1093/intimm/dxu047

[84] Baranovskii AG, Buneva VN, Doronin BM, Nevinsky GA. Immuniglobulins from blood of patients with multiple sclerosis like catalytic heterogeneous nucleases. Russian Journal of Immunology. 2008;**2**:405-419

[85] Buneva VN, Nevinsky GA. Exceptional diversity of catalytic antibodies with varying activity in the blood of autoimmune and viral disease patients. Molekuliarnaia Biologiia (Moscow). 2017;**51**:969-984. DOI: 10.7868/S002689841706009X

[86] Andrievskaia OA, Kanyshkova TG, Iamkovoi VI, Buneva VN, Nevinskii GA. Monoclonal antibodies to DNA hydrolyze RNA better than DNA. Doklady Akademii Nauk (Moscow). 1997;**355**:401-403. PMID: 9376783

[87] Vlassov AV, Helm M, Florentz C, Naumov VA, Breusov AA, Buneva VN, Giege R, Nevinsky GA. Variability of substrate specificity of serum antibodies obtained from patients with different autoimmune and viral diseases in reaction of tRNA hydrolysis. Russian Journal of Immunology. 1999;**4**:25-32. PMID: 12687113

[88] Polosukhina DI, Kanyshkova TG, Doronin BM, Tyshkevich OB, Buneva VN, Boiko AN, Gusev E., Favorova OO, Nevinsky GA. Hydrolysis of myelin basic protein by polyclonal catalytic IgGs from the sera of patients with multiple sclerosis. Journal of Cellular and Molecular Medicine. 2004;**8**:359-368. PMID: 15491511

[89] Polosukhina DI, Buneva VN, Doronin BM, Tyshkevich OB, Boiko AN, Gusev EI, Favorova OO, Nevinsky GA. Hydrolysis of myelin basic protein by IgM and IgA antibodies from the sera of patients with multiple sclerosis. Medical Science Monitor. 2005;**11**:BR266-BR272. PMID: 16049372

[90] Polosukhina DI, Kanyshkova TG, Doronin BM, Tyshkevich OB, Buneva VN, Boiko AN, Gusev EI, Favorova OO, Nevinsky GA. Metal-dependent hydrolysis of myelin basic protein by IgGs from the sera of patients with multiple sclerosis. Immunology Letters. 2006;**103**:75-81. DOI: 10.1016/j.imlet.2005.10.018

[91] Legostaeva GA, Polosukhina DI, Bezuglova AM, Doronin BM, Buneva VN, Nevinsky GA. Affinity and catalytic heterogeneity of polyclonal myelin basic protein-hydrolyzing IgGs from sera of patients with multiple sclerosis. Journal of Cellular and Molecular Medicine. 2010;**14**:699-709. DOI: 10.1111/j.1582-4934.2009.00738.x

[92] Bezuglova AM, Konenkova LP, Doronin BM, Buneva VN, Nevinsky GA. Affinity and catalytic heterogeneity and metal-dependence of polyclonal myelin basic protein-hydrolyzing IgGs from sera of patients with systemic lupus erythematosus. Journal of Molecular Recognition. 2011;**24**:960-974. DOI: 10.1002/jmr.1143

[93] Bezuglova AM, Konenkova LP, Buneva VN, Nevinsky GA. IgGs containing light chains of the λ-and κ-type and of all subclasses (IgG1-IgG4) from the sera of patients with systemic lupus erythematosus hydrolyze myelin basic protein. International Immunology. 2012;**24**:759-770. DOI: 10.1093/intimm/dxs071

[94] Bezuglova AM, Dmitrenok PS, Konenkova LP, Buneva VN, Nevinsky GA. Multiple sites of the cleavage of 17- and 19-mer encephalytogenic oligopeptides corresponding to human myelin basic protein (MBP) by specific anti-MBP antibodies from patients with systemic lupus erythematosus. Peptides. 2012;**37**:69-78. DOI: 10.1016/j.peptides.2012.07.003

[95] Timofeeva AM, Dmitrenok PS, Konenkova LP, Buneva VN, Nevinsky GA. Multiple sites of the cleavage of 21- and 25-mer encephalytogenic oligopeptides corresponding to human myelin basic protein (MBP) by specific anti-MBP antibodies from patients with systemic lupus erythematosus. PLoS One. 2013;**8**:e51600. DOI: 10.1371/journal.pone.0051600

[96] O'Connor KC, Bar-Or A, Hafler DA. The neuroimmunology of multiple sclerosis: Possible roles of T and B lymphocytes in immunopathogenesis. Journal of Clinical Immunology. 2001;**21**:81-92. PMID: 11332657

[97] Timofeeva AM, Buneva VN, Nevinsky GA. Systemic lupus erythematosus: molecular cloning and analysis of 22 individual recombinant monoclonal kappa light chains specifically hydrolyzing human myelin basic protein. Journal of Molecular Recognition. 2015;**28**:614-627. DOI: 10.1002/jmr

[98] Timofeeva AM, Buneva VN, Nevinsky GA. Systemic lupus erythematosus: Molecular cloning and analysis of recombinant monoclonal kappa light chain NGTA1-Me-pro with two metalloprotease active centers. Molecular BioSystems. 2016;**12**:3556-3566. DOI: 10.1039/c6mb00573j

[99] Timofeeva AM, Ivanisenko NV, Buneva VN, Nevinsky GA. Systemic lupus erythematosus: Molecular cloning and analysis of recombinant monoclonal kappa light chain NGTA2-Me-pro-Tr possessing two different activities-trypsin-like and metalloprotease. International Immunology. 2015;**27**:633-645. DOI: 10.1093/intimm/dxv042

[100] Timofeeva AM, Buneva VN, Nevinsky GA. SLE: Unusual recombinant monoclonal light chain ngta3-pro-dnase possessing three different activities trypsin-like, metalloprotease and DNase. Lupus: Open Access. 2017;**2**(2):1-12

[101] Odintsova ES, Zaksas NP, Buneva VN, Nevinsky GA. Metal dependent hydrolysis of β-casein by sIgA antibodies from human milk. Journal of Molecular Recognition. 2011;**24**:45-59. DOI: 10.1002/jmr.1022

[102] Odintsova ES, Kharitonova MA, Baranovskii AG, Sizyakina LP, Buneva VN, Nevinsky GA. Proteolytic activity of IgG antibodies from blood of acquired immunodeficiency syndrome patients. Biochemistry (Moscow). 2006;**71**:251-261. PMID: 16545061

[103] Odintsova ES, Baranova SV, Dmitrenok PS, Rasskazov VA, Calmels C, Parissi V, Andreola ML, Buneva VN, Zakharova OD, Nevinsky GA. Antibodies to HIV integrase catalyze site-specific degradation of their antigen. International Immunology. 2011;**23**:601-612. DOI: 10.1093/intimm/dxr065

[104] Baranova SV, Buneva VN, Kharitonova MA, Sizyakina LP, Calmels C, Andreola ML, Parissi V, Zakharova OD, Nevinsky GA. HIV-1 integrase-hydrolyzing IgM antibodies from sera of HIV-infected patients. International Immunology. 2010;**22**:671-680. DOI: 10.1093/intimm/dxq051

[105] Baranova SV, Buneva VN, Kharitonova MA, Sizyakina LP, Zakharova OD, Nevinsky GA. Diversity of integrase-hydrolyzing IgGs and IgMs from sera of HIV-infected patients. Biochemistry (Moscow). 2011;**76**:1300-1311. DOI: 10.1134/S0006297911120030

[106] Baranova SV, Buneva VN, Nevinsky GA. Antibodies from the sera of HIV-infected patients efficiently hydrolyze all human histones. Journal of Molecular Recognition. 2016;**29**:346-362. DOI: 10.1002/jmr.2534

Chapter 3

Trace Elements in Hair: Relevance to Air Pollution

Jun-ichi Chikawa, Jeremy Salter, Hiroki Shima,
Takaaki Tsuchida, Takashi Ueda,
Kousaku Yamada and Shingo Yamamoto

Additional information is available at the end of the chapter

http://dx.doi.org/10.5772/intechopen.74373

Abstract

Elemental concentrations of single hair samples taken from 2003 to 2012 had been evaluated by X-ray fluorescence for the assessment of the relation between calcium and cancer. Early results implied a mechanism linking hair and serum element concentrations with a shift in element levels over time. After 2009, pollution-attributable differences were seen in the levels of Ca, Sr, P, Cl, Br, K, S, elements under renal control by parathyroid hormone (PTH), as well as Cu, Zn, Ti. Especially, hair taken from February to March 2011 showed low [Cu] and [Zn] indicating about half of the normal serum level and often three orders of magnitude higher [Ti] than typical. These specimens also showed higher serum [S] than usual, and except for one patient with PTH-related disease, all the subjects had the normal or lower hair calcium than typical for earlier years. Almost all the subjects showed store-operated Ca channel gating. The pollution era is associated with an increase in hair Na, a decrease in K, and abnormally low P, suggesting a functional deterioration of Na^+/K^+-ATPase. These results can be attributed to increases in serum Ca and S coincident with breathing the polluted air; the incorporated Ca closes the ion channels of hair matrix cells but may be moved with P to bone, resulting in the abnormal P deficiency, likely producing an ATP shortage in serum. This insufficient ATP supply may result in inactivated molecular pumps and hypokalemia contributing to fatal ventricular fibrillation in patients with myocardial infarction. The pollution increase [S] in serum may be excreted by forming sulfide compounds with Cu and Zn, resulting in Cu deficiency necessary for making elastin to repair damage in blood vessels. The K and Cu deficiencies observed appear to account for the reported increase in infarction mortality after high-pollution days.

Keywords: calcium, sulfur, ion channels, parathyroid hormone, Na^+/K^+-ATPase, hypokalemia, yellow haze, copper, zinc

1. Introduction

Synchrotron X-ray fluorescence analysis of single hair segments was achieved by Iida and Noma [1]. Today, elemental distribution in hair microstructures has been observed especially in cosmetic studies [2] and occasionally in environmental studies [3]. In our previous work [4–6], the study of the relations between elemental concentrations in serum and hair (total concentration instead of structural distribution) was employed for our inquiries into links between cancer and calcium metabolism. X-ray fluorescence (XRF) detects many elements, and in time it became clear that the spectra acquired for cancer assessment also showed pollution-related trends.

Pollution particles smaller than 10 and 2.5 μm suspended in the atmosphere are referred to as "PM 10" and "PM 2.5" (fine Particulate Matter). An association between daily mean PM concentration and daily mortality was shown by a statistical model [7–10]. Also, correlations between PM and cancer were investigated [9]. The PM 2.5 is mainly attributed to soot particles contained in gas emissions from diesel vehicles and manufacturing facilities and contains various substances; combustion-associated gases include sulfur and nitrogen oxides. The PM includes wind-blown yellow sand that often comes to Japan [10] by desertification in the continent. Such particulates have reached California, British Columbia, and the French Alps [11–14]. Today, air pollution PM 2.5 is a universal problem, routinely affecting most of the world, although most obvious in and downwind of industrial areas. PM 2.5 is too small to be filtered by the conventional gauze mask and can deposit materials in capillary vessels in the lung [15].

In this study, to explore the possible origins of the mortality increase observed among cardiac patients, elemental inflow from polluted air into blood has been investigated by review of X-ray fluorescence analyses (XFA) of hair using the ratio of characteristic X-ray peaks to background scatter [4–6]. Since the scatter is a function of the mass of the sample within the beam, the peak-to-scatter ratio (P/S) can be used as a unitless relative concentration of each detected element, independent of hair thickness and shape. With the relationships of serum and hair elements given by the equations in **Table 1** previously established [5], we obtained useful approximations of element levels in serum.

XFA for scalp hair has revealed ion channel gating of hair matrix (HM) cells [4]. By the principle of "inflow-outflow equality," the content of an element in growing hair must be equal to the inflow into the HM cells from blood [4, 5], and the elements admitted through ion channels occur in hair at two distinct levels produced by the closing or opening (gating) of the relevant channels (in vivo). By such channel gating, homeostasis of cellular essential elements can be maintained. Especially, Ca is an overall regulator of ion gating. We had given ten subjects 2-week oral calcium supplementation; the (dried) serum samples showed a single value for Ca [5]. Similarly, no significant variation was seen among the subjects for Sr, Cl, Br, K, S, and P, elements under renal homeostatic control, although in nonsupplemented subjects, considerable variation is usual [4–6]. Calcium is the central player for the homeostatic control of the elements, and usually, therefore, store-operated Ca channels are activated to maintain

$[Fe]_S = [Fe]_P$	$[Fe]_H = [Fe]_P = 15$	(4)
$[Cu]_S = [Cu]_P$	$[Cu]_H = [Cu]_P = 20$	(5)
$[Zn]_S = [Zn]_P$	$[Zn]_H = [Zn]_P^2 = 400$	(6)
$[S]_P = [S]_I$	$[S]_{HC} = [S]_P = 20$	(7)
	$[S]_{HO} = (1/2)[S]_I^2 = 200$	(8)
$[Ca]_P = [Ca]_I$	$[Ca]_{HC} = [Ca]_P = 10$	(9)
	$[Ca]_{HO} = (1/2)[Ca]_I^2 = 50$	(10)
$[Sr]_P = [Sr]_I$	$[Sr]_{HC} = [Sr]_P = 10$	(11)
	$[Sr]_{HO} = (1/2)\{[Sr]_P+[Sr]_I\}^2 = 200$	(12)
$[Cl]_P = 0.04[Cl]_I$	$[Cl]_{HC} = [Cl]_P = 10$	(13)
	$[Cl]_{HO} = \{2[Cl]_I\}^{1/2} = 22$	(14)
$[Br]_P = 0.04[Br]_I$	$[Br]_{HC} = [Br]_P = 10$	(15)
	$[Br]_{HO} = \{2[Br]_I\}^{1/2} = 22$	(16)
$[K]_S = [K]_I$	$[K]_{HC} = 7.1[K]_S = 300$	(17)
$[P]_P = [P]_I = (1/4)[P]_S$	$[P]_{HC} \geqq 10$	(18)
	$[P]_{HO} = 5\,[P]_I^{1/2} = 5$	(19)

Numerical values of peak/scatter as apparent concentrations of element X defined by Eq. (2). Eq. (1): $[X]_S = [X]_I + [X]_P$. Subscripts: H = hair, S = serum, I = serum Ion, P = serum Protein, OH = Hair produced during Open ion channels, HC = Hair produced during Closed ion channels.
Dried serum was measured to be $[Na]_S = 10$ by the definition $[X] = P/S$ Eq. (2), and hair usually shows no Na peak, that is, $[Na]_H = 1$. This resulting ratio corresponds to established values: [Na] = 142 mmol/L in serum and [Na] = 14 mmol/L in cell [23]. The standard concentration $[X]_H$ given by Eq. (2), of course, can be converted into the conventional expression such as $[Ca]_{HC} = 0.49$ mg/g and $[Ca]_{HO} = 2.5$ mg/g [5].

Table 1. Standards of hair $[X]_H$ and dried serum $[X]_S$.

the normal intracellular [Ca]. Thus, hair elements constitute a record of the combination of serum elements and ion channel function.

The store-operated Ca channels on the plasma membrane are understood to open when Ca^{2+} stores are depleted at the endoplasmic reticulum (ER) [16–18]. "Store-operated ion channels" adjust the intracellular Ca ion level toward the normal, and an XFA scan along hair shows that the normal $[Ca]_{HC} = 10$ was maintained despite the ongoing channel gating revealed by the noted fluctuation in $[Sr]_H$ [6]. Therefore, the store-operated channels gate due to shortage of Ca stored in serum protein [5, 6], corresponding to hair Ca less than the normal ($[Ca]_{HC} < 10$ by Eq. (9) in **Table 1**).

However, when the serum Ca deficiency further proceeds beyond the range covered by the store-operated Ca entry (SOCE), the deficiency increases the secretion of parathyroid hormone (PTH), which causes PTH-activated Ca channel gating. Such channel activity is due to membrane voltage and propagates from channel to channel, resulting in the upper range $[Ca]_H > 10$

and reaching the maximum $[Ca]_{HO} = 50$ and $[Sr]_{HO} = 200$ [Eqs. (10) and (12) in **Table 1**]. Ca oral supplementation immediately transits this highest level into the normal or less than normal $[Ca]_{HC} \leqq 10$ and $[Sr]_{HC} \leqq 10$; PTH regulates the Ca channel(s) of HM cells [4–6]. As a typical example, de Groot et al. [19] elucidated the epithelial Ca channel TRPV-5 activated by PTH, which is responsible for Ca reabsorption in renal tubule [20]. Today, for utilizing the channel on-off action for biosensing applications, artificial cell membrane systems have been widely investigated [21].

Thus, calcium has a very high essentiality and homeostasis. The serum standard values for subjects with Ca supplementation are given in **Table 1**. The hair standards were calculated from the serum standards and confirmed by the *P*/*S* FXA [5, 6]. For this work, Ca may be treated as the major regulator of ion channels and may react to a change in serum Ca level in just 15–20 min [22].

Because sulfur-containing amino acids, methionine and cysteine are components of almost all protein molecules, sulfur has also high essentiality and homeostasis and is contained as the ionic sulfur species (SO_4^{2-}) in serum [23, 24]. Its relation between serum and hair is similar to that of Ca as seen from Eqs. (7)–(10) in **Table 1**, although the sulfate ion channels have not been reported to the knowledge of the authors [5].

We have observed elemental levels in the hair of thousands of people from 2003 to the present day. Samples after 2009 show significant changes in hair elements, and today the intrinsic hair element levels cannot be seen any more. However, the homeostasis of Ca and S is maintained even with their great inflow into serum from the polluted air at the sacrifice of other important elements responsible for heart activity, resulting in the increased mortality in myocardial infarction cases up to 7 days following short-term pollution [25–27].

2. Samples and method

All the hair and blood samples were collected after informed consent was obtained in accordance with the ethical standards of Hyogo College of Medicine.

X-ray fluorescence analysis (XFA) of the hair samples was carried out using synchrotron radiation at the Photon Factory's (PF) BL4A beamline in the same way as previously [4–6]: excitation energy was 17.4 keV (0.71 Å), the hair was suspended into the X-ray beam in vacuum, and fluorescence detected using a lithium-drifted silicon detector. Because almost all our subjects dye their hair, to avoid hair contamination, only dye-free fresh hair root (length about 1 mm) was used for single-point evaluation. Datum was typically collected for a minute in the range of 0.5–17.5 keV, and the fluorescence peaks evaluated on the log-scale plot by height, all k-alphas except the Ca K-beta peak at 4.0 keV used to avoid interferences. Since hair grows at about 1 cm per month, each data point corresponds to about 3 days of hair growth. The variation of concentrations with time in **Figure 1** was observed by scanning along hair strands using a beam width of 0.05 mm.

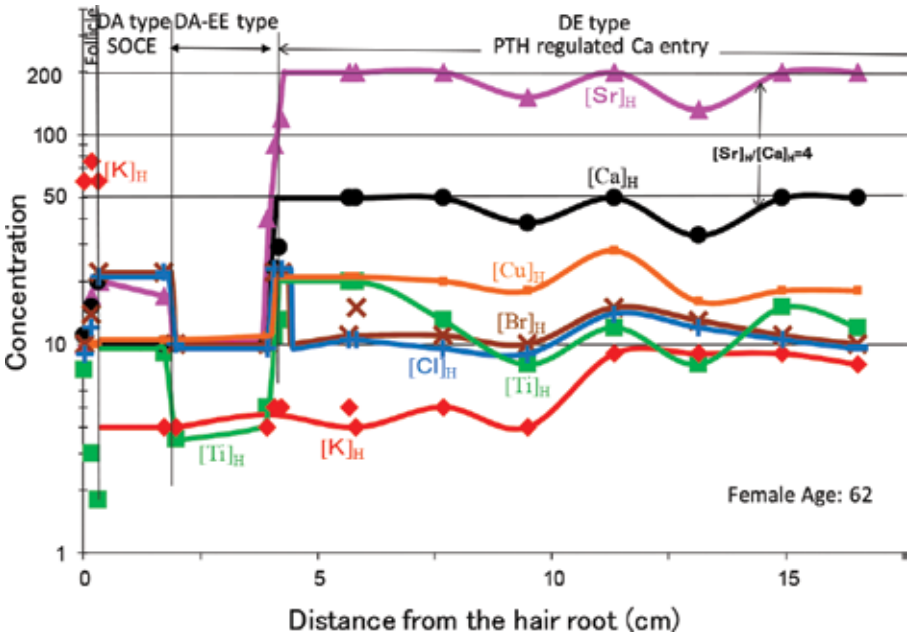

Figure 1. Typical Ca deficiency observed along a single hair strand by scanning 0.05-mm-width XFA. Transitions of DE type (PTH-regulated Ca entry), DA-EE type (Ca channel closing with a low $[K]_H$), and DA type (store-operated Ca entry, SOCE) can be seen with the $[Ca]_H$ variation due to the Ca channel gating, resulting in synchronized variations for $[Cu]_H$, $[Ti]_H$, $[K]_H$, $[Cl]_H$, and $[Br]_H$. In the SOCE region (DA type), $[Ti]_H$ and $[Sr]_H$ are still high, and other elements have the standard levels. Female subject age: 62.

3. Concentration relations between serum and hair

Serum contains water at 90–92% and Ca at 8.5–10.2 mg/dL; these Ca values correspond to 92 and 90% water contents, respectively, with negligible [Ca] variations in dried serum. Dried serum is calculated to have Ca at 1 mg/g. Hair can be regarded as serum protein containing mineral elements. For example, Cu exists mainly not as free ions, only bound to serum protein, and the reported serum $[Cu]_S$ of 17 μmol/L [28] becomes dried serum concentration of 207 μmol/kg, which is in good agreement with the reported hair Cu concentration of 190–200 μmol/kg. Therefore, any element in serum protein has about the same concentration in hair, if no ions flow into the hair.

In most cases, the total concentration of element X in dried serum, $[X]_S$, is the sum of

$$[X]_S = [X]_I + [X]_P \tag{1}$$

$[X]_I$ and $[X]_P$, the concentrations of ionic and protein-bound X, respectively. By the principle of the inflow-outflow equality, X's hair concentrations $[X]_H$ can occur in two levels depending on whether the ion channels for element X are gating or closing;

$[X]_{HO}$ = hair concentration in the case of the gating (open) ion channels.

$[X]_{HC}$ = hair concentration in the case of the closing ion channels.

For specimen mass M within the excitation X-ray beam in XFA, the peak height P for element X must be $P = kM[X]$, with k, a proportional constant, so $\log[X] = \log P - \log kM$. Logarithmic spectra for thick and thin specimens having the same concentration can be superimposed by moving one to the other vertically, that is, $\log kM = \log S$, and.

$$\log [X] = \log P - \log S = \log (P/S), \tag{2}$$

independently of the specimen thickness, where S is the background due to X-rays scattered by the specimen. Eq. (2) is valid even for thick specimens because the X-ray absorption occurs for P and S in the same way. (The hair was suspended in the X-ray beam in vacuum, so there is no other mass to contribute background scatter.) Using this definition for [X], the relations between $[X]_H$ and $[X]_S$ obtained in the previous paper [5] are listed in **Table 1** (also, see **Figure 3**).

As seen from the foregoing argument, the background S is due to serum (hair) protein (nonprotein solids: 3–4%). According to the Gamble [23] gram, the ionic element species are controlled to maintain electric neutrality with [Protein$^-$] in serum. Then, the ratio of the number of X atoms to the number of the protein molecules within the excitation X-ray beam in XFA, which is proportional to $[X] = P/S$, is under homeostatic control. If congener elements, X and Z, have a proportionality, we have [X] = [Z] by the definition Eq. (2), as $[Cl]_H = [Br]_H$ in **Table 1**. The concentration by Eq. (2) can be considered to use the standard value of each element as a unit and results in a new concentration system to show the relationship of elements in dried serum, cell, and hair.

For an element Z such as Cu, Fe, and Zn being protein-bound and having no ion in serum, the value $\log[Z]_H = [\log P - \log S]_H$ is normalized for comparing their concentrations by.

$$\log [Z]_H = [\log P - \log S]_H / \left([\log P - \log S]_H\right)_{st} \tag{3}$$

using the standard $([\log P - \log S]_H)_{st}$ for hair. The standard values for the Ca-supplemented healthy subjects are $[Cu]_H = 20$, $[Fe]_H = 15$ and $[Zn]_H = 400$ (**Table 1**).

By the principle of "inflow-outflow equality," hair composition reveals ion channel closing and opening. There may be many kinds of ion channels and receptors, some yet unknown. Though sulfate ion channels have not been reported, we observed upper $[S]_{HO}$ and lower $[S]_{HC}$ levels in hair, suggesting the existence of S-related ion channels [5] (designated as S or SO_4^{2-} channels).

Although channel gating produces a short pulsed inflow into the cell each time, the messenger protein binds with one of the associated receptors; such gating can occur so frequently as to bring the intracellular ion concentration $[X]_{CI}$ to serum ion concentration $[X]_I$. Since the $[X]_{CI}$ is kept at the serum $[X]_I$ by the channels' flow, $[X]_{HO}$ is determined by $[X]_I$ (see **Table 1**).

In HM cells, Ca can enter primarily as ionic ($[Ca]_{CI}$) with few protein-bound atoms ($[Ca]_{CP} = 0$). The cellular Ca concentration $[Ca]_C$ is equal to cell ion concentration $[Ca]_{CI}$, that is, $[Ca]_C = [Ca]_{CI}$. Ca is incorporated as a pair of atoms into the hair protein molecules formed in the HM cells [29]. The reaction rate of the pair formation is proportional to the

ion collision probability, $\{[Ca]_{CI}\}^2$, in the HM cell. The dissociation rate of two Ca pair atoms in the protein is proportional to twice the $[Ca]_H$. $[Ca]_H$ is in equilibrium with cell $[Ca]_C$; the rates are equal, $2r[Ca]_H = q\{[Ca]_{CI}\}^2$, where r and q are the proportional constants. When the channel gating frequency is high enough to result in $[Ca]_{CI} = [Ca]_I$ (=10), we have $[Ca]_{HO} = 50$. Therefore, $q = r$ and $[Ca]_{HO} = (1/2)[Ca]_I^2$. For a channel gating frequency, we can express as.

$$[Ca]_H = (1/2)[Ca]_{CI}^2.$$

Sr is assumed to be distributed equally as ion and protein-bound atom in HM cells, as established previously, that is, $[Sr]_{CI} = [Sr]_{CP}$. Similarly, we have

$$[Sr]_H = (1/2)\{[Sr]_{CI}+[Sr]_{CP}\}^2.$$

According to the definition $[X]_H = P/S$ by Eq. (2), the congener proportionality is expressed as $[Ca]_{CI} = [Sr]_{CI} = [Sr]_{CP}$, and the Sr/Ca ratio becomes $[Sr]_H/[Ca]_H = 4$. This agrees with experimental results (see **Figure 1**).

As seen above, when Ca channel gating takes place, the $[Sr]_H/[Ca]_H = 4$. For Ca channel closing, only the Ca and Sr on serum protein are incorporated into HM cells, resulting in $[Sr]_H = [Ca]_H = 10$ by Eqs. (9) and (11), $[Sr]_H/[Ca]_H = 1$. Thus, in this work, $[Sr]_H$ is a useful marker for channel gating.

Here, we first consider the hair elements without pollution. For dried serum from Ca-supplemented five male and five female subjects, a single concentration value for each element in **Table 1** was found. Ca appears to be the central and overriding player in the regulation of various elements; by ensuring normal serum Ca with a Ca supplement, all other elements under renal control (Sr, Cl, Br, K, S, P) become normal [5]. We have the Ca standard

$$[Ca]_S = [Ca]_I + [Ca]_P = 20 \text{ and } [Ca]_P = [Ca]_I = 10 \text{ (Dried serum)}$$

$$[Ca]_H = [Ca]_P = (1/2)\,[Ca]_S = 10 \text{ (Hair)}$$

with closed Ca channels (only serum protein can enter the HM cells, so $[Ca]_H$ must be equal to $[Ca]_P$ in steady-state hair growth).

Unfortunately, almost all humans have "ordinary deficiencies" in Ca in varying degrees [30, 31]. Calcium balance is maintained in kidney; Ca is freely filtered by the glomerulus, and the quantity of Ca filtered each day of over 10 g is far greater than the content of the entire ECF compartment [20]. Therefore, ~98% of the filtered Ca must be reabsorbed along the renal tubule. Approximately 70% of filtered Ca is reabsorbed passively in the proximal tubule. The remaining reabsorption is controlled by the Ca-sensor, CaSR, on the basolateral membrane of the tubular cells. Consequently, we have a tendency to fall into Ca deficiency. The ranges of $[Ca]_H < 10$ and $[Ca]_H > 10$ are due to Ca deficiency with deviations toward acidosis $[Cl]_H > 10$ and alkalosis $[Cl]_H < 10$, respectively. Two kinds of known Ca channels account for the results seen in hair analysis; the store-operated channel and PTH-operated channel are activated in the ranges of $[Ca]_H \leqq 10$ and $[Ca]_H > 10$, respectively.

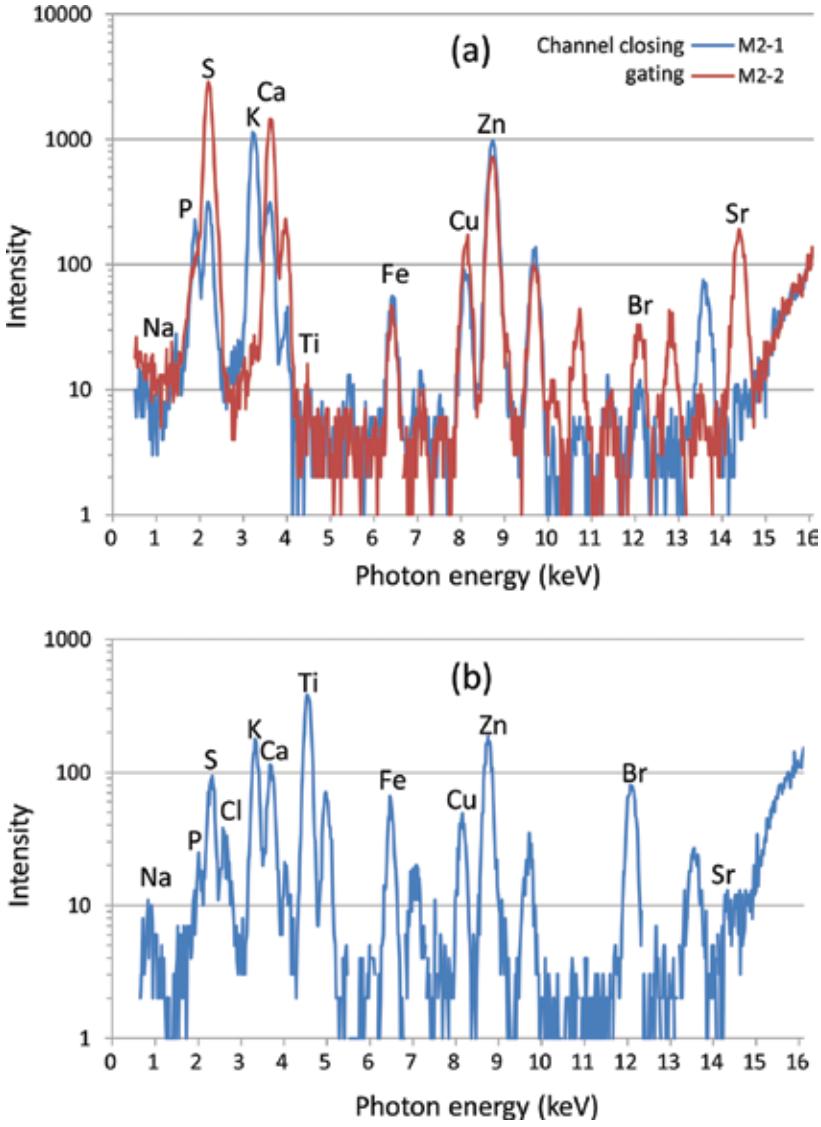

Figure 2. X-ray fluorescence spectra of single hair samples. (a) With ion channel closing and gating of Ca, K and S (SO_4^{2-}) in the hair matrix cells without pollution. Compare the peak heights with the levels listed in **Table 1**. (b) Typical example of hair with the pollution (F150 in **Figure 5**) showing a very high Ti peak and clearly recognized Na peak [Compare with (a)]. The [Ca] is lower than the normal, with store-operated Ca channel gating. The k-alpha peaks are labeled (see Section 2) (16.5–17.5 keV omitted to preserve useful scale).

Figure 1 gives a typical example showing the effects of both the store-operated and PTH-regulated Ca channels. The single strand from a 62-year-old female was analyzed from root to tip with the 0.05-mm-width excitation beam. As time progresses from right to left, the Ca deficiency is improving; the high-level $[Ca]_H$ = 50 ($[Sr]_H$ = 200) continues for a long term (12 months) from the tip, with deviations downward, keeping $[Sr]_H/[Ca]_H = 4$ and then abruptly

decreases to the low-level $[Ca]_H = 10$ standard, with $[Sr]_H/[Ca]_H = 1$ due to Ca channel closing, for about 2 months. Furthermore, the standard $[Ca]_H = 10$ is maintained for about 1.5 months by gating the store-operated Ca channels (SOCE) with $[Sr]_H/[Ca]_H$~2; $[Ti]_H$ is as high as $[Ti]_H$~10, with open Cl channels $[Cl]_H = [Br]_H = 22$ (acidosis: DA type). At the follicle (root), the concentrations become singular values, which will be reported elsewhere.

The observed process can be divided into three regions by the abrupt Sr change; the regions labeled "SOCE," DA-EE type with Ca channel closing, and "PTH regulated Ca entry." The store-operated Ca entry (SOCE) channel system is for maintaining the intracellular Ca at the normal by channel gating when the depletion of Ca storage in the cell occurs. For hair, therefore, the store-operated Ca channels must work for $[Ca]_H \leqq 10$ so as to keep the normal $[Ca]_H = 10$, as reported earlier [6]. In contrast, the "PTH-regulated Ca entry" region indicates greater inflow of Ca and Sr through the gating Ca channels; the electrical signal initiated by the activation of the receptor PTH1R propagates rapidly over the surface of the cell due to the opening of other ion channels that are sensitive to the voltage change caused by the initial channel opening, as observed for renal epithelial Ca channel (TRPV5) as a typical example by de Groot et al [19]. For the hair Ca level, the channel gating frequency depends on serum [PTH] and causes the downward deviations from $[Ca]_H = 50$ and $[Sr]_H = 200$. Based on such results, the deduced type of Ca channel is referred to as "PTH-regulated Ca channels." Typical XFA spectra in **Figure 2(a)** show Ca channel closing and opening (gating) accompanied by levels changes for P (HPO_4^{2-}), S (SO_4^{2-}) and K^+.

By taking into account, both the PTH-regulated and store-operated Ca channels, Ca deficiency can be classified into five distinct types, as summarized in **Table 2**. These five types describe the Ca patterns typical in the region before PM pollution was notable.

DE type has Ca deficiency for excitation of the PTH-regulated Ca channel gating resulting in a high-level $[Ca]_H > 10$ due to the Ca^{2+} inflow into HM cells.

The Ca^{2+} and Sr^{2+} inflow through the gating channels may become toxic [30, 31], resulting in abnormally high $[Cu]_H$ and/or $[Ti]_H$ and the inequality $[Cl]_H < [Br]_H$ (disordered chloride shift), which can be taken as the deterioration of hepatocytes and erythrocytes, respectively. In **Figure 1**, when the PTH-regulated Ca channels are closed, $[Cu]_H$ and $[Cl]_H$ become normal for the EE-type ($[Cu]_H = 10$, $[Cl]_H = 10$). In the store-operated SOCE region, the $[Ti]_H$ is high, that is, $[Ti]_H$~10 (for normal $[Ti]_H$ ~1), suggesting deterioration of Ti excretion as a consequence of Sr inflow into hepatocytes.

When the gating accumulates $[Ca^{2+}]$ and $[Sr^{2+}]$ to ionic serum levels in HM cells, that is, $[Ca]_{CI} = [Ca]_I = 10$ and $[Sr]_{CI} = [Sr]_I = 10$, we have the maximum $[Ca]_{HO} = 50$ and $[Sr]_{HO} = 200$ in **Table 1**. An 8-month lasting $[Ca]_{HO} = 50$ was observed for chronic Ca deficiency [6], as referred to as LD type (long-term Ca deficiency). "LD type" often causes fatty liver [31].

DO type (Ca deficiency with Overplus in serum) has Ca channels closed in $[Ca]_H > 10$ by an increase of serum $[Ca^{2+}]$ with bone resorption [22, 30, 31], which results in serum alkalosis accompanied by a high $[Ca]_P$ (=$[Ca]_H > 10$ for closed Ca channels). Consequently, we have $[Ca]_H = [Sr]_H > 10$ with $[Cl]_H = [Br]_H < 10$. In this case, the serum [PTH] becomes so low as to result in a high $[K]_H$ and a low $[S]_H$ ([5]. Also, see Section 5.2.)

LD type: Long-term continuation of DE type due to chronic Ca deficiency.

DE type: PTH-regulated Ca channel gating.

$10 < [Ca]_H \leq 50$ with $[Sr]_H/[Ca]_H = 4$.

Ca (Sr) inflow into cells deteriorates their functions:

$[Cu]_H > 10$ and/or high $[Ti]_H$ by deteriorated metal excretion in hepatocytes.

$[Cl]_H > [Br]_H$ or $[Cl]_H < [Br]_H$ by deteriorated chloride shift in erythrocytes

PTH inhibits H^+/Na^+-exchange and Na^+-anion cotransport in renal tubule:

high $[H^+]$ in serum, K^+/H^+ exchange in cells, and $[K]_H \lesssim 10$.

low $[SO_4^{2-}]$ in serum, $[S]_H = 200$ by gating sulfate ion channels Eq. (8).

Serum: $[Ca]_I \lesssim 10$ and $[Ca]_P \lesssim 10$. High [PTH]. Acidosis.

DO type: PTH-regulated Ca channel closing with bone resorption by Ca deficiency.

$[Ca]_H = [Sr]_H \gtrsim 10$ with $[Cl]_H = ([Br]_H) < 10$ (Alkalosis), $[K]_H = 200$, $[S]_H = 20$.

Ca in serum protein increases with the alkalosis ($[Ca]_H = [Ca]_P$).

Serum: $[Ca]_I > 10$ and $[Ca]_P > 10$. [PTH]~0. Highly alkalosis.

EE type: Ever closing of Ca channels by Ca sufficient "Ever Enough".(No deficiency).

$[Ca]_H = [Sr]_H = 10$, $[Cl]_H = ([Br]_H) \lesssim 10$, $[K]_H = 200$, $[S]_H = 20$, $[P]_H \gtrsim 10$.

Serum: $[Ca]_I = 10$ and $[Ca]_P = 10$. [PTH]~0. Slightly alkalosis.

DA type: PTH-regulated Ca channel closing and Store-operated channel gating.

$[Ca]_H = 10$ with $1 < [Sr]_H/[Ca]_H \leqq 4$ and $[Ca]_H < 10$ with $[Sr]_H/[Ca]_H = 4$.

($[Cu]_H = 10$, $[Cl]_H > 10$, $[Ti]_H$: high)

PTH inhibits H^+/Na^+-exchange and Na^+-anion cotransport in renal tubule:

high $[H^+]$ in serum, K^+/H^+ exchange in cells, and $[K]_H \lesssim 10$.

low $[SO_4^{2-}]$ in serum, $[S]_H = 200$ by gating sulfate ion channels Eq. (8).

Serum: $[Ca]_I \lesssim 10$ and $[Ca]_P \lesssim 10$. Mean [PTH]. Acidosis.

Table 2. Classification of Ca deficiency observed in hair with Eqs. (2) and (3).

In summary, for $[Ca]_H > 10$, hair Ca is by PTH-regulated Ca channels, DE for gating and DO type for closing.

At $[Ca]_H = 10$, if the normal state of $[Ca]_H = [Sr]_H = 10$ continues steadily, we can call this EE type (Ca ever enough to close Ca channels). Some healthy subjects have been found to keep EE type more than several months.

Usually, however, transitions between open and closed Ca channels occur at $[Ca]_H = 10$, resulting in $1 < [Sr]_H/[Ca]_H < 4$. Scanning the 50-μm width X-ray beam along the hair, in earlier work [6], we observed the $[Ca]_H$ maintained at $[Ca]_H = 10$ (normal) during the variation of the $[Sr]_H$ by Ca channel gating. Therefore, the observed Ca channel gating is due to some kind of store-operated type to be activated at $[Ca]_H = [Ca]_P \leqq 10$. It was concluded that transition between $[Ca]_I$-sensitive (PTH-regulated) and $[Ca]_P$-sensitive (store-operated) channel gating occurs at $[Ca]_H = 10$.

In $[Ca]_H < 10$, the subjects have store-operated Ca channel gating with $[Sr]_H/[Ca]_H = 4$ (DA type). In this case, PTH-regulated channels are closed, and the hair Ca is due to Ca bound on serum protein, that is, $[Ca]_H = [Ca]_P < 10$. If the serum [PTH] is still high enough to inhibit the H^+/Na^+ exchangers from excreting H^+ in renal proximal convoluted tubular cells [32], serum $[H^+]$ increases; this deviation of serum pH toward acidosis ($[Cl]_H = [Br]_H >> 10$ "DA type) ionizes the protein-bound Ca to increase serum $[Ca^{2+}]$. Therefore, Ca in serum protein is a stockpile that the body can tap in cases of Ca deficiency. Oral calcium supplementation shows no immediate effects on $[Ca]_H < 10$ and $[Sr]_H/[Ca]_H = 4$ (2-month Ca supplementation is needed).

Normally, molecular pumps on cell membrane expel Ca^{2+} ions (closing the Ca channels) so that the intracellular $[Ca^{2+}]$ is nearly zero. This creates a state for signal Ca^{2+} inflow through the associated channels. However, when Ca^{2+} stores are depleted at the endoplasmic reticulum (ER), the store-operated Ca channels open [17, 18, 33], as Cahalan [16] illustrated clearly; STIM proteins in the ER open the store-operated "Orai" Ca^{2+} channels and inhibit voltage-gated $Ca_V1.2$ channels in plasma membrane. Because of the ubiquitous Ca-sensing STIM proteins, this store-operated Ca channel gating may be assumed to be similar to that we observed in the hair [5, 6]. Then, Ca depletion in the ER likely occurs with the depletion of the Ca stored on serum proteins ($[Ca]_P = [Ca]_H < 10$ with closed PTH-regulated Ca channels).

By 2-month supplementation of Ca 900 mg/day (3ACa) [34], LD type recovers to DO to DA type; the level of Ca deficiency is in the decreasing order of LD, DE, DO, and DA (see **Table 2**).

4. Hair elements with minor effects of air pollution before 2009

In Japan, notable air pollution had not been frequent until 2009. **Figure 3** shows results from hair samples obtained before 2009, and elemental concentrations evaluated for the hair roots of 50 randomly selected subjects of each sex between their 30s and 70s; the labels' Roman numerals stand for each age period, and the bar graph is in order of age.

By the criteria listed in **Table 2**, we can determine the type of each subject in **Figure 3** as labeled in **Figure 3(b)**. Examining **Figure 3(a)** and **(b)**, the high $[Cu]_H$ and $[Ti]_H$ are parallel with Sr-indicated gating ($10 < [Ca]_H \leq 50$ with $[Sr]_H/[Ca]_H = 4$), and thus related to opening of PTH-regulated Ca channels (DE type) causing deterioration of hepatic Cu and Ti excretion. Similar results can be seen for some DA-type subjects indicated by "LD-DA," which are the DA type with $[Ca]_H < 10$ with $[Cl]_H >> 10$ at present and were LD type in past. This means that recovery from Ca entry takes a long time. There are also many intrinsic DA-type subjects ($[Ca]_H < 10$ with $[Cl]_H >> 10$) having the normal Cu level. Many have $[Sr]_H/[Ca]_H = 4$ by the opening of store-operated Ca channels.

In this way, we obtained the results showing all the subjects with Ca deficiency in varying degrees; 24 out of 50 are DA type, 20 are DO type, and 4 are DE type, 2 are LD-DA type for the male, and 31 out of 50 are DA type, 9 are DO type, and 6 are DE type, 4 are LD-DA type for the female. This means that DA type, the least severe type of Ca deficiency, occurs in half of the subjects, regardless of gender. The second level in severity (and the second step in cases of

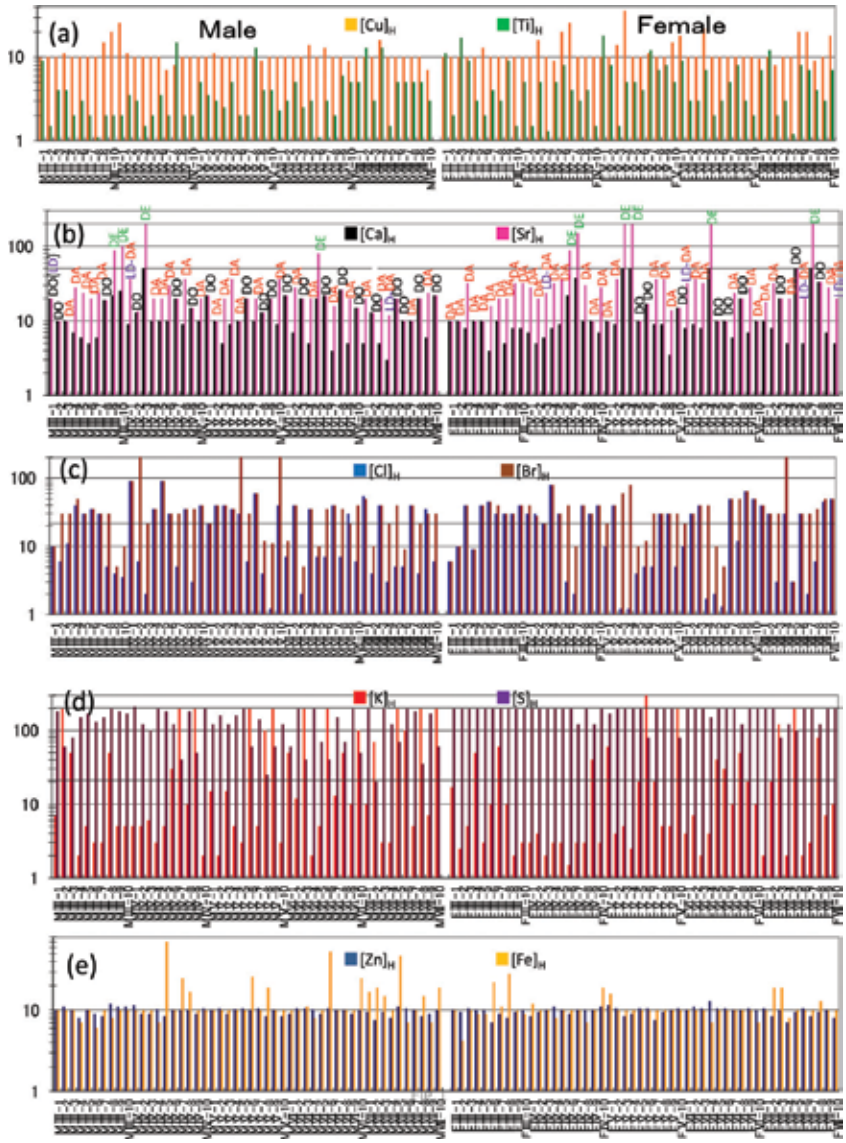

Figure 3. Hair concentrations observed for 50 randomly selected male and female subjects aged between 30 and 70. The hair samples were obtained before 2009 and show little or minor effects of air pollution. The bars graphed are in order of age and the Roman numerals in the subject labels stand for age period. (a) $[Cu]_H$ and $[Ti]_H$. The essential element Cu shows most values close to the homeostatic standard at $[Cu]_H = 10$ by Eq. (3), while Ti has a variety in $[Ti]_H$ by Eq. (2). (b) $[Ca]_H$ and $[Sr]_H$ having two separate standard levels with close and open Ca channels, $[Ca]_H = 10$ *vs.* $[Ca]_H = 50$ and $[Sr]_H = 10$ *vs.* $[Sr]_H = 200$, respectively. (c) $[Cl]_H$ and $[Br]_H$ having two separate standard levels at $[Cl]_H = [Br]_H = 10$ *vs.* $[Cl]_H = [Br]_H = 22$. (d) $[K]_H$ with the normal $[K]_H = 200$ and $[S]_H$ having two separate standard levels, $[S]_H = 20$ *vs.* $[S]_H = 200$. (e) $[Zn]_H$ and $[Fe]_H$ showing values close to the standard at $[Zn]_H = 10$ and $[Fe]_H = 10$ normalized by Eq. (3).

increasing deficiency), DO type, is more common for the male, and LD type is more common for the female, that is, the male appears to tolerate Ca deficiency by bone resorption, and the female by Ca channel gating.

In **Figure 3(d)**, almost all the females in our studies have the maximum $[S]_H = 200$ (SO_4^{2-} channel opening) due to Ca deficiency, and the normal $[S]_H = 20$ cannot be seen. For the males, $[S]_H$ values are slightly lower than the maximum, the two subjects MV-8 and MVII-2 (DO type) have the standard $[S]_H = 20$, and 10 subjects have the normal $[K]_H = 200$ (in DO type), which can be achieved by pumping K^+ into the HM cells with Na^+/K^+-ATPase.

Figure 3(e) shows hair $[Zn]_H$ and $[Fe]_H$ for the same subjects. Zinc values are well regulated around the standard; $[Zn]_H$ is consistent with $[Zn]_H = [Zn]_S^2$. This implies that Zn atoms on the serum protein are incorporated into the hair protein in pairs, in the same manner as Ca (Ca in hair protein also exists as a pair of atoms) [5].

5. Air pollution observed by hair analysis in February 2011

The effect of air pollution on hair elements in Japan is discernible from 2009 onward. Especially, from February to March 2011, very high contents of Ti in hair were observed, as seen in **Figures 4–6**, corresponding to a period of yellow haze, and indicating PM from the mainland desert [35].

Figures 4 and **5** are from female subjects under 60 years old and above, respectively. **Figure 6** is from male subjects between 23 and 83. The bar graphs are in order of age. Almost all hair samples were taken in February 2011. Three-orders of magnitude higher $[Ti]_H$ can be seen. Such high levels of $[Ti]_H$ were also observed for hair samples obtained in Tokyo area in this period.

All the people in the area must have breathed the polluted air containing Ti. However, about 80% of the female subjects younger than 60 (**Figure 4**) have $[Ti]_H > 10$, and less than 30% of the male subjects showed this effect. **Figures 4–6(c)** show the $[Cl]_H$ and $[Br]_H$ for the same subjects. The correspondence between the high $[Ti]_H$ and high $[Cl]_H$ (and $[Br]_H$) is clear. The high $[Ti]_H$ should be attributed to the deterioration of the liver's function to excrete Ti into bile caused by Sr^{2+} inflow into hepatocytes. The $[Cl]_H$ abnormality can be attributed to Ca^{2+} inflow (in past) into erythrocytes through open Ca^{2+} channels (a PTH effect) ultimately caused by Ca deficiency. Recovery of Ca levels requires months of oral supplementation. Therefore, the observed $[Ti]_H$ and $[Cl]_H$ abnormalities mean that the affected subjects were LD type in past even if Ca is sufficient when the hair was taken. The observed difference between the sexes is due to most of the male subjects being DO type. Although all the subjects breathed the polluted air, the pollution effect depends on the Ca-deficiency history of the individuals. However, all elements Ca, Sr, Cl, Br, P, K, S, Cu, and Zn changed their levels in hair from those in **Figure 3**.

5.1. Store-operated Ca channel gating induced by the pollution

Ca contained in the polluted air, probably as calcium silicate, sulfate and carbonate, is breathed into the lung and must increase $[Ca^{2+}]$ in serum. As seen in **Figures 4–6(b)**, all the subjects have $[Ca]_H$ levels normal or less than the normal, that is, $[Ca]_H \lesssim 10$, except the subject labeled "F073" having parathyroid gland dysfunction. This means that PTH-regulated Ca channels are closed with the air pollution. Comparison with **Figure 3(b)** indicates that breathing the

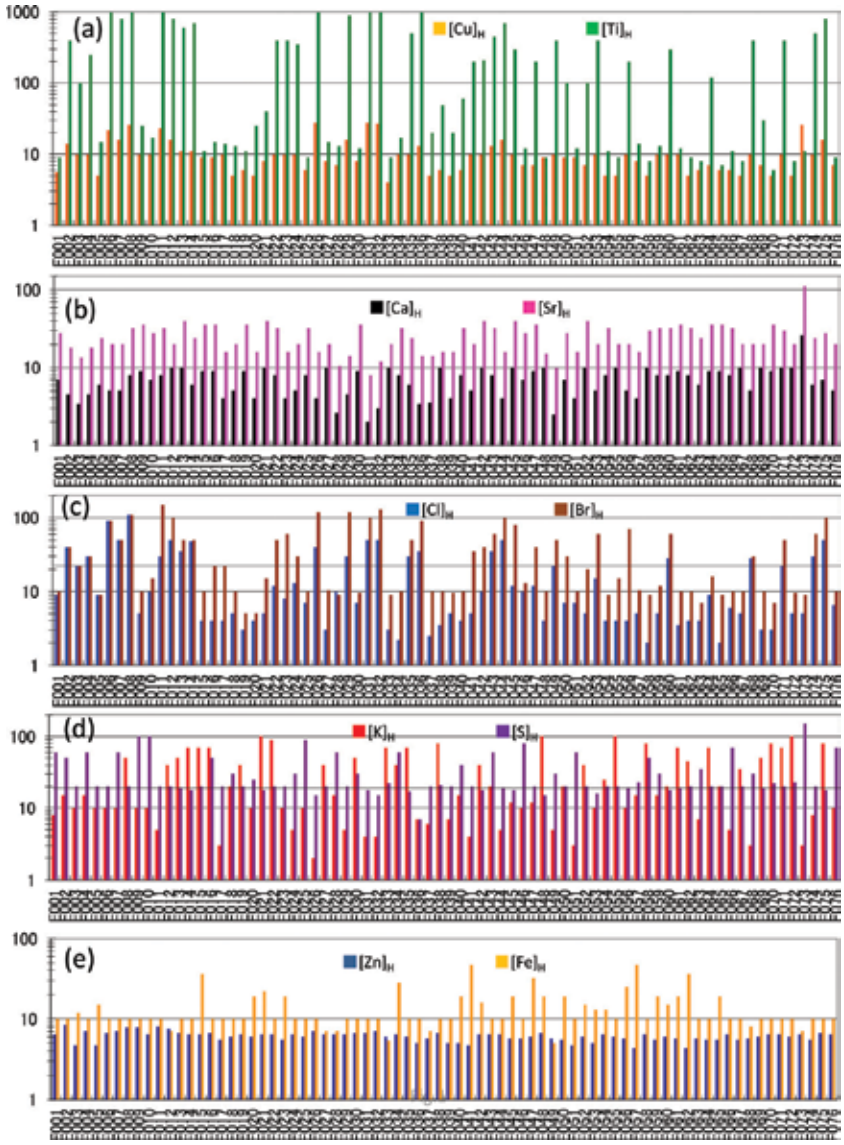

Figure 4. Effect of the air pollution on elements in hair root obtained in February 2011 from female subjects younger than 60. The bar graphs are in order of age from 23. Compare with **Figure 3**. (a) $[Cu]_H$ and $[Ti]_H$. Although the subjects younger than 42 (F019) have the normal $[Cu]_H = 10$ by Eq. (3), the $[Cu]_H$ level for the older is lower than the normal. The $[Ti]_H$ level by Eq. (2) is high for all the subjects; $[Ti]_H > 1000$ for the several subjects with the maximum of 2000 for F036 (age: 48), reflecting the atmosphere polluted with Ti. The high levels for $[Cu]_H$ and/or $[Ti]_H$ are consistent with deterioration of liver function. (b) $[Ca]_H$ and $[Sr]_H$. All the subjects have $[Ca]_H \leqq 10$ due to PTH-regulated Ca channel closing except F073 (parathyroid gland dysfunction, $[Sr]_H/[Ca]_H = 4$ by PTH). (c) $[Cl]_H$ and $[Br]_H$. As a whole, $[Cl]_H$ (and $[Br]_H$) is lower than that for **Figure 3** by a deviation to alkalosis with a high $[Ca^{2+}]$ in serum. The very high $[Ti]_H$ in (a) is associated with the high $[Cl]_H$ ($[Br]_H$) (acidosis). (d) $[K]_H$ and $[S]_H$. Many subjects have the lower standard $[S]_H = 20$ with closing the ion channels attributable to breathing S in the polluted air. (e) $[Zn]_H$ and $[Fe]_H$ normalized by Eq. (3). All the subjects have low $[Zn]_H$ values (indicating 1/4 of the normal hair level), while the standard $[Fe]_H$ is seen for many subjects. The pollution effects shown here are for hair samples collected in Hyogo Prefecture. The similar effects are confirmed for those in Yokohama.

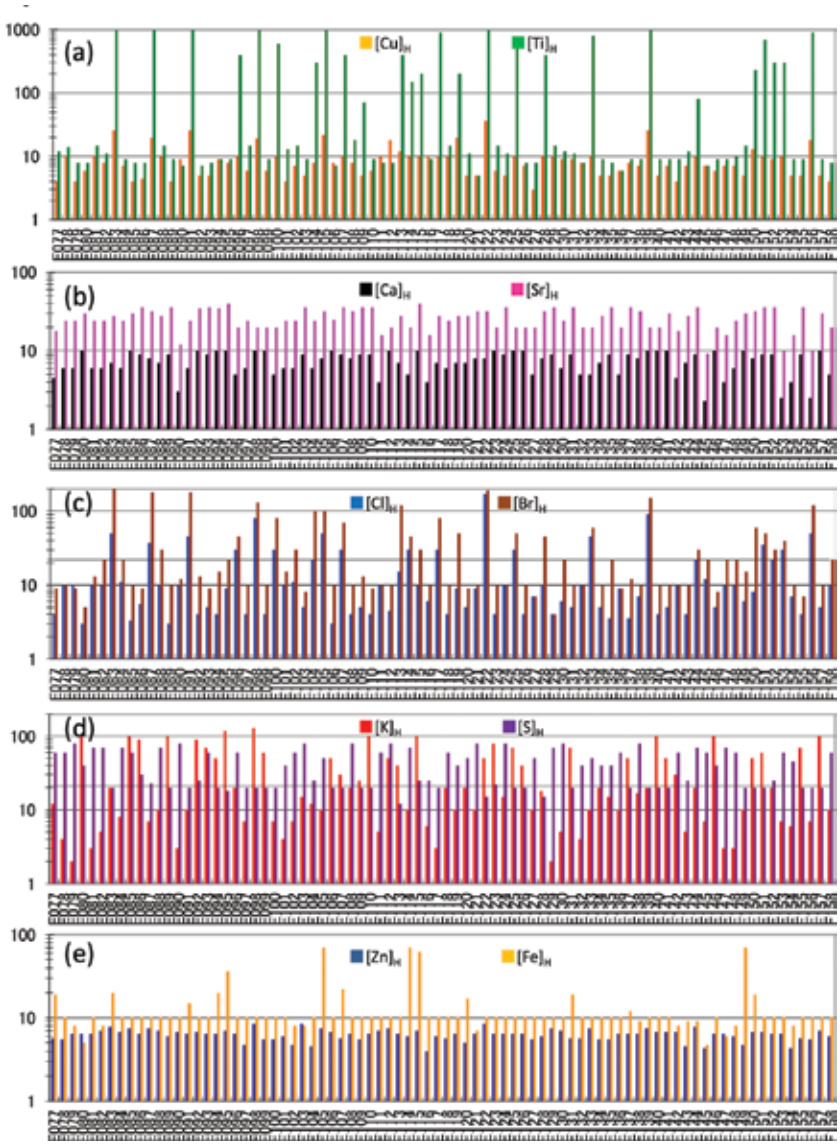

Figure 5. Effect of the air pollution on elements in hair root obtained in February 2011 from female subjects aged from 60 to 83. The bar graphs are in order of age. Compare with **Figure 3**. (a) $[Cu]_H$ and $[Ti]_H$. Almost all the subjects have $[Cu]_H < 10$ by Eq. (3). The $[Ti]_H$ level by Eq. (2) is high for all the subjects; $[Ti]_H > 1000$ for the several subjects with the maximum of 3000 for F122 (age: 69). (b) $[Ca]_H$ and $[Sr]_H$. All the subjects have $[Ca]_H \leqq 10$ due to PTH-regulated Ca channel closing. (c) $[Cl]_H$ and $[Br]_H$. As a whole, $[Cl]_H$ ($[Br]_H$) is lower than that for **Figure 3** by a deviation to alkalosis with a high $[Ca^{2+}]$ in serum. Also, see the correspondence between very high $[Ti]_H$ in (a) and high $[Cl]_H$ ($[Br]_H$). (d) $[K]_H$ and $[S]_H$. The lower standard $[S]_H = 20$ is due to breathing S in the polluted air. (e) $[Zn]_H$ and $[Fe]_H$ normalized by Eq. (3). All the subjects have low $[Zn]_H$ values (1/4 of the normal), with the standard $[Fe]_H$ for many subjects.

polluted air (yellow sands) has an effect as if Ca supplements were taken. However, to increase Ca stored in serum protein to the normal $[Ca]_H = [Ca]_P = 10$, long-term Ca supplementation over 2 months with 900 mg/day is required. Therefore, the closing of PTH-regulated Ca

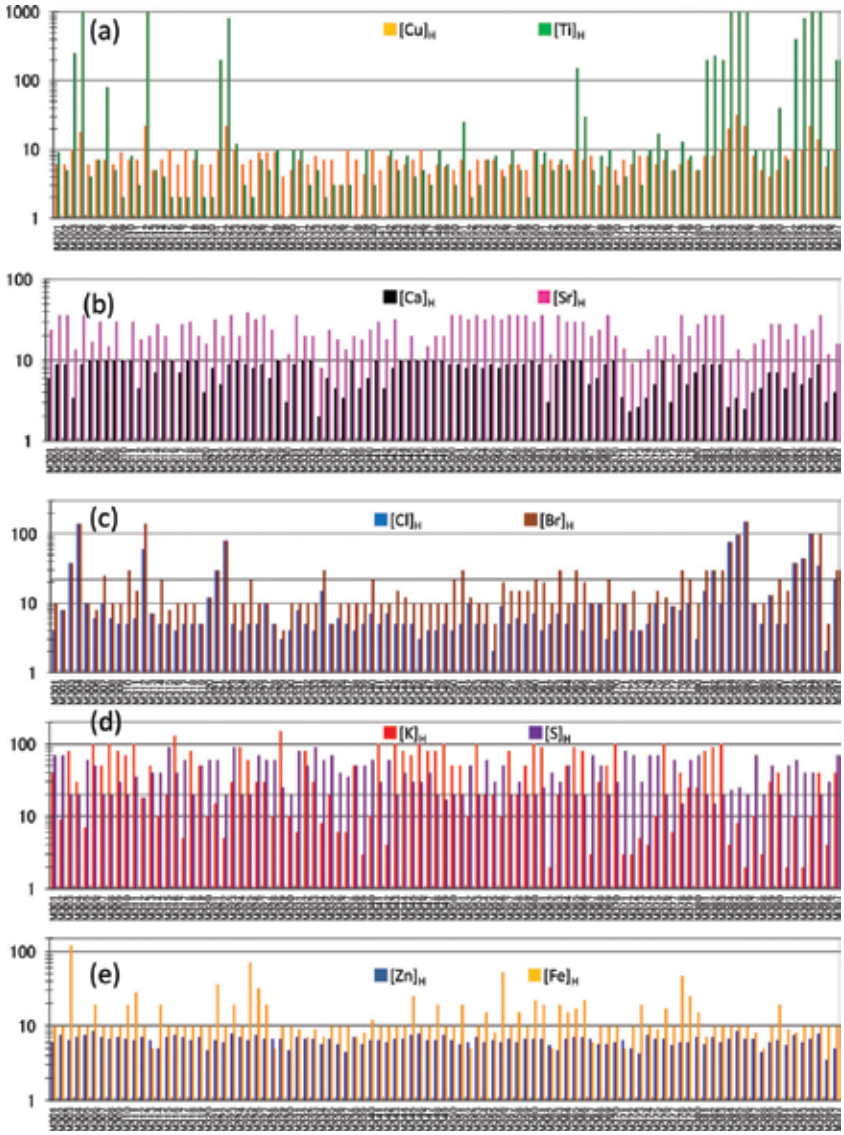

Figure 6. Effect of the air pollution on elements in hair root obtained in February 2011 from male subjects aged from 26 to 87. The bar graphs are in order of age. Compare with **Figure 3**. (a) $[Cu]_H$ and $[Ti]_H$. Almost all the subjects have $[Cu]_H < 10$ by Eq. (3). The high $[Ti]_H > 1000$ is seen for several subjects with the maximum of 3000 for M385 (age: 75). (b) $[Ca]_H$ and $[Sr]_H$. All the subjects have $[Ca]_H \leqq 10$ due to PTH-regulated Ca channel closing. (c) $[Cl]_H$ and $[Br]_H$. As a whole, $[Cl]_H$ ($[Br]_H$) is lower than that for **Figure 3** by a deviation to alkalosis with a high $[Ca^{2+}]$ in serum. Also, see the correspondence between very high $[Ti]_H$ in (a) and high $[Cl]_H$ ($[Br]_H$). (d) $[K]_H$ and $[S]_H$. The lower standard $[S]_H = 20$ is due to breathing S in the polluted air. (e) $[Zn]_H$ and $[Fe]_H$ normalized by Eq. (3). All the subjects have low $[Zn]_H$ values (1/4 of the normal), with the standard $[Fe]_H$ for many subjects.

channels results in activation of the store-operated Ca channels; all the female subjects in **Figures 4** and **5** and almost all male subjects in **Figure 6** have $[Ca]_H < 10$ with $[Sr]_H/[Ca]_H = 4$ or $[Ca]_H = 10$ with $1 < [Sr]_H/[Ca]_H \leqq 4$ produced by store-operated Ca channel opening. In other words, the pollution mainly changes the Ca channel gating into the store-operated type, which, if

this is by activation of the STIM proteins, inhibits voltage-gated Ca^{2+} channels ($Ca_v1.2$) responsible for activating heart muscle cells [33]. This may be taken as a risk factor for cardiovascular mortality (especially in cardiac patients) and to a lesser degree, for all persons.

5.2. Deterioration of molecular pumps in membrane by the pollution

Both the $[K]_H$ and $[S]_H$ for the same subjects are shown in **Figures 4–6(d)**. As seen in **Figure 3(d)**, almost all subjects without air pollution have low $[K]_H < 10$ and high $[S]_H = 200$ due to the PTH inhibition of both the excretion of H^+ (K^+/H^+ exchange in the cells) and the reabsorption of SO_4^{2-} in renal tubules, respectively [32]. The deficiency of SO_4^{2-} in serum causes ion channel gating into cells, through which SO_4^{2-} inflows into HM cells to give $[S]_H = 200$ (maximum by Eq. (8) in **Table 1**). However, the air pollution (apparently containing sulfur species) increases $[SO_4^{2-}]$ in serum in addition to the $[Ca^{2+}]$ increase as have been seen in **Figures 4–6(b)**, resulting in the lower level $[S]_H = 20$ due to ion channel closing. In **Figures 4–6(d)**, many subjects have the normal $[S]_H = 20$, which had been seldom seen without air pollution (before 2009) due to common dietary Ca deficiencies. We can conclude that the air pollution overfills $[Ca^{2+}]$ and $[SO_4^{2-}]$ in serum.

$[K]_H$ is proportional to the intracellular [K], which strongly depends on K^+ transfer between cell and serum which is influenced by β-catecholamines, insulin, aldosterone, pH, and osmolality [36]. Each hair analysis gives the mean concentration for about 3 days (Section 2) and primarily shows the H^+/K^+ exchange depending on pH. In acidosis, H^+ ions move into cells and, to maintain electrical balance, K^+ ions move out into the serum, resulting in a low $[K]_H$, and vice-versa in alkalosis. The pollution increases the serum $[Ca^{2+}]$ and shifts the subject from acidosis to alkalosis. Therefore, there seen many high values of $[K]_H$ in **Figures 4–6(d)**. However, the $[K]_H$ values never reach the maximum level of $[K]_H = 200$ seen in **Figure 3(d)**. Since it is the maximum that is proportional to the serum $[K^+]$ [5], the $[K]_H$~100 observed as the maximum indicates the serum $[K]_S$ at about a half of the normal, that is, hypokalemia defined as a $[K]_S < 3.5$ mmol/L, as opposed to the normal 5 mmol/L [23]. The maximum $[K]_H = 200$ can be reached by pumping K ions by the molecular pump, Na^+/K^+-ATPase, which expels three sodium ions from the cell and takes in two potassium ions. If the pumping power deteriorates, therefore, the decrease of the $[K]_H$ maximum level must occur with an increase of $[Na]_H$. This can be seen in the typical example, **Figure 2(b)**, for a hair sample (F150) having a high $[Ti]_H$ from PM pollution; the Na Kα peak at 1.04 keV appears clearly, in contrast to the nonpolluted samples in **Figure 2(a)**. Despite the high internal absorbance of sodium's 1.04 keV X-ray emission, such Na peaks were observed for many subjects in **Figures 4–6**. It may be concluded that the function of Na^+/K^+-ATPase in cell membrane is deteriorated by the pollution.

Molecular ion pumps such as Na^+/K^+-ATPase work with the energy supply of fully phosphated ATP. Therefore, serum [P] is important in their deterioration. Both of P and Ca in serum are closely associated in an equilibrium relation with bone. The effect of the pollution on hair $[P]_H$ is seen in **Figure 7**; **Figure 7(a)–(d)** shows $[P]_H$ values observed for the hair samples in **Figures 3–6**. As has been reported [5], hair has the upper level of $[P]_H \gtrsim 10$ and lower level of $[P]_H = 5$ by Eq. (2). In **Figure 7(a)** without pollution, 12 out of 50 males and 7 out of 50 female subjects have the upper level $[P]_H \gtrsim 10$. Usually, $[P]_H < 5$ lower than the standard cannot be observed without air pollution [**Figure 7(a)**]. With the pollution, however, many hair samples

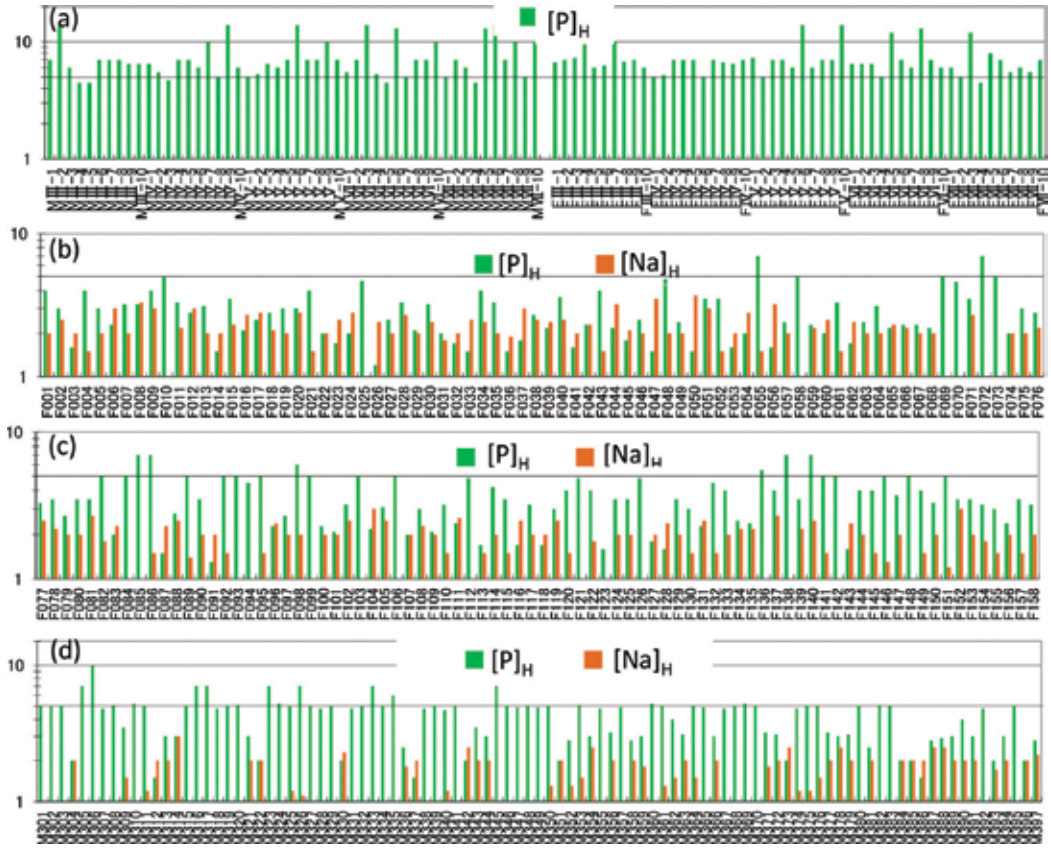

Figure 7. Association between $[P]_H$ and $[Na]_H$ with inactive Na^+/K^+-ATPase due to the air pollution. (a) $[P]_H$ without air pollution for the male and female subjects in **Figure 3**. The upper and lower levels are seen at $[P]_H \gtrsim 10$ and $[P]_H = 5$, respectively. $[Na]_H$ is not seen by the normal Na^+/K + -ATPase. (b) and (c) show $[P]_H$ and $[Na]_H$ for the female subjects in **Figures 4** and **5**, respectively. $[P]_H$ lower than the usual lower level is seen with the appearance of $[Na]_H$ peak. (d) $[P]_H$ for the male subjects in **Figure 6**; the low $[P]_H$ is accompanied by the $[Na]_H$ peak. The low $[P]_H$ values are often seen for the male over 60 (M351: 63). The abnormally low $[P]_H$ indicates insufficient energy supply to the Na^+/K^+-ATPase. Breathing the polluted air increases serum $[Ca^{2+}]$ which moves to bone, accompanied by P to cause P deficiency.

in **Figure 7(b)–(d)** showed $[P]_H$ = 1.5–3.5, much lower than the usual lower level. Also, the upper level $[P]_H \gtrsim 10$ is not seen, except for the subject labeled "M306," in **Figure 7(b)-(d)**. As a whole, $[P]_H$ is decreased by the air pollution; by Eq. (19) in **Table 1**, serum $[P]_I$ ($[HPO_4^{2-}]$) is calculated to be a half of the normal for $[P]_H = 3.5$ and 1/4 for $[P]_H = 2.5$, taking $[P]_H = 5$ for the lower standard. This serum $[P]_I$ decrease may be explained as the pollution-induced excess Ca moving with P to bone by forming insoluble Ca × PO_4; serum HPO_4^{2-} moving to bone must lower serum $[P]_S$ [20, 22, 32], and the deterioration of molecular pumps seems due to insufficient energy supply. Therefore, we can see the correlation between $[P]_H$ and $[Na]_H$; the low $[P]_H$ is accompanied by appearance of $[Na]_H$ peak as seen in **Figure 7(b)-(d)**. ($[Na]_H$ peaks were not seen in **Figure 7(a)** without pollution).

The serum [K] is regulated with free filtration at the glomerulus and by excretion-reabsorption in renal tubules. The reabsorption is produced by H^+/K^+-ATPase [36] which is also deteriorated by the insufficient ATP supply, resulting in the hypokalemia understood from the hair level. This pollution's effect is serious; even mild or moderate hypokalemia increases the risks of morbidity and mortality in patients with cardiovascular disease [36, 37].

According to the meta-analysis for 57,158 patients with acute myocardial infarction (AMI) [37], primary ventricular fibrillation (PVF) is lethal and occurs without signs or symptoms of heart failure or cardiogenic shock. It was shown that patients with PVF had a lower serum K level before the event compared with patients without PVF. Though the weighted mean difference was small (−0.27 mmol/L), the finding of lower serum K before PVF was very consistent. The association between low [K] and PVF was confirmed in clinical settings. Patients with PVF have lower heart rates for interior AMI and higher rates for anterior AMI. It can be concluded that the hypokalemia due to PM causes a mortality increase in AMI [25, 26] even 1 day after PM pollution increases. Also, it is well known that PVF results in blood stagnation in atrium to form clots having the risk for brain infarction.

The $[P]_H$ decrease as observed in **Figure 7** never takes place with oral Ca supplementation, which leads to the upper level $[P]_H \geqq 10$ with $[Cl]_H = [Br]_H = 10$ [5]. The direct Ca intake by breathing the polluted air into the lung is essentially different from absorption through the GI tract and produces deficiency in the intracellular main ions [23], HPO_4^{2-} and K^+.

In observation of [Na] and [P] by FXA, absorption of the Na Kα and P Kα by the specimen must greatly reduce the number of 1.04 and 2.01 keV photons reaching the detector. However, although low keV X-rays are received from only the hair surface, the calculation of concentration of *P*/*S* by Eq. (2) is valid because the absorption for the peak *P* and background *S* is produced by the same matrix. The observation of $[Na]_H$ increase and $[P]_H$ decrease is consistent with the emerging pattern and should not be dismissed because of the low sampling volume inherent.

5.3. Reduction of serum Cu and Zn with the pollution

Another effect of the pollution is the decrease of $[Cu]_H = [Cu]_S$ and $[Zn]_H = [Zn]_S^2$ [with the definition by Eq. (2)]. As seen from the comparison of **Figures 4–6(a)** and **(e)** with **Figure 3(a)** and **(e)** showing their normalized values by Eq. (3), most subjects have the normal $[Fe]_H = 10$ independent of pollution, but decreases of Cu and Zn, $[Cu]_H < 10$ and $[Zn]_H < 10$, are seen with the pollution. The $[Cu]_H$ decrease depends upon age, and many subjects older than 60 have $[Cu]_H = [Cu]_S < 5$ less than a half of normal. The $[Zn]_H$ decrease takes place about equally for the male and female populations studied. We estimate the average hair zinc level in **Figures 4–6(e)** to be 1/4 of normal, that is, the air pollution therefore decreases serum $[Zn]_S$ to half of normal by Eq. (6) in **Table 1**. The decrease in serum Cu and Zn may be due to S inflow into serum from air pollution, which then forms compounds such as CuS and ZnS which may be excreted from the liver and pancreas, respectively. Both Cu and Zn are essential elements. For Zn, the normal serum concentration is in the range of 0.08–0.15 mg/dL, and its lower limit is 0.06–0.07 mg/dL. A decrease by half is therefore dangerous.

Zinc serves as a structural center for maintaining the higher-order structure of protein. Zinc participates in the activity of more than 70 enzymes, including carbonic anhydrase (CA) and dehydrogenase. Almost all proteins related to gene expression contain Zn as a DNA-binding motif "zinc finger." Zinc is essential for physiological functions such as growth, gestation, taste, and participates in immunity, brain development, insulin biosynthesis, and so on [38]. Therefore, the air-pollution's effect on serum Zn is serious to many aspects of health.

The reduction of serum $[Cu]_S$ due to the pollution can also give an answer to the question of the increase of myocardial infarction mortality. It is firmly established that the formation of elastin protein, which gives elasticity to blood vessels, is copper-dependent [39–41], and Cu deficiency degenerates smooth muscle cells in the aortic walls. It was observed that elastin increases at the damage sites (scar) on aortic walls [41]. This indicates that elastin is necessary to correct damages, which, if unrepaired, trigger both aortic rupture and infarction. Therefore, the Cu deficiency due to PM can cause a mortality increase of myocardial infarction [25].

Here, it should be noted that we encountered many subjects having the normal $[S]_H = 20$ in **Figures 4–6(d)**, in contrast to **Figure 3(d)** showing $[S]_H = 200$. This observation indicates that the serum [S] remains normal by excreting the excess [S] incorporated from the pollution together with Cu, and Zn [implying the essentiality for some sulfur species, referred to as sulfate, having its own or accessible ion channels. See **Figure 2(a)**].

6. Differences in pollution effect between the sexes

The normal levels of hair elements are the same for male and female. However, the pollution effects show differences as seen clearly in **Figures 4–7**. As described in Section 4, male and female deal with Ca deficiency differently; DO type is more common for the mail, and LD type is more common for the female, that is, males tolerate Ca deficiency with Ca channels closed by bone resorption, and females have a tendency to open the PTH-regulated Ca channels without bone resorption. The resulting Ca and/or Sr inflow through the channels causes deterioration of the hepatocytes' function to excrete pollutants into bile; a dysfunction that persists for months. Consequently, the pollution effect appears greater for the female; more female subjects have the high $[Ti]_H$ as seen in **Figures 4–6(a)**.

In **Figure 7**, the appearance of $[Na]_H$ due to the excess serum Ca by breathing the polluted air shows difference between the sexes clearly; male can accommodate the excess Ca on serum protein as expected from the fact that DO type is more common for male.

The pollution's effect to decrease $[Cu]_H$ and $[Zn]_H$ can be recognized in **Figures 4–6(a)** and **(e)**. However, no difference between the sexes is clear; this implies these elements have no relation to the Ca metabolism, suggesting an association with the excess [S] in serum due to the pollution. By forming sulfide species, zinc and copper are excreted mainly with pancreatic fluid and bile into the gut, respectively.

The observed relation between the sexes leads to the conclusion that the serum element levels change so as to eliminate the excess Ca and S inhaled from the air pollution.

7. Conclusion

Hair calcium depends on both PTH-regulated and store-operated Ca^{2+} channels; oral Ca supplementation transits hair Ca level from the Ca upper level ($[Ca]_H = 50$) to the lower level (normal $[Ca]_H = 10$) by closing PTH-regulated Ca channels of hair matrix cells (HM cells), and gives no effects on the store-operated channels which are activated by the decrease of stock Ca bound on serum protein. In-vitro studies ([16–18] show store-operated "Orai" Ca channels activate when Ca^{2+} stores are depleted at the endoplasmic reticulum (ER). Together with hair studies (in vivo), our analysis concludes that the store-operated and PTH-regulated Ca channels activate with depletion of $[Ca]_P$ and $[Ca]_I$ in Eq. (1), respectively, both of which are regulated by PTH.

Without air pollution before 2009, a half of the 100 subjects were classified as mildly calcium-deficient DA type ($[Ca]_H = [Ca]_P < 10$ with $[Cl]_H > > 10$), and the other half are of more severe Ca deficiency related to PTH-regulated Ca channels ($[Ca]_I < 10$).

The air pollution from February to March 2011 overfilled Ca ($[Ca^{2+}]$) and S ($[SO_4^{2-}]$) in serum. Consequently, except one patient with parathyroid gland dysfunction, all the subjects had the normal or lower $[Ca]_H \lesssim 10$ (with $[Cl]_H < 10$) produced by closed PTH-regulated Ca channels, and almost all the subjects had store-operated Ca channel gating, which, if done by the STIM proteins, inhibits voltage-gated Ca channels and worsens cardiac risks.

The overfilled Ca and S in serum has consequences: we expect that Ca is removed as the phosphate to bone and S is removed to bile and pancreatic fluid as excretable metal sulfides, resulting in loss of needed Zn and Cu. Serum [K] as well as [Cu] and [Zn] decrease to half of the normal level with air pollution. The excessive Ca^{2+} results in a notable deficiency of serum [P]. It must create a shortage of ATP, which deteriorates cell membrane molecular pumps such as H^+/K^+-ATPase and Na^+/K^+-ATPase, responsible for the renal K reabsorption, resulting in hypokalemia to produce fatal ventricular fibrillation in patients with myocardial infarction accompanied with heart rate variability [26]. It is well known that even mild or moderate hypokalemia increases the risks of mortality in patients with cardiovascular diseases. Abnormal intracellular [K] and [Na] due to the inactive molecular pumps may be also responsible for heart rate variability. (K^+ and Na^+ regulate and form the electric pulses commanding myocardial movement.)

The excessive [S] in serum may decrease toward the normal by forming sulfide compounds with Cu and Zn, which are excreted from the liver and pancreas, resulting in deficiency of Cu necessary for the formation of elastin protein to repair damage in blood vessels. Thus, the sulfur species in the pollution may provide a second increase the mortality in myocardial infarction [25].

In summation, hair analysis shows that post-2009 air pollution causes serious deficiencies in serum K, P, Cu, and Zn, and is likely responsible for various diseases.

Finally, it is emphasized that the deterioration of Na^+/K^+-ATPase (**Figure 7**) is a serious pollution effect because Na^+/K^+-ATPase exists in all cells, for example, more than half of brain energy dissipation is due to Na^+/K^+-ATPase; the pollution effect on neurodegenerative disease [42] is conceivable.

Acknowledgements

This work has been performed under the approval of the Photon Factory (Proposal No. 2005R15, 2006G408, 2009Y011, 2009Y022, 2010Y023) in collaboration with industry (Health Analysis Laboratory, Ltd.). The authors would like to express their sincere thanks to Professor A. Iida, Photon Factory, for his great help with the experiments at BL-4A. His sophisticated instrumentation made it possible to analyze the hair roots from thousands of people.

Author details

Jun-ichi Chikawa[1]*, Jeremy Salter[1], Hiroki Shima[2], Takaaki Tsuchida[3], Takashi Ueda[4], Kousaku Yamada[1] and Shingo Yamamoto[5]

*Address all correspondence to: chikawa@hyogosta.jp

1 Hyogo Science and Technology Association, Himeji, Japan

2 Shima Institute in Quantum Medicine, Osaka, Japan

3 National Cancer Centre, Tokyo, Japan

4 Ueda Heart Clinic, Tatsuno-shi, Hyogo, Japan

5 Hyogo College of Medicine, Nishinomiya, Hyogo, Japan

References

[1] Iida A, Noma T. Nuclear Instruments & Methods. 1993;**B82**:129-138

[2] Ito A, Inoue T, Kawai T, Taki Y, Inoue S, Shimizu T, Shinohara K. AIP Conference Proceedings 1696. 020021-1-5; 2016

[3] Noguchi T, Itai T, Kawaguchi M, Takahasshi S, Tanabe S. Applicability of human hair as a bioindicator for trace elements exposure. In: Kawaguchi M, Misaki K, Sato H, Yokokawa T, Itai T, Nguyen TM, Ono J, Tanabe S, editors. Environmental Chemistry. Vol. 6. Tokyo: Terra Scientific Publishing; 2012. pp. 73-77

[4] Chikawa J, Yamada K, Akimoto T, Sakurai H, Yasui H, Yamamoto H, Okabe S, Ebara M. Journal of X-Ray Science and Technology. 2007;**15**:109-129

[5] Chikawa J, Mouri Y, Shima H, Yamada K, Yamamoto H, Yamamoto S. Journal of X-ray Science and Technology. 2014;**22**:471-491

[6] Chikawa J, Mouri Y, Shima H, Yamada K, Yamamoto H, Yamamoto S. Journal of X-ray Science and Technology. 2014;**22**:587-603

[7] Dockery DW, Pope CA III, Xu X, Spengler JD, Ware JH, Fay ME, Ferris BG Jr, Speizer FE. The New England Journal of Medicine. 1993;**329**:1753-1759

[8] Pope CA III, Thun MJ, Namboodiri MM, Dockery DW, Evans JS, Speizer FE, Heath CW Jr. American Journal of Respiratory and Critical Care Medicine. 1995;**151**:669-674

[9] Pope CA III, Burnett RT, Thun MJ, Calle EF, Krewski D, Ito K, Thurston GD. Journal of the American Medical Association. 2002;**287**:1132-1141

[10] Ueda K, Nitta H, Ono M, Takeuchi A. Journal of the Air & Waste Management Association. 2009;**59**:1212-1218

[11] Creamean JM, Suski KJ, Rosenfeld D, Cazorla A, DeMott PJ, Sullivan RC, White AB, Ralph FM, Minnis P, Comstock JM, Tomlinson JM, Prather KA. Science. 2013;**339**: 1572-1578

[12] Goudie AS, Middleton NJ. Desert Dust in the Global System. Amsterdam: Springer; 2006

[13] Grousset FG, Ginoux P, Bory A, Biscaye PE. Case study of a Chinese dust plume reaching the French Alps. Geophysical Research Letters. 2003;**30**:1277-1280

[14] Husar RB, Tratt DM, Schichtel BA, Falke SR, Li F, Jaffe D, Gassó S, Gill T, Laulainen NS, Lu F, Reheis MC, Chun Y, Westphal D, Holben BN, Gueymard C, McKendry I, Kuring N, Feldman GC, McClain C, Frouin RJ, Merrill J, DuBois D, Vignola F, Murayama T, Nickovic S, Wilson WE, Sassen K, Sugimoto N, Malm WC. Journal of Geophysical Research. 2001;**106**:18317-18330

[15] Fernandez TA, Casan CP. Archivos de Bronconeumología. 2012;**48**:240-246

[16] Cahalan MD. Science. 2010;**330**:43-44

[17] Park CY, Shcheglovitov A, Dolmetsch R. Science. 2010;**330**:101-105

[18] Wang Y, Deng X, Mancarella S, Hendron E, Eguchi S, Soboloff J, Tang XD, Gill DL. Science. 2010;**330**:105-109

[19] de Groot T, Lee K, Langeslag M, Xi Q, Jalink K, Bindels RJM, Hoenderop JGJ. Journal of the American Society of Nephrology. 2009;**20**:1693-1704

[20] Favus MJ, Bushinsky DA, Lemann J Jr. Regulation of calcium, magnesium, and phosphate metabolism. In: Favus MJ, editor. Primer on the Metabolic Bone Diseases and Disorders of Mineral Metabolism (Chapter 13, 6th edition). American Society for Bone and Mineral Research: Washington, DC; 2006. pp. 76-83

[21] Osaki T, Takeuchi S. Analytical Chemistry. 2017;**89**:216-231

[22] Brown EM, Jüppner H. Parathyroid hormone: Syntheses, secretion, and action. In: Favus MJ, editor. Primer on the Metabolic Bone Diseases and Disorders of Mineral Metabolism (Chapter 15, 6th edition). Washington, DC: American Society for Bone and Mineral Research; 2006. pp. 90-99

[23] Gamble JL. Chemical Anatomy, Physiology and Pathology of Extracellular Fluid: A Lecture Syllabus. Cambridge, MA: Harvard University Press; 1949

[24] Kraut JE, Madias NE. Clinical Journal of American Society of Nephrology. 2007;**2**:162-174

[25] Mustafic H, Escolano S, Empana P. JAMA. 2012;**307**:713-721

[26] Pope CA III, Verrier RI, Lovett EG, Larson AC, Raizenne ME, Kanner RE, Schuwartz J, Villegas GM, Gold DR, Dockery DW. American Heart Journal. 1999;**138**:890-899

[27] Pope CA III, Muhlestein JB, May HT, Renlund DG, Anderson JL, Horne BD. Circulation. 2006;**114**:2443-2448

[28] Cornelis R, Fuentes-Arderiu X, Bruunshuus I, Templeton D. Pure and Applied Chemistry. 1997;**69**:2593-2606

[29] Aksirov AM, Gerasimov VS, Kondratyev VI, Korneev VN, Kulipanov GN, Lanina NF, Letyagin VP, Mezentsev NA, Sergienko PM, Tolochko BP, Trounova VA, Vazina AA. Nuclear Instruments & Methods. 2001;**A470**:380-387

[30] Fujita T. Journal of Bone and Mineral Metabolism. 1998;**16**:195-205

[31] Fujita T, Palumieri GMA. Journal of Bone and Mineral Metabolism. 2000;**18**:109-125

[32] Bringhurst FR. Physiologic actions of PTH and PTHrP II. Renal actions. In: Bilezikian JP, Marcus R, Levine MA, editors. The Parathyroids, Basic and Clinical Concepts (Chapter 14, 2nd edition). San Diego: Academic Press; 2001. pp. 227-243

[33] Clapham DE. Cell. 2007;**131**:1047-1058

[34] Fujita T. Journal of Bone and Mineral Metabolism. 1996;**14**:31-34

[35] Zhang R, Shen Z, Cheng T, Zhang M, Liu Y. Aerosol and Air Quality Research. 2010;**10**: 67-75

[36] Greenlee M, Wingo CS, McDonough AA, Youn J-H, Kone BC. Annals of Internal Medicine. 2009;**150**:619-625

[37] Gheeraert PJ, De Buyzere ML, Taeymans YM, Gillebert TC, Henriques JP, De Backer G, De Bacquer D. European Heart Journal. 2006;**27**:2499-2510. [PMID: 16952926]

[38] Cunnane SC. Zinc, Clinical and Biochemical Significance. CRC Press; 1988

[39] Miller EJ, Martin GR, Mecca CE, Piez KA. The Journal of Biological Chemistry. 1965;**240**: 3623-3627

[40] Prohaska JR, Heller L. The Journal of Nutrition. 1982;**112**:2142-2150

[41] Wildgruber M, Bielicki I, Aichler M, Kosanke K, Feuchtinger A, Settles M, Onthank DC, Cesati RR, Robinson SP, Huber AM, Rummeny EJ, Walch AK, Botnar RM. Assessment of myocardial infarction and postinfarction scar remodelling with an elastin-specific magnetic resonance agent. Circular Cardiovascular Imaging. 2014;**7**:321-329

[42] Kioumourtzoglou M-A, Schwartz JD, Weisskopf MG, Melly SJ, Wang Y, Dominici F, Zanobetti A. Environmental Health Perspectives. 2016;**124**:23-29

Chapter 4

Relation of Trace Elements on Dental Health

Mehmet Sinan Doğan

Additional information is available at the end of the chapter

http://dx.doi.org/10.5772/intechopen.75899

Abstract

Trace elements (TEs) play an important role in human health. Toxic effects are caused by deficiency or excess of TEs. TEs have significant effects on both dental health and human health. It participates in important biological polyphosphate compound functions such as ATP, DNA, and RNA. TEs are present at different concentrations in the tooth structure. Changes in the density of some TEs affect tooth. The alteration of the density of some TEs makes the teeth more susceptible to caries. Others are protective against caries formation. Important TEs zinc (Zn), phosphorus (P), and magnesium (Mg) have important effects on dental health. Measuring the TE values through tissue sampling to identify and correct these effects has an important effect. In general, tissue samples such as blood, urine, teeth, nails, and hair are used in TE studies. Teeth are accepted as appropriate indication of TEs. As a result, TEs have significant effects on healthy tooth formation.

Keywords: trace elements, teeth health, human health, dental caries, dental structure

1. Introduction

About 96% of life materials consist of carbon, hydrogen, and nitrogen elements. Almost 50% of the known elements are at measurable concentrations in life system. In humans and other mammals, physiological activities of 23 elements are known, 11 of which are classified as trace elements (TEs). TEs consist of transition elements [vanadium, chromium, manganese (Mn), iron (Fe), cobalt, copper (Cu), zinc (Zn), and molybdenum] and non-metal elements [selenium (Se), fluorine, and iodine]. TEs are, unlike sodium, calcium, magnesium, potassium, and chlorine, which are considered as macronutrients and required at larger amounts, fall into the micro-nutrient category, which is required at negligible levels (usually lower than 100 mg/day). Major and TEs play an essential role in human health. Lack or abundance of these elements due to natural or man-made reasons can lead to critical clinic consequences [1–4].

A tooth consists of hard tissue (enamel, dentine, and cement) and soft tissue (pulp and periodontal ligaments), and has TE in its structure. A tooth has a multicellular structure which can cooperate functionally with maxillofacial area [5].

2. Enamel

Enamel is the hard tissue that covers the surface of the tooth. The function of this layer is to protect dentine-pulp complex. Enamel is the hardest and most resistant tissue in the body. It consists of 95% inorganic material (calcium hydroxyapatite crystals), 2% organic material (proteins such as amylogenic, enameline, ameloblastin, and tuftelin, among others), and 3% water [6–8]. A negligible part of the 95% inorganic material is represented by TEs. As a result of the analyses conducted using different methods in tooth enameling several chemical components are observed. These components include phosphorus (P), calcium (Ca), magnesium (Mg), zinc (Zn), lead (Pb), cobalt (Co), fluorine (F), iron (Fe), aluminum (Al), and selenium (Se). Inorganic structure of enamel consists of 36.1 Ca, 17.3 P, 3.0 carbon oxide, 0.5 Mg, 0.2 Na, 0.3 potassium (K), 0.016 F, 0.1 sulfur (S), 0.01 copper (Cu), 0.016 Zn, 0.003 silicon (Si); and low levels of silver (Ag), strontium (Sr), barium (Ba), chromium (Cr), manganese (Mn), vanadium (V), aluminum (Al), lithium (Li), and selenium (Se). TE is placed in the human tooth enamel from the environment during and after the mineralization and maturation period of the tooth [9].

3. Dentin

The dentin consists of 70% inorganic material (hydroxyapatite crystals and TEs), 18% organic material (type I collagen fiber and proteins such as osteonectin, osteopontin, osteoclastin-like dentin Gla protein, dentin phosphorene, dentin matrix protein, and dentin sialoprotein) and 12% water [6–8].

The inorganic material of dentin contains about 40 elements, ranging from 1000 ppm (i.e., Zn, Sr., Fe, Al, B, Ba, Pb, etc.) to 100 ppb (i.e., Ni, Li, Ag, As, Se, Nb, Hg, etc.) [10–12].

The ratio of TE in human dentin varies according to age and sex. Cobalt can be higher in women, while lead can be higher in men [13].

4. Cementum

Cementum is a special connective tissue that connects the periodontal ligament to the root surface, covering the outermost layer of the calcite matrix on the root surface [14].

Cement is a vascular and unlimited mineralized tissue. It is the interface between dentin and periodontal ligament and contributes to the repair and renewal of periodontal tissue after injury [15].

The inorganic component of cement is similar to bone, dentin, and enamel. The basic mineral component of the cement is hydroxyapatite with amorphous calcium phosphate (Ca10 (PO4) 6 (OH) 2). The crystallinity of the cement inorganic component is lower than other calcifying tissues [16]. As a result, cement is decalcified more easily, while it has a tendency to coalesce for the adsorption of surrounding ions (i.e., fluoride). In general, the cement of adult mature teeth has higher fluoride content compared to other calcifying tissues. Mg content of the cement is about half of that in the dentin. There is a gradual increase in Mg in the deep layers of the cement [14].

5. Dental pulp

Tooth pulp developing from dental papilla consists of odontoblast, fibroblast, blood, and neural veins [17]. Odontoblast cells are the most important cells of the pulp. As the cells responsible for the construction of dentin and pre-dentin, they are also responsible for reparative dentin make-up in pathological cases [5, 18]. Pulp cells, especially fibroblasts, produce several inflammatory mediators such as IL-8, IL-6, and vascular endothelial growth factor in cases which threaten the health of the pulp. Tooth pulp performs a series of biological activities such as nutrition, sensitiveness, construction, and protection. The change in blood pressure and flow in the veins coming from apical region essentially affects the health of the pulp. When tooth pulp is damaged due to mechanical, chemical, thermal and microbial irritants, local tissue reactions and lymphatic, vascular inflammatory responses occur. The existence of dentin affected by oral bacteria which lead to the formation of caries is most important reasons for pulp inflammation [19].

Dental caries is a microbiological infectious disease of the teeth that results in the destruction of dental calcified tissues. There must be three factors for the formation of dental caries; bacteria (from mutans Streptococci and Lactobacillus species), susceptible tooth surface (host), and nutrient (diet) to provide bacterial growth [20, 21]. Changes in the density of TEs due to some environmental and genetic impacts have some effects on human and dental health. The change in density of some elements can lead to dental caries. Based on the previous studies on humans and animals, some classifications have been made on the impact of TE on dental caries [4, 9].

Cariostatic elements: Fluoride (F), Phosphorus (P).

Mildly cariostatic: Mo, V, Cu, Sr., B, Li, Au.

Doubtful: Be, Co, Mn, Sn, Zn, Br, I.

Caries inert: Ba, Al, Ni, Fe, Pd, Ti.

Caries promoting: Se, Mg, Cd, Pt, Pb, Si.

In addition, there is another classification with regard to the impact of TE on dental health:

Cariostatic elements: Molybdenum, Vanadium, Fluoride, Strontium, Lithium.

Caries-promoting elements: Selenium, Cadmium, Lead, Manganese, Copper, Zinc.

The effect on dental and oral tissues of elements and their features.

6. Fluoride (F)

Fluoride is an essential part of the organized matrix in hard tissues such as teeth and bones and is found in the form of fluorapatite. In addition, it can combine with calcium and stimulate osteoblastic activity. The daily recommended amount of fluoride is 0.7 mg for 1–3 ages, 1 mg for 4–8 ages, 2 mg for 9–13 ages, 3 mg for 14–18 ages, 4 mg for males above 18 years of age and 3 mg for females above 18 years of age.

Fluoride need of the body is met by drinking water, food, and tea [22].

The most well-known function of fluorine is a prevention of tooth caries. As a result of the changes created by this function dental structure, the resistance of enamel increases. In addition, it prevents the proliferation of bacteria in dental plaque. It also accelerates remineralization [4, 23].

However, during calcification of the teeth, it can lead to dental fluorosis due to excessive fluorine concentration. Dental fluorosis is a kind of enamel hypoplasia. Dental fluorosis has varying strengths from lesions in the form of white small spots on the enamel to loss of material in dental structure. The impact of excessive fluoride intake on the dental structure is a function of such factors as the fluoride concentration in drinking water, exposure amount, exposure period, and development period of the tooth [24, 25].

7. Vanadium (V)

Vanadium is found naturally in the soil, water, and air. Natural sources of vanadium include continental dust, sea aerosol, and volcanic emissions. The release of vanadium is associated with industrial sources such as oil refineries and power plants, especially using vanadium-rich petroleum and coal. Most foods contain naturally low vanadium concentrations. Sea products generally contain vanadium at a higher concentration than the meat of land animals. Daily vanadium uptake was reported in the range of 0.01–0.02 mg [26].

Although the role of vanadium in the development of dental caries is not clear, animal studies showed that it reduces dental caries. It is seen that when hamsters on Cariogenic diet are given vanadium, the formation of dental caries decreased. In addition, a study conducted on rats reported that when they are given intraperitoneal vanadium, the formation of dental caries reduced. On the contrary, some studies on monkeys showed that monkeys fed with water including vanadium content suffered from higher dental caries incidents [4].

8. Strontium (Sr)

Strontium is an element found everywhere in the environment. Stable and radioactive strontium compounds are used in many industrial processes and find applications in research and medical fields. Although strontium is not considered an important element and does not have a known biological role, it is present in all living organisms. Strontium resembles

calcium element in its properties; like calcium, it is taken up and is preferably implanted into the bone. Strontium may have both beneficial and deleterious effects on humans, depending on the amount received [27].

High strontium content is related to low caries incidence. Epidemiological studies conducted on males determined that dental caries cases involve high strontium content. One study compared good and decayed enamels and found out that strontium was higher in the good enamel. In addition, it is reported that strontium ratio in tooth decreased with aging; strontium ratio is found to be higher in young people compared to the elderly [4].

Apatites with strontium settlement are more difficult to remove from enamel compared to pure calcium component and it is stated that solution of enamel remineralized without strontium is more difficult than enamel remineralized with strontium. For this reason, it is believed that strontium adds resistance to hydroxyapatites against the solution. Strontium settlement in tooth enamel makes apatite crystal more resistant to caries due to the hetero-ionic change of calcium. The resistance of apatite crystals against demineralization which occurs as a result of acid attacks is increased [28].

9. Lithium (li)

More than 90% of lithium is eliminated from the human body through the kidney. The human serum has been reported to have a lithium half-life of less than 24 hours [29].

Lithium exposure through drinking water and other environmental sources can also affect thyroid function. Lithium is used in the treatment of bipolar disorders. Lithium is found to have an indirect relationship with tooth caries. It is reported that dental caries incidence reduces in the existence of lithium. One study conducted to control the relation between lithium and dental caries determined that it reduced the dental caries incidence in humans [4]. It has also been reported the histopathologic changes in the structure of salivary glands [30].

Lithium exposure through drinking water and other environmental sources can also affect thyroid function [31**]**.

10. Copper (cu)

Copper plays an essential role in our metabolism as it is involved in the functions of several critical enzymes [28, 32].

Copper is defined as a material which increases caries. In decayed teeth, a higher level of copper is found compared to healthy teeth. Higher caries prevalence is found to be related to the existence of copper in water, food, soil or vegetables [4].

Conducted studies showed that serum copper level is significantly higher in patients with oral leukoplakia and oral submucous fibrosis and also malignant tumors such as squamous cell carcinoma [22].

Copper concentration is found to be higher compared to the enamel of healthy and primary teeth than the enamel of decayed teeth [25].

Recommended daily copper level is 340 mcg/day for 1–3 ages, 440 mcg/day for 4–8 ages, 700 mcg/day for 9–13 ages, 890 mcg/day for 14–18 ages, 900 mcg/day for males and females above 18 years of age, and 1000 mcg/day for pregnant and 1300 mcg/day for nursing women.

Copper is mostly found in oysters, sea animals with shell, whole grains, hazelnuts, potatoes, greeneries with dark leaves, dried fruits and animal products such as kidneys and livers [22].

11. Selenium (se)

Selenium is a vital trace element which is an essential component of antioxidant enzymes. Selenium salts are required for several cellular functions in the human body but their excessive amount is toxic [33].

Selenium is found in liver, kidneys, sea products, meat, grains, grain products, milk products, fruits, and vegetables. The recommended daily intake is 70 micrograms [22].

Selenium is a non-metallic element which is found epidemically in nature and absorbed by the body through food or inhalation. Selenium is reported to be involved in synthetic hydroxyapatite as anionic Se^{+4} through phosphate change with selenite. The ionic radius of Se^{+4} (0.50 Å) is higher than P^{+5} (Phosphate) (0.35 Å) value. For this reason, the fabric parameter increases after it is settled in synthetic hydroxyapatites [34–36].

It is found out that selenium leads to structural changes in dental dentin and mandibular condyles. Increase in dental caries emerged in the case of selenium intake. Some studies show that there is a direct relationship between caries sensitiveness and selenium ejected with urine [4].

It is reported that selenium is settled in the micro-crystal structure of the enamel at the beginning of the decay and made it more sensitive toward dissolution [25].

In addition, it is reported that decrease in selenium level in the body leads to oxidative stresses. A recent study found out that patients with oral mucositis due to a high level of chemotherapy effectively reduced the term and seriousness of oral mucositis and, in addition, sufficient selenium reinforcement can produce cytoprotective impact and antiulcer activity [22, 37].

12. Manganese (Mn)

Manganese content in food products varies considerably. It is highest in peanuts and grains; it is found in lowest concentration in milk products, meat, poultry, fish, and sea products. In addition, manganese can be found in coffee and tea which constitute 10% of daily intake. The body of an adult has 15 mg manganese on average which is typically seen in the nucleic acid. The daily requirement is approximately 2–5 mg/day. Manganese functions are considered as an enzyme activator and a part of metalloenzymes. Manganese is found in all mammal tissues at

concentrations varying from 0.3 to 2.9 ug manganese/g. Tissues rich in mitochondria and pigments (for example, retina, dark skin) tend to have high manganese concentrations. Bones, livers, pancreas, and kidneys typically have higher manganese concentrations than other tissues. The most important manganese store is in the bones. There are 49 elements in enamel hydroxyapatite crystals; one of them is manganese, which is usually in very slight percentages. The manganese concentrations in enamel are between 0.08 and 20 ppm, equivalent to 0.08–20 mg/kg and dentine between 0.6 and 1000 ppm. Mn concentration is at enamel-dentin limit at the external surface of enamel and higher at permanent dentition compared to primary dentition [29, 30].

Manganese is a TE which can be included in enamel through food, air, and water. In addition, Mn has the potential of changing Ca place at HAP. Several studies reported that Mn has the ability to include in synthetic HAP without degrading the crystal area size [34, 38].

Manganese is increasingly related to decay prevalence. One study found out that in areas where manganese content is higher, dental caries incidence in males increased. Therefore, it is emphasized that manganese encourages caries [4].

13. Zinc (Zn)

There are 2–4 grams of zinc scattered throughout the human body. Zinc is stored in the prostate, eye parts, brain, muscles, bones, kidney, and liver. It is the second most abundant transition metal in organisms after iron and is the only metal seen in all enzyme classes. In blood plasma, zinc is carried and bound to albumin (60%) and transferrin (10%). Zinc concentration in blood plasma always remains unchanged regardless of the zinc intake [22, 39, 40].

The daily average requirement of zinc is 15–20 mg/day. Approximately 2–5 mg/day is expelled through pancreas and intestines. Plasma zinc level decreases in such cases as pregnancy, loss of liquid, oral contraceptive usage, blood loss, acute myocardial infarction, infections, and malignity [41].

Zinc plays an essential role in cell reproduction, differentiation, and metabolic activities. Zinc also supports normal growth in pregnancy, childhood, and adolescence periods [28, 42, 43]. Zinc is mostly found in animal products like meat, milk, and in fishes. Zinc bio adjustment is low in phytonutrients [22].

The role of zinc in the development of dental caries is controversial. One study which analyzed the existence of TEs in children found zinc levels of children with more dental caries to be higher. In addition, it has been found out that zinc concentration in caries enamel of milk teeth was higher. However, another study showed that existence of zinc in saliva decreased the development of dental caries [4, 44, 45].

Contrary to the foregoing, zinc is added to oral health products in order to control plaques, reduce halitosis and delay tartar development. The zinc released from mouthwash solutions and toothpastes can continue to exist in plaque and saliva for a long time. Low zinc concentrations can reduce enamel demineralization. However, their anticariogenic impact is still controversial. Zinc deficiency is reported to be a potential risk factor for oral and

periodontal patients. Parakeratotic changes in cheeks, tongue, and esophagus are indicators of zinc deficiency. Serum zinc level has been found to be at lower levels in patients with potentially premalignant disorders such as oral leukoplakia [22, 43, 46].

14. Cadmium (Cd)

Cadmium is found in some vegetables (leaved vegetables, potatoes, grains, and seeds) and animal food (liver and kidney). The moment cadmium enters the body, it accumulates in the liver and bones and is expelled very slowly (cadmium reference). Cadmium is an active element in soil and can be received by plants easily. As a result of being received by plants and entering the food chain or possibility of reaching water environment by being washed from the soil, it creates a significant environmental problem. In addition, the downward carriage of cadmium from the soil with chelating agents accelerates and it can lead to pollution in drinking and irrigation waters as it enters underground water sources [47, 48]. Exposure to cadmium is related to some various systematic health impacts such as kidney failure, skeleton disorders, and cardiovascular diseases [49]. Cadmium can be released from intraoral alloys in dentistry patients and accumulate in teeth and mouth tissues, which are strictly bound to metallothioneins [50]. The relation has been found between cadmium and the increase in decay prevalence. However, it is stated that settlement of cadmium in teeth after growth is not effective on caries. Some studies conducted on test animals indicate that there is a strong relationship between the formation of dental caries and cadmium intake in dental development period [4]. The increase of exposure to and dispersion of this toxic material is becoming increasingly important on the systematic and oral health of sensitive populations such as children [49].

15. Lead (Pb)

People can be exposed to lead through contaminated food and beverage, resulting from industrial activity [51]. Lead is added to the food chain especially through vegetables growing on contaminated soil. Lead can be transferred with plants and grass from contaminated soil, which potentially leads to the accumulation of toxic metals in vegetating ruminants and especially in cattle. The accumulation of lead creates toxic effects in cattle; it also leads to toxic effects in people who consume meat and milk contaminated with toxic metals [52].

It is a harmful and toxic metal for the human body. Lead has the ability to translocation with Ca^{+2} at the HAP of teeth. For this reason, it downsizes the HAP crystals [34, 53].

Lead is transferred to the tissues of the body such as teeth through environment or nutrition. It is determined to have an encouraging effect on dental caries. In addition, it is found out that lead increases the formation of enamel hypoplasia. A positive correlation has been found between saliva lead levels and decay development of children with early childhood decays. Thus, lead plays an essential role in the development of new caries lesions [4, 53, 54].

16. Iron (Fe)

Unlike other TE, iron (Fe) is abundant in nature and a biologically essential component of every living organism. Nevertheless, despite geological abundance, when oxygen contacts iron, hardly soluble oxides are created. For this reason, it is not easily received by organisms [55].

These are most common dietary resources for iron: liver, meat, poultry products and fish; cereals, green leafy vegetables, pulses, nuts, oilseeds, and dried fruits [22].

As an essential element, iron mostly enters the body with green vegetables. It is reported that iron concentrations are low in enamel [34].

The amount of Fe is 4–5 gm in healthy individuals. Iron (Fe) is a trace metal that is necessary to ensure that almost all organisms survive. Participation in heme and iron–sulfur cluster containing proteins allows Fe to participate in a variety of vital functions such as oxygen transport, DNA synthesis, metabolic energy, and cellular respiration [56].

Some studies reported that iron can act as preventive for dental caries. The study reported that adding 2 mmol/L $FeSO_4.7H_2O$ to acidic drinks reduced mineral loss and human enamel preserved the surface microhardness [57, 58].

In addition, some iron addition products used for iron deficiency anemia are reported to have a cariostatic effect and delayed the emergence of dental caries in human teeth. As a result of iron deficiency, angular cheilitis, atrophic glossitis, diffused oral mucosal atrophy, candidal infections, oral premalignant lesions, and stomatitis can be seen in the oral region [22].

Besides all these explanations, some factors change the density of the TEs on the teeth such as exposure to electromagnetic fields, Wi-Fi, radio frequencies emitted from mobile phones, environmental pollution, excessive fertilization of soil, natural disasters, and dental anomalies [3, 27, 49, 50].

Author details

Mehmet Sinan Doğan

Address all correspondence to: dtlider@hotmail.com

Faculty of Dentistry, Harran University, Pediatric Dentistry, Şanlıurfa, Turkey

References

[1] Fraga CG. Relevance, essentiality and toxicity of trace elements in human health. Molecular Aspects of Medicine. 2005;**26**(4-5):235-244

[2] Brown CJ, Chenery SR, Smith B, Mason C, Tomkins A, Roberts GJ, et al. Environmental influences on the trace elementcontent of teeth implications for disease and nutritional-status. Archives of Oral Biology. 2004;**49**:705-717

[3] Dogan MS, Yavas MC, Yavuz Y, Erdogan S, Yener İ, Simsek İ, et al. Effect of electromagnetic fields and antioxidants on the trace element content of rat teeth. Drug Design, Development and Therapy. 2017;**11**:1393-1398

[4] Pathak MU, Shetty V, Kalra D. Trace elements and oral health: A systematic review. Journal of Advanced Oral Research. 2016;**7**(2):12-20

[5] Oshima M, Tsuji T. Functional tooth regenerative therapy: Tooth tissue regeneration and whole-tooth replacement. Odontology. 2014;**102**(2):123-136

[6] Medina S, Salazar L, Mejía C, Moreno F. In vitro behavior of the dentin and enamel calcium hydroxyapatite in human premolars subjected to high temperatures. DYNA. 2016;**83**(195):34-41

[7] Garant PR. Oral Cells and Tissues. Chicago: Quintessence Books; 2003

[8] Nanci A. Ten Cate's Oral Histology: Development, Structure, and Function. 8th ed. St. Louis: Elsevier Mosby; 2008

[9] Shashikiran ND, Subba Reddy VV, Hiremath MC. Estimation of trace elements in sound and carious enamel of primary and permanent teeth by atomic absorption spectrophotometry: An in vitro study. Indian Journal of Dental Research. 2007;**18**:157-162

[10] Teruel Jde D, Alcolea A, Hernández A, Ruiz AJ. Comparison of chemical composition of enamel and dentine in human, bovine, porcine and ovine teeth. Archives of Oral Biology. 2015;**60**(5):768-775

[11] Kang D, Amarasiriwardena D, Goodman AH. Application of laser ablation–inductively coupled plasma–mass spectrometry (LA–ICP–MS) to investigate trace metal spatial distributions in human tooth enamel and dentine growth layers and pulp. Analytical and Bioanalytical Chemistry. 2004;**378**:1608-1615

[12] He LH, Swain MV. Understanding the mechanical behavior of human enamel from its structural and compositional characteristics. The Journal of the Mechanical Behavior of Biomedical. 2008;**1**:18-29

[13] Kumagai A, Fujita Y, Endo S, Itai K. Concentrations of trace element in human dentin by sex and age. Forensic Science International. 2012;**219**(1-3):29-32

[14] Tziafas D. Composition and structure of cementum: Strategies for bonding. In: Eliades G, Watts D, Eliades T, editors. Dental Hard Tissues and Bonding. Berlin/Heidelberg: Springer; 2005. pp. 177-193

[15] Papagerakis P, Mitsiadis T. Development and structure of teeth and periodontal tissues. In: Primer on the Metabolic Bone Diseases and Disorders of Mineral Metabolism. 8th ed. New York: John Wiley & Sons; 2013

[16] ten Cate AR. Oral Histology. Development, Structure and Function. 5th ed. St. Louis: Mosby; 1998

[17] Hsieh SC, Tsao JT, Lew WZ, Chan YH, Lee LW, Lin CT, Huang YK, Huang HM. Static magnetic field attenuates lipopolysaccharide-induced inflammation in pulp cells by affecting cell membrane stability. Scientific World Journal. 2015;**2015**:492683

[18] Han G, Hu M, Zhang Y, Jiang H. Pulp vitality and histologic changes in human dental pulp after the application of moderate and severe intrusive orthodontic forces. American Journal of Orthodontics and Dentofacial Orthopedics. 2013;**144**(4):518-522

[19] Doğan MS, Yavaş MC, Günay A, Yavuz İ, Deveci E, Akkuş Z, et al. The protective effect of melatonin and Ganoderma lucidum against the negative effects of extremely low frequency electric and magnetic fields on pulp structure in rat teeth. Biotechnology and Biotechnological Equipment. 2017;**31**(5):979-988

[20] Kutsch VK. Dental caries: An updated medical model of risk assessment. The Journal of Prosthetic Dentistry. 2014;**111**(4):280-285

[21] Fontana M, Young DA, Wolff MS. Evidence-based caries, risk assessment, and treatment. Dental Clinics of North America. 2009;**53**(1):149-161

[22] Bhattacharya PT, Misra SR, Hussain M. Nutritional aspects of essential trace elements in oral health and disease: An extensive review. Scientifica. 2016;**2016**:12-24. DOI: 10.1155/2016/5464373

[23] Alcântara PC, Alexandria AK, Souza IP, Maia LC. In situ effect oftitanium tetrafluoride and sodium fluoride on artificially decayedhuman enamel. Brazilian Dental Journal. 2014;**25**:28-32

[24] Shafer WG, Hine MK, Levy BM. A Textbook of Oral Pathology. 4th ed. Chennai: Elsevier India; 2004

[25] Amin W, Almimar F, Alawi M. Quantitative analysis of trace elements in sound and carious enamel of primary and permanent dentitions. BJMMR. 2016;**11**(6):1-10

[26] US Department of Health and Human Services. Toxicological Profile for Vanadium; 2012

[27] Höllriegl V, München HZ. Strontium in the environment and possible human health effects. In: Nriagu JO, editor. Encyclopedia of Environmental Health. Burlington: Elsevier; 2011. pp. 268-275

[28] Prashanth L, Kattapagari KK, Chitturi RT, Baddam VRR, Prasad LK. A review on role of essential trace elements in health and disease. Journal Dr. NTR University of Health Sciences. 2015;**4**(2):75-78

[29] Usuda K, Kono K, Dote T, Watanabe M, Shimizu H, Tanimoto Y, et al. An overview of boron, lithium, and strontium in human health and profiles of these elements in urine of Japanese. Environmental Health and Preventive Medicine. 2007;**12**(6):231-237

[30] Özcan I. The histopathologic effects of lithium on rat salivary glands. ACTA Pharmaceutica Sciencia. 2000;**42**(4):107-111

[31] Broberg K, Concha G, Engström K, Lindvall M, Grander M, Vahter M. Lithium in drinking water and thyroid function. Environmental Health Perspectives. 2011;**119**:827-830

[32] Alves RD, Souza TM, Lima KC. Titanium tetra fluoride and dental caries: A systematic review. Journal of Applied Oral Science. 2005;**13**:325-328

[33] Rayman MP. Selenium and human health. The Lancet. 2012;**379**(9822):1256-1268

[34] Qamar Z, Haji Abdul Rahim ZB, Chew HP, Fatima T. Influence of trace elements on dental enamel properties: A review. Journal of the Pakistan Medical Association. 2017; **67**(1):116-120

[35] Monteil-Rivera F, Fedoroff M, Jeanjean J, Minel L, Barthes MG, et al. Sorption of selenite (SeO_3^{2-}) on hydroxyapatite: An exchange process. The Journal of Colloid and Interface Science. 2000;**221**:291-300

[36] Ma J, Wang Y, Zhou L, Zhang S. Preparation and characterization of selenite substituted hydroxyapatite. Materials Science and Engineering C: Materials for Biological Applications. 2013;**33**:440-445

[37] Jahangard-Rafsanjani Z, Gholami K, Hadjibabaie M, Shamshiri AR, Alimoghadam K, Sarayani A, et al. The efficacy of selenium in prevention of oral mucositis in patients undergoing hematopoietic SCT: A randomized clinical trial. Bone Marrow Transplantation. 2013;**48**(6):832-836

[38] Li Y, Widodo J, Lim S, Ooi C. Synthesis and cyto compatibility of manganese (II) and iron (III) substituted hydroxyapatite nanoparticles. Journal of Materials Science. 2012;**47**:754-763

[39] Broadley MR, White PJ, Hammond JP, Zelko I, Lux A. Zinc in plants. New Phytologist. 2007;**173**(4):677-702

[40] Whitney EN, Rolfes SR. Understanding Nutrition, Thomson Learning. 10th ed. Boston: Cengage Learning; 2010

[41] Kamberi B, Hoxha V, Kqiku L, Pertl C. The manganese content of human permanent teeth. Acta Stomatologica Croatica. 2009;**43**:83-88

[42] Franklin RB, Costello LC. Zinc as an anti-tumor agent in prostate cancer and in other cancers. Archives of Biochemistry and Biophysics. 2007;**463**:211-217

[43] Das M, Das R. Need of education and awareness towards zinc supplementation: A review. Journal of Nutrition and Metabolism. 2012;**4**(3):45-50

[44] Hussein AS, Ghasheer HF, Ramli NM, Schroth RJ, Abu-Hassan MI. Salivary trace elements in relation to dental caries in a group of multi-ethnic school children in Shah Alam, Malaysia. European Journal of Paediatric Dentistry. 2013;**14**:113-118

[45] Uçkardes Y, Tekçiçek M, Ozmert EN, Yurdakök K. The effect of systemic zinc supplementation on oral health in low socioeconomic level children. The Turkish Journal of Pediatrics. 2009;**51**:424-428

[46] Jayadeep A, Raveendran Pillai K, Kannan S, Nalinakumari KR, Mathew B, Krishnan Nair M, et al. Serum levels of copper, zinc, iron and ceru plasmin in oral leukoplakia

and squamous cell carcinoma. Journal of Experimental & Clinical Cancer Research. 1997;**16**(3):295-300

[47] Benredjem Z, Delimi R. Use of extracting agent for decadmiation of phosphate rock. Physics Procedia. 2009;**2**(3):1455-1460

[48] AlKhader AMF. The impact of phosphorus fertilizers on heavy metals content of soils and vegetables grown on selected farms in Jordan. Agrotechnology. 2015;**5**(1):1-15

[49] Arora M, Weuve J, Schwartz J, Wright RO. Association of environmental cadmium exposure with pediatric dental caries. Environmental Health Perspectives. 2008;**116**(6):821-825

[50] Guzzi G, Pigatto PD, Ronchi A. Periodontal disease and environmental cadmium exposure. Environmental Health Perspectives. 2009;**117**(12):535

[51] Barbosa F Jr, Tanus-Santos JE, Gerlach RF, Parsons PJ. A critical review of biomarkers used for monitoring human exposure to lead: Advantages, limitations, and future needs. Environmental Health Perspectives. 2005;**113**(12):1669-1674

[52] Pilarczyk R, Wójcik J, Czerniak P, Sablik P, Pilarczyk B, Tomza-Marciniak A. Concentrations of toxic heavy metals and trace elements in raw milk of Simmental and Holstein-Friesian cows from organic farm. Environmental Monitoring and Assessment. 2013;**185**(10):8383-8392

[53] Mavropoulos E, Rossi AM, Costa AM, Perez CAC, Moreira JC, Saldanha M. Studies on the mechanisms of lead immobilization by hydroxyapatite. Environmental Science and Technology. 2002;**36**:1625-1629

[54] Pradeep KK, Hegde AM. Lead exposure and its relation to dentalcaries in children. The Journal of Clinical Pediatric Dentistry. 2013;**38**:71-74

[55] Abbaspour N, Hurrell R, Kelishadi R. Review on iron and its importance for human health. Journal of Research in Medical Sciences. 2014;**19**(2):164-174

[56] Gozzelino R, Arosio P. Iron homeostasis in health and disease. International Journal of Molecular Sciences. 2016;**17**(1):130

[57] Tsanidou E, Nena E, Rossos A, Lendengolts Z, Nikolaidis C, Tselebonis A, Constantinidis TC. Caries prevalence and manganese and iron levels of drinking water in school children living in a rural/semi-urban region of north-eastern Greece. Environmental Health and Preventive Medicine. 2015;**20**(6):404-409

[58] Xavier AM, Rai K, Hegde AM, Shetty S. A spectroscopic and surface microhardness study on enamel exposed to beverages supplemented with lower iron concentrations. The Journal of Clinical Pediatric Dentistry. 2015;**39**(2):161-167

Chapter 5

Trace Elements in the Human Milk

Manuel de Rezende Pinto and
Agostinho A. Almeida

Additional information is available at the end of the chapter

http://dx.doi.org/10.5772/intechopen.76436

Abstract

Human breast milk is considered to be the perfect food for infants, specifically adapted to their needs. Before birth, the mother transfers all the nutrients and bioactive components to the fetus through the placenta. After birth, these substances have to be transferred through colostrum and milk. In particular, human breast milk is supposed to provide all the essential trace elements that are required by the normal term newborn infant. Therefore, the composition of human breast milk and its changes during lactation is a topic of major importance and has been the subject for intensive research. Conversely, human milk can also be a transfer medium of undesirable (toxic) elements from the mother to the infant. An extensive review of the most recent literature was carried out focusing on the current trace elements levels and their changes during lactation. For several elements, there is a consistent knowledge of their characteristic concentrations throughout the various stages of lactation, their dependence on maternal nutritional status, inter-individual and geographical variability, metabolic pathways, inter-elemental relationships, and effects on child development. For many other elements, this knowledge does not exist or is quite limited.

Keywords: breast milk, breastfeeding, micronutrients, trace elements, temporal changes

1. Introduction

The nutritional requirements during breastfeeding are among the most important in human development. The production of 750–1000 ml of human milk per day represents the transfer from the mother to the infant of approximately 2100–2520 kJ, as energy-producing macronutrients (carbohydrates, proteins, and lipids) [1].

Likewise, all the vitamins and minerals (both macrominerals and trace elements) needed to support the child's growth and development are transferred in the same way.

According to current recommendations, the newborn should whenever possible be exclusively breastfed for the first 6 months of life [2]. Breast milk is then the only nutritional source of the child at this stage. Among these nutrients, macrominerals and essential trace elements are particularly noteworthy.

Maternal nutritional deficiencies in these elements may occur during lactation, affecting the mother's health. If this is reflected in the volume and quality of the milk, it will lead to nutritional deficiencies in the child, consequently affecting its development and health status.

The characterization of the composition of the human milk, in relation to these elements, is therefore of the utmost importance and has attracted much attention for many years.

On the other hand, breast milk can be a source of exposure of the child to various xenobiotics, including toxic trace elements.

A systematization of the current knowledge about the typical ("normal") levels of trace elements in human milk and the major factors responsible for their variability was the main objective of the present review. It is expected to be a useful tool for future studies and in the formulation of breast milk substitutes.

2. Human breast milk

Human milk is a complex secretion produced by the mammary glands of postpartum women [3]. It is generally assumed that the average volume of breast milk ingested by a nursing infant is about 600 ml/day.

2.1. Macronutrients

The composition of breast milk in terms of macronutrients varies during lactation. According to a recent review [4], the mean concentration of main macronutrients in mature milk from full-term women is estimated to be approximately 0.9–1.2 g/dL for protein, 3.2–3.6 g/dL for lipids, and 6.7–7.8 g/dL for lactose. The total energy is estimated to be approximately 65–70 kcal/dL, and is highly correlated with the lipids content. These macronutrients have three different sources: synthesis in the lactocyte, dietary origin, and maternal stores [4].

The nutritional quality of breast milk tends to be highly conserved for most of the macronutrients, independently of the maternal diet [4].

2.2. Micronutrients

Micronutrients, usually considered as the vitamins and the minerals (both the macrominerals and the trace elements), are fundamental for the proper development of the child. They are essential in the formation and regeneration of tissues, as well as in regulating most of the functions of the body's systems, leading its deficiency to disease, and serious malformations in

the baby and the child. Many of these micronutrients are also involved in the body's defense functions [1]. Minerals are closely related to the action of the remaining nutrients, affecting their absorption, metabolism, and excretion [1].

Contrarily to the generality of the macronutrients, it is documented that when maternal nutrition is inadequate, significant changes in milk composition may occur for some of its micronutrients (e.g., some fatty acids and vitamins, sodium, potassium, chloride, phosphorus, copper, zinc, manganese, and iron). The correlation between the levels of minerals in breast milk and the mother's diet is variable from element to element, being in some cases strongly linked to the mother's intake and body stores [4].

These changes have important implications for the growth and development of the breastfed infants [5]. It is also documented that there are differences regarding the milk composition between the different races [6].

3. Trace elements in human milk

3.1. Essential trace elements

3.1.1. Boron

Little is known about the biochemical function of boron in human tissues. Signs of boron deficiency depend on the nutritional levels of aluminum, calcium, cholecalciferol, magnesium, methionine, and potassium. It affects calcium and magnesium concentrations in plasma and tissues, plasma alkaline phosphatase, and bone calcification [7]. The toxicity of boron is very low orally. There is no clear definition of symptoms of chronic boron intoxication in humans [7]. The levels of boron in breast milk seem to increase during lactation [8]. Average concentration of 0.14 μg/L was observed in mature milk [8].

3.1.2. Chromium

Chromium, as trivalent chromium, is an essential nutrient that enhances the action of insulin and, consequently, the metabolism of carbohydrates, lipids, and proteins. It has been suggested that the active form of chromium, the so-called "glucose tolerance factor," is a complex of chromium, nicotinic acid, and the amino acids glycine, cysteine, and glutamic acid. Biochemically, it affects the ability of the transmembrane insulin receptor to interact with insulin [7]. Chromium deficiency causes glucose intolerance similar to diabetes mellitus, elevated plasma free fatty acids levels, changes in nitrogen metabolism, weight loss, neuropathy, and respiratory depression [7]. The toxicity of trivalent chromium is so low that no effects of administering excessive amounts of this species could be observed. Hexavalent chromium, by contrast, is extremely toxic [7]. The concentrations of chromium in breast milk are very low and present a great variability [8, 9]. They may be increased during 21–89 and 90–180 days of lactation [8, 9].

Element	Average or interval (mg/L)	Time after delivery[1]	Milk type[2]	n	Country[3]	Analytical technique[4]	[Ref] year
B	0.000145	1–20 mo	M	205	ARE	ICP-MS	[8] 2008
Co	0.00019[b]	—	—	27	AUT	ICP-SFMS	[45] 2000
	0.0002–0.0007	—	—	—	—	—	[20] 2001
	0.00085	2–8 w	M	19	CZE DEU POL	ICP-MS	[46] 2002
	0.000009	1–20 mo	M	205	ARE	ICP-MS	[8] 2008
	0.00069	2 d	C	34	PRT	ICP-MS	[12] 2008
	0.00072	1 mo	M	19			
Cr	0.0243[b]	—	—	27	AUT	ICP-SFMS	[45] 2000
	0.0009–0.0012	0–7 mo	—	6–45	—	—	[20] 2001
	0.0108	2–8 w	M	19	CZE DEU POL	ICP-MS	[46] 2002
	0.017–0.076	1–365 d	—	—	JPN	ICP-AES	[9] 2005
	0.000689	1–20 mo	M	205	ARE	ICP-MS	[8] 2008
	0.000173	1–191 d	M	79	JPN	ICP-MS	[75] 2008
Cu	0.4[b]	—	—	27	AUT	ICP-SFMS	[45] 2000
	0.11–0.62	1–293 d	—	6–50	—	—	[20] 2001
	0.54	1–7 d	C	50	BRA	TXRF	[76] 2002
	0.162	2 mo	M	32	TUR	FAAS	[53] 2005
	0.35	—	M	—	JPN	ICP-AES	[9] 2005
	0.066	1 mo	M	41	IND	ICP-AES	[37] 2006
	0.056	3 d	C	41			
	0.41519	1–20 mo	M	205	ARE	ICP-MS	[8] 2008
	0.403	—	—	120	ARE	ICP-MS	[54] 2008
	0.760	2 d	C	34	PRT	ICP-MS	[12] 2008
	0.498	1 mo	M	19			
	0.506	1 w	C	44	KOR	GFAAS (Zeeman)	[14] 2012
	0.489	2 w	T	32			
	0.384	4 w	M	22			
	0.356	6 w	M	26			
	0.303	8 w	M	22			
	0.301	12 w	M	9			
	0.3	—	—	27	IRN	FAAS	[77] 2015
	0.587	5–17 d	T	55	GTM	ICP-MS	[72] 2016
	0.460	18–46 d	M	73			
	0.262	4–6 mo	M	100			
	0.220	—	—	12	AUS	ICP-MS	[51] 2016

Element	Average or interval (mg/L)	Time after delivery[1]	Milk type[2]	n	Country[3]	Analytical technique[4]	[Ref] year
	0.16952	2–6 w	M	20	USA	ICP-MS	[48] 2017
	0.13094	1–7 w	M	6	NAM		
	0.18687	2–6 w	M	23	POL		
	0.21104	3–7 w	M	21	ARG		
Fe	0.38[b]	—	—	27	AUT	ICP-SFMS	[45] 2000
	0.3–0.6	—	—	—	—	—	[20] 2001
	1.72	1–7 d	C	50	BRA	TXRF	[76] 2002
	1.19	—	M	—	JPN	ICP-AES	[9] 2005
	0.5	30–45 d	M	31	USA (Texas)	AAS	[19] 2008
	0.4	75–90 d		17			
	0.36	—	—	27	IRN	FAAS	[77] 2015
	0.558	5–17 d	T	55	GTM	ICP-MS	[72] 2016
	0.581	18–46 d	M	73			
	0.320	4–6 mo	M	100			
	0.047	—	—	12	AUS	ICP-MS	[51] 2016
	1.27	2–6 w	M	20	USA	ICP-MS	[48] 2017
	1.53	1–7 w	M	6	NAM	ICP-MS	
	1	2–6 w	M	23	POL	ICP-MS	
	0.99	3–7 w	M	21	ARG	ICP-MS	
I	0.098–0.247	14 d–3.5 y	—	14–24	—	—	[20] 2001
	0.0478	30–45 d	M	31	USA (Texas)	NAA	[19] 2009
	0.0423	75–90 d		17			
	0.113	—	—	12	AUS	ICP-MS	[51] 2016
Mn	0.003–0.01	—	—	—	—	—	[20] 2001
	0.000929	1–20 mo	M	205	ARE	ICP-MS	[8] 2008
	0.011	—	M	—	JPN	ICP-AES	[9] 2005
	0.0077	2 d	C	34	PRT	ICP-MS	[12] 2008
	0.0049	1 mo	M	19			
	0.133	1 w	C	44	KOR	GFAAS (Zeeman)	[14] 2012
	0.127	2 w	T	32			
	0.125	4 w	M	22			
	0.123	6 w	M	26			
	0.127	8 w	M	22			
	0.108	12 w	M	9			
	0.012	5–17 d	T	55	GTM	ICP-MS	[72] 2016

Element	Average or interval (mg/L)	Time after delivery[1]	Milk type[2]	n	Country[3]	Analytical technique[4]	[Ref] year
	0.011	18–46 d	M	73			
	0.0077	4–6 mo	M	100			
	0.00137	—	—	12	AUS	ICP-MS	[51] 2016
	0.00271	2–6 w	M	20	USA	ICP-MS	[48] 2017
	0.0116	1–7 w	M	6	NAM	ICP-MS	
	0.00161	2–6 w	M	23	POL	ICP-MS	
	0.00762	3–7 w	M	21	ARG	ICP-MS	
Mo	0.0002–0.017	1–293 d	—	6–46	—	—	[29] 2000
	0.00072	2–8 w	M	19	CZE DEU POL	ICP-MS	[46] 2002
	0.000348	1–20 mo	M	205	ARE	ICP-MS	[8] 2008
	0.000542	1–191 d	M	79	JPN	ICP-MS	[75] 2008
	0.00037	—	—	12	AUS	ICP-MS	[51] 2016
Se	0.0056–0.08	1–869 d	—	5–241	—	—	[29] 2000
	0.017[b]	—	—	27	AUT	ICP-SFMS	[45] 2000
	0.0163	2–3 mo	M	31	ESP	ICP-AES	[28] 2003
	0.017	—	M	—	JPN	ICP-AES	[9] 2005
	0.010623	1–20 mo	M	205	ARE	ICP-MS	[8] 2008
	0.0159	30–45 d	M	31	USA (Texas)	NAA	[19] 2008
	0.0157	75–90 d		17			
	0.0722	2 d	C	34	PRT	ICP-MS	[12] 2008
	0.0321	1 mo	M	19			
	0.0118	1 w	C	44	KOR	GFAAS (Zeeman)	[14] 2012
	0.0114	2 w	T	32			
	0.0127	4 w	M	22			
	0.0114	6 w	M	26			
	0.0108	8 w	M	22			
	0.0105	12 w	M	9			
	0.017	5–17 d	T	55	GTM	ICP-MS	[72] 2016
	0.017	18–46 d	M	73			
	0.013	4–6 mo	M	100			
	0.0143	—	—	12	AUS	ICP-MS	[51] 2016
Zn	0.8–4.7	2 d–2 y	—	6–71	—	—	[20] 2001
	6.97	1–7 d	C	50	BRA	TXRF	[76] 2002
	1.2	2 mo	M	32	TUR	FAAS	[53] 2005
	1.45	—	M	—	JPN	ICP-AES	[9] 2005

Element	Average or interval (mg/L)	Time after delivery[1]	Milk type[2]	n	Country[3]	Analytical technique[4]	[Ref] year
	0.255	3 d	C	41	IND	ICP-AES	[37] 2006
	0.276	1 mo	M	41			
	2.1	30–45 d	M	31	USA (Texas)	FAAS	[19] 2008
	2	75–90 d		17			
	1.468	1–20 mo	M	205	ARE	ICP-MS	[8] 2008
	2.730	—	—	120	ARE	ICP-MS	[54] 2008
	12.137	2 d	C	34	PRT	ICP-MS	[12] 2008
	2.785	1 mo	M	19			
	7.8	1 w	C	44	KOR	GFAAS (Zeeman)	[14] 2012
	9.1	2 w	T	32			
	7.2	4 w	M	22			
	8	6 w	M	26			
	7.4	8 w	M	22			
	6.6	12 w	M	9			
	2.34	—	—	27	IRN	FAAS	[77] 2015
	4.36	5–17 d	T	55	GTM	ICP-MS	[72] 2016
	3.47	18–46 d	M	73			
	1.44	4–6 mo	M	100			
	1.390	—	—	12	AUS	ICP-MS	[51] 2016
Ag	0.00041[b]	—	—	27	AUT	ICP-SFMS	[45] 2000
	0.00078	2–8 w	M	19	CZE DEU POL	ICP-MS	[46] 2002
	0.000005	1–20 mo	M	205	ARE	ICP-MS	[8] 2008
Al	0.067	—	—	27	AUT	ICP-SFMS	[45] 2000
	0.007056	1–20 mo	M	205	ARE	ICP-MS	[8] 2008
	0.05645	1–4 d	C	45	TWN	GFAAS	[43] 2014
	0.03657	5–10 d	T	45			
	0.01811	30–35 d	M	45			
	0.01344	60–65 d	M	45			
As	0.0067[b]	—	—	27	AUT	ICP-SFMS	[45] 2000
	0.00025–0.003	—	—	—	—	—	[20] 2001
	0.000089	1–20 mo	M	205	ARE	ICP-MS	[8] 2008
	0.000196	—	—	120	ARE	ICP-MS	[54] 2008
	0.0078	2 d	C	34	PRT	ICP-MS	[12] 2008
	0.0058	1 mo	M	19			
	0.00150	1–4 d	C	45	TWN	GFAAS	[43] 2014

Element	Average or interval (mg/L)	Time after delivery[1]	Milk type[2]	n	Country[3]	Analytical technique[4]	[Ref] year
	0.00068	5–10 d	T	45			
	0.00027	30–35 d	M	45			
	0.00016	60–65 d	M	45			
	0.00347	2–6 w	M	20	USA	ICP-MS	[48] 2017
	0.00668	1–7 w	M	6	NAM	ICP-MS	
	0.00386	2–6 w	M	23	POL	ICP-MS	
	0.00451	3–7 w	M	21	ARG	ICP-MS	
	0.00236	—	—	74	LBN	GFAAS	[47] 2018
Au	0.00029[b]	—	—	27	AUT	ICP-SFMS	[45] 2000
	0.0001–0.0021	—	—	—	AUT	ICP-SFMS	[59] 2000
Ba	0.000017	1–20 mo	M	205	ARE	ICP-MS	[8] 2008
Be	0.000008	1–20 mo	M	205	ARE	ICP-MS	[8] 2008
Bi	0.000002	1–20 mo	M	205	ARE	ICP-MS	[8] 2008
Br	0.812	—	—	12	AUS	ICP-MS	[51] 2016
Cd	<0.001	—	—	—	—	—	[20] 2001
	0.000097	2 mo	M	32	TUR	FAAS	[53] 2005
	0.000003	1–20 mo	M	205	ARE	ICP-MS	[8] 2008
	0.00027	—	—	120	ARE	ICP-MS	[54] 2008
	0.00137	1–4 d	C	45	TWN	GFAAS	[43] 2014
	0.00065	5–10 d	T	45			
	0.00049	30–35 d	M	45			
	0.00034	60–65 d	M	45			
	0.00087	—	—	74	LBN	GFAAS	[47] 2018
Ce	0.00012	2–8 w	M	19	CZE DEU POL	ICP-MS	[46] 2002
	0.0000154	—	—	11	DEU	ICP-MS	[56] 2010
	0.0000157	—	—	51	DEU	ICP-MS	
	0.0000139	—	—	26	ESP	ICP-MS	
Cs	0.001–0.005	—	—	—	—	—	[20] 2001
Ga	0.00052	2–8 w	M	19	CZE DEU POL	ICP-MS	[46] 2002
Hg	0.000030–0.00062	—	—	17	CAN	CV-AFS	[78] 1994
	0.000146–0.000237	—	—	33	CAN	—	[79] 1997
	0.001–0.003	—	—	—	—	—	[20] 2001
	0.000008	1–20 mo	M	205	ARE	ICP-MS	[8] 2008
	0.000115	—	—	120	ARE	ICP-MS	[54] 2008

Element	Average or interval (mg/L)	Time after delivery[1]	Milk type[2]	n	Country[3]	Analytical technique[4]	[Ref] year
	0.00289–0.01333	—	—	10–15	IRN	DC/Au-amal	[80] 2012
	0.000008	1–20 mo	M	205	ARE	ICP-MS	[8] 2008
La	0.00007	2–8 w	M	19	CZE DEU POL	ICP-MS	[46] 2002
	0.000002	1–20 mo	M	205	ARE	ICP-MS	[8] 2008
Li	0.000005	1–20 mo	M	205	ARE	ICP-MS	[8] 2008
Nb	0.00004	2–8 w	M	19	CZE DEU POL	ICP-MS	[46] 2002
Ni	0.00079[b]	—	—	27	AUT	ICP-SFMS	[45] 2000
	0.010–0.020	—	—	—	—	—	[20] 2001
	0.48	2 mo	M	32	TUR	FAAS	[53] 2005
	0.0076	2 d	C	34	PRT	ICP-MS	[12] 2008
	0.0058	1 mo	M	19			
	0.002581	1–20 mo	M	205	ARE	ICP-MS	[8] 2008
Pb	0.001–0.005	—	—	—	—	—	[20] 2001
	0.000019	1–20 mo	M	205	ARE	ICP-MS	[8] 2008
	0.00151	—	—	120	ARE	ICP-MS	[54] 2008
	0.00155	2 d	C	34	PRT	ICP-MS	[12] 2008
	0.00094	1 mo	M	19			
	0.01322	1–4 d	C	45	TWN	GFAAS	[43] 2014
	0.00892	5–10 d	T	45			
	0.01172	30–35 d	M	45			
	0.00293	60–65 d	M	45			
	0.00077	2–6 w	M	20	USA	ICP-MS	[48] 2017
	0.00215	1–7 w	M	6	NAM	ICP-MS	
	0.00102	2–6 w	M	23	POL	ICP-MS	
	0.00059	3–7 w	M	21	ARG	ICP-MS	
	0.01817	—	—	74	LBN	GFAAS	[47] 2018
Pt	< 0.00001[b]	—	—	27	AUT	ICP-SFMS	[45] 2000
Rb	0.3–1.2	—	—	—	—	—	[20] 2001
	32.176[a]	2–15 d	T	40	IRN	NAA	[71] 2014
	1.12	5–17 d	T	55	GTM	ICP-MS	[72] 2016
	1.05	18–46 d	M	73			
	0.810	4–6 mo	M	100			
Ru	0.00015	2–8 w	M	19	CZE DEU POL	ICP-MS	[46] 2002

Element	Average or interval (mg/L)	Time after delivery[1]	Milk type[2]	n	Country[3]	Analytical technique[4]	[Ref] year
Sb	0.00014	2–8 w	M	19	CZE DEU POL	ICP-MS	[46] 2002
	0.000352	1–20 mo	M	205	ARE	ICP-MS	[8] 2008
Sc	0.00019[b]	—	—	27	AUT	ICP-SFMS	[45] 2000
Sn	<0.001- < 0.002	—	—	—	—	—	[20] 2001
Sr	0.044	5–17 d	T	55	GTM	ICP-MS	[72] 2016
	0.046	18–46 d	M	73			
	0.046	4–6 mo	M	100			
Ti	0.0063[b]	—	—	27	AUT	ICP-SFMS	[45] 2000
	0.270	2–8 w	M	19	CZE DEU POL	ICP-MS	[46] 2002
Th	0.00002	2–8 w	M	19	CZE DEU POL	ICP-MS	[46] 2002
U	0.00003	2–8 w	M	19	CZE DEU POL	ICP-MS	[46] 2002
V	0.00018[b]	—	—	27	AUT	ICP-SFMS	[45] 2000

[1]d: day(s); w: week(s); mo: month(s); y: year(s); t: term; pt: pre-term.
[2]C: colostrum; T: transition milk; M: mature milk.
[3]Countries according to ISO 3166-1 A3.
[4]ICP-MS: inductively coupled plasma mass spectrometry; ICP-SFMS: inductively coupled plasma sector field mass spectrometry; TXRF: total reflection X-ray fluorescence; FAAS: flame atomic absorption spectroscopy; ICP-AES: inductively coupled plasma atomic emission spectroscopy; GFAAS: graphite furnace atomic absorption spectroscopy; NAA: neutron activation analysis; CV-AFS: cold vapor atomic fluorescence spectroscopy; DC/Au-amal: direct combustion/Au amalgam.
[a]mg/kg, as dry matter.
[b]median.

Table 1. Summary of available data on trace element levels in human milk.

3.1.3. Cobalt

Cobalt is a constituent of vitamin B12 and has been linked to the synthesis of antibodies and phagocytic activity in neutrophils and macrophages [10, 11]. Increased cobalt levels were observed throughout lactation [10, 12]. It has been speculated that this increase would be related to the increased needs arising from the infants' production of humoral antibodies, which starts during the third and fourth month of life, when the passage of the passive acquired immunity to active acquired immunity occurs [13]. Another study reported no significant changes in cobalt levels in breast milk throughout the various stages of lactation [8]. Plasma cobalt was higher in blood plasma of 12–14-week-old infants fed breast milk compared to healthy adults [8]. Cobalt levels in maternal plasma have a negative correlation with their concentration of breast milk [8].

3.1.4. Copper

Copper is present in biological tissues mainly in the form of organic complexes, most of them being enzymatic systems. The metabolic processes in which copper dependent enzymes are

involved include the use of oxygen in cellular respiration and the synthesis of essential biomolecules such as the complex proteins of the skeleton and blood vessels connective tissues and a variety of neuroactive compounds of the central nervous system. It is estimated that an adult individual contains between 50 and 120 mg of copper in the whole body [7]. Copper in the blood is distributed by plasma and erythrocytes, of which 60% is associated with metalloenzyme Cu,Zn-superoxide dismutase (SOD), the rest being linked to other proteins and amino acids [7]. Plasma copper levels in the adult range between 0.8 and 1.2 mg/L and are not significantly influenced by feeding. In women, they are about 10% higher, and may be three times higher during pregnancy [7]. In plasma, about 93% of copper is bound to ceruloplasmin, a protein with multiple functions, particularly involved in the metabolism of iron [7]. In adulthood, copper deficiency is associated with hypochromic anemia, neutropenia, hypopigmentation, deficient bone formation with osteoporosis, and vascular deficiencies [7]. The deficiency of this element in the infant is related to identical symptoms [7, 14]. Copper is mainly accumulated in the liver, especially during the third trimester of pregnancy. Premature infants tend to have lower copper stores compared to full-term children [14]. There is a decrease in copper concentration in milk during lactation, reaching a minimum of 0.08–0.10 mg/L in mature milk between 6 months and 1 year [15]. This trend is consistent with the majority of published results by other authors during this same period of lactation [8, 9, 12, 15]. One author reported a slight increase in copper concentration in breast milk in the first month, from 0.25–0.29 mg/L in colostrum to 0.37–0.41 mg/L in mature milk [15]. The effect of iron dietary supplementation of the mother in serum and milk cooper levels is not clear. Some authors reported a decrease in cooper milk associated with iron supplementation [16, 17], but a noncorrelation have also been reported [18].

3.1.5. Iodine

Iodine is an essential constituent of the thyroid hormones thyroxine (T4) and triiodothyronine (T3). These hormones are involved in the regulation of various enzymes and metabolic processes. The organs most subject to its regulation are the developing brain, muscles, heart, pituitary gland, and kidneys [19, 20]. Iodine is thus absolutely essential for life in mammals [20]. The increase in perinatal mortality associated with iodine deficiency and a reduction in birth weight are described [7]. Since the newborn's brain has only reached about one-third of its size, continuing its accelerated growth until 2 years of age, thyroid hormones and iodine keep playing a key role throughout this period. Populations with severe iodine deficiencies present a high risk of mental retardation and cretinism [7, 19, 21]. Iodine adequate intake is 110 and 130 μg/day for first and second semester of life, respectively [22]. The concentration of iodine in breast milk is strongly correlated with the dietary intake of the mother [19]. The nutritional intake of iodine in the nursing woman (recommended dietary allowance) should be of 220 μg/day [22]. Iodine content in breast milk as shown to be strongly reduced by mother's smoking habits [23].

3.1.6. Iron

Iron is an essential component of several proteins, including enzymes, cytochromes, myoglobin, and hemoglobin. Nearly two-thirds of body iron is found in the hemoglobin of circulating

red blood cells, involved in oxygen transport. About 25% is stored as rapidly mobilizable reserves and the remaining 15% is in muscle myoglobin [22]. The individual iron reserves have a great influence on its absorption. Elevated reserves inhibit the gastrointestinal absorption of iron. Absorption occurs in the small intestine [22]. Iron deficiency results in anemia, which represents the most frequent nutritional deficiency of essential elements. The main symptoms are reduced work capacity and delayed psychomotor development in the child, with cognitive deficit [22]. Anemia is also the most prevalent disease in children [24]. During the first 6 months after delivery, iron concentration in breast milk is relatively stable, ranging from 0.21 to 0.27 mg/L. Some authors have reported that, after this period, iron levels in breast milk tend to fall very significantly to values between 0.08 and 0.10 mg/L [15]. Other authors observed quite constant levels throughout lactation [9]. No differences were found associated with the mother's age, number of children, or number of previously breastfed infants [15]. Likewise, the iron content in the maternal diet did not showed a significant correlation with iron concentration in breast milk [19, 25].

3.1.7. Manganese

Manganese is an essential nutrient, involved in the formation of bone tissue and in specific reactions related to the metabolism of amino acids, cholesterol, and carbohydrates. Manganese metalloenzymes include arginase, glutamine synthetase, phosphoenolpyruvate decarboxylase, and Mn-superoxide dismutase (Mn-SOD), the mitochondrial correspondent to Cu,Zn-SOD (cytoplasmic) [7]. Only a small part of the manganese ingested is absorbed. Absorption occurs through an active transport process [7]. Although there are symptoms associated with manganese deficiency, it was not possible to clearly establish a relationship between low dietary intakes and health problems. Manganese toxicity causes central nervous system effects similar to those of Parkinson's disease [14, 22]. In one study in Japanese women, the concentrations of manganese in breast milk showed a very low variability throughout the lactation period [9]. Other studies however reported that breast milk concentrations decrease throughout lactation [8]. Also, a direct correlation between maternal plasma levels and breast milk concentration has been observed [8]. A significant reduction in milk manganese content during lactation was also observed in a small study of 29 well-nourished mothers in the United Arab Emirates [8, 12].

3.1.8. Molybdenum

Molybdenum is a cofactor of a small number of enzymes, such as sulfite oxidase, xanthine oxidase, and aldehyde oxidase, involved in the catabolism of sulfur amino acids and heterocyclic compounds such as purines and pyrimidines [20]. In all Mo-enzymes, functional molybdenum is present in the form of an organic component, molybdopterin [20]. Dietary molybdenum deficiencies are associated with growth problems, neurological disorders, and premature death [26]. On the other hand, its excess is associated with an increase in susceptibility to gout, hyperuricemia, and xanthuria [26]. Concentrations of molybdenum in breast milk increase significantly during lactation [8].

3.1.9. Selenium

The best known metabolic role of selenium in mammals was as a component of the enzyme glutathione peroxidase, which, together with vitamin E, catalase, and superoxide dismutase, is a key player of the body's antioxidant defense system. More recently, its role in P-selenoprotein has been discovered, and there is also increasing evidence of the involvement of a selenoprotein in the synthesis of the hormone triiodothyronine from thyroxine [20, 27]. Keshan's disease is a cardiomyopathy associated with selenium deficiency, which mainly affects children and women of childbearing age. Also, Kashin-Beck disease, an osteoarthropathy, is associated with selenium deficiency in soils (and consequently in food), affecting children between 5 and 13 years [7, 28, 29]. Chronic selenium toxicity is characterized primarily by hair loss and changes in nail morphology. In some cases, there is the development of skin lesions and central nervous system disturbances, being the biochemical mechanism unknown [20, 28]. There is evidence of a negative correlation between the supply of selenium and the prevalence of breast, prostate, colon, pancreatic, lung, and bladder cancer [30]. The concentration of selenium in breast milk is directly dependent on the mother's selenium dietary intake [9, 31–33]. In one study, the selenium breast milk concentrations were studied according to the region of residence of the lactating mother. Two selenium-rich regions (Portuguesa) and one control region (Yaracuy) were compared. A significant increase of selenium was observed, from 42.9 μg/L for the control region to 56.6 and 112.2 μg/L for the two seleniferous regions [31]. Other authors reported selenium levels in the first month between 12.7 and 32.1 μg/L [12, 14, 19]. There appears to be a significant inverse correlation between selenium and zinc concentrations in breast milk. Also, mothers with higher dietary selenium intakes present lower concentrations of zinc in breast milk [31]. Studies of zinc binding compounds in breastmilk allowed the identification of six compounds with affinity for selenium too. It was possible to identify one of those compounds as the citrate, which is the main low molecular weight zinc binder. The decrease in zinc concentration in breast milk is then related to the concentration of citrate, which in turn depends on the concentration of selenium in plasma. High levels of selenium observed in seleniferous regions induced reduction of citrate in milk, probably by the suppression of the mechanism of citrate production in the Golgi apparatus described by Linzell [31, 34]. In the case of premature infants, since their reserves of selenium at birth are low, it is of the utmost importance the supply of this element in adequate concentrations through breast milk, which is clearly dependent, as mentioned above, on geographical aspects, the nutritional intake of the mother and the lactation phase [12, 28, 35].

3.1.10. Zinc

In the cell, zinc is involved in catalytic, structural, and regulatory functions [20]. The biochemical role of zinc results from its presence in hundreds of enzymatic systems and as a stabilizer of the molecular structure of cellular substructures. Examples of zinc metalloenzymes are RNA polymerase, alcohol dehydrogenase, carbonic anhydrase, and alkaline phosphatase [20]. Zinc is involved in the synthesis and degradation of carbohydrates, lipids, proteins, and nucleic acids. It plays an essential role in gene expression [7]. The skeletal muscle contains about 60% of the total zinc of the body, being the bone mass

responsible for about 30% [36]. Severe zinc deficiency is associated with clinical symptoms such as delayed growth, delayed sexual and skeletal maturation, dermatitis, diarrhea, alopecia, poor appetite, behavioral changes, and increased susceptibility to disease, as result of immune system malfunction [20, 37]. Generally, mild zinc deficiency occurs without a convenient diagnosis. When detected, it is usually related to a reduced growth rate and poor resistance to infections. Acute zinc poisoning is rare. The manifestations are nausea, vomiting, diarrhea, fever, and lethargy. In the case of chronic exposure to zinc, interference with other elements, particularly with copper, occurs. The zinc/copper interaction causes an excess of zinc to result in a reduction of copper levels (by decreasing its absorption at the gastrointestinal tract) [7]. Zinc metabolism is still subject to interference with other elements. For example, if iron is present at high levels in diet, it may decrease the absorption of zinc, and this aspect should be considered when, during pregnancy and lactation, the control of iron levels is attempted through the use of dietary supplements. Other authors observed that dietary supplementation of the mother with iron did not significantly interfere with their plasma zinc levels nor with zinc levels in breast milk [18, 19, 38]. Also, calcium and phosphorus may interfere with the absorption of zinc, and there are also contradictory studies of the effect of these two elements [20]. Due to the abovementioned zinc/copper antagonism, high concentrations of zinc in breast milk may result in copper deficiency, since zinc can competitively inhibit copper absorption in the gastrointestinal tract of the child. Metallothionein appears to play a relevant role in this process [39]. As for selenium, zinc is accumulated by the fetus during the third trimester of pregnancy [14]. Zinc may be about 15 times more concentrated in breast milk than in the mother's plasma, evidencing an active transport mechanism, and its essential role for the child's development [12, 31]. There is a rapid and significant decrease in the concentration of zinc in breast milk throughout the lactation period, significantly during the first month [12]. This evidence is supported by several published studies [8, 14, 15, 40]. There were no differences associated with the mother's number of children or lactation history. Regarding the age of the mother, it was found that the concentration of zinc tends to increase (higher values for ages greater than 30 years) [15]. Significantly higher zinc values were observed in breast milk between the third and seventh days in mothers with preterm infants, compared to those with full-term infants [37].

3.2. Non-essential/toxic trace elements

3.2.1. Aluminum

Brain function of children exposed to this metal can be seriously affected [41]. Relevant sources of exposure are not only breast milk of mothers exposed to relevant levels of aluminum, but also infant Al-adjuvanted vaccination, like hepatitis B [41, 42]. Aluminum milk levels decrease significantly over the nursing, ranging from 0.056 mg/L in colostrum to 0.013 mg/L in mature milk [43]. Older mothers' (>25 years) milk present a higher aluminum concentration than the younger ones [44]. There is no relevant data available related to aluminum exposure during early life, and its correlation with brain function. Concentrations in human milk varying between 7.056 and 67 μg/L are described [8, 43, 45].

3.2.2. Antimony

The calculated transfer factor from food into human milk, calculated as the element concentration in food (g/kg) divided by the element concentration in milk (g/L), has been determined as 13.2 [46]. The reported concentration in human breast milk is between 0.14 and 0.35 μg/L.

3.2.3. Arsenic

Arsenic occurs in trivalent and pentavalent forms in food, water, and the environment. The biological effects of arsenic strongly depend on the actual chemical specie it is present, with inorganic forms being more toxic than most organic forms. Inorganic forms are methylated in the human body, giving rise to less toxic compounds, which are then excreted through urine [7]. Acute intoxication with arsenic is rare and is characterized by nausea, vomiting, diarrhea, and acute abdominal pain. Chronic intoxication is caused by exposure to natural sources, contaminated food, or water, or other accidental source [7]. In a recent study, presence of arsenic was observed in 63.51% of samples, with an average concentration of 2.36 μg/L [47], consistent with results from other authors [12, 20, 45, 48]. Arsenic presence in human milk is associated with cereal and fish intake [47].

3.2.4. Barium

No nutritional requirements are set for barium in mammals, and its origin is probably associated with plant sources, following metabolic pathways similar to the elements of the same group in the periodic table, such as calcium and strontium [11]. Barium levels in milk may be dependent of mother diet [11]. Concentrations of 0.017 μg/L have been reported [8].

3.2.5. Beryllium

Beryllium compounds are very toxic [49], and chronic beryllium disease has been observed in children living near a beryllium factory [50]. There is a high probability that this element can be transferred from mother to child through breast milk [50]. Concentration of 0.008 μg/L has been reported in breast milk [8].

3.2.6. Bismuth

This element has been reported in breast milk at a concentration of 0.002 μg/L [8].

3.2.7. Bromide

Described as having an important function in tissue development, cellular structure and membrane integrity, its presence in breast milk was reported in a recent study at a concentration of 0.812 mg/L [51].

3.2.8. Cadmium

The main source of exposure to cadmium is tobacco smoke. It is estimated that about 10% of mothers smoke during pregnancy, and the percentage of those who return to smoking during

lactation is even higher [23]. Smoking contributes to increased levels of some metals in breast milk. Cadmium is the one of highest concern because it is an IARC type 1 carcinogen, altering the metabolism of other micronutrients, such as copper, iron, magnesium, selenium, and zinc. Cadmium levels are about four times higher in the breast milk of smoking mothers compared to non-smoking ones [23]. It has been reported that metallothionein levels are about half in smoking mothers. This seems to indicate a protective mechanism to the child, since the toxicity of the metallothionein-Cd complex is higher than that of inorganic cadmium [52]. Concentrations of cadmium in human milk varying between 0.003 and 1.37 μg/L are described [8, 20, 43, 47, 53, 54].

3.2.9. Cerium

There is no evidence that it is an essential element [11], neither transport from mother to infant through milk [55, 56]. Concentrations in human milk varying between 0.0139 and 0.12 μg/L are described [46, 56].

3.2.10. Cesium

There is no evidence that it is an essential element [11]. It has been reported ^{137}Cs in breast milk after the reactor accident at Chernobyl [57]. Concentrations in human milk varying between 1 and 5 μg/L are described [20].

3.2.11. Gallium

The presence of ^{67}Ga in human breast milk has been described [58]. A concentration of 0.52 μg/L was reported [46].

3.2.12. Gold

Traces of gold have been found in breast milk, and it is assumed an association with the use of jewelry or dental amalgams [59]. Concentrations varying between 0.1 and 2.1 μg/L are described [45, 59].

3.2.13. Lanthanum

There is no evidence that it is an essential element [11]. The calculated transfer factor from food into the human milk has been determined as 13.8 [46]. The reported concentration in human breast milk is between 0.002 and 0.07 μg/L [8, 46].

3.2.14. Lead

Lead blood levels in the worldwide population have been decreasing significantly since the 1970s, largely due to the reduction of sources of environmental contamination, mainly the virtual elimination of this element from automobile fuels, but also from other sources of exposure such as paints, plumbing, ceramics, cosmetics, welding of food cans, etc. [60]. In young American children, it is reported that the levels of lead above 100 μg/L will mainly be related to exposure to particulate matter resulting from the degradation of paints used in homes [60]. The relationship between elevated levels of lead in children's blood and the

occurrence of intellectual development deficits (decreased IQ) is well known [60, 61]. In the human body, most of the lead is deposited in the bones (bones and teeth contain more than 90% of the body's total lead load) [62]. Lead mobilization of the human skeleton during pregnancy and lactation has been described [63, 64], resulting in a transgenerational transfer from the mother to the child. The mother consumption of calcium-rich foods reduces the risk of increased concentrations of lead in breast milk (>100 μg/L) [65, 66]. Iron also interferes with the absorption and toxicity of lead in children, causing a reduction of lead absorption. The hematological effects and intellectual deficit caused by lead are antagonized by an iron-rich diet [60]. A great inter-individual variability was observed in the concentration of lead in breast milk, which may be three orders of magnitude [67]. Concentrations varying between 0.019 and 18.17 μg/L are reported [8, 12, 20, 43, 47, 48, 54].

3.2.15. Lithium

Although clinical recommendations discourage the treatment of lactating mothers with lithium for bipolar disorder, studies demonstrate a concentration reduction in half from mother serum to milk, and also from milk to infant plasma, in the same proportions, with no serious adverse effects [68]. Concentrations of 0.005 μg/L in human milk are reported [8].

3.2.16. Mercury

Mercury is a highly toxic metal. Like lead, it causes depletion of glutathione as well as the protein sulfhydryl binding groups, resulting in the production of reactive oxygen species, such as superoxide anion and hydroxyl radicals [69]. Mercury levels in breast milk vary considerably depending on the mother's place of residence, lactation stage, age, and diet. An increase in mercury levels in mother's plasma and breast milk during lactation is described [8]. Concentrations varying between 0.008 and 3 μg/L are reported [70].

3.2.17. Nickel

Nickel role in some human physiological function is unknown [11]. However, it is reported that in case of severe nickel depletion, growth and hematopoiesis are depressed [7]. Due to its high homeostatic regulation, the symptoms of nickel poisoning are simply related to gastrointestinal irritation [7]. A decrease in nickel concentration throughout lactation is described [12]. Concentrations varying between 0.79 and 480 μg/L are reported [8, 12, 20, 45, 53].

3.2.18. Niobium

The calculated transfer factor from food into human milk was determined as 20.7 [46]. A mean concentration of 0.04 μg/L in human milk was reported [46].

3.2.19. Platinum

Undetectable levels were reported for platinum in human milk [45].

3.2.20. Rubidium

A relatively abundant element in body fluids and tissues, rubidium is also present in breast milk, having a behavior similar to that of potassium, although no rubidium-dependent biochemical functions are known [71]. Concentrations of rubidium in human milk ranging from 0.3 to 1.2 μg/L have been reported [20, 71, 72].

3.2.21. Ruthenium

The calculated transfer factor from food into human milk was determined as 4.1 [46]. Concentrations of 0.15 μg/L in human milk have been reported [46].

3.2.22. Scandium

Median concentrations of scandium in human milk of 0.19 μg/L are reported [45].

3.2.23. Silver

Silver has been found in breast milk, and it is speculated that it also originates from the use of jewelry or dental amalgams [59]. Concentrations varying between 0.005 and 0.78 μg/L are reported [8, 45, 46].

3.2.24. Strontium

There is no evidence of the nutritional importance of this element, although it is known that it is concentrated in the bone mass [11]. Biokinetic model for strontium in the lactating woman from bone to milk have been described [73]. Concentrations in human milk varying between 44 and 46 μg/L are reported [72].

3.2.25. Thorium

The calculated transfer factor from food into human milk was determined as 20.2 [46]. A concentration of 0.2 μg/L in human milk was reported [46].

3.2.26. Tin

There is no evidence that tin is an essential element [11]. Signs of chronic exposure to inorganic tin include decreased growth and anemia [7]. Also, organic tin compounds were studied and no significant transport could be observed from mother diet to milk [74]. Undetectable levels were reported [20].

3.2.27. Titanium

The calculated transfer factor from food into human milk for titanium was determined as 5.6 [46]. Concentrations in human milk varying between 6.3 and 270 μg/L are reported [45, 46].

3.2.28. Uranium

The calculated transfer factor from food into human milk for uranium was determined as 21.3 [46]. A concentration of 0.03 μg/L in the human milk was reported [46].

3.2.29. Vanadium

No defined biochemical function has been identified for vanadium in the higher animals. Vanadium is a relatively toxic element, with the most frequent symptoms being intestinal disturbances and greenish tongue [7]. A concentration of 0.18 μg/L in human milk was reported [45].

4. Concluding remarks

Breast milk is for many children, in the first months of life, their unique source of nutrients, including trace elements essential for their healthy growth and development.

Although by definition trace elements are present in breast milk at relatively low concentrations, they play a crucial role in multiple physiological processes.

All of them show a great inter-individual variability in the breast milk, generally tending to decrease during lactation.

The variability of trace element levels in breast milk related to geographic, environmental, and dietary factors is well studied for several of them. For others, there is still insufficient knowledge about these aspects.

The advances in sensitivity and specificity of the analytical instrumentation occurred in recent years have made it possible to determine several elements which had not been studied until then. On the other hand, the higher reliability of current analytical techniques and the higher awareness about the importance of contamination control makes the more recently published results much more reliable.

It should be noted that the nutritional value of breast milk regarding a particular trace element does not depend on its total analytical concentration but on its bioavailable fraction; however, studies on this topic are very scarce.

Knowing to what extent the mother's supplementation can adequately correct any deficiencies in milk quality in terms of trace element levels is another important issue that should be studied.

Acknowledgements

This work received financial support from the European Union (FEDER funds POCI/01/0145/FEDER/007265) and National Funds (FCT/MEC, Fundação para a Ciência e Tecnologia and Ministério da Educação e Ciência) under the Partnership Agreement PT2020 UID/QUI/50006/2013.

Author details

Manuel de Rezende Pinto and Agostinho A. Almeida*

*Address all correspondence to: aalmeida@ff.up.pt

LAQV, REQUIMTE, Departamento de Ciências Químicas, Laboratório de Química Aplicada, Faculdade de Farmácia, Universidade do Porto, Porto, Portugal

References

[1] Picciano MF. Nutrient composition of human milk. Pediatric Clinics of North America. 2001;**48**(1):53-67

[2] WHO. Exclusive Breastfeeding. 2018. Available from: http://www.who.int/nutrition/topics/exclusive_breastfeeding/en/ [Accessed: February 22, 2018]

[3] Kent JC. How breastfeeding works. Journal of Midwifery & Women's Health. 2007;**52**(6): 564-570

[4] Ballard O, Morrow AL. Human milk composition nutrients and bioactive factors. Pediatric Clinics of North America. 2013;**60**(1):49-74

[5] Qian JH et al. Breast milk macro- and micronutrient composition in lactating mothers from suburban and urban shanghai. Journal of Paediatrics and Child Health. 2010;**46**(3): 115-120

[6] Rueda R et al. Gestational age and origin of human milk influence total lipid and fatty acid contents. Annals of Nutrition and Metabolism. 1998;**42**(1):12-22

[7] World Health Organization, International atomic energy agency & food and agriculture organization of the United Nations. Trace Elements in Human Nutrition and Health. Geneva: World Health Organization; 1996

[8] Abdulrazzaq YM et al. Trace element composition of plasma and breast milk of well-nourished women. Journal of Environmental Science and Health, Part A-Toxic/Hazardous Substances & Environmental Engineering. 2008;**43**(3):329-334

[9] Yamawaki N et al. Macronutrient, mineral and trace element composition of breast milk from Japanese women. Journal of Trace Elements in Medicine and Biology. 2005;**19**(2–3): 171-181

[10] Krachler M et al. Changes in the concentrations of trace elements in human milk during lactation. Journal of Trace Elements in Medicine and Biology. 1998;**12**(3):159-176

[11] Friel JK et al. Elemental composition of human milk from mothers of premature and full-term infants during the first 3 months of lactation. Biological Trace Element Research. 1999;**67**(3):225-247

[12] Almeida AA et al. Trace elements in human milk: Correlation with blood levels, inter-element correlations and changes in concentration during the first month of lactation. Journal of Trace Elements in Medicine and Biology. 2008;**22**(3):196-205

[13] Rossipal E, Krachler M. Pattern of trace elements in human milk during the course of lactation. Nutrition Research. 1998;**18**(1):11-24

[14] Kim SY et al. Longitudinal study on trace mineral compositions (selenium, zinc, copper, manganese) in korean human preterm milk. Journal of Korean Medical Science. 2012; **27**(5):532-536

[15] Lin TH et al. Longitudinal changes in Ca, mg, Fe, cu, and Zn in breast milk of women in Taiwan over a lactation period of one year. Biological Trace Element Research. 1998;**62**(1–2): 31-41

[16] Bloxam DL et al. Maternal zinc during oral iron supplementation in pregnancy—A preliminary study. Clinical Science. 1989;**76**(1):59-65

[17] Hambidge KM et al. Acute effects of iron therapy on zinc status during pregnancy. Obstetrics and Gynecology. 1987;**70**(4):593-596

[18] Arnaud J et al. Effect of iron supplementation during pregnancy on trace-element (cu, se, Zn) concentrations in serum and breast-milk from Nigerian women. Annals of Nutrition and Metabolism. 1993;**37**(5):262-271

[19] Hannan MA et al. Maternal milk concentration of zinc, iron, selenium, and iodine and its relationship to dietary intakes. Biological Trace Element Research. 2009;**127**(1):6-15

[20] Institute of Medicine (U.S.). Panel on Micronutrients, DRI: Dietary Reference Intakes for Vitamin a, Vitamin K, Arsenic, Boron, Chromium, Copper, Iodine, Iron, Manganese, Molybdenum, Nickel, Silicon, Vanadium, and Zinc. Washington, D.C.: National Academy Press; 2001

[21] Laurberg P et al. Iodine nutrition in breast-fed infants is impaired by maternal smoking. Journal of Clinical Endocrinology and Metabolism. 2004;**89**(1):181-187

[22] Otten JJ, Hellwig JP, Meyers LD. DRI, Dietary Reference Intakes: The Essential Guide to Nutrient Requirements. Washington, D.C.: National Academies Press; 2006. xiii, 543p

[23] Napierala M et al. Tobacco smoking and breastfeeding: Effect on the lactation process, breast milk composition and infant development. A critical review. Environmental Research. 2016;**151**:321-338

[24] Casey CE, Hambidge KM, Neville MC. Studies in human lactation—Zinc, copper, manganese and chromium in human-milk in the 1st month of lactation. American Journal of Clinical Nutrition. 1985;**41**(6):1193-1200

[25] Murray MJ et al. Effect of iron status of nigerian mothers on that of their infants at birth and 6-months, and on concentration of Fe in breast-milk. British Journal of Nutrition. 1978;**39**(3):627-630

[26] Gupta VK et al. A comparative study on PVC based sensors in determination of molybdenum. Analytical Methods. 2011;**3**(2):334-342

[27] Bratter P, de Bratter VEN. Influence of high dietary selenium intake on the thyroid hormone level in human serum. Journal of Trace Elements in Medicine and Biology. 1996; **10**(3):163-166

[28] Navarro-Blasco I, Alvarez-Galindo JI. Selenium content of Spanish infant formulae and human milk: Influence of protein matrix, interactions with other trace elements and estimation of dietary intake by infants. Journal of Trace Elements in Medicine and Biology. 2003;**17**(4):277-289

[29] Institute of Medicine (U.S.). Panel on Dietary Antioxidants and Related Compounds, Dietary Reference Intakes for Vitamin C, Vitamin E, Selenium, and Carotenoids. Washington, D.C.: National Academy Press; 2000

[30] Campbell JD. Lifestyle, minerals and health. Medical Hypotheses. 2001;**57**(5):521-531

[31] Bratter P et al. Maternal selenium status influences the concentration and binding pattern of zinc in human milk. Journal of Trace Elements in Medicine and Biology. 1997;**11**(4):203-209

[32] Bianchi MLP et al. Dietary intake of selenium and its concentration in breast milk. Biological Trace Element Research. 1999;**70**(3):273-277

[33] Benemariya H, Robberecht H, Deelstra H. Copper, zinc and selenium concentrations in milk from middle-class women in Burundi (Africa) throughout the first 10 months of lactation. Science of the Total Environment. 1995;**164**(2):161-174

[34] Linzell JL, Mepham TB, Peaker M. Secretion of citrate into milk. Journal of Physiology (London). 1976;**260**(3):739-750

[35] Litov RE, Combs GF. Selenium in pediatric nutrition. Pediatrics. 1991;**87**(3):339-357

[36] Devi CB et al. Zinc in human health. Journal of Dental and Medical Sciences. 2014;**13**(7 ver. II): 18-23

[37] Narang APS et al. Comparative study of trace elements of human milk in preterm and term mothers. Trace Elements and Electrolytes. 2006;**23**(2):99-102

[38] Domellof M et al. Iron, zinc, and copper concentrations in breast milk are independent of maternal mineral status. American Journal of Clinical Nutrition. 2004;**79**(1):111-115

[39] Kaur K et al. Zinc: The metal of life. Comprehensive Reviews in Food Science and Food Safety. 2014;**13**(4):358-376

[40] Wasowicz W et al. Selenium, zinc, and copper concentrations in the blood and milk of lactating women. Biological Trace Element Research. 2001;**79**(3):221-233

[41] Dórea JG. Aluminium concentrations in human milk: Additional comments on exposure issues in the neonate. Pediatrics and Neonatology. 2014;**55**(2):81-82

[42] Dórea JG, Marques RC. Infants' exposure to aluminum from vaccines and breast milk during the first 6 months. Journal of Exposure Science & Environmental Epidemiology. 2009;**20**(7):598-601

[43] Chao H-H et al. Arsenic, cadmium, lead, and aluminium concentrations in human milk at early stages of lactation. Pediatrics and Neonatology. 2014;**55**(2):127-134

[44] Mandić ML et al. Aluminium levels in human milk. Science of the Total Environment. 1995;**170**(3):165-170

[45] Krachler M et al. Concentrations of selected trace elements in human milk and in infant formulas determined by magnetic sector field inductively coupled plasma-mass spectrometry. Biological Trace Element Research. 2000;**76**(2):97-112

[46] Wappelhorst O et al. Transfer of selected elements from food into human milk. Nutrition. 2002;**18**(4):316-322

[47] Bassil M et al. Lead, cadmium and arsenic in human milk and their socio-demographic and lifestyle determinants in Lebanon. Chemosphere. 2018;**191**:911-921

[48] Klein LD et al. Concentrations of trace elements in human milk: Comparisons among women in Argentina, Namibia, Poland, and the United States. PLoS One. 2017;**12**(8):1-16

[49] International Program on Chemical Safety. Concise International Chemical Assessment Document. Geneva: World Health Organization; 1998

[50] US Department of Health and Human Services, Public Health Service, Agency for Toxic Substances and Disease Registry. Toxicological Profile for Beryllium. Atlanta, Georgia. Agency for Toxic Substances and Disease Registry. 2002

[51] Mohd-Taufek N et al. The simultaneous analysis of eight essential trace elements in human milk by ICP-MS. Food Analytical Methods. 2016;**9**(7):2068-2075

[52] Milnerowicz H, Chmarek M. Influence of smoking on metallothionein level and other proteins binding essential metals in human milk. Acta Paediatrica. 2005;**94**(4):402-406

[53] Elmastas M et al. Determinations of copper, zinc, cadmium, and nickel in cows', goats', ewes', and human milk samples using flame atomic absorption spectrometry (FAAS)-microwave digestion. Analytical Letters. 2005;**38**(1):157-165

[54] Kosanovic M et al. Simultaneous determination of cadmium, mercury, lead, arsenic, copper, and zinc in human breast milk by ICP-MS/microwave digestion. Analytical Letters. 2008;**41**(3):406-416

[55] Michalke B et al. Cerium in human milk samples and its transfer from blood to milk: Is there an elevated nutritional risk for breast-fed babies? Pure and Applied Chemistry. 2012; **84**(2):313-324

[56] Höllriegl V et al. Measurement of cerium in human breast milk and blood samples. Journal of Trace Elements in Medicine and Biology. 2010;**24**(3):193-199

[57] Gattavecchia E et al. Cesium-137 levels in breast-milk and placentae after fallout from the reactor accident at Chernobyl. Health Physics. 1989;**56**(2):245-248

[58] Larson SM, Schall GL. Gallium-67 concentration in human breast milk. Journal of the American Medical Association. 1971;**218**(2):257

[59] Prohaska T et al. Determination of trace elements in human milk by inductively coupled plasma sector field mass spectrometry (ICP-SFMS). Journal of Analytical Atomic Spectrometry. 2000;**15**(4):335-340

[60] Gulson BL et al. Dietary intakes of selected elements from longitudinal 6-day duplicate diets for pregnant and nonpregnant subjects and elemental concentrations of breast milk and infant formula. Environmental Research. 2001;**87**(3):160-174

[61] Canfield RL, Jusko TA, Kordas K. Environmental lead exposure and children's cognitive function. Rivista Italiana di Pediatria (The Italian Journal of Pediatrics). 2005;**31**(6):293-300

[62] Christopher P et al. Pathophysiology and Etiology of Lead Toxicity. 2015. Available from: http://emedicine.medscape.com/article/2060369 [Accessed: February 22, 2018]

[63] Gulson BL et al. Pregnancy increases mobilization of lead from maternal skeleton. Journal of Laboratory and Clinical Medicine. 1997;**130**(1):51-62

[64] Gulson BL et al. Mobilization of lead from the skeleton during the postnatal period is larger than during pregnancy. Journal of Laboratory and Clinical Medicine. 1998;**131**(4): 324-329

[65] Farias P et al. Blood lead levels in pregnant women of high and low socioeconomic status in Mexico City. Environmental Health Perspectives. 1996;**104**(10):1070-1074

[66] Hernandez Avila M et al. Dietary and environmental determinants of blood and bone lead levels in lactating postpartum women living in Mexico City. Environmental Health Perspectives. 1996;**104**(10):1076-1082

[67] De Felip E et al. Priority persistent contaminants in people dwelling in critical areas of Campania region, Italy (SEBIOREC biomonitoring study). Science of the Total Environment. 2014;**487**:420-435

[68] Viguera AC et al. Lithium in breast milk and nursing infants: Clinical implications. Journal of Womens Health. 2007;**16**(6):933-933

[69] Stohs SJ, Bagchi D. Oxidative mechanisms in the toxicity of metal-ions. Free Radical Biology and Medicine. 1995;**18**(2):321-336

[70] Dorea JG. Mercury and lead during breast-feeding. British Journal of Nutrition. 2004; **92**(1):21-40

[71] Khatami SF et al. Breast milk concentration of rubidium in lactating mothers by instrumental neutron activation analysis method. Iranian Journal of Pediatrics. 2014;**24**(6): 692-696

[72] Li C et al. Minerals and trace elements in human breast milk are associated with Guatemalan infant anthropometric outcomes within the first 6 months. Journal of Nutrition. 2016;**146**(10):2067-2074

[73] Shagina NB et al. Strontium biokinetic model for the lactating woman and transfer to breast milk: Application to Techa River studies. Journal of Radiological Protection. 2015; **35**(3):677-694

[74] Mino Y et al. Determination of organotins in human breast milk by gas chromatography with flame photometric detection. Journal of Health Science. 2008;**54**(2):224-228

[75] Yoshida M et al. Molybdenum and chromium concentrations in breast milk from Japanese women. Bioscience, Biotechnology, and Biochemistry. 2008;**72**(8):2247-2250

[76] da Costa RSS et al. Trace elements content of colostrum milk in Brazil. Journal of Food Composition and Analysis. 2002;**15**(1):27-33

[77] Mandavi R et al. A pilot study of synbiotic supplementation on breast milk mineral concentrations and growth of exclusively breast fed infants. Journal of Trace Elements in Medicine and Biology. 2015;**30**:25-29

[78] Winfield SA et al. Measurement of total mercury in biological specimens by cold vapor atomic fluorescence spectrometry. Clinical Chemistry. 1994;**40**(2):206-210

[79] Vimy MJ et al. Mercury from maternal "silver" tooth fillings in sheep and human breast milk—A source of neonatal exposure. Biological Trace Element Research. 1997;**56**(2):143-152

[80] Norouzi E, Bahramifar N, Ghasempouri SM. Effect of teeth amalgam on mercury levels in the colostrums human milk in Lenjan. Environmental Monitoring and Assessment. 2012; **184**(1):375-380

Section 3

Environmental Trace Elements

Chapter 6

Trace Elements in Suspended Particulate Matter and Sediments of the Cai River: Nha Trang Bay Estuarine System (South China Sea)

Sofia Koukina and Nikolay Lobus

Additional information is available at the end of the chapter

http://dx.doi.org/10.5772/intechopen.76471

Abstract

The distribution of particulate form of organic carbon (POC), Al, Fe, Ti, Li, Zn, Pb, U, Sc, Sn, Bi, Zr, Ba, As, Sr, W, V, Co, Cu, Ni, Mo, Cr, Mn, Ba, Sn, Sb, Hg, and Ag in the Cai river and Nha Trang Bay generally followed the distribution of total suspended matter (SPM) and was characterized by the most significant loss in the frontal zone of the estuary with highest horizontal gradients within the salinity interval of 8–20‰. The most part of these elements are supplied to the estuary with the Cai river discharge. Sedimentary Al, Fe, Ti, Li, Sc, Co, Cs, Zr, Cr, Zn, Co, Ni, Cu, Pb, Sn, and V are most likely controlled by the accumulation of their most fine-grained host minerals in sea floor depression of the bay. Sedimentary Bi, W, As, U, and Mo are mainly deposited with the coarse river material near the river mouth. The distribution of Ca, Sr, Mn, and Ba is largely controlled by the total inorganic carbon (TIC) content in the sediments. Metal form study revealed the highest percent contents of the labile forms for Mn, Co, and Pb in the sediments. The high levels of weak acid-soluble Pb and Co (30% and 43% of the total content in sediment, on average, respectively) contributes to a contamination problem in the Nha Trang Bay which arises from the Cai River discharge.

Keywords: Vietnam, tropical estuary, trace elements, selective extraction, bioavailable metal forms

1. Introduction

Southeast Asia has experienced a rapid and colossal economic growth with Vietnam being one of the fastest growing countries. Most development activities (e.g., industry, agriculture,

human settlement, tourism, and transport) take place in coastal zones [1–4]. This hazard is increased by the high vulnerability of these areas to environmental changes. The Cai River and the Nha Trang Bay of the South China Sea are inhabited by unique biota. This region is now exposed to the multiple anthropogenic stressors such as human settlement, agriculture and aquaculture, tourism and transport [5].

Over the past two decades, comprehensive studies of the organic geochemistry patterns and contamination levels and trends in the Nha Trang Bay have been undertaken [6–14]. The most recent research of the abundance, distribution and speciation of the major and trace elements in the sediments allowed to track the fate of potential contaminants in the Cai River—Nha Trang Bay estuarine system along the salinity gradient [5, 15]. It was shown that most trace element contents were at natural levels and are derived from the composition of rocks and soils in the watershed. A severe enrichment of Ag was most likely derived from metal-rich detrital heavy minerals. Geochemical fractionation of the riverine material generally determined the metal enrichment in surface sediments along the salinity gradient. The parts of actually and potentially bioavailable forms were most elevated for Mn and Pb (up to 36 and 32% of total content, respectively). Overall, the most bioavailable parts of trace elements were associated with easily soluble amorphous Fe and Mn oxyhydroxides.

In estuarine region, suspended particulate matter (SPM) acts as a major carrier as trace elements get adsorbed on to major elements like Fe and Mn oxyhydroxides and organic matter and get precipitated, where coarse material may settle into the estuarine system as sediments and finer materials get transported into the ocean [16–18]. It is important to study major and trace elements, as excess input of these metals may settle into the estuary due to salinity gradient [19–22]. The present study summarises the data on the abundance, distribution, partition, speciation and bioavailability of major and trace elements in the suspended particulate matter (SPM) and surface sediments of the Cai River estuary under multiple stresses.

2. Materials and methods

2.1. Environmental setting

The Cai River, its estuary and the adjacent part of the Nha Trang Bay belong to the Central Southern Coastal Region of Vietnam (Khanh Hoa Province). The fresh river water ($S < 0.1‰$) and saline South China Sea water ($S \approx 36‰$) form a major water-mixing zone. The fill dam built 8 km upstream from the river mouth limits the water exchange and marks the riverine boundary of the water-mixing zone (**Figure 1**). The Cai River estuary and Nha Trang Bay can be divided into three sub-zones: (1) river ($S < 0.1‰$), (2) transitional waters (estuary) ($0.1‰ > S > 32‰$) and (3) sea (bay) ($S > 32‰$). In the transitional waters, the salinity (S) increases from the river to the sea and from the surface to the bottom. The water column is

highly stratified with the pronounced horizontal and vertical salinity gradients [5]. The climate seasonality and human activities (such as urbanisation, land use, damming, tourism, coastal construction, transportation, aquaculture and fisheries) expose the Nha Trang Bay to multiple pressures [14, 23–26].

2.2. Field work

The water and sediment samples were collected in the Cai River estuary and Nha Trang Bay in July 2013 along the salinity gradient at five locations for surface water layer (sts. 1, 3, 4, 7, 8, **Figure 1**) and at seven locations for surface sediments (sts. 2–8, **Figure 1**). The sampling stations were located in the riverine (st. 1), transitional (sts. 2–4) and marine (sts. 5–8) sub-zones of the dry season.

The surface water samples were obtained using a plastic Niskin bottle. The temperature, alkalinity and salinity of the water samples were measured on-board immediately after collection using portable conductivity apparatuses HI 98129 Combo and HI 98302 DIST 2 (Hanna Instruments, Germany). The suspended particulate matter was collected by filtering of water samples in an all-glass filtering system, on pre-weighted filters: 0.45 μm polycarbonate filters (Millipore-Isopore) for total suspended matter (TSM); combusted and pre-weighted glass fibre filters (Whatman GF/F) for particulate organic carbon (POC) and acid-clean cellulose filters (Millipore HA) for geochemical analyses. In the laboratory, all filters were rinsed with 250 ml Milli-Q water to remove salts and dried to constant weight at 60°C.

The surface sediment sampling, transportation and preparation procedures were performed using standard clean techniques that were described elsewhere [5].

2.3. Analytical methods

The surface sediment samples were subjected to grain size and mineral composition analyses. The grain size analysis was performed by wet sieving [27, 28].

The dissolved organic carbon in water samples was determined by high-temperature (at 680°C) thermocatalitic oxidation with dispersion-free IP detection. The total carbon (TC) contents in suspended particulate matter (SPM) and sediment samples were determined by dry burning at 900°C in oxygen flow and the total inorganic carbon (TIC) contents were determined by dry burning at 200°C with H_3PO_4. The DOC, TC and TIC analyses were performed with the analyser TOC 5000-V-CPH (Shimudzu Co., Japan). The total organic carbon (TOC) contents were determined as a difference between TC and TIC contents in the samples [10].

For the total Al, Fe, Ti, Ca, Na, Mn, Li, V, Cr, Co, Ni, Cu, Zn, As, Sr., Zr, Mo, Cd, Ag, Sn, Sb, Cs, Ba, Pb, Bi and U content analysis, the samples were subjected to the total acidic dissolution in HNO_3 + HF + $HClO_4$ in an open system with further determination of element contents using

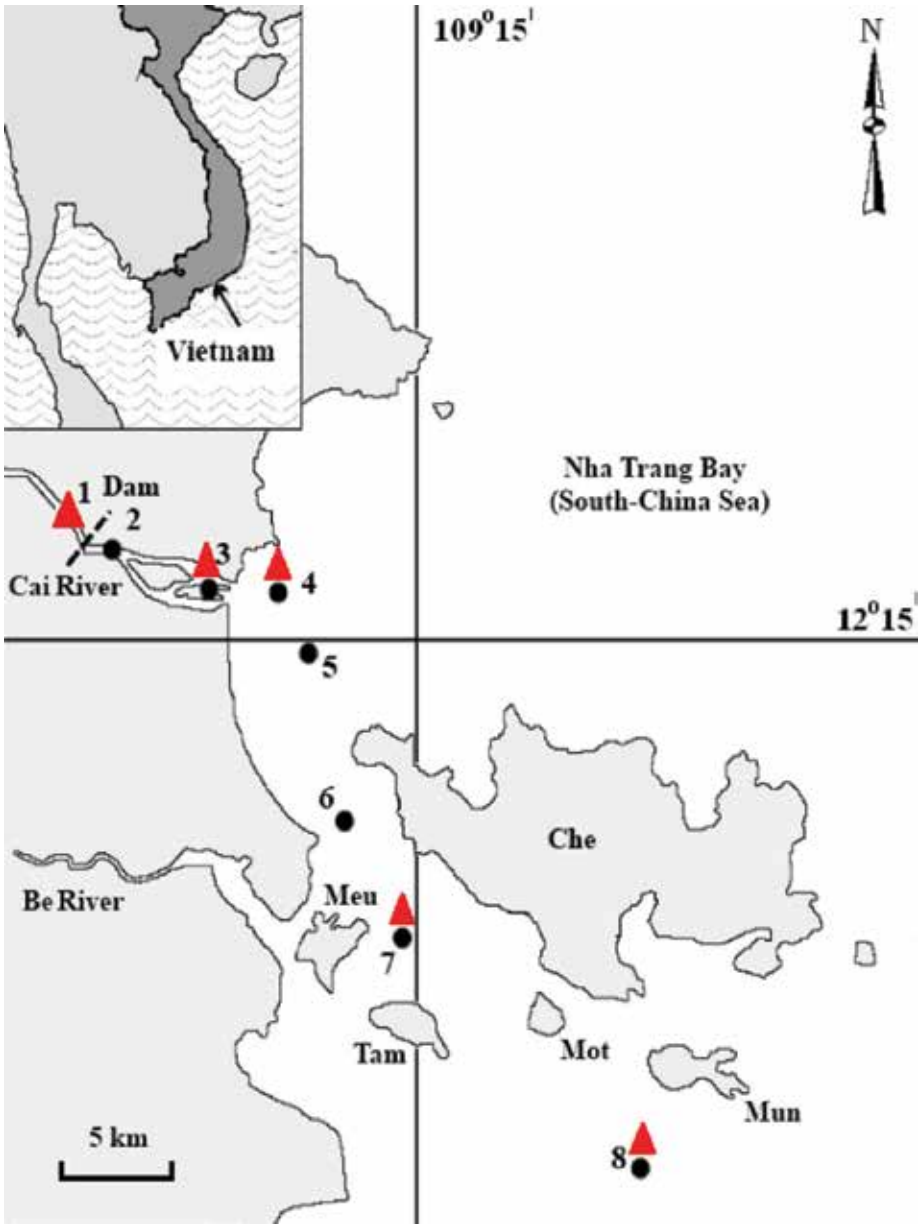

Figure 1. Location of study sites.

the ICP method on the X-7 ICP-MS spectrometer (Thermo Scientific, USA) [29]. The detailed sample decomposition and analytical procedures are described elsewhere [16]. The Hg content was determined in the dry samples using a pyrolyse method on the RA-915+ spectrometer with background correction and a two-chamber atomiser PYRO-915+ (Lumex, Russia) [9, 14].

http://dx.doi.org/10.5772/intechopen.76471

To assess the chemical form of selected metals (Fe, Mn, Cr, Zn, Cu, Pb, Ni and Co) in the sediments, the samples were subjected to single chemical reagent (single-step) extraction procedures. The weak-acid-soluble (labile) metals were extracted using 25% acetic acid, the oxalate-soluble metals were extracted using ammonium oxalate-oxalic acid buffered solution at pH 3.2 (Tamm extraction), the pyrophosphate-soluble metals were extracted by 0.1 M sodium pyrophosphate. To isolate the weak acid-soluble metals, 15 ml of 25% acetic acid was added to 1.1 g of dry sample in polypropylene vials and shaken in a mechanical shaker for 6 h with acetic acid. Then, each extract with the sediment was filtrated into a 25 ml glass volumetric flask. The sediment on the filter was washed with 10 ml of distilled water and the wash water was added to the flask [27]. To isolate the amorphous iron oxides and their associated microelements, 50 ml of ammonium oxalate-oxalic acid buffered (Tamm) solution was added to 1.1 g of dry sample in the 250 ml flat bottom flask, shaken for 1 h and filtrated to a 250 ml glass volumetric flask. The sediment on the filter was washed with 10 ml of distilled water that was mixed with a small amount of oxalic acid and the wash water was added to the flask. Then, the filter with sediment was added to the sediment in the flat-bottom flask and subjected to one more repeated extraction and the extract was added to the 250 ml volumetric flask [30]. To isolate the organically bound metals, 15 ml of 0.1 M sodium pyrophosphate was added to 1.1 g of dry sample in polypropylene vials and shaken in a mechanical shaker for 15 min, left for 24 h and then filtrated to a 250 ml glass volumetric flask. The sediment on the filter was washed with 10 ml of 0.1 M sodium pyrophosphate and the wash water was added to the flask [31]. The metal contents in the extracts were further determined using an atomic absorption spectrometer (AAS) Hitachi 180–8 (Hitachi Co., Japan) in the Analytical Centre of Moscow State Lomonosov University.

The relative accuracy of the analytical determinations was within the standard deviations that were established by the certified reference materials (CRM) SDO-1 (Russia) (for SiO_2, TOC and TIC), SRM 521-84P (Russia) (for Na_2O, Al_2O_3, S_{total}, K_2O, CaO, MnO, Fe_2O_3, Li, V, Cr, Zn, As, Sr., Zr, Mo, Ag, Sn, Ba, Pb), AGV-2 (USA) (for MgO, P_2O_5, TiO_2, Co, Ni, Cu, Sr., Sb, Cs, U) and Mess-3 (Canada) (for Hg).

3. Results and discussion

3.1. Abundance and distribution of major and trace elements in surface SPM

The hydrology of the riverine sub-zone of the studied part of the Cai River—Nha Trang Bay estuarine system is strongly influenced by the fill dam. The surface fresh water layer flows seaward over the dam, while the upstream penetration of the near-bottom saline water lenses is blocked [5]. In July 2013, the salinity of the surface fresh-water layer varied from 0% to 36‰. The frontal zone of the contact of fresh and saline waters occurred downstream from the fill dam (sts. 2–3, **Figure 1**), where the horizontal salinity gradient was 3.5‰ per 1 km distance. The temperature (T) of the water column varied in narrow ranges and decreased from

the river to the sea from 30 to 29°C in the surface water layer. The pH of the water column increased from neutral in the riverine waters (pH 7) to low-alkaline in the transitional and sea waters (pH 8–9). The dissolved organic carbon (DOC) concentration in the surface water layer varied within the ranges 1.1–2.5 mg l^{-1} and was distributed uniformly (2.3-2.5 mg l^{-1}) in the frontal zone and transitional waters and exhibited a minimum of 1.1 mg l^{-1} in the marine part of the transect at salinity >30‰ (**Figure 2**).

The suspended particulate matter (SPM) showed a concentration maximum of 50 mg l^{-1} near the river mouth (sts. 1) at salinity 0‰ and then a decrease seaward to the values of around 1 mg l^{-1} at salinities 32–36‰, following from the sedimentation of the coarsest fluvial material in the frontal zone of the estuary at the sharp decrease in the river flow velocity enhanced by the dam influence (**Figure 2**). The distribution pattern of particulate organic carbon (POC) was close to the SPM distribution. The maximal POC concentration (1–1.25 mg l–1) was found in the fluvial part of the estuary (sts. 1–3) at salinities 0–8‰ because of an intensive sedimentation of the organically enriched suspended river material in the frontal zone of the estuary. In the transitional waters, the POC concentration lowers seaward to 0.94 mg l^{-1}at salinities around 20‰ and further to 0.18–0.21 mg l^{-1} at salinities 32–36‰ (**Figure 2**). The organic carbon content in the SPM (POC, % of dry SPM weight) varied within the range 2–17%. The higher organic carbon content >10% was found in SPM of the marine waters at the salinity >30‰ (**Table 1**).

The distribution of particulate form of Al, Fe, Ti, Li, Zn, Pb, U, Sc, Sn, Bi, Zr, Ba, As, Sr., W, V and Ag followed the distribution of total suspended matter and was characterised by a maximum in the river water and then a sharp decrease seaward of element relative concentration (in μg l^{-1}) with highest horizontal gradients within the salinity interval of 8–20% (**Figure 3**). The absolute concentration of these elements (in μg $g^{-1}$of the dry SPM weight) followed the same trend of decreasing seaward but was elevated in the both riverine and transitional waters (0–20‰) (**Table 1**, **Figure 3**). The most significant losses of suspended elements occurred in the frontal to transitional zone of the estuary (0–20‰) by an intensive sedimentation of dissolved and suspended river material. The most part of these elements must be supplied to the estuary with the Cai River discharge. In estuaries, the flocculation and coagulation of riverine microcolloids are initiated when the salinity increases. These processes are accompanied by a rapid scavenging of dissolved trace elements from the water column. Further deposition of newly-formed aggregates contributes to the enrichment of sediments in trace elements [32].

The distribution of particulate form of Co, Cu, Ni, Mo and Cr and, in some lesser extent, Mn, Ba, Sn, Sb and Hg is characterised by the most significant loss in the frontal zone of the estuary where the coarsest river material enriched in detrital minerals is deposited at the sharp decrease of the river flow velocity enhanced by the dam (**Table 1**, **Figure 3**). Both relative (in μg l^{-1}) and absolute (in μg g^{-1} of the dry SPM weight) concentrations of these elements sharply decrease with the highest horizontal gradients at the initial salinity rise (0–8‰). The depletion in these elements in the transitional waters (at salinities 8–32‰) was followed by negligible increase of their relative concentrations and significant increase of

http://dx.doi.org/10.5772/intechopen.76471

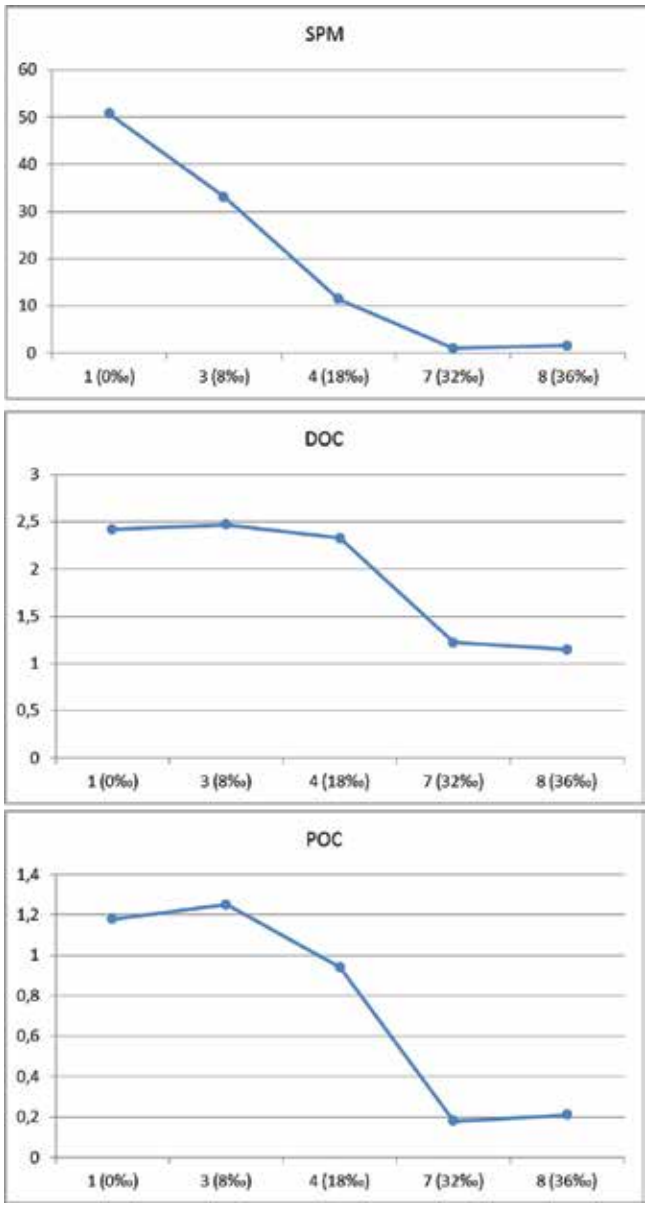

Figure 2. SPM, DOC and POC concentrations in surface water layer (in mg l^{-1}).

absolute concentrations of Co, Cu, Ni, Mo, and Cr at salinities 32–36‰ (**Table 1**, **Figure 3**). In the stratified Cai River estuary, the significant part of the particulate trace elements may be carried out seaward with the surface water layer. In the marine part of the estuary, with a homogenisation of the water column, most of the fine-grained material of surface water layer enriched in clay minerals, carbonates and trace metals is deposited [5]. Since SPM in

Station (S ‰)	1 (0‰)	3 (8‰)	4 (18‰)	7 (32‰)	8 (36‰)
Li	57.09	60.32	57.37	9.50	8.67
Al	15.11	15.41	14.61	1.30	0.78
Ca	0.31	0.16	0.16	0.83	0.82
Sc	15.85	15.42	16.17	5.65	3.52
Ti	0.18	0.15	0.12	0.03	0.02
V	94.07	109.59	127.60	63.59	17.39
Cr	187.21	57.34	72.09	66.18	91.86
Mn	737.05	410.08	342.46	461.65	479.05
Fe	4.67	4.77	5.31	0.45	0.25
Co	175.41	13.66	12.24	60.91	116.96
Ni	384.24	52.48	61.56	119.56	171.20
Cu	201.66	31.60	34.25	119.16	201.11
Zn	116.07	119.56	103.54	28.00	35.7
As	42.42	34.88	39.85	6.61	89.64
Sr	45.32	46.63	61.39	201.82	201.40
Zr	27.46	22.74	22.62	4.25	2.52
Mo	51.58	9.13	9.45	10.97	13.57
Ag	0.22	0.18	0.22	0.25	0.13
Sn	9.19	8.56	6.57	2.53	1.77
Sb	0.97	0.93	0.94	0.22	0.20
Cs	16.30	15.12	11.80	0.97	0.77
Ba	286.38	205.25	248.46	28.48	157.93
W	12.01	5.63	5.43	1.64	1.06
Hg	0.89	0.49	1.11	2.28	0.91
Pb	65.17	63.05	75.28	44.76	26.88
Bi	9.66	9.84	14.59	1.14	0.42
U	9.08	10.33	8.77	0.49	0.43
POC	3.68	3.85	9.39	7.87	7.29

Table 1. Major and trace elements contents in SPM (in μg g^{-1}, except for Al, Fe, Ti, Mn, Ca and POC in % of dry weight).

transitional and marine waters were enriched in organic carbon, the particulate organic matter of terrigenous and/or planktonogenous origin most probably contributed to trace element accumulation in SPM in the bay.

http://dx.doi.org/10.5772/intechopen.76471

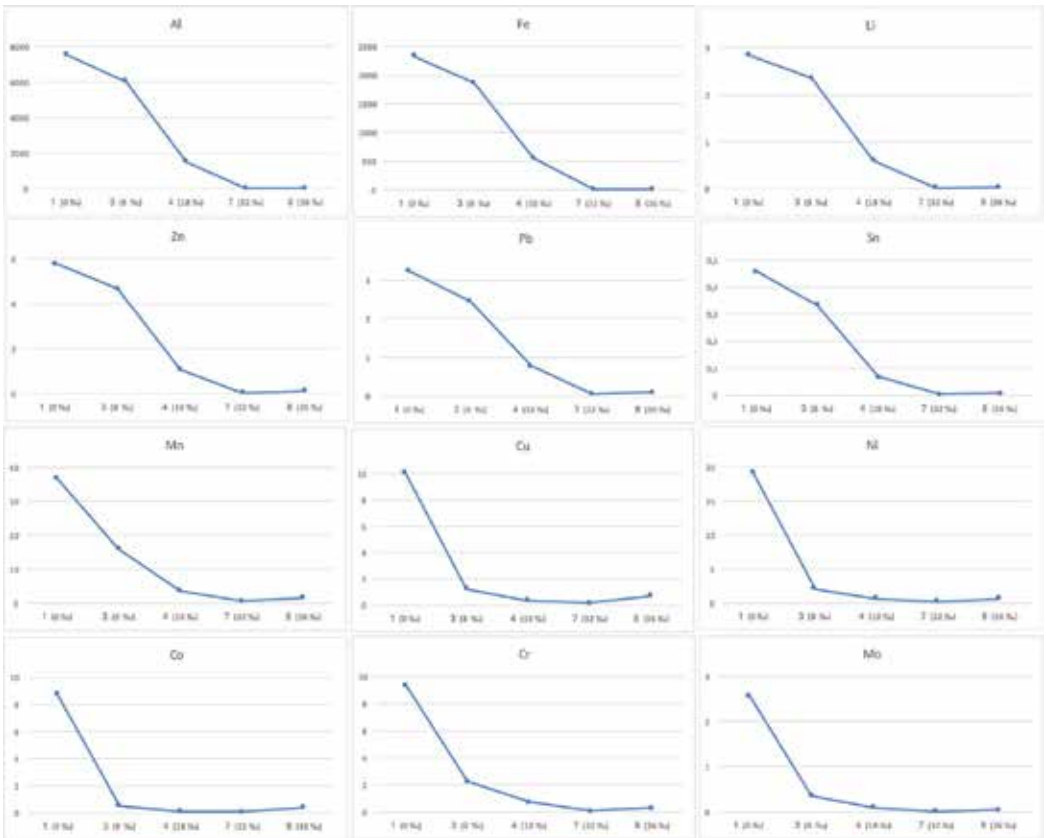

Figure 3. Major and trace elements contents in SPM (in μg l^{-1}).

3.2. Abundance and distribution of major and trace elements in surface sediments

The percent of the content of sand- (63 μm–2 mm), silt- (2–63 μm) and clay- (<2 μm) sized material in the studied sediments is shown in **Table 2**. The sediments near the river mouth were mostly sandy, while the coarsest sediment is from station 4. Downstream, in the transitional sub-zone, the sediment contains less sand and more silt and clay. The most fine-grained sediment, with the highest clay content, is from marine stations 7–8.

The total contents of Al, Fe, Ca, Mn, Ti, TOC and TIC are reported in **Table 3**. The mean contents of the major elements are within the range of the Clark contents in shale, pelagic clays and average world riverbed sediments [33–37]. The distribution of Fe and Ti in the river-sea transect is similar to that of Al. The observed distribution of major elements in the sediments illustrates the grain size and mineral fractionation processes. Al, Fe, Ti and Mn (to a lesser extent) increase seaward in the sediments with the clay-sized materials.

The distribution of the inorganic carbon (TIC) content in the sediments along the river-sea transect is characterised by only two significant values in the marine part (2,1 % at st. 7 and

Stations	Sand (63 μm–2 mm)	Silt (2–63 μm)	Clay (<2 μm)	TOC	TIC
2	49.58	23.96	26.46	1.77	0
3	47.81	28.28	23.91	1.49	0
4	71.03	19.23	9.74	0.89	0
5	28.47	47.48	24.05	1.55	0
6	49.31	37.6	13.09	1.76	0
7	3.26	42.69	54.05	0.61	2.11
8	2.37	28.96	68.67	1.02	0.88

Table 2. Sand, silt, clay, TOC and TIC contents in sediments (in % of dry weight).

0.88% at st. 8). Sedimentary organic carbon (TOC) varied within the range of 0.6–1.8% and showed no affinity to the other major or trace elements that were studied. This may be due to the intensive microbial decomposition of particulate organic matter, which occurs in the water column during estuarine sedimentation processes [38, 39]. The post-depositional diagenetic reactions, which are enhanced by resuspension processes at sediment disturbance events (such as tides, storms and upwelling), may also contribute to a destruction of sedimentary organic matter and the formation of organic-poor sediments [40].

The mean content of the major part of the studied trace elements (Li, V, Cr, Co, Ni, Cu, Zn, As, Sr, Zr, Mo, Cd, Sn, Sb, Cs, Ba, Hg and Pb) in the sediments from the Cai River estuary and Nha Trang Bay is lower or corresponds to the reference values for shale, pelagic clays and the average world riverbed sediments (**Table 3**). The Ag content was negligible or below the detection limit at all locations along the salinity gradient. Thus, natural enrichment of Ag reported in the previous study [19] had a temporary/impact character [33–37]. However, relative sediment enrichment with Bi, W and, at some sites, with Sr. needs special study.

To normalise the obtained geochemical data for the grain-size effects and identify the enrichment zones along the salinity gradient, the metal/Al ratios were calculated [27, 41, 42]. The distribution of metal/Al ratios along the Cai River—Nha Trang Bay transect is provided in **Figure 4**. The results revealed associations of elements that are characterised by a similar geochemical behaviour in the sediments along the salinity gradient. Sedimentary Fe, Ti, Li, Sc, Co, Cs, Zr, Cr, Zn, Co, Ni, Cu, Pb, Sn, V As, U and Mo varied in relatively narrow ranges. Major part of these elements tended to increase seaward with an elevation at station 7 at heightened carbonate content. The observed distribution of the normalised trace element contents reflects the association with and/or inclusion of Fe, Ti, Li and trace elements in the lattices of clay minerals that constitute the bulk of the fine-grained sedimentary material accumulated in the sea floor depression in the bay [42]. Sedimentary Bi and W decreased significantly from river to the sea. These elements may be associated with the coarsest river material enriched in detrital minerals which is mostly deposited in the riverine part of the estuary. The distribution of Sr. and Ca and, in a lesser extent, of Mn and Ba is largely controlled by the total inorganic carbon (TIC) content in the sediments. These elements form low-soluble carbonates in aquatic environments [36]. The distribution of trace elements in

Element	Mean	SD	Range	Shale[a]	Pelagic clay[a]	River sed[b]
Al	10.8	2.05	7.67–12.23	8.8	8.4	4.3
Fe	3.98	0.64	2.46–4.51	4.72	6.5	2.5
Ti	0.36	0.05	0.25–0.40	0.46	0.46	0.31
Mn	0.04	0.01	0.03–0.06	0.085	0.67	0.05
Ca	1.26	1.93	0.36–6.16	1.6	1.0	1.7
Li	47.9	8.2	34.7–62.7	66	57	20
V	89.3	12.0	61.4–100	130	120	50
Cr	45.8	9.9	27.9–66.7	90	90	50
Co	8.5	1.8	4.9–12.2	19	74	15
Ni	23.2	6.12	14.2–38.1	50	230	25
Cu	18.5	4.12	12.1–26.9	45	250	20
Zn	104.6	16.17	69.8–121	95	170	60
As	22.2	6.3	12.2–30.9	13	20	6
Sr	145	166	61.3–605	170	180	150
Zr	85.2	10.4	61.7–104	160	150	250
Mo	3.0	1.5	0.6–5.1	2.6	27	1.5
Ag	0.1	0.01	0.07–0.1	0.07	0.11	0.1
Sn	5.9	1.3	3.7–7.9	3.0	4.0	4.0
Sb	1.2	0.2	0.9–1.4	1.5	1.0	2.0
Cs	11.1	1.6	7.9–13.1	5.0	6.0	4.0
Ba	274	18	256–323	580	2300	290
Hg	0.03	0.01	0.02–0.05	0.18	0.10	0.05
Pb	54.4	11.0	35.1–61.6	20	80	15
Bi	9.5	9.0	0.9–27.6	0.43	0.53	0.2
U	6.6	1.5	3.9–8.0	2.7	2.6	3
W	10.4	7.2	2.4–24.6	0.3	0.42	0.4
TOC	1.36	0.39	0.61–1.77	—	—	1.4
TIC	1.49	0.69	<0.01–2.10	—	—	0.4

[a]Cited from [24].
[b]Cited from [46].

Table 3. Major and trace elements contents in sediments (in μg g^{-1}, except for Al, Fe, Ti, Mn, Ca, TOC and TIC in % of dry weight).

sediments is strongly influenced by the water column stratification because of the natural fractionation and deposition of materials of different grain sizes at sites, which are determined by hydrodynamic conditions [5, 13, 43, 44].

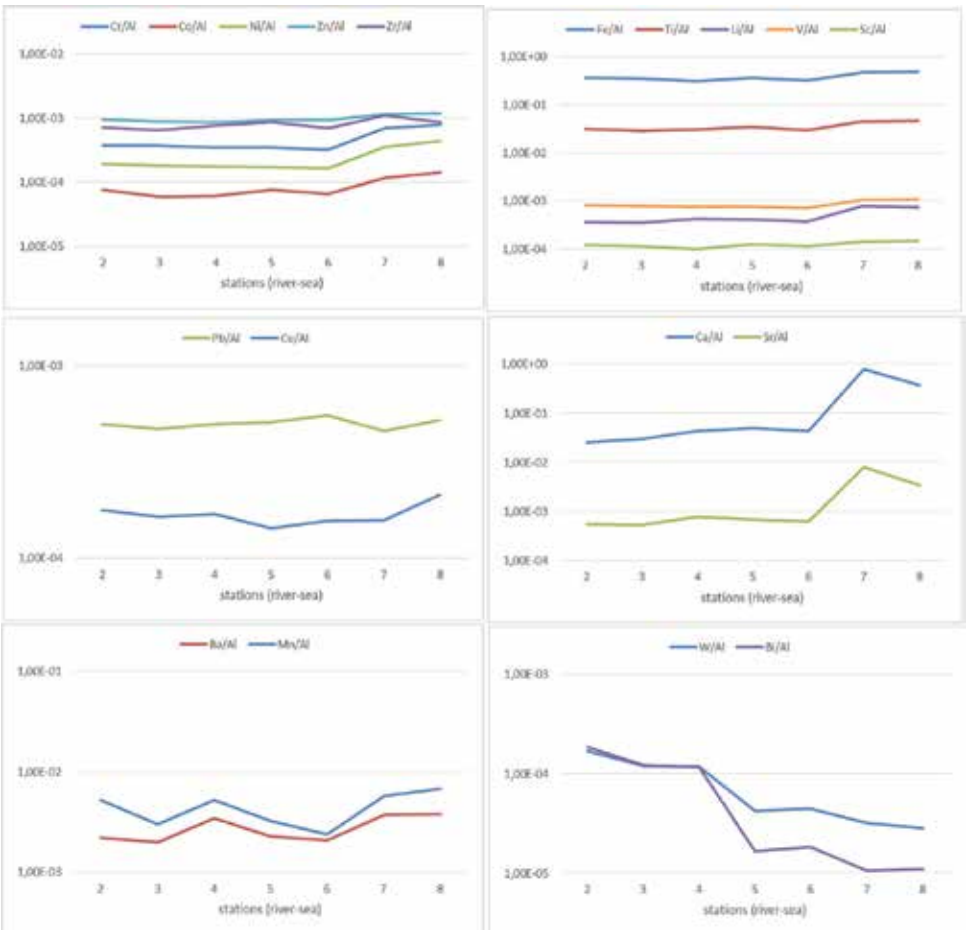

Figure 4. Element/Al ratio in sediments.

3.3. Speciation of major and trace elements in surface sediments

Major and trace elements are bound to a variety of sediment fractions that range from easily extractable (and bioavailable) to resistant residual mineral phases [45–49]. The total contents of the oxalate-soluble, pyrophosphate-soluble and weak-acid-soluble forms of Fe, Mn, Cr, Zn, Cu, Pb, Ni and Co are provided in **Table 4**. In this work, ammonium oxalate (pH 3.2–3.3) served to mobilise the easily soluble amorphous Fe-oxyhydroxides and acid-soluble fulvates [30, 31, 50]. Sodium pyrophosphate (pH 10) was used to remove organically bound metals from the sediments. This extract also mobilised part of easily soluble amorphous Fe-oxyhydroxides [13]. Acetic acid removed the labile metals in ion exchange positions, the easily soluble amorphous compounds of iron and manganese, the carbonates and the metals that are weakly held in organic matter [27].

The total content of the oxalate-soluble (amorphous) Fe increased from the river to the sea, whereas its percent content varied insignificantly (18–24% of the total content) and is the

highest in sediments in the frontal zone (sts. 2–3). The percent content of the weak-acid-soluble Fe, which is mostly comprised of easily soluble amorphous oxides, was constant in the transitional zone (10–11% of the total content), reached the maximum of 18% in the coarsest sediment from station 4 and lowered to 7–8% in the bay sediments. The percent content of the pyrophosphate-soluble Fe was low and decreased from 6–1% of the total Fe along the salinity gradient. The total and percent contents of oxalate-soluble Mn (18–58%), weak-acid-soluble Mn (13–54%) and pyrophosphate-soluble Mn (9–28%) were the highest in the coarse sediments of the frontal zone (sts. 2–3). Seaward, the contents of the studied forms of Mn decreased in the sediments in the transitional sub-zone (sts. 4–6) and increased again in the bay (sts. 7–8).

The oxalate-soluble form comprised 9–14% (12% on average) of the total content for Cr, 3–11% (8%) for Pb, 5–11% (7%) for Zn, 3–23%(15%) for Cu, 5–12% (9%) for Ni and 13–22% (17%) for Co. The weak-acid-soluble form comprised 8–12% (9% on average) of the total content for Cr, 23–34% (30%) for Pb, 4–19% (12%) for Zn, 1–8% (2%) for Cu, 8–24% (17%) for Ni and 20–66% (44%) for Co. The contents of pyrophosphate-soluble form were below the detection limit for Ni and Co. This form comprised 0.3–3% (2% on average) of the total content for Cr, 5–17% (11%) for Pb, 1–16% (10%) for Zn and 1–26% (12%) for Cu. According to the comparative extractability from sediments, Ni, Zn, Cr and Cu are low-labile and mainly occur in the residual phase. These metals were mainly extracted in the detrital fraction, which emphasises the importance of natural weathering and erosion in drainage basins. Fe and Zn are moderately labile and occur in the less resistant phases such as crystallised Fe/Mn oxides and organic compounds that may be a threat in the long term. Mn, Co and Pb are labile, held in ion exchange positions, bound to easily soluble amorphous Fe/Mn compounds and weakly held in organic matter. The high levels of acid-soluble Pb and Co (30 and 43% of the total content on average, respectively) compared to previously studied estuarine and coastal sediments contributes to a contamination problem in the Nha Trang Bay, which arises from the Cai River discharges, while the elevated level of easily reducible and organically bound Pb fractions (8 and 11% of the total content on average, respectively) also contributes to the anthropogenic input of Pb [5, 13].

The contents of oxalate-soluble (amorphous) forms were higher than the contents of pyrophosphate-soluble (organically bound) forms at all sites for Fe, Mn, Ni, Co and Cr (**Table 4**). Therefore, the most bioavailable parts of Ni, Co and Cr are bound to amorphous Fe and Mn oxyhydroxides and acid-soluble organic compounds. The contents of pyrophosphate-soluble forms were higher than the contents of oxalate-soluble forms at most of the sites for Pb, Zn and at some sites for Cu. Among the elements studied, most of the bioavailable Pb, Zn and Cu was most likely bound to organic substances. According to the mean determined amounts of the oxalate-soluble, pyrophosphate-soluble and weak-acid-soluble forms, the studied elements can be arranged in the following increasing order of average potential bioavailability: Cr < Ni < Cu < Zn < Fe < <Pb < Co < <Mn. The most bioavailable trace elements in sediments that were studied were scavenged by amorphous iron oxyhydroxides in the course of estuarine sedimentation. This result supports the fact that Fe and Mn oxyhydroxides largely control the bioavailability in sediments [7, 19, 32].

Figure 5 illustrates the distribution of the ecologically most significant weak-acid-soluble (labile) fraction along the river-sea transect. Mn, Co and Pb have the highest percent contents of the labile form but exhibit different spatial distributions showing some sporadic enrichments

Stations	Cu	Zn	Ni	Co	Pb	Cr	Fe	Mn
Weak acid-soluble								
2	0.4	18	5.6	4	16.4	3.4	4540	344
3	0.4	14	4.8	4.6	14	4.8	5620	144
4	0.2	13.2	3.4	2.2	13.4	3.2	2840	36
5	0.2	14	3	6	16	4.8	7640	58
6	≤0.2	4	2.4	1.8	12	5.2	2660	164
7	0.2	15.8	3	3.4	20	3.4	3440	52
8	≤0.2	7.6	5	2.6	15.6	5.6	2920	264
Mean	0.525	12.9	3.82	3.6	15.84	4.22	4244	133.6
Mean (% of total content)	2.8	12.3	16.5	42.4	29.1	9.2	10.6	32.0
Pyrophosphate-soluble								
2	5.6	18.6	≤0.2	≤0.2	4.8	1	2580	180
3	2	10.4	≤0.2	≤0.2	7	0.8	2940	82
4	2.6	9	≤0.2	≤0.2	7	≤0.2	1300	30
5	0.8	14.8	≤0.2	≤0.2	5.4	0.4	1480	32
6	0.4	1.2	≤0.2	≤0.2	5	0.8	420	50
7	1	13.4	≤0.2	≤0.2	9.6	1.6	1360	42
8	0.2	2	≤0.2	≤0.2	7.6	≤0.2	600	90
Mean	2.24	10.84	≤0.2	≤0.2	5.74	1	1652	65.9
Mean (% of total content)	12.1	10.4	—	—	10.6	2.2	4.1	15.8
Oxalate-soluble								
2	3	5.6	1.4	1.6	5.4	5.3	11,300	375
3	3.7	7	2.2	1	6.8	5.2	10,550	172
4	2.5	8	1.6	0.6	3.4	4	5480	75
5	2.1	6.8	1.3	2.2	5.4	6	8250	87
6	0.4	6.5	2.2	1.2	1.1	7	7500	158
7	4.4	8.7	2.6	1.5	4.1	5	7550	90
8	0.5	8.1	2	1.9	1.2	6.2	8430	255
Mean	2.93	7.42	2	1.44	4.56	5.57	8572	152.1
Mean (% of total content)	15.8	7.1	8.6	16.9	8.4	12.2	21.5	36.4

Table 4. Major and trace element form contents in sediments (in μg g^{-1}).

http://dx.doi.org/10.5772/intechopen.76471

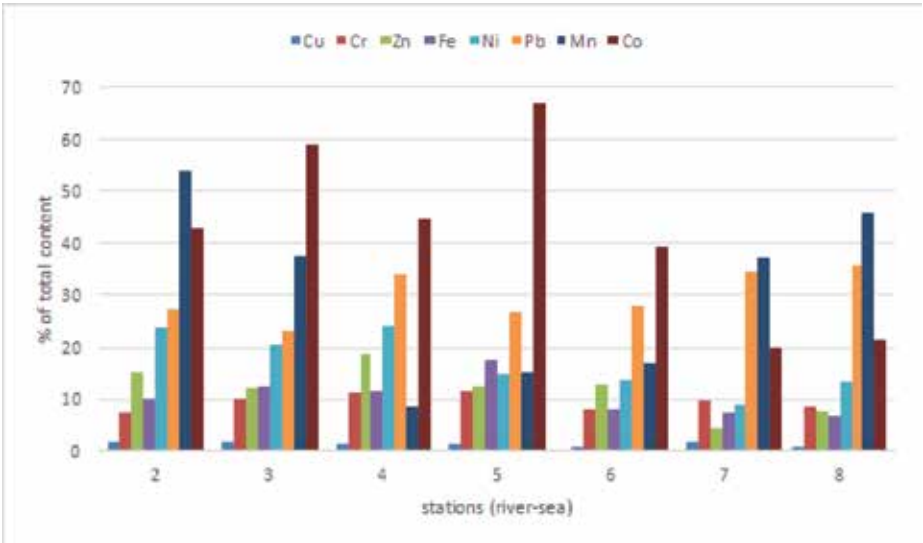

Figure 5. Weak acid-soluble (labile) metal form in sediments.

along the salinity gradient. Thus, the distribution of the most abundant labile Co is complicated by a pronounced maximum of 67% in the sediment at station 5. The sediments are mostly enriched with labile Fe, Zn, Cr and Ni in the frontal and transitional sub-zones (sts. 2–5). Cu exhibit the lowest contents of the labile form. Therefore, in the studied sediments, Cu is most likely bound to the residual mineral phase that is comprised of detrital heavy minerals.

4. Conclusions

The suspended particulate matter (SPM) showed a concentration maximum (50 mg l^{-1}) near the river mouth and then a decrease seaward to the values of around 1 mg l^{-1} at salinities 32–36‰, following from the sedimentation of the coarsest fluvial material in the frontal zone of the estuary at the sharp decrease in the river flow velocity enhanced by the dam influence. The distribution pattern of particulate organic carbon (POC) was close to the SPM distribution and varied within the range 0.18–1.25 mg l^{-1}. The organic carbon content in the SPM (POC, % of dry SPM weight) varied within the range 2–17%. The higher organic carbon content >10% was found in SPM of the marine waters at the salinity >30‰.

The distribution of particulate form of Al, Fe, Ti, Li, Zn, Pb, U, Sc, Sn, Bi, Zr, Ba, As, Sr., W, V and Ag followed the distribution of total suspended matter and was characterised by a maximum in the river water and then a sharp decrease seaward of element relative concentration (in μg l^{-1}) with highest horizontal gradients within the salinity interval of 8–20%. The most part of these elements must be supplied to the estuary with the Cai River discharge. The distribution of particulate form of Co, Cu, Ni, Mo and Cr and, in a lesser extent, Mn, Ba, Sn, Sb and Hg is characterised by the most significant loss in the frontal zone of the estuary where the coarsest river material enriched in detrital minerals and pronounced increase of their absolute concentrations

at salinities 32–36‰. In the stratified Cai River estuary, the significant part of the particulate trace elements may be carried out seaward with the surface water layer. In the marine part of the estuary, with a homogenisation of the water column, most of the fine-grained material of surface water layer enriched in organic matter and trace metals is deposited.

Sedimentary Fe, Ti, Li, Sc, Co, Cs, Zr, Cr, Zn, Co, Ni, Cu, Pb, Sn, V As, U and Mo varied in relatively narrow ranges along the salinity gradient and tend to increase seaward. These elements are most likely controlled by the accumulation of their most fine-grained aluminosilicate host minerals and materials in the sea floor depression of the marine sub-zone. Sedimentary Bi and W, are generally uniformly low but tend to decrease seaward. These elements may be associated with the coarsest river material enriched in detrital minerals which is mostly deposited in the riverine part of the estuary. The distribution of Sr. and Ca and, in a lesser extent, of Mn and Ba is largely controlled by the total inorganic carbon (TIC) content in the sediments.

The distribution of trace elements in SPM and sediments of Cai River—Nha Trang Bay estuarine system is strongly influenced by the water column stratification because of the natural fractionation and deposition of materials of different grain sizes at sites, which are determined by hydrodynamic conditions.

Assuming that the mean determined amounts of the oxalate-soluble, pyrophosphate-soluble and weak-acid-soluble forms are a measure of the potential metal bioavailability in sediments of the Cai River—Nha Trang Bay estuarine system, the studied elements can be arranged in the following increasing order of average potential bioavailability: Cr < Ni < Cu < Zn < Fe < <Pb < Co < <Mn. This sequence is true for sediments in different sub-zones of the water-mixing zone: estuary (transitional waters) and sea (bay). Metal form study revealed the highest percent contents of the labile (weak acid-soluble) form for Mn, Co and Pb in the sediments. The high levels of labile Pb and Co (30 and 43% of the total content in sediment, on average, respectively) contribute to a heavy metal contamination problem in the Nha Trang Bay, which arises from the Cai River discharge. The elevated level of amorphous (oxalate-soluble) and organically bound (pyrophosphate-soluble) Pb fractions (8 and 11% of the total content in sediment, on average, respectively) also contribute to the anthropogenic input of Pb. The most bioavailable parts of the studied trace metals are associated with easily soluble amorphous Fe and Mn oxyhydroxides.

Acknowledgements

This research was performed in the framework of the state assignment of FASO Russia (theme No. 0149-2018-0005).

Author details

Sofia Koukina* and Nikolay Lobus

*Address all correspondence to: skoukina@gmail.com

Shirshov Institute of Oceanology of RAS, Russia

References

[1] Bayen S. Occurrence, bioavailabiliy and toxic effects of trace metals and organic contaminants in mangrove ecosystems: A review. Environment International. 2012;**48**:84-101

[2] Costa-Böddeker S et al. Ecological risk assessment of a coastal zone in Southern Vietnam: Spatial distribution and content of heavy metals in water and surface sediments of the Thi Vai estuary and Can Gio Mangrove Forest. Marine Pollution Bulletin 2017;**114**(2):1141-1151

[3] Guor-Cheng F, Hung-Chieh Y. Heavy metals in the river sediments of Asian countries of Taiwan, China, Japan, India and Vietnam during 1999-2009. Environmental Forensics. 2010;**11**:201-206

[4] Motuzova GV, Hong Van NT. The geochemistry of major and trace elements in the agricultural terrain of South Vietnam. Journal of Geochemical Exploration. 1999;**66**:407-411

[5] Koukina SE, Lobus NV, Peresypkin VI, Dara OM, Smurov AV. Abundance, distribution and bioavailability of major and trace elements in surface sediments from the Cai River estuary and Nha Trang Bay (South China Sea, Vietnam). Estuarine, Coastal and Shelf Science. 2017;**198**:450-460

[6] Britaev TA, editor. Benthic Fauna of the Bay of Nhatrang. Southern Vietnam, Moscow, Russia: KMK; 2007. p. 248

[7] Burton GA Jr. Metal bioavailability and toxicity in sediments. Critical Reviews in Environmental Science and Technology. 2010;**40**(9-10):852-907

[8] Chernova EN, Sergeeva OS. Metal concentrations in Sargassum algae from coastal waters of Nha Trang Bay (South China Sea). Russian Journal of Marine Biology. 2008;**34**(1):57-63

[9] Lobus NV, Komov VT. Mercury in the muscle tissue of fish in the central and South Vietnam. Inland Water Biology. 2016;**9**(3):319-328

[10] Peresypkin VI, Smurov AV, Shulga NA, Safonova ES, Smurova TG, Bang CV. Composition of the organic matter of the water, suspended matter, and bottom sediments in Nha Trang Bay in Vietnam in the South China Sea. Oceanology. 2011;**51**:959-968

[11] Romano S, Mugnai C, Giuliani S, Turetta C, Huu CN, Belucci LG, Nhon DH, Caporaglio G, Frignani M. Metals in sediment cores from nine coastal lagoons in Central Vietnam. American Journal of Environmental Sciences. 2012;**8**:130-142

[12] Baturin GN, Lobus NV, Peresypkin VI, Komov VT. Geochemistry of channel drifts of the Kai river (Vietnam) and sediments of its mouth zone. Oceanology. 2014;**54**(6):788-797

[13] Koukina SE, Vetrov AA. Metal forms in sediments from Arctic coastal environments in Kandalaksha Bay, White Sea, under separation processes. Estuarine, Coastal and Shelf Science. 2013;**130**:21-29

[14] Lobus NV, Komov VT, Nguen THT. Mercury concentration in ecosystem components in water bodies and streams in Khanh Hoa province (Central Vietnam). Water Resources. 2011;**38**(6):799-805

[15] Lobus NV, Peresypkin VI, Shulga NA, Drozdova AN, Gusev ES. Dissolved, particulate, and sedimentary organic matter in the Cai River basin (Nha Trang Bay of the South China Sea). Oceanology. 2015;**55**(3):339-346

[16] Millward GE, Turner A. Trace metals in estuaries. In: Salbu B, Steinnes E, editors. Trace Elements in Natural Waters. Boca Raton, FL: CRC Press; 1995. pp. 223-245

[17] Morris AW, Howland RJM, Bale AJ. Dissolved aluminium in the Tamar estuary, Southwest England. Geochim et Cosmochimacta. 1986;**50**:189-197

[18] Suja S, Kessarkar PM, Fernandes LL, Kurian S, Tomer A. Spatial and temporal distribution of metals in suspended particulate matter of the Kali estuary, India. Estuarine, Coastal and Shelf Science. 2017;**196**:10-21

[19] Bianchi TS. Biogeochemistry of Estuaries. NY, USA: Oxford Press; 2007. p. 706

[20] Briant N, Bancon-Montignya C, Elbaz-Poulichet F, Freydier R, Delpouxa S, Cossa D. Trace elements in the sediments of a large Mediterranean marina (port Camargue, France): Levels and contamination history. Marine Pollution Bulletin. 2013;**73**:78-85

[21] Chaillou G, Schäfer J, Blanc G, Anschutz P. Mobility of Mo, U, As, and Sb within modern turbidities. Marine Geology. 2008;**254**:171-179

[22] Wolanski E. Estuarine Ecohydrology. Amsterdam, Netherlands: Elsevier; 2007. p. 157

[23] Pavlov DS, Zvorikin DD, editors. Ecologia vnytrennich vod Vietnama. Moscow, Russia: KMK; 2014. p. 435 (in Russian)

[24] Pavlov DS, Novikov GG, Levenko BA. Osobennosti struktury I funktzionirovaniya pribrezhnyh ecosystem Yuzhno-Kitaiskogo moria. GEOS, Moscow, Russia; 2006. p. 280 (in Russian, with English abstract)

[25] Nghia ND, Lunestad BT, Trung TS, Son NT, Maage A. Heavy metals in the farming environment and in some selected aquaculture species in the van Phong Bay and Nha Trang Bay of the Khanh Hoa Province in Vietnam Ngo. Bulletin of Environmental Contamination and Toxicology. 2009;**82**:75-79

[26] Jennerjahn TC, Mitchell SB. Pressures, stresses shocks and trends in estuarine ecosystems – An introduction and synthesis. Estuarine, Coastal and Shelf Science. 2013;**130**:1-8

[27] Loring DH, Rantala RTT. Manual for geochemical analyses of marine sediments and suspended particulate matter. Earth-Science Reviews. 1992;**32**:235-283

[28] Moore DM, Reynolds RC. X-ray Diffraction and the Identification and Analysis of Clay Minerals. New York, USA: Oxford University Press; 1997. 400 p

[29] Karandashev VK, Turanov AN, Orlova TA, Lezhnev AE, Nosenko SV, Zolotareva NI, Moskvina IR. Use of the inductively coupled plasma mass spectrometry for element analysis of environmental objects. Inorganic Materials. 2008;**44**:1491-1500

[30] Vodyanitskii YN. On the dissolution of Iron minerals in Tamm's reagent. Eurasian Soil Science. 2001;**34**(10):1086-1096

[31] Vorobyova LF, editor. Teoriya I praktika khimicheskogo analiza pochv. GEOS, Moscow, Russia; 2006. p. 400. (in Russian, With English Abstract)

[32] Saulnier I, Mucci A. Trace metal remobilization following the resuspension of estuarine sediments: Saguenay Fjord, Canada. Applied Geochemistry. 2000;**15**:203-222

[33] Li YH. Distribution patterns of the elements in the ocean. Geochimica et Cosmochimica Acta. 1991;**55**:3223-3240

[34] Long ER, MacDonald DD. Recommended uses of empirically derived, sediment quality guidelines for marine and estuarine ecosystems. Human and Ecological Risk Assessment. 1998;**4**(5):1019-1039

[35] Long ER, MacDonald DD, Smith SL, Calder FD. Incidence of adverse biological effects within ranges of chemical concentrations in marine and estuarine sediments. Environmental Management. 1995;**19**:81-97

[36] Savenko VS. Chemical composition of world river's suspended matter. Khimichesky sostav vzveshennikh nanosov rek mira. GEOS, Moscow, Russia; 2006. 175 p. (in Russian, With English Abstract)

[37] Shahid M, Ferrand E, Schreck E, Dumat C. Behavior and impact of zirconium in the soil-plant system: Plant uptake and phytotoxicity. Reviews of Environmental Contamination and Toxicology. 2013;**221**:107-127

[38] Romankevich EA. Geochemistry of Organic Matter in the Ocean. Berlin, Germany: Springer; 1984. 334 p

[39] Romankevich EA, Vetrov AA. Masses of carbon in the Earth's hydrosphere. Geochemistry International. 2013;**51**(6):431-455

[40] Eggleton J, Thomas KV. A review of factors affecting the release and bioavailability of contaminants during sediment disturbance events. Environment International. 2004; **30**:973-980

[41] Gensemer RW, Playle RC. The bioavailability and toxicity of aluminum in aquatic environments. Critical Reviews in Environmental Science and Technology. 1999;**29**(4):315-450

[42] Loring D.H, Dahle S, Naes K, Dos Santos J, Skei J.M, Matishov G.G.1998. Arsenic and other trace metals in sediments from the Pechora Sea, Russia. Aquatic Geochemistry 4, 233-252

[43] Koukina SE, Calafat-Frau A, Hummel H, Palerud R. Trace metals in suspended particulate matter and sediments from the Severnaya Dvina estuary, Russian Arctic. Polar Record. 2001;**37**:249-256

[44] Shevchenko VP, Dolotov YS, Filatov NN, Alexeeva TN, Fillipov AS, Noethig E-M, Novigatsky AN, Pautova LA, Platonov AV, Politova NV, Ratkova TN, Stein R. Biogeochemistry of the Kem' river estuary, White Sea (Russia). Hydrology and Earth System Sciences. 2005;**9**(1-2):57-66

[45] Fedotov PS, Kördel W, Miró M, Peijnenburg WJGM, Wennrich R, Huang P-M. Extraction and fractionation methods for exposure assessment of trace metals, metalloids, and hazardous organic compounds in terrestrial environments. Critical Reviews in Environmental Science and Technology. 2012;**42**(11):1117-1171

[46] Hass A, Fine P. Sequential selective extraction procedures for the study of heavy metals in soils, sediments, and waste materials – A critical review. Critical Reviews in Environmental Science and Technology. 2010;**40**(5):365-399

[47] Krishnamurti GSR. Chemical methods for assessing contaminant bioavailability in soils. In: Naidu R, editor. Chemical Bioavailability in Terrestrial Environments. Oxford, UK: Elsevier; 2008. pp. 495-520

[48] Kukina SE, Sadovnikova LK, Calafat-Frau A, Palerud R, Hummel H. Forms of metals in bottom sediments from some estuaries of the basins of the white and Barents seas. Geochemistry International. 1999;**37**(12):1197-1202

[49] Tack FMG, Verloo MG. Chemical speciation and fractionation in soil and sediment heavy metal analysis: A review. International Journal of Environmental Analytical Chemistry. 1995;**59**(2-4):225-238

[50] Ladonin DV. Heavy metal compounds in soils: Problems and methods of study. Eurasian Soil Science. 2002;**35**(6):605-613

Chapter 7

A Simple and Highly Structured Procaine Hydrochloride as Fluorescent Quenching Chemosensor for Trace Determination of Mercury Species in Water

Dyab A. Al-Eryani, Waqas Ahmad, Zeinab M. Saigl,
Hassan Alwael, Saleh O. Bahaffi,
Yousry M. Moustafa and Mohammad S. El-Shahawi

Additional information is available at the end of the chapter

http://dx.doi.org/10.5772/intechopen.73397

Abstract

An ultrasensitive, simple and highly selective spectrofluorometric strategy for quantifying traces of mercury(II) in environmental water has been established using the fluorescent probe procaine hydrochloride ($PQ^+.Cl^-$). The procedure was based upon the formation of the ternary ion associate complex $[(PQ^+)_2.(HgI_4)^{2-}]$ between $PQ^+.Cl^-$ and mercury(II) in iodide media at pH 9.0–10.0 with its subsequent extraction onto dichloromethane accompanied by a change in fluorescence intensity at $\lambda_{ex/em}$ = 268/333 nm. The developed strategy exhibited a linear range of 1–114 μg L^{-1} with lower limit of detection (LOD) and quantification (LOQ) of mercury(II) 1.3 and 3.98 nM, respectively. Intra and inter-day laboratory accuracy and precision for trace analysis of mercury(II) in water were performed. Complexed mercury(II) in environmental water, chemical speciation and successful literature comparison was performed. The proposed system offered excellent selectivity towards mercury(II) ions examined in the presence of competent ions in excess, relevant to real water samples. The method was applied for analysis of mercury(II) in tap water samples. Statistical comparison (Student's *t* and *F* tests) of the proposed method with the reference ICP-OES method revealed no significant differences in the accuracy and precision.

Keywords: spectrofluorometry, mercury(II), fluorescence, procaine hydrochloride, quenching, ternary ion associate complex

1. Introduction

Heavy metal pollution is global level environmental concern, which poses serious implications towards human health [1, 2]. Heavy metal pollution has attained considerable interest

in the recent past [3]. Among heavy metals, mercury is considered among the most toxic and dangerous ion due to its wide existence as an ore cinnabar in nature and its applications as pigment vermilion, detoxification/anticorrosive medicines and mercury fulminate detonator in explosives [3, 4]. Due to its wide presence in environment, it enters the biological membranes through respiratory and gastrointestinal tissues [4, 5]. It can also cause permanent harm to the endocrine and central nervous systems if accumulated in the food chain and ultimately in human body [5–13]. Moreover, a low-level exposure of mercury will affect the endocrine and nervous systems, brain and kidneys [14, 15].

Several forms of mercury including elemental, organic and inorganic or elemental display different levels of toxicity and contamination in natural water resources and drinking water [2]. The most stable and prevalent form of mercury that contributes to wider contamination is the solvated divalent mercuric ion (Hg^{2+}), due to its high solubility in water [16]. The US Environmental Protection Agency (US-EPA) and World Health Organization (WHO) have set the permissible level (MPL) for mercury to 10 nM [1, 17]. Traces of mercury ions have shown significant toxicity, and therefore developing highly sensitive methodologies are considered essential [18]. Thus, recent trends have been oriented towards developing highly sensitive and selective procedures for monitoring and/or enrichment of mercury in various water samples [20–22].

Several analytical procedures, including atomic absorption and emission spectrometry (AAS, AES) [19, 20], inductively coupled plasma-optical emission spectrometry (ICP-OES) [21], ion exchange chromatography [22], mechanical filtration [23], chemical precipitation [24], reverse osmosis, flotation [25, 26] and membrane separation [27], are reported for mercury determination. On the other hand, numerous liquid and solid phase extraction methods such as liquid-liquid extraction (LLE) [28], carbon nanotubes [29], graphene oxide [30–33] and polymers [34–36] have been reported for routine analysis of mercury(II). However, most of these methods require sophisticated equipment unavailable for use in developing countries with numerous other limitations like high cost, complications in their proper operation, selectivity and sensitivity [34, 35].

Recently, several molecular probe-based sensors using organic chromophores, quantum dots (QDs), small fluorescent organic molecules, proteins, antibodies and conjugated polymers coupled with several spectrometric and electrochemical techniques are reported for mercury(II) determination [36–53]. Some of these methods suffere from solubility issues, low stability, lower sensitivity and selectivity, complicated synthesis procedures and environmentally unfriendliness to monitor mercury(II) in biological and environmental samples. Hence, the work presented in this chapter is focused on: (i) developing a simple, highly selective and sensitive extractive spectrofluorometric LLE for trace determination of mercury(II) species in water samples using the ion pairing reagent 4-amino-N-(2-diethylaminoethyl) benzamide hydrochloride namely procaine hydrochloride and abbreviated as ($PQ^+.Cl^-$) (**Figure 1**) [54–59]; (ii) the utility of the proposed extractive LLE for trace determination of mercury ions in environmental water samples and finally (iii) validation and assignment of the most probable stoichiometry and chemical equilibria and fluorescence quenching mechanism of the produced ternary ion associate complex [$(PQ^+)_2.(HgI_4)^{2-}$] of $[HgI_4]^{2-}$ with the proposed ion pairing reagent [60–64].

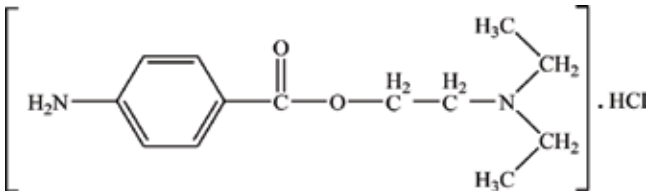

Figure 1. Chemical structure of procaine hydrochloride.

2. Experimental

2.1. Reagents and materials

Glasswares were pre-cleaned with HNO_3 (20% m/v), acetone and deionized water. Analytical reagent grade chemicals and solvents were used as received. Low-density polyethylene (LDPE) bottles, Nalgene were used for storage of the stock solutions. A stock solution (1.0 mg mL^{-1}) of standard mercury(II) solution was prepared in ultra-pure water. Stock solution (1000 μM) of mercury(II) was prepared from $HgCl_2$ (BDH Chemicals, Poole, England) in ultra-pure water. More dilute solutions of mercury(II) ions were prepared by series dilution in deionized water. Potassium iodide solution (10% w/v) was prepared in ultra-pure water. Stock solutions of other cations were synthesized either from their chloride or nitrate salts in deionized water. Britton-Robinson (B-R) (pH 2–11) buffers were prepared from BDH purchased H_3BO_3, H_3PO_4, CH_3COOH and NaOH in deionized water as reported [65]. A stock solution (1000 μM) of procaine hydrochloride (Sigma–Aldrich) was prepared by dissolving the required weight in aqueous solution.

2.2. Apparatus

Fluorescent measurements were recorded on a Perkin-Elmer LS55 spectrofluorometer, USA equipped with quartz cuvettes of path length 10 × 10 mm. UV-visible (190–1100 nm) spectra were recorded on a Perkin-Elmer spectrophotometer (Lambda 25, Shelton, CT, USA). For method validation, a Perkin-Elmer inductively coupled plasma-optical emission spectrometry (ICP-OES) (California, CT, USA) was utilized for mercury determination at the optimum operational parameters (**Table 1**). Deionized water was obtained from Milli-Q Plus system (Millipore, Bedford, MA, USA). A digital micropipette (Plus-Sed) and pH meter (inoLap pH/ion level 2) were used for preparation of stock and more diluted solutions of reagent and mercury(II) and pH measurements, respectively.

2.3. Recommended procedures

2.3.1. Spectrophotometric procedure

Appropriate volume (1.0 mL) of various mercury(II) concentrations (1.0×10^{-5} to 8×10^{-5} M) was transferred to a series of glass test tubes (10.0 mL) followed by addition of 100 μL KI (10% w/v). The solutions were made up to the mark with Britton-Robinson (B-R) buffer solution of pH 10 after

Parameter	Unit
RF power	1400 W
Nebulizer flow	0.7 L/min
Auxiliary flow	0.3 L/min
Plasma flow	10.0 L/min
Sample pump flow	1 mL/min
Plasma viewing	Axial
Processing mode	Area
Replicates	3
Nebulizer type	Cross-flow (Gim Tip)
Spray chamber	Scott (Ryton)
Injector	Scott (Ryton)
Analytical wavelength	Hg 194.2 nm

Table 1. Operational parameters of ICP-OES for analysis of mercury.

adding 1.0 mL (1.0×10^{-4} M) of procaine hydrochloride. The solution mixtures were shaken well for 3.0 min with dichloromethane (5.0 mL). After equilibrium, the organic phase was separated out, shaken with anhydrous Na_2SO_4 to remove trace of water and finally the absorbance of the organic extract was finally measured at λ_{max} 310 nm *versus* the reagent blank at room temperature.

2.3.2. Spectrofluorometric procedure

In a series of glass test tubes (10.0 mL), appropriate concentrations (20–140 nM) of mercury(II) and 100 μL of 10% KI (w/v) were added. The test solutions were completed to the mark with B-R buffer of pH 10.0 after adding 1.0 mL (20 μM) of $PQ^+.Cl^-$ and shaken well for 3.0 min with dichloromethane (5.0 mL). The organic phase was separated after equilibrium, shaken with anhydrous Na_2SO_4 and analyzed at $\lambda_{ex/em}$ = 268/333 nm *versus* a reagent blank at room temperature. The quenched fluorescence in signal intensity (ΔF) of $PQ^+.Cl^-$ by mercury(II) was computed employing the following equation:

$$\Delta F = F_0 - F \quad (1)$$

where F_0 and F are the fluorescence intensities of the reagent before and after addition of mercury(II) under the optimized analytical parameters, respectively. The fluorescence signal intensity (F) of the formed ion associate complex was measured *versus* a reagent blank as described above. The quenched fluorescence (ΔF) was finally determined. Following the recommended procedures, the selectivity of the proposed method was examined in the presence of a series of the concurrent diverse ions, e.g. Ca^{2+}, Ba^{2+}, Cu^{2+}, Pb^{2+}, Fe^{3+}, As^{3+}, Ag^+, Al^{3+} Sn^{2+}, Cd^{2+}, Bi^{3+}, WO_4^{2-}, MnO_4^-, F^-, CO_3^{2-}, SO_4^{2-} in the presence of mercury(II) at 2.0 μg L^{-1}.

2.3.3. Calibration curve of mercury(II)

To construct the linear calibration plot, a series of solutions (10.0 mL) containing various known (5.0 mL, 20–140 nM) concentrations of mercury(II) and $PQ^{+}.Cl^{-}$ (1.0 mL, 20 μM) were transferred to measuring flask (25 mL) prepared. The test solutions were completed to the mark with B-R buffer of pH 10 and shaken well with dichloromethane (5.0 mL) for 3.0 min. After equilibrium, the organic phase was separated out, shaken with anhydrous Na_2SO_4 and analyzed at $\lambda_{ex/em}$ = 268/333 nm *versus* a reagent blank at room temperature. The quenched fluorescence signal intensity (ΔF) of the formed colorless complex species was finally measured *versus* a reagent blank as described above.

2.4. Analytical applications

In LDPE sample bottles, pre-cleaned as described in Section 3.2.1, tap water samples were collected from the laboratories of the Department of Chemistry, King Abdul Aziz University, Jeddah, KSA and immediately filtered through 0.25 μm cellulose membrane filters before analysis and stored in LDPE bottles. The sample solutions were then spiked with known concentration (20–100 nM) of mercury(II). The fluorescence intensity of the test solutions were measured at ($\lambda_{ex/em}$ = 268/333 nm) under the optimized experimental conditions of mercury(II) by standard addition plot. The concentration and the percent recovery of the mercury(II) added to water samples were finally computed.

3. Results and discussion

3.1. Electronic and fluorescence spectra of reagent and its mercury(1I) ion associate complex

The absorption spectrum of the ion pairing reagent $PQ^{+}.Cl^{-}$ is demonstrated in **Figure 2**. The spectrum showed one well-defined band at 290 nm and was safely assigned to $n \rightarrow \pi^*$ electronic transitions [66, 67]. The electronic absorption spectra of the developed ternary ion associate complex $[(PQ^{+})_2.(HgI_4)^{2-}]$ of $PQ^{+}.Cl^{-}$ (4×10^{-5} M) with mercury(II) (1×10^{-5} M) in the presence of an excess aqueous KI (10% w/v) were recorded and a well-defined absorption peak at 310 nm was noticed (**Figure 2**). The most probable formation mechanism of ion associate complex of mercury can be expressed as follows [68–73]:

$$Hg^{2+} + 4I^{-} \rightleftharpoons [HgI_4]^{2-} \tag{2}$$

$$2[PQ^{+}]_{aq} + [HgI_4]^{2-}_{aq} + nS_{org} \rightleftharpoons \{[PQ^{+}]_2.[HgI_4]^{2-}.nS\}_{org} \tag{3}$$

As shown in **Figure 3**, the solution of reagent blank $PQ^{+}.Cl^{-}$ with concentration of 5.0 μM exhibits a strong fluorescence intensity at $\lambda_{ex/em}$ = 268/333 nm in dichloromethane [68, 74–76]. The strong fluorescence band of $PQ^{+}.Cl^{-}$ can be quenched after addition of 40 nM Hg(II) and increases after adding excess of mercury(II), through the formation of ternary ion associate

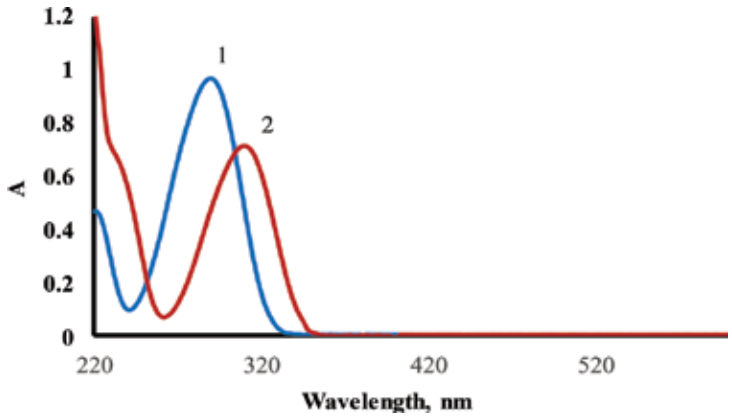

Figure 2. Electronic spectra of the $PQ^+.Cl^-$ (4×10^{-5} M) (1) and its ternary ion associate complex $[(PQ^+)_2.(HgI_4)^{2-}]$ in dichloromethane (2). Condition: Mercury (1×10^{-5} M).

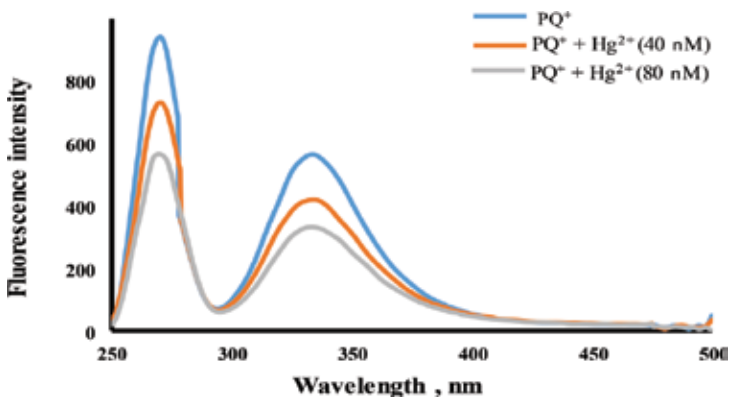

Figure 3. Fluorescence spectra of $PQ^+.Cl^-$ (5.0 μM) and its ternary ion associate complex $[(PQ^+)_2.(HgI_4)^{2-}]$ with mercury(II) ions (40, 80 nM).

complex $[(PQ^+)_2.(HgI_4)^{2-}]$ (**Figure 3**) between $PQ^+.Cl^-$ and HgI_4^{2-} [60]. Hence, this sensing principle by virtue of quenching was successfully applied for sensitive spectrofluorometric determination of mercury(II).

3.2. Analytical parameters

The effect of various experimental conditions on the fluorescence characteristics of both ion associate complex was studied, including type of solvents, pH, reagent concentration and equilibrium time.

3.2.1. Effect of solvent

The influence of extraction solvent, e.g. n-hexane, chloroform, dichloromethane, toluene and cyclohexane, on the fluorescence quenching of the formed mercury(II) complex was studied. The results are demonstrated in **Figure 4**. Stable and maximum change in fluorescence

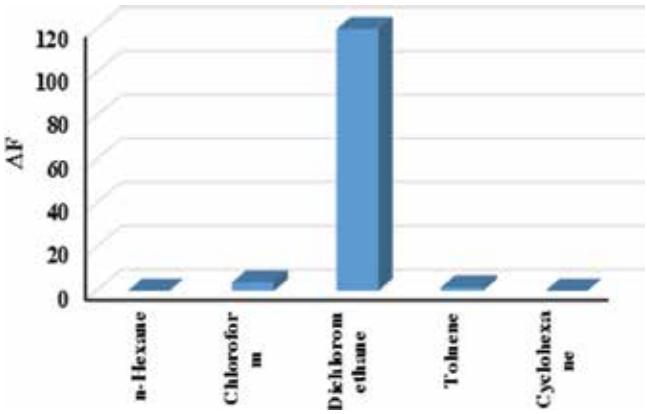

Figure 4. Influence of type extraction solvent on the fluorescence quenching of $PQ^+.Cl^-$ (5.0 μM) reagent by $K_2[HgI_4]$ (80 nM).

quenching was observed in dichloromethane. Therefore, a detailed study on the influence of dichloromethane volume on the fluorescence quenching of $PQ^+.Cl^-$ reagent by mercury(II) was critically studied (**Figure 5**). Thus, dichloromethane was adopted at 2.0 mL volume in the subsequent work pertaining to its higher performance compared to other volume fractions.

3.2.2. Effect of pH

The effect of pH on the fluorescence quenching of the formed mercury(II)-PQ^+ complex was studied in B-R (pH 3–12) buffer solutions. Maximum quenching by mercury(II) quencher was achieved at pH ≈ 9–10. The extraction rate at pH < 10.0 for ternary ion associate complex $[(PQ^+)_2.(HgI_4)^{2-}]$ was lower. Several factors including hydrolysis, instability and/or incomplete extraction, and the slow dissociation of the complex $K_2[HgI_4]^{2-}$ account for the decrease in the amount of mercury extracted at pH values other than pH ≈ 9–10 [62, 63]. Thus, in the next work, the solution media were adopted at pH ≈ 10 due to the ease in formation of the ternary ion associate complex $[(PQ^+)_2.(HgI_4)^{2-}]$.

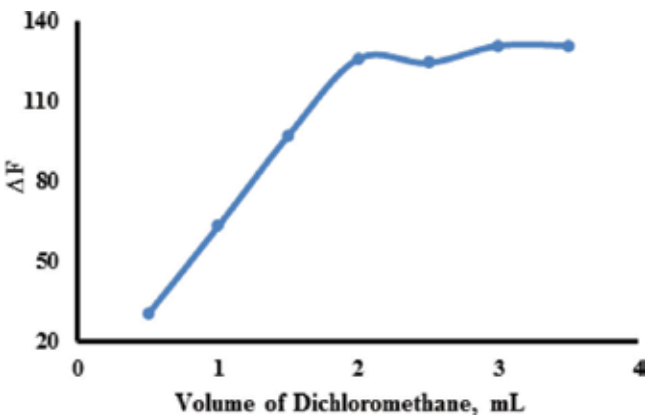

Figure 5. Influence of dichloromethane volume on the fluorescence quenching of $PQ^+.Cl^-$ (5.0 μM) reagent by mercury (80 nM).

3.2.3. Effect of extraction time

The stability and the fluorescence signal intensity of the emission spectrum of the formed ternary ion associate complex $[(PQ^{+})_2.(HgI_4)^{2-}]$ considerably depend on the reaction time. Therefore, the fluorescence intensity of the emission spectrum of the ternary ion associate complex $[(PQ^{+})_2.(HgI_4)^{2-}]$ was measured at various time intervals (0.5–14 min) at $\lambda_{ex/em}$ = 268/333 nm at the optimum conditions. The results are demonstrated in **Figure 6**. Maximum stability in signal intensity was achieved after 2.0 min and remained constant for longer time up to 14.0 min. Therefore, a standing time of 2.0 min was adopted in the subsequent work.

3.2.4. Effect of $PQ^{+}.Cl^{-}$ concentration

The influence of $PQ^{+}.Cl^{-}$ concentration on the fluorescence quenching of mercury(II) at concentration of 80 nM was studied in KI (0.1% w/v). Thus, various fractions of $PQ^{+}.Cl^{-}$ solution were added to $[HgI_4]^{2-}$. The fluorescence quenching (ΔF) increased on increasing $PQ^{+}.Cl^{-}$ concentration up to 5.0 μM and leveled off at higher concentration. This possible self-absorption and aggregation of the reagent at high concentration contribute to this enhanced behavior [77]. Thus, in the subsequent work, a concentration of 5.0 μM of $PQ^{+}.Cl^{-}$ was selected, capable of successfully quantifying the target up to trace level proportions.

3.3. Selectivity

Microenvironment resembling real sample matrix containing competent interfering ion was designed to critically examine the applicability of the proposed method. Thus, the quenching in the fluorescence intensity of the ternary ion associate complex $[(PQ^{+})_2.(HgI_4)^{2-}]$ before and after adding the interfering ions in the presence of relatively high concentration (50–500 μgL^{-1}) of other metal ions (K^{+}, Ca^{2+}, Ba^{2+}, Cu^{2+}, Pb^{2+}, Fe^{3+}, As^{3+}, Ag^{+}, Al^{3+} Sn^{2+}, Cd^{2+}, Bi^{3+}, WO_4^{2-}, MnO_4^{-}, F^{-}, CO_3^{2-}, SO_4^{2-}) under the same condition was studied. The results are shown in **Figure 7**, where no noticeable quenching changes were observed. The data indicated that

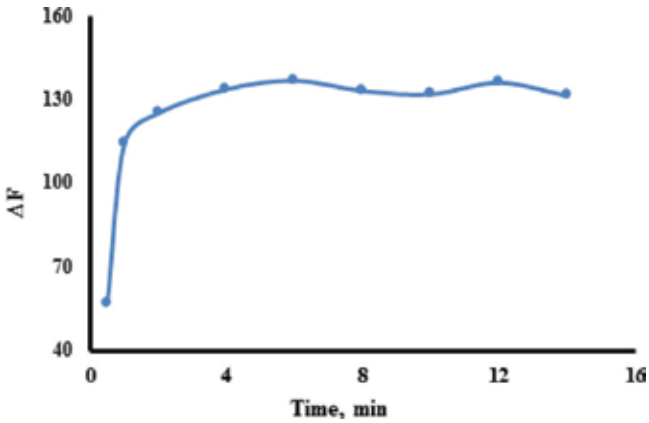

Figure 6. Plot of time *vs.* the fluorescence quenching of $PQ^{+}.Cl^{-}$ (5.0 μM) reagent by mercury (80 nM).

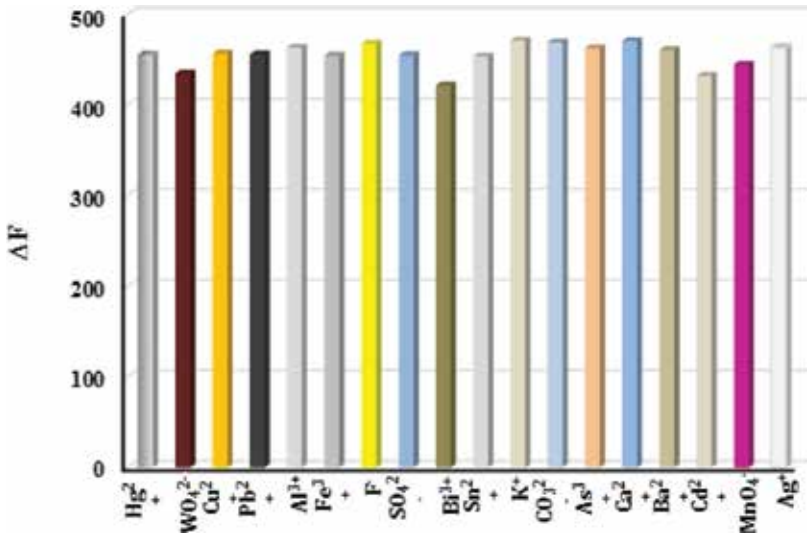

Figure 7. The values of quenching fluorescence intensity of $PQ^+.Cl^-$ (5.0 μgL^{-1}) with addition of Hg(II) (2.0 μgL^{-1}) in the presence of different metal ions (500 μgL^{-1}) in KI (0.1% w/v).

$PQ^+.Cl^-$ possess good selectivity in probing mercury(II). As shown in **Figure 7**, the signal intensity in the presence of 2.0 μg L^{-1} mercury(II) mixed with 500 μg L^{-1} of other metal ions in KI (0.1% w/v) was found similar to mercury(II) alone at 2.0 μg L^{-1} in KI (0.1% w/v). Thus, it can be concluded that the probe is selective towards mercury(II) in the presence of potent interfering ions in higher concentration.

3.4. Analytical performance

Under the optimized experimental conditions, the influence of various known mercury(II) concentrations (20–140 nM) on the fluorescence spectra of mercury(II)-PQ^+ was recorded. The plot of mercury(II) concentrations (20–140 nM) *versus* ΔF was linear (**Figure 8**) with the following regression equation:

$$\Delta F = 1.6354\,[C]\,(nM) - 3.3971 \quad (4)$$

where C and ΔF are the concentration of mercury(II) ions and quenched fluorescence, respectively.

The precision of the method was checked by means of ANOVA by performing five successive replicates per day for 5 days for a typical sample containing 100 nM mercury(II) (**Table 2**).

The precision of the proposed method was evaluated. The calculated value of *F* (F = 1.64) (**Table 3**) was found lower than the tabulated *F* value (F = 2.87) at 95% confidence level [78]. The obtained LOD and LOQ [78] for the proposed method for mercury(II) species were 1.3 and 3.98 nM, respectively. This value was significantly lower than the maximum allowable mercury concentration (10.0 nM) by USEPA in drinking water [17]. The proposed method

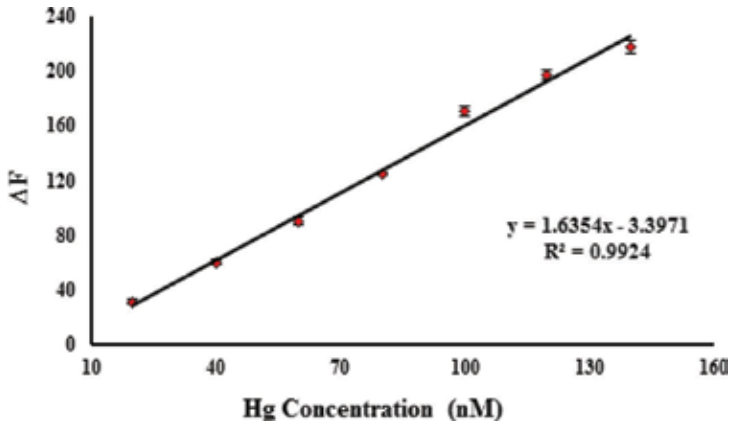

Figure 8. Calibration plot of ternary ion associate complex $[(PQ^+)_2.(HgI_4)^{2-}]$. Conditions: Mercury(II) (20–140 nM), PQ^+ (5.0 μM) and KI (0.1% w/v) pH ≈ 10 at $\lambda_{ex/em}$ = 268/333 nm.

could be considered for routine analysis of mercury due to high precision and selectivity in real samples in the presence of excess relevant competent ions. Moreover, the utility of the proposed method was finally evaluated by comparing the analytical features of the proposed method with a wide range of promising studies in literature. It includes successful comparison with a series of published fluorescence [30, 37–41, 43], electrochemical sensor [42], spectrophotometric [44, 48], colorimetry [45, 49], chemiluminescence [46], single-crystal X-ray diffraction [47], electrochemiluminescence biosensor [50], X-ray fluorescence (XRF) [51], differential pulse voltammetry [36, 52], ICP-OES [21], electrochemical [50] and X-ray photoelectron spectroscopy (XPS) [53], in terms of LOD and LOQ (**Table 4**).

3.5. Fluorescence quenching mechanism

The fluorescence quenching process of $PQ^+.Cl^-$ by mercury(II) as a quencher was critically investigated to evaluate the fluorescence mechanism for the formed ternary ion associate complex $[(PQ^+)_2.(HgI_4)^{2-}]$ [60, 62–64]. The fluorescence spectra of $PQ^+.Cl^-$ ($\lambda_{ex}/\lambda_{em}$ 268/330 nm)

Replicate	First day ΔF	Second day ΔF	Third day ΔF	Fourth day ΔF	Fifth day ΔF
1	167.00	163.88	166.10	159.40	167.59
2	164.47	168.70	163.75	162.32	165.55
3	161.81	166.43	167.99	166.78	166.34
4	160.53	166.45	161.69	164.76	164.00
5	165.70	162.44	165.08	161.13	169.45
Mean	163.90	165.58	164.92	162.88	166.59
SD	2.69	2.45	2.38	2.93	2.06

Table 2. Five days and five replicates per day determined the quenching fluorescence intensity of the reagent $PQ.Cl^-$ by mercury(II) (100 nM) added.

Source of variation	Sum of squares (SS)	Degrees of freedom (df)	Mean square (MS)	F value S_1/S_2
Between days	41.55	4	10.39	1.64
Within days	126.77	20	6.34	
Total	168.32	24		

†S_1: Regression mean square. S_2: Mean square error.

Table 3. Analysis of variance (ANOVA) for the linear equation results†.

Technique	Reagent	LOD	Ref
Fluorescence	(2-Pyridylmethyl)(2-quinolylmethyl) amine	2.6×10^{-8} M	[37]
Fluorescence	Rhodamine hydrazine and 2-hydroxy-acetophenone	150×10^{-9} M	[38]
Fluorescence	Phenylamine-oligothiophene	4.39×10^{-7} M	[39]
Fluorescence	Squaraine–bis(rhodamine-B)	6.47×10^{-6} M	[40]
Fluorescence	Rhodamine (R-2)	1×10^{-8} M	[41]
Electrochemical sensor	DNA-generated gold amalgam	0.002×10^{-9} M	[42]
Fluorescence	Rhodamine 6G derivative and AuNPs	0.75×10^{-9} M	[43]
Fluorescence	1,4-Bis(styryl)benzene	7×10^{-9} M	[44]
Colorimetry	Au-NPs	0.0084×10^{-9} M	[45]
Chemiluminescence	Rhodamine B and gold nanoprisms	0.027×10^{-9} M	[46]
Single-crystal X-ray diffraction	1-[(5-Benzyl-1,3-thiazol-2-yl) diazenyl] naphthalene-2-ol	0.41×10^{-6} M	[47]
Spectrophotometric	bis(2-Ethylhexyl) phosphate	3.5×10^{-9} M	[48]
Colorimetry	Carrageenan-functionalized Ag/AgCl nanoparticles	1×10^{-6} M	[49]
Electrochemiluminescence biosensor	tris-(Bipyridine) $(Ru(bpy)_3^{2+})$/ cyclodextrins-Au nanoparticles(CD-AuNps)/ Nafion	0.1×10^{-9} M	[50]
X-ray fluorescence (XRF)	—	37×10^{-6} M	[51]
Differential pulse voltammetry	Polypyrrole decorated graphene/β-cyclodextrin	0.47×10^{-9} M	[36]
Inductively coupled plasma-optical emission spectrometry (ICP-OES)	—	0.15×10^{-9} M	[21]
Differential pulse voltammetry	Copper cobalt hexacyanoferrate	80×10^{-9} M	[52]
Electrochemical and X-ray photoelectron spectroscopy(XPS)	1-Undecanethiol assembled Au substrate	4.5×10^{-9} M	[53]
Fluorescence	DNA-functionalized-graphene	4.1×10^{-9} M	[30]
Spectrofluorometry	Procaine hydrochloride	1.3×10^{-9} M	Present work

Table 4. Analytical features of different methods employed for mercury(II) determination.

upon introduction of varying concentrations (0.3–1.0 μg L^{-1}) of quencher (mercury(II) ions) are shown in **Figure 9**. The fluorescence intensity of $PQ^+.Cl^-$ decreases regularly with increasing quencher concentration. The Stern-Volmer (K_{SV}) constant was calculated by employing the equation:

$$F_0/F = 1 + K_{SV}[Q] \quad (5)$$

where F_0 and F are the fluorescence signals in the absence and presence of $[HgI_4]^{2-}$ quencher, respectively. K_{SV} is the Stern-Volmer constant and [Q] is the quencher concentration. The values of K_{SV} and correlation factor calculated by plotting fluorescence quenching (ΔF) of $PQ^+.Cl^-$ *versus* $[Hg^{2+}]$ were found equal to 1.87×10^6 L g^{-1} mol^{-1} and 0.9909, respectively.

The chemical composition of the ternary ion associate complex $[(PQ^+)_2.(HgI_4)^{2-}]$ was determined from the Benesi-Hildebrand linear model by employing the following equation [77, 79–82]:

$$\frac{1}{(F_o - F)} = \frac{1}{(F - F_\infty)} + \frac{1}{(F - F_\infty) \times K \times [Q]^2} \quad (6)$$

where F_∞ represents the emission intensity of the ternary ion associate complex $[(PQ^+)_2.(HgI_4)^{2-}]$ at equilibrium and *K* is association constant. The number of the binding sites (n) and the apparent binding constant (K) of $PQ^+.Cl^-$ that independently binds to equivalent sites on a macromolecule were determined from the linear plot of Benesi-Hildebrand ($1/(I\text{-}I_o)$ *versus* 1/([Mercury(II)]). The plot revealed formation of 1:2 stoichiometry of $[HgI_4]$:$PQ^+.Cl^-$ molar ratio in the produced ternary ion associate complex $[(PQ^+)_2.(HgI_4)^{2-}]$. The calculated association constant *K* was found equal to 73 M^{-1}.

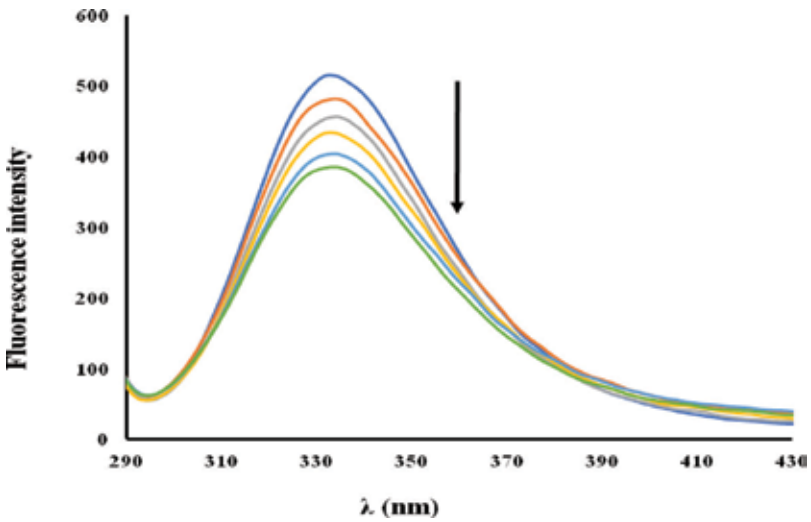

Figure 9. Fluorescence quenching spectra of $PQ^+.Cl^-$ (5.0 μM) in the presence of various concentrations (20–80 nM) of the mercury(II) ions. Conditions: KI (0.1% w/v) pH ≈ 10, at $\lambda_{ex/em}$ = 268/333 nm.

Samples	Spiked (nM/L)	Proposed method	Proposed PQ+ method	ICP-OES	
		Detected (nM) mean ± *SD*	Recovery (%)	Detected (nM) mean ± *SD*	Recovery (%)
Tap water 1	20	20.97 ± 0.50	104.7	20.54 ± 0.63	102.7
Tap water 2	40	39.11 ± 1.25	97.78	39.22 ± 0.92	98.05
Tap water 3	60	61.74 ± 3.07	102.23	62.58 ± 0.72	104.3
Tap water 4	80	78.51 ± 1.63	98.14	77.88 ± 1.21	97.35
Tap water 5	100	97.74 ± 3.51	97.74	98.37 ± 1.30	98.37

[†]Average ± standard deviation (n = 5).

Table 5. Analytical data mercury(II) assay by the developed and ICP-OES methods[†].

3.6. Analytical applications

Applications of the proposed method were tested for analysis of mercury(II) in tap water samples (King Abdulaziz University, Jeddah, KSA). Samples were spiked with known concentrations (20–100 nM) of mercury(II) ion and analyzed by the developed method. In each sample, the fluorescence quenching of $PQ^+.Cl^-$ was immediately measured after spiking of mercury(II) onto the water samples. For method validation, mercury(II) concentrations in the spiked samples were also determined by the standard ICP-OES method. The results are summarized in **Table 5**. The recovery percentage of the measured mercury(II) added to the real samples by the developed and the standard ICP-OES methods was in the range from 97.74 to 104.7% and 98.05 to 102.7%, respectively. The calculated values of the Student's *t* and *F* tests were found lower than the tabulated Student's *t* and *F* tests at 0.05 probability [78] revealing no significant differences between both methods. Thus, it can be concluded that the proposed fluorescence probe can be used as a potential assay for sensing of mercury(II) in complex matrices.

4. Conclusion

A new and facile extractive spectrofluorometric method for cost effective, precise, accurate and selective determination of trace levels of mercury(II) in water. The proposed method was based upon formation of ternary ion associate complex $[(PQ^+)_2.(HgI_4)^{2-}]$ between $[HgI_4]^{2-}$ and the fluorescence probe $PQ^+.Cl^-$. The proposed system offered excellent selectivity towards mercury(II) ions over most anions and metal cations. The detection process could be performed quickly at room temperature without any catalyst or oxidizer. The proposed method provides LOD (1.3 nM) lower than the value set by WHO (10 nM) and USEPA for drinkable water [1, 17]. The developed method is easy to operate as it does not require sophisticated experimental techniques, and the proposed assay is useful for point-of care applications. Moreover, the method opens capable ways for developing fluorescence assay strategies. The proposed approach was validated successfully by analysis of mercury(II) in environmental

water samples by ICP-OES data and statistical treatment of data in terms of significant tests, e.g. *F* and Student's *t* tests. The method could be expanded for ultra-trace analysis of mercury(II) ions in water after on-line enrichment on nanosized solid phase extractor, e.g. polyurethane foam packed column followed by elution with selective reagent [83] and/or its proposed coupling with the advanced microextraction techniques [84]. Therefore, the present work suggested the suitability of the proposed method for use in routine analysis and applicable strategy for analysis of mercury(II) in complex matrices.

Author details

Dyab A. Al-Eryani[1,2], Waqas Ahmad[1], Zeinab M. Saigl[1], Hassan Alwael[1], Saleh O. Bahaffi[1], Yousry M. Moustafa[3] and Mohammad S. El-Shahawi[1,4†*]

*Address all correspondence to: mohammad_el_shahawi@yahoo.co.uk

1 Department of Chemistry, Faculty of Science, King Abdulaziz University, Jeddah, Saudi Arabia

2 Department of Chemistry, Faculty of Applied Science, Thamar University, Thamar, Yemen

3 Faculty of Applied Science, Umm Al-Qura University, Makkah, Saudi Arabia

4 Department of Chemistry, Faculty of Science, Damiatta University, Damiatta, Egypt

†The author is on sabbatical leave from the Department of Chemistry, Faculty of Science, Damiatta University, Damiatta, Egypt.

References

[1] World Health Organization (WHO). Guidelines for Drinking Water, 4th ed. Switzerland; 2011

[2] Elinder CG, Gerhardsson L, Oberdoerster G. Biological monitoring of toxic metals-overview. In: Biological Monitoring of Toxic Metals. US: Springer; 1988. pp. 1-71

[3] Aragay G, Pons J, Merkoci A. Recent trends in macro-, micro-, and nanomaterial-based tools and strategies for heavy-metal detection. Chemical Reviews. 2011;**111**:3433-3458

[4] Lin YH, Tseng WL. Ultrasensitive sensing of Hg^{2+} and CH_3Hg^+ based on the fluorescence quenching of lysozyme type VI-stabilized gold nanoclusters. Analytical Chemistry. 2010;**82**:9194-9200

[5] Wen D, Deng L, Guo SJ, Dong SJ. Self-powered sensor for trace Hg^{2+} detection. Analytical Chemistry. 2011;**83**:3968-3972

[6] Ye BC, Yin BC. Highly sensitive detection of mercury(II) ions by fluorescence polarization enhanced by gold nanoparticles. Angewandte Chemie, International Edition. 2008;**47**:8386-8389

[7] Liu DB, Qu WS, Chen WW, Zhang W, Wang Z, Jiang XY. Highly sensitive, colorimetric detection of mercury(II) in aqueous media by quaternary ammonium group-capped gold nanoparticles at room temperature. Analytical Chemistry. 2010;**82**:9606-9610

[8] Deng L, Ouyang XY, Jin JY, Ma C, Jiang Y, Zheng J, Li JS, Li YH, Tan WH, Yang RH. Exploiting the higher specificity of silver amalgamation: Selective detection of mercury(II) by forming Ag/hg amalgam. Analytical Chemistry. 2013;**85**:8594-8600

[9] Wei H, Wang ZD, Yang LM, Tian SL, Hou CJ, Lu Y. Lysozyme-stabilized gold fluorescent cluster: Synthesis and application as Hg^{2+} sensor. Analyst. 2010;**135**:1406-1410

[10] Charlet L, Chapron Y, Faller P, Kirsch R, Stone AT, Baveye PC. Neurodegenerative diseases and exposure to the environmental metals Mn, Pb, and hg. Coordination Chemistry Reviews. 2012;**256**:2147-2163

[11] Holmes P, James KAF, Levy LS. Is low-level environmental mercury exposure of concern to human health? Science of the Total Environment. 2009;**408**:171-182

[12] Lu H, Xiong L, Liu H, Yu M, Shen Z, Li F, You X. A highly selective and sensitive fluorescent turn-on sensor for Hg^{2+} and its application in live cell imaging. Organic & Biomolecular Chemistry. 2009;**7**:2554-2558

[13] Liu W, Chen J, Xu L, Wu J, Xu H, Zhang H, Wang P. Reversible "off-on" fluorescent chemosensor for Hg^{2+} based on rhodamine derivative. Spectrochimica Acta A. 2012;**85**:38-42

[14] Deng L, Zhou Z, Li J, Li T, Dong S. Fluorescent silver nanoclusters in hybridized DNA duplexes for the turn-on detection of Hg^{2+} ions. Chemical Communications. 2011;**47**: 11065-11067

[15] Ma LJ, Li Y, Li L, Sun J, Tian C, Wu Y. A protein-supported fluorescent reagent for the highly-sensitive and selective detection of mercury ions in aqueous solution and live cells. Chemical Communications. 2008:6345-6347

[16] Du J, Liu M, Lou X, Zhao T, Wang Z, Xue Y, Zhao J, Xu Y. Highly sensitive and selective chip-based fluorescent sensor for mercuric ion: Development and comparison of turn-on and turn-off systems. Analytical Chemistry. 2012;**84**:8060-8066

[17] MacLean JL, Morishita K, Liu J. DNA stabilized silver nanoclusters for ratiometric and visual detection of Hg^{2+} its immobilization in hydrogels. Biosensors & Bioelectronics. 2013;**48**:82-86

[18] Nolan EM, Lippard SJ. Tools and tactics for the optical detection of mercuric ion. Chemical Reviews. 2008;**108**:3443-3480

[19] Ghaedi M, Fathi MR, Shokrollahi A, Shajarat F. Highly selective and sensitive preconcentration of mercury ion and determination by cold vapor atomic absorption spectroscopy. Analytical Letters. 2006;**39**:1171-1185

[20] Turker AR, Cabuk D, Yalcinkaya O. Preconcentration, speciation spectrometry, and determination of mercury by solid phase extraction with cold vapor atomic absorption. Analytical Letters. 2013;**46**:1155-1170

[21] Silva TS, Conte C, Santos JO, Simas ES, Freitas SC, Raices RLS, Quiterio SL. Spectrometric method for determination of inorganic contaminants (arsenic, cadmium, lead and mercury) in smooth weakfish fish. LWT-Food Science and Technology. 2017;**76**:87-94

[22] Oehmen A, Vergel D, Fradinho J, Reis MAM, Crespo JG, Velizarov S. Mercury removal from water streams through the ion exchange membrane bioreactor concept. Journal of Hazardous Materials. 2014;**264**:65-70

[23] Biester H, Schuhmacher P, Muèller G. Effectiveness of mossy tin filters to remove mercury from aqueous solution by Hg(II) reduction and Hg(0) amalgamation. Water Research. 2000;**34**:2031-2036

[24] Huttenloch P, Roehl KE, Czurda K. Use of copper shavings to remove mercury from contaminated groundwater or wastewater by amalgamation. Environmental Science & Technology. 2003;**37**:4269-4273

[25] Chojnacki A, Chojnacka K, Hoffman J, Gorecki H. The application of natural zeolites for mercury removal: From laboratory tests to industrial scale. Minerals Engineering. 2004;**17**:933-937

[26] Evangelista SM, DeOliveira E, Castro GR, Zara LF, Prado AGS. Hexagonal mesoporous silica modified with 2-mercaptothiazoline for removing mercury from water solution. Surface Science. 2007;**601**:2194-2202

[27] Lopes CB, Otero M, Coimbra J, Pereira E, Rocha J, Lin Z, Duarte A. Removal of low concentration Hg^{2+} from natural waters by microporous and layered titanosilicates. Microporous and Mesoporous Materials. 2007;**103**:325-332

[28] Fábrega FM, Mansur MB. Liquid–liquid extraction of mercury(II) from hydrochloric acid solutions by aliquat 336. Hydrometallurgy. 2007;**87**:83-90

[29] Pokhrel LR, Ettore N, Jacobs ZL, Zarr A, Weir MH, Scheuerman PR, Kanel SR, Dubey B. Novel carbon nanotube (CNT)-based ultrasensitive sensors for trace mercury(II) detection in water: A review. Science of the Total Environment. 2017;**574**:1379-1388

[30] Liu Y, Wang X, Wu H. Reusable DNA-functionalized-graphene for ultrasensitive mercury (II) detection and removal. Biosensors and Bioelectronics. 2017;**87**:129-135

[31] Wang N, Lin M, Dai H, Ma H. Functionalized gold nanoparticles/reduced graphene oxide nanocomposites for ultrasensitive electrochemical sensing of mercury ions based on thymine–mercury–thymine structure. Biosensors and Bioelectronics. 2016;**79**: 320-326

[32] Henriques B, Goncalves G, Emami N, Pereira E, Vila M, Marques PAAP. Optimized graphene oxide foam with enhanced performance and high selectivity for mercury removal from water. Journal of Hazardous Materials. 2016;**301**:453-461

[33] Borthakur P, Darabdhara G, Das MR, Boukherroub R, Szunerits S. Solvothermal synthesis of CoS/reduced porous graphene oxide nanocomposite for selective colorimetric detection of Hg(II) ion in aqueous medium. Sensors and Actuators B. 2017;**244**:684-692

[34] Saad A, Bakas I, Piquemal JY, Nowakc S, Abderrabba M, Chehimi MM. Mesoporous silica/polyacrylamide composite: Preparation by UV-graft photopolymerization, characterization and use as Hg(II) adsorbent. Applied Surface Science. 2016;**367**:181-189

[35] Li R, Liu L, Yang F. Preparation of polyaniline/reduced graphene oxide nanocomposite and its application in adsorption of aqueous Hg(II). Chemical Engineering Journal. 2013;**229**:460-468

[36] Palanisamy S, Thangavelu K, Chen SM, Velusamy V, Chang MH, Chen TW, Al-Hemaid FMA, Ali MA, Ramaraj SK. Synthesis and characterization of polypyrrole decorated graphene/β-cyclodextrin composite for low level electrochemical detection of mercury (II) in water. Sensors and Actuators B. 2017;**243**:888-894

[37] Kim JH, Noh JY, Hwang IH, Lee JJ, Kim C. A NBD-based selective colorimetric and fluorescent chemosensor for Hg^{2+}. Tetrahedron Letters. 2013;**54**:4001-4005

[38] Ozdemir M. A rhodamine-based colorimetric and fluorescent probe for dual sensing of Cu^{2+} and Hg^{2+} ions. Journal of Photochemistry and Photobiology A: Chemistry. 2016; **318**:7-13

[39] Niu Q, Wu X, Zhang S, Li T, Cui Y, Li X. A highly selective and sensitive fluorescent sensor for the rapid detection of Hg^{2+} based on phenylamine-oligothiophene derivative. Spectrochimica Acta Part A: Molecular and Biomolecular Spectroscopy. 2016;**153**:143-146

[40] Lee S, Rao BA, Son YA. A highly selective fluorescent chemosensor for Hg^{2+} based on a squaraine–bis(rhodamine-B) derivative: Part II. Sensors and Actuators B. 2015;**210**:519-532

[41] Dong Z, Tian X, Chen Y, Hou J, Guo Y, Sun J, Ma J. A highly selective fluorescent chemosensor for Hg^{2+} based on rhodamine B and its application as a molecular logic gate. Dyes and Pigments. 2013;**97**:324-329

[42] Tang J, Huang Y, Zhang C, Liu H, Tang D. DNA-based electrochemical determination of mercury(II) by exploiting the catalytic formation of gold amalgam and of silver nanoparticles. Microchimica Acta. 2016;**183**:1805-1812

[43] Brasca R, Onaindia MC, Goicoechea HC, Peña AM, Culzoni MJ. Highly selective and ultrasensitive turn-on luminescence chemosensor for mercury (II) determination based on the rhodamine 6G derivative FC1 and au nanoparticles. Sensors. 2016;**16**:1652

[44] Le VS, Jeong JE, Huynh HT, Lee J, Woo HY. An ionic 1,4-bis(styryl)benzene-based fluorescent probe for mercury(II) detection in water via deprotection of the thioacetal group. Sensors. 2016;**16**:2082

[45] Chen Y, Yao L, Deng Y, Pan D, Ogabiela E, Cao J, Adeloju SB, Chen W. Rapid and ultrasensitive colorimetric detection of mercury(II) by chemically initiated aggregation of gold nanoparticles. Microchimica Acta. 2015;**182**:2147-2154

[46] Oskoei YM, Bagheri N, Hassanzadeh J. Ultrasensitive determination of mercury(II) using a chemiluminescence system composed of permanganate, rhodamine B and gold nanoprisms. Microchimica Acta. 2015;**182**:1635-1642

[47] Tupys A, Kalembkiewicz J, Bazel Y, Zapała L, Dranka M, Ostapiuk Y, Tymoshuk O, Woznicka E. 1-[(5-Benzyl-1,3-thiazol-2-yl)diazenyl]naphthalene-2-ol:X-ray structure, spectroscopic characterization, dissociation studies and application in mercury(II) detection. Journal of Molecular Structure. 2017;**1127**:722-733

[48] Fashi A, Yaftian MR, Zamani A. Electromembrane extraction-preconcentration followed by microvolume UV–Vis spectrophotometric determination of mercury in water and fish samples. Food Chemistry. 2017;**221**:714-720

[49] Narayanana KB, Han SS. Highly selective and quantitative colorimetric detection of mercury(II) ions by carrageenan-functionalized Ag/AgCl nanoparticles. Carbohydrate Polymers. 2017;**160**:90-96

[50] Cheng L, Wei B, He LL, Mao L, Zhang J, Ceng J, Kong D, Chen C, Cui H, Hong N, Fan H. "Off-on"switching electrochemiluminescence biosensor for mercury(II) detection based on molecular recognition technology. Analytical Biochemistry. 2017;**518**:46-52

[51] Brent RN, Winesa H, Luther J, Irving N, Collins J, Drake BL. Validation of handheld X-ray fluorescence for in situ measurement of mercury in soils. Journal of Environmental Chemical Engineering. 2017;**5**:768-775

[52] Sharma VV, Tonelli D, Guadagnini L, Gazzano M. Copper-cobalt hexacyanoferrate modified glassy carbon electrode for an indirect electrochemical determination of mercury. Sensors and Actuators B. 2017;**238**:9-15

[53] Li XQ, Liang HQ, Cao Z, Xiao Q, Xiao ZL, Song LB, Chen D, Wang FL. Simple and rapid mercury ion selective electrode based on 1-undecanethiol assembled au substrate and its recognition mechanism. Materials Science and Engineering C. 2017;**72**:26-33

[54] Brunton LL, Chbner BA, Knollmann BC. Goodman & Gilman's, The Pharmacological Basic of Therapeutics, 12th ed. USA: McGraw-Hill; 2011

[55] Miller RD, Cohen NI, Eriksson LI, Fleisher LA, Wiener JP, Young WL. Miller's Anesthesia, 8th ed. Saunders, USA: An Imprint of Elsevier Inc.; 2015

[56] Merino C, Junquera E, Barbero JJ, Aicart E. Effect of the presence of β-cyclodextrin on the solution behavior of procaine hydrochloride. Spectroscopic and thermodynamic studies. Langmuir. 2000;**16**:1557-1565

[57] Lee AG. Interactions between anaesthetics amines and lipid mixtures. Biochimica et Biophysica Acta. 1976;**448**:34-44

[58] Bartucci R, Mollica P, Sapia P, Sportelli L. Procain interaction with DPPC multilayers: An ESR spin label investigation. Applied Magnetic Resonance. 1998;**15**:181-195

[59] Polasek M, Gas B. Determination of limiting ionic mobilities and dissociation constants of some local anaesthetics. Journal of Chromatography. 1992;**596**:265-270

[60] El-Shahawi MS, Al Khateeb LA. Spectrofluorometric determination and chemical speciation of trace concentrations of tungsten species in water using the ion pairing reagent procaine hydrochloride. Talanta. 2012;**88**:587-592

[61] Soni S, Pal A. Spectroscopic studies on host–guest interactions of α- and β-cyclodextrin with lidocaine hydrochloride and procaine hydrochloride. Journal of Solution Chemistry. 2016;**45**:665-674

[62] El-Shahawi MS, Alwael H, Arafat A, Al-Sibaai AA, Bashammakh AS, Al-Harbi EA. Kinetics and thermodynamic characteristics of cadmium(II) sorption from water using procaine hydrochloride physically impregnated polyurethane foam. Journal of Industrial and Engineering Chemistry. 2015;**28**:147-152

[63] El-Shahawi MS, Bashammakh AS, Orief MI, Alsibaai AA, Al-Harbi EA. Separation and determination of cadmium in water by foam column prior to inductively coupled plasma optical emission spectrometry. Journal of Industrial and Engineering Chemistry. 2014;**20**:308-314

[64] El-Shahawia MS, Hamza A, Al-Sibaai AA, Al-Saidi HM. Fast and selective removal of trace concentrations of bismuth (III) from water onto procaine hydrochloride loaded polyurethane foams sorbent: Kinetics and thermodynamics of bismuth (III) study. Chemical Engineering Journal. 2011;**173**:29-35

[65] Vogel AI. Quantitative Inorganic Analysis. 3rd ed. England: Longmans Group Ltd.; 1966

[66] Sawyer DT, Heinemann WR, Beebe JM. Chemistry Experiments for Instrumental Methods. New York: John Wiley & Sons; 1984

[67] Santoni G, Mura P, Pinzauti S, Lombardo E, Gratteri P. Simultaneous UV spectrophotometric determination of procaine hydrochloride and phenazone in an otic formulation. International Journal of Pharmaceutics. 1990;**64**:235-238

[68] Xu LX, Shen YX, Wang HY, Jiang JG, Xiao Y. Spectrophotometric determination of procaine hydrochloride in pharmaceutical products using 1,2-naphthoquinone-4-sulfonic acid as the chromogenic reagent. Spectrochimica Acta Part A. 2003;**59**:3103-3110

[69] Sekine T, Ishli T. Studies of the liquid-liquid partition systems. VII. The solvent extraction of mercury(II) chloride, bromide, iodide and thiocyanate with some organic solvent. Bulletin of the Chemical Society of Japan. 1970;**43**:2422-2429

[70] Sharma RP, Singh A, Venugopalan P, Smolentsev AI, Gubanov AI. Stabilizing effects of large counter ion: Synthesis, characterization and single crystal X-ray structure determination of $[Co(NH_3)_6][HgI_4]I{\cdot}H_2O$. Journal of Molecular Structure. 2010;**975**:1-4

[71] Pourreza N, Behpour M. Column preconcentration of mercury as HgI_4^{2-} using methyltrioctylammonium chloride-naphthalene adsorbent with subsequent anodic stripping-differential pulse voltammetric determination. Analytica Chimica Acta. 2003;**481**:23-28

[72] Liu J, Huang Y, Cai W, Li P, Li X, Li L, Lin S. Determination of trace mercury by solid substrate room temperature phosphorimetry based on an ionic associate $[(Rhod.6G)_2]^{2+}{\cdot}[HgI_4]^{2-}$. International Journal of Environmental Analytical Chemistry. 2005;**85**:387-397

[73] Yowloo AY, Lay YP, Kutty MG, Timpe O, Behrens M, Hamid SBA. Spectrophotometric determination of mercury with iodide and rhodamine B. Sains Malaysiana. 2012;**41**:213-218

[74] Sun Y, Ma L, Wang HY, Tang B. Determination of procaine hydrochloride by fluorimetry. Guang Pu Xue Yu Guang Pu Fen Xi. 2002;**22**:637-640

[75] Carretero AS, Blanco CC, Peinado SF, El-Bergmi R, Gutierrez AF. Fluorimetric determination of procaine in pharmaceutical preparations based on its reaction with fluorescamine. Journal of Pharmaceutical and Biomedical Analysis. 1999;**21**:969-974

[76] Sanchez FG, Rubio ALR, Blanco CC, Lopez MH, Gomez JCM, Carnero C. Enhanced fluorimetric determination of procaine in pharmaceutical preparations by aqueous β-cyclodextrin inclusion and non-aqueous competitive action. Analytica Chimica Acta. 1988;**205**:139-147

[77] Valeur B. Molecular Fluorescence Principles and Applications. Weinheim, Federal Republic of Germany: Wiley-VCH Verlag GmbH; 2002

[78] Miller JC, Miller JN. Statistics for Analytical Chemistry. 6th ed. New York.: Ellis-Howood; 2010

[79] Skoog DA, West DM, Holler FJ, Crouch SR. Fundamental of Analytical Chemistry. 9th ed. Belmont, USA: Cengage Learning; 2014

[80] Maafi M, Laassis B, Aaron JJ. Photochemically induced fluorescence investigation of a β-cyclodextrin: Azure A inclusion complex and determination of analytical parameters. Journal of Inclusion Phenomena and Molecular Recognition in Chemistry. 1995; **22**:235-247

[81] Abdel-Shafi AA, Al-Shihry SS. Fluorescence enhancement of 1-napthol-5-sulfonate by forming inclusion complex with β-cyclodextrin in aqueous solution. Spectrochimica Acta Part A. 2009;**72**:533-537

[82] Al-Shihry SS. Spectroscopic studies of inclusion complexes of 1-naphthol-4-sulfonate with β-cyclodextrin in aqueous solution. Spectrochimica Acta Part A. 2005;**61**:2439-2443

[83] Kiwan AM, E1-Shahawi MS, Aldhaheri SM, Saleh MH. Sensitive detection and semiquantitative determination of mercury(II) and lead(II) in aqueous media using polyurethane foam immobilized 1,5-di-(2-fluorophenyl)-3-mercaptoformazan. Talanta. 1997;**45**: 203-211

[84] Fernandez E, Vidal L, Costa-Garcia A, Canals A. Mercury determination in urine samples by nanostructured screen-printed carbon electrodes after vortex-assisted ionic liquid dispersive liquid-liquid microextraction. Analytica Chimica Acta. 2016;**915**:49-55

Chapter 8

Biomonitoring of Trace Metals in the Coastal Waters Using Bivalve Molluscs

Periyadan K. Krishnakumar,
Mohammad A. Qurban and Geetha Sasikumar

Additional information is available at the end of the chapter

http://dx.doi.org/10.5772/intechopen.76938

Abstract

Several environmental contaminants including toxic trace metals are being discharged into the coastal environment causing serious threat to marine organisms and posing public health risk. Marine bivalves (mussel, oyster, and clam) have been successfully used as sentinel organisms for monitoring contaminant levels, including trace metals, in coastal waters around the globe. Chemical analyses measure the contaminants present in the biota but do not necessarily reveal potential biological effects. Therefore, the need to detect and assess the effects of contaminants, especially at low concentrations, has led to the development of molecular markers of contaminant effects called biomarkers. Owing to their short time of response, biomarkers in marine bivalves are used as early warning signals of biological effects caused by environmental pollutants. Research into the development and application of accurate biomarker-based monitoring tools for the environmental contaminants has been intensified in several developed countries.

Keywords: bivalves, bioaccumulation, biomarkers, trace metals, mussel watch

1. Introduction

Marine pollution is a major problem that has negative effects on the ocean's ecosystems. Economic developments and urbanization are taking place at an accelerated rate in the coastal zones across the world, putting enormous pressures on coastal waters and marine habitats. Incidents of coastal and marine water pollution have increased throughout the world, mainly due to discharges from rivers, increased surface run-off, drainage from expanding port areas, oil spills, discharges from shipping activities, and domestic and industrial effluent discharges.

Most of the world's wastes around 20 billion tons per year end up in the sea, often without any preliminary processing.

Trace metals are introduced into the coastal waters through natural process and anthropogenic activities. The natural process includes river discharge, rock weathering, wind-generated dust from arid and semi-arid regions of the continents, and hydrothermal circulation at mid-ocean ridges. The anthropogenic sources of metals include agriculture, fossil fuel extraction, refining and burning, chemical production, and intentional and accidental discharges. Trace levels of trace metals naturally occur in the marine environment, and many of them at low concentrations are essential for marine life. However, if their concentrations exceed the natural levels, it will cause a serious threat to marine life. Monitoring and assessment programs are routinely conducted in the coastal waters for planning and implementing mitigation measures to control trace metal pollution. Historically as one of the simple and widely used monitoring techniques, sampling, and analysis of seawater and sediment are being employed for estimating the levels of contaminants including trace metals in coastal waters. Instead of using water or sediment samples, tissue concentrations of contaminants in marine organisms, especially bivalves, are being used as a reliable method for assessing the coastal water quality since 1960s [1–4].

Most of the marine bivalves such as mussels, oysters, and clams are commercially important groups, and several of them are being used for coastal farming around the globe and as popular seafood. Since late 1960s and early 1970s, bivalves such as mussels were used for biomonitoring trace metals in coastal waters [3, 5]. In biomonitoring, tissue burden of trace metals in marine organisms are analyzed, and the biological responses of organisms are measured to assess changes in the environmental quality caused by toxic contaminants [6–8]. This chapter will attempt to provide an overview of the basic concept, methods and the present status of the biomonitoring of trace metals in the coastal waters using bivalve molluscs.

2. Why bivalves

Generally, bivalves are suspension feeders or deposit feeders, or even utilize both feeding methods. They feed on microscopic algae, bacteria, and detritus through filter feeding process. They draw water from the posterior ventral side through the inhalant siphon, and the water passes through the gills and gets expelled through the exhalent siphon. In this process, they filter large quantities of seawater, and the water filtering capacity of typical natural mussel beds has been calculated as 7–12 m^3, m^{-1}, h^{-1} [9, 10]. One single adult blue mussel pumps around 50 ml of seawater per minute during active feeding [11]. As bivalves filter large quantiles of seawater, their tissues absorb some of the contaminants present in water and food particles. Bivalves accumulate trace metals from the surrounding aquatic medium across the cellular membrane (dissolved source) and from the food materials (dietary source) [12].

Historically, bivalve molluscs are considered as valuable marine organisms for environmental monitoring and used as biomonitors of chemical pollution of coastal waters [3, 5, 13]. Bivalves are widely distributed from the North Pole to the South Pole, sessile in nature, and easy to sample and available in a suitable size for chemical analysis. Bivalves are also resistant to a wide

http://dx.doi.org/10.5772/intechopen.76938

Figure 1. Common marine bivalves and their habitats from the Indian coast. (A) Intertidal rocky area showing green mussel beds from the south west coast of India; (B) green mussel *Perna viridis;* (C) enlarged view of green mussels; (D) oyster bed consisting of *Crassostrea madrasensis* and *Saccostrea cucullata* exposed during low tide; and (E) enlarged view of *C. madrasensis and S. cucullata;* (E) clam bed consisting of *Meretrix casta* and (F) enlarged view of the clam *Paphia malabarica*.

range of contaminants and may thrive even in highly polluted environments [3, 14]. These qualities make them a group of candidate species for biomonitoring programs across the globe. As filter feeders, they bioaccumulate various contaminants and their tissue concentrations provide a time-integrated picture of contaminants in the environment [15, 16]. It has been reported that bivalves accumulate trace metals in their tissues at levels up to 100–100,000 times higher than the concentrations observed in the seawater in which they live [5, 17]. Therefore, several chemical contaminants, including trace metals, present at undetectable levels in seawater can be detected in bivalve tissues. Different species of clams, mussels, and oysters have widespread distribution across the continents (**Figure 1**), and many of those species have been successfully used for monitoring the concentrations of contaminants in the marine environment [5].

3. Metal bioaccumulation in bivalves

Cobalt, copper, chromium, iron, magnesium, manganese, molybdenum, nickel, selenium, and zinc are essential metals that are required for various biochemical and physiological functions of animals [18] while other metals such as aluminum, antinomy, arsenic, barium, cadmium, gold, lead, lithium, mercury, nickel, platinum, silver, strontium, tin, titanium, and vanadium have no

established biological functions and are considered as non-essential metals [19]. However, the essential metals will be harmful to the organisms if their concentrations exceed the natural levels. The expert's group of International Council for the Exploration of the Sea (ICES) and Oslo and Paris Conventions (OSPAR) highlighted the trace metals such as arsenic, cadmium, chromium, copper, mercury, nickel, lead, and zinc in the marine environment as key substances of concern [20].

Bivalves accumulate both essential and non-essential metals in their soft tissues above the background levels in seawater or sediments, and this process is called bioaccumulation. Bioaccumulation is a good integrative indicator of the chemical exposures of marine organisms such as bivalves in polluted waters [21]. Trace metals cannot be metabolized by organisms, and hence bioaccumulation of trace metals is of particular value as an exposure indicator. However, metal bioaccumulation can be complex. The bioaccumulation levels in mollusks differ among metals in the same bivalve species and among species [13, 21–23] due to the biological role of different metals and to specific strategies of accumulation [23]. In addition, the metal bioaccumulation in bivalves depends on the marine environmental factors (temperature, pH, salinity, co-occurrence of metals, etc.) and the biological conditions (age, sex, sexual maturity stage, etc.) of the species [24, 25].

The gill tissue of bivalves constitutes a key interface for the uptake of dissolved metal ions from water followed by the mantle tissue, and the uptake of metals bound to particulate material is achieved via the digestive tract, in particular, via the digestive gland [23]. Generally, in bivalves, maximum concentrations of metals have been reported in the digestive gland and/or gill tissue followed by mantle and muscle tissue [26, 27]. The bioaccumulation of trace metals in bivalve tissues is dependent on different metabolic processes occurring within specific cell types in target tissues. Metallothioneins (MTs), the low-molecular-weight proteins present in organisms including bivalves are involved in the intracellular regulation of metals such as Cu, Zn, and Cd [28]. Epithelial cells of gill and mantle can synthesize MT and sequester metals into the lysosomes for further transport in circulating hemocytes [29].

4. Bivalves as sentinel organisms

Sentinel organisms accumulate contaminants in their tissues without any harmful effects and can be measured in a sensitive manner the amount of contaminants that are biologically available [30]. Several comprehensive reviews have been published on the use of bivalve molluscs as sentinel organisms and as biomonitors of metal pollution [5, 12, 20, 31–35]. These reviews and studies provide an in-depth discussion on metal bioaccumulation and metal bioavailability, highlighting the historical usage of bivalves in environmental studies.

Most of the bivalves such as clams, mussels, and oysters, fulfill the criteria required for a typical sentinel organisms and being successfully used as spatial and temporal trend indicators of contaminants in monitoring program from several parts of the world [3, 7, 12, 14–16, 36–39]. The tissue concentrations of various toxic trace metals in wild mussel species from various regions worldwide are summarized in **Table 1**. The tissue concentrations ranged from low to high values depending upon the environmental status of the study area.

Country	Mussel Species	Ag	Al	As	Cd	Cr	Co	Cu	Fe	Hg	Ni	Pb	Zn	Ti	Se	V	Sr	Ba	Mn	Ref.
San Francisco Bay, USA	*Mytilus edulis* mg/kg dry wt				6.9	4.05							92		4.6					[97, 98]
Claisebrook Cove, Western Australia	*Xenostrobus sp.* mg/kg wet wt		12–61	0.46–0.75	0.21–0.27	0.05–0.17	0.06–0.16	1.7–2.2		<0.01	0.22–85	0.08–0.52	6–9.6		0.34–0.57				3.3–28	[99]
South Island New Zealand	*Perna canaliculatus* mg/kg dry wt			5.35–27.48	0.14–1.67			2.19–18.25			0.08–5.83	0.13–1.53	45.31–147.18							[100]
Offshore South China Sea	*Bathymodiolus platifrons* mg/kg dry wt	2.6–25.13	2.16–6.73	5.89–10.03	0.78–4.35	0.81–1.72	0.1–0.45	5.53–42.31	14.28–56.07		0.42–1.25	4.41–4.8	33.76–79.04				17.98–45.78	2.69–4.06	4.5–8.01	[101]
East coast of China	*Perna viridis* mg/kg dry wt	0.01–0.14		12.64–20.95	0.48–5.31	1.51–10.93		1.45–28.55	96.62–1002		1.3–4.78	0.44–2.93	66.05–231							[102]
East Adriatic Sea, Croatia	*Mytilus galloprovincialis* mg/kg dry wt			4–30		1–2.9		3.7–11.1	53.4–719		0.8–5	2–7	59.1–273						2–13	[103]
Adriatic Sea (Montenegro coasts)	*Mytilus galloprovincialis* mg/kg dry wt							4.6–17.2	128–603				132–345						7.3–85.0	[104]
Tyrrhenian Sea (Gulf of Gaeta)	*Mytilus galloprovincialis* mg/kg dry wt							5.5–11.5					123–180							[105]
Marmara Sea (NW coasts)	*Mytilus galloprovincialis* mg/kg dry wt							6.7–9.5	120–415				208–320						4.5–11.7	[106]

http://dx.doi.org/10.5772/intechopen.76938

Country	Mussel Species	Ag	Al	As	Cd	Cr	Co	Cu	Fe	Hg	Ni	Pb	Zn	Ti	Se	V	Sr	Ba	Mn	Ref.
Aegean Sea	*Mytilus galloprovincialis* *mg/kg dry wt*							3.5–5.3	48.6–49.9				17.8–28.5						2.6–4.7	[107]
N Atlantic (Spanish Gallician coasts)	*Mytilus galloprovincialis* *mg/kg dry wt*							3.9–9.7					159–351							[108]
Island of Gossa (W coast of Norway)	*Mytilus galloprovincialis* *mg/kg dry wt*							1.3–1.8	11.0–11.7				13.3–15.2							[109]
Spain Cantabrian Coast	*Mytilus galloprovincialis* mg/kg *dry weight*			14.6–31.5	0.4–2.3	2.6–5.7	0.4–69.3	9.1–34.8			1.5–15.4	1.1–13.3	202.7–300.8		5.8–8.7	1.7–7.1			5.6–55.3	[110]
N Aegean Sea (Strait of Canakkale)	*Mytilus galloprovincialis* *mg/kg dry wt*							0.7–12.9	24.3–82.0				43.8–133.5						0.4–4.8	[111]
Trinidad	*Perna viridis* mg/kg *wet weight*				0.01–0.61	0.06–0.2		1.02–1.98		0.03–0.07	0.3–0.75		11.3–40.37							[112]
Venezuela	*Perna viridis* mg/kg *wet weight*				0.02–0.05	0.12–0.16		1.42–3.43		0.02–0.08	0.22–1.3		8.75–16.38							[112]
Italy Tyrrhenian coastal areas	*Mytilus galloprovincialis* mg/kg *dry weight*				0.33–0.49	0.46–1.31		5.51–11.5				1.67–2.49	123–180							[105]
Black Sea (Turkish coasts)	*Mytilus galloprovincialis* *mg/kg dry wt*							11.7–23.3					312–396						46.9–73.0	[113]

Country	Mussel Species	Ag	Al	As	Cd	Cr	Co	Cu	Fe	Hg	Ni	Pb	Zn	Ti	Se	V	Sr	Ba	Mn	Ref.
Turkey Eastern Aegean Sea	*Mytilus galloprovincialis* mg/kg *dry weight*				0.24–0.49	0.32–7.27		2.44–5.49		0.11–0.15		0.84–2.41	75.9–201							[114]
Italy Venice Lagoon	*Mytilus galloprovincialis* mg/kg *dry weight*				1.16–6.59	0.16–2.75		3.55–10.8				1.08–4.27	135–400							[115]
Brazil	*Mytella guyanensis* mg/kg *dry weight*		778–2458	1.44–23.1	Bdl–1.42	Bdl–3.13	Bdl–611	6.03–102	Bdl–1820	Bdl–0.35		Bdl–19.4	50.8–141		Bdl–49.6	Bdl–6.93	35.5–95.8	Bdl–88.7	30.7–3520	[116]
India	*Perna viridis* mg/kg *wet weight*				0.24–3.49	Bdl–0.46		Bdl–1.84	Bdl–235.6		Bdl–2.89	Bdl–1.95	Bdl–17.36						1.91–8.77	[15]

Table 1. Selected trace metal concentrations in the soft tissue of wild mussel species from various regions worldwide.

http://dx.doi.org/10.5772/intechopen.76938

4.1. Mussel watch programs

Mussels and other marine bivalves are widely used as sentinel organisms in "mussel watch" programs for indicating levels of pollutants in the coastal marine environment due to their ability to bioaccumulate organic or toxic elements [40]. Under mussel watch program, environmental contaminants (trace metals, hydrocarbons, pesticides, etc.) accumulated in the soft tissue of natural, cultured, or deployed bivalves (clams, mussels, and oysters) collected from a set of defined geographical locations over a time-span of several years are systematically and repeatedly measured for assessing and comparing the coastal water quality [5, 40–42]. A prominent example is the US Mussel Watch Program originally started in 1976 [3, 43] and established as the Mussel Watch component of National Oceanic and Atmospheric Administration's (NOAA) National Status and Trends (NST) program during 1986–2012 [44, 45, 46]. In spite of the criticisms and limitations [47], the US mussel watch results made valuable contributions to our understanding of trace metal contamination and its biogeochemistry in coastal ecosystems [5].

Project phase and year	Study areas	Bivalve species	List of contaminants	References
IMW Phase I (Initial Implementation): 1991–1993	South America, Central America, Mexico and Caribbean	Blue mussels (*Mytilus* sp.) 134 stations Oysters (*Crassostrea* sp.)–18 stations Other bivalves–24 stations	Total Polychlorinated biphenyls (PCBs), total Chlordane (CHLs), and total HCHs	[5, 117]
IMW Phase II 1997–1999	Asia Pacific Region (Japan, South Korea, Russia, China, the Philippines, Vietnam, Malaysia, Cambodia, Thailand, Indonesia and India)	Blue mussel, (*M. edulis*), and the green mussel (*Perna viridis*).	Total PCBs, dichloro diphenyl trichloroethane and its metabolites (DDTs), CHLs, hexachlorocyclohexane isomers (HCHs) and hexachlorobenzene (HCB), polychlorinated dibenzo-p-dioxins and furans (PCDDs/Fs), coplanar PCBs (Co-PCBs), Butyltins (BTs) and some heavy metals	[38, 118–121]
IMW Pilot Study—Black Sea. 1996–1997	Six Black Sea Countries (Bulgaria, Georgia, Romania, Russia, Turkey and Ukraine).	Blue mussels (*M. galloprovincialis*)- 5–13 sites	PAHs, PCBs, DDTs	[122]
Western Mediterranean Basin and the International Mediterranean Commission (CISEM) Mussel Watch program. 2002–2006	The coasts of the Western Mediterranean Basin (Spain, France, Italy, North Tunisia, Algeria and Morocco)	Caged mussels (*Mytilus* sp.) deployed at 122 sites	Heavy metals, chlorinated pesticides and PCBs and PAHs	[123–125]

Table 2. Details of the International Mussel Watch (IMW) program conducted from various parts of the globe [5].

Later, the contaminant monitoring programs similar to mussel watch were implemented throughout the world either for monitoring long-term spatial and temporal pollution trends covering large marine region containing multiple monitoring stations and several anthropogenic contamination sources [36–38, 48–51] or for monitoring and solving local pollution problems covering a small geographical areas [7, 8, 15, 32, 52–58].

The mussel watch program initiated in USA has led to the formation of the International Mussel Watch (IMW) Projects [5]. It was initiated by the International Oceanographic Commission (IOC) in collaboration with the United Nations Environment Program (UNEP) and the US NOAA. **Table 2** summarizes the details of the international mussel watch program conducted from different geographical locations. Recently, the advantages and limitations of the mussel watch concept were discussed 40 years after its inception [5].

5. Biomarkers of exposure in bivalves

Chemical analyses of bivalve tissue samples measure the contaminants present but do not necessarily reveal potential biological effects on bivalves. Therefore, biomarkers were developed to assess the health status of the marine organisms, especially bivalves. Biomarkers are the early warning signals about the health status of bivalves exposed to toxic contaminants, because a toxic effect or response will be apparent at the molecular or cellular level before it is noticeable at higher biological levels. The concept of biomarker is borrowed from medical science, which describes a measurable indicator such as blood cholesterol profile connected to relevant clinical endpoints like atherosclerosis and heart attack. The biochemical biomarkers (acetylcholinesterase inhibition for exposure to neurotoxic compounds, cytochrome P450 for detoxification of polycyclic aromatic hydrocarbons (PAHs) and polychlorinated biphenyls (PCBs), and the different methods to detect genotoxicity), which are used in marine environmental monitoring are still used in humans [59–61].

During the last decade, several biomarkers sensitive to contaminant exposure and/or impact have been developed as tools for use in marine environmental monitoring and impact assessment [7, 8, 62]. During the same time, various monitoring agencies began to focus on locating the source of contamination and fates as well as the impact as contaminants are usually discharged into the coastal waters, especially estuaries, where effects have been most significantly detected. The European Union's Water Framework Directive (WFD) also stressed the requirement of monitoring programs to assess the achievement of good chemical and ecological status for all water bodies by 2015 [63]. In the past 30–40 years, numerous biomarkers have been developed on bivalve mollusks, especially mussels (see **Table 3**) with the objective to apply them for environmental biomonitoring. Biomarkers based on responses at physiological level, cellular/tissue level, and molecular level of bivalve molluscs are developed and recommended as tools for studying the effects of contaminants on field and laboratory exposed bivalves, especially mussels [6, 64–66]. Research into the development and application of accurate biomarker-based monitoring tools for the environmental contaminants has been intensified in several developed countries, and they are using several biomarkers based in marine bivalves to monitor the environmental quality of coastal and estuarine waters [20].

Group	Biomarker name	Description	References
Bivalve Physiology	Body Condition Index (BCI)	Assessment of tissue weight in comparison with shell cavity volume or shell length	[7, 59, 126]
	Stress on stress response (SOS)	Assessment of survival rate during aerial exposure	[71]
	Scope for growth (SFG)	Measurement of physiological energy balance	[59, 76]
Metal-binding cysteine-rich proteins	Metallothioneins (MTs)	Measurement of metal binding proteins in tissue samples. Compensatory mechanism during exposure to heavy metals (Cd, Fe, Hg, Zn, As)	[28]
Cellular Responses	Lysosomal membrane stability (LMS); lipofuscin and neutral lipids accumulation	Assessment of the condition of lysosomes and the related cell injury	[7, 8, 61]
DNA integrity markers	Micronuclei	Assessment of toxic impact on chromosomes	[91, 92, 127]
	DNA adducts	DNA damage assessment	[91, 92, 128]
	Comet assay	Single cell DNA damage assessment	[91, 92, 128]

Table 3. List of biomarkers routinely used for monitoring the coastal waters quality using marine bivalves.

5.1. Physiological biomarkers

The biological indicators of health in bivalves such as Body Condition Index (BCI), stress on stress response (SOS), and scope for growth (SCF) have been recommended as broad markers of stress caused by either environmental changes or contaminants [59, 64, 67–70]. The stress on stress response is a simple test, which measures the mortality rate (time to kill 50% of the sample) of bivalves when exposed to air [70, 71]. The SOS test examines whether stress caused by environmental changes or contaminants have altered the capacity of bivalves to survive under adverse conditions such as aerial exposure. The body condition index (ratio between soft tissue dry/wet weights to its overall size) is a general indicator of favorable growth conditions as well as the overall biological status. The body condition index is routinely used in aquaculture and environmental monitoring studies to assess the health condition of mussels [7, 25, 72].

The growth, reproduction, and survival of bivalves depend on the availability of sufficient energy reserve in their body. Exposure to contaminants negatively affects the energy balance of bivalves due to the high-energy demand for maintaining homeostasis at the expense of growth, storage, defense, and reproduction [73]. Fitness of an individual organism can be measured in terms of Scope for Growth (SfG), which is the measurement of physiological energy balance and it ranges from optimal (positive values) to stressed conditions (negative values) when the organism is exposed to contaminants or unfavorable environmental conditions [74, 75]. The SFG has been widely used in field monitoring studies [76, 77]. The SFG and the growth rates of mussels were drastically reduced when mussels from uncontaminated sites were transplanted along known pollution gradients or placed in the most contaminated areas [78, 79].

5.2. Cellular biomarkers

The digestive gland cells in bivalves play a key role in digestive and absorptive processes and also in the detoxification and excretion of contaminants [80]. The lysosomal system in the digestive cells was identified as the main target site for the toxic effects of most of the environmental contaminants including trace metals [81]. Lysosomal responses to cell injury due to contaminant exposure or stress caused by environmental changes fall into three categories: (1) changes in lysosomal contents, (2) changes in fusion events, and (3) changes in membrane permeability [81].

Changes in lysosomal membrane permeability of bivalves can be measured using the lysosomal membrane stability (LMS) test [82–84]. The LMS test can be conducted by using two different methodologies: (i) a cytochemical method using cryostat sections of digestive gland tissue and (ii) an in vivo cytochemical method using hemolymph cells. Biomarkers such as LMS, accumulation of lipofuscin and neutral lipids in bivalves were successfully used for coastal pollution monitoring studies [7, 8, 69, 70, 82–84]. Subsequently, different regional conventions have recommended the use of LMS as a general stress biomarker of chemical pollution within the framework of the pollution biomonitoring programs [67, 68, 85]. The proposed integrated assessment approach of contaminants and their effects in the NE Atlantic Baltic Sea Action Plan and in the Mediterranean Ecosystem Approach (EcAp) have included the LMS in mussels as one of the core biomarkers [86–88].

It has been demonstrated that metallothioneins (inducible low molecular, sulfhydryl proteins) levels in the digestive cells of bivalves will be induced after exposure to trace metals such as Cd, Cu, and Zn [89]. The induction of metallothioneins (MT) in bivalves has been proposed as biomarkers of trace metal stress, and it has been recommended to use in coastal pollution monitoring studies [67, 68, 85, 90].

5.3. Biomarkers of genotoxicity

A wide variety of chemical contaminants capable of directly or indirectly damaging the DNA of marine organisms are being discharged into the marine environment. These genotoxic chemicals are capable of inducing some changes in the molecular and cellular levels of marine bivalves [91, 92]. Two well-known tests, micronucleus assay and comet assay, are being widely used to assess the genotoxic effects of environmental contaminants on marine bivalves [91, 92]. The micronucleus assay is used to detect the structural and numerical chromosomal changes while the comet assay (single-cell gel electrophoresis) is used to detect DNA strand breaks in marine bivalves.

6. Coastal pollution monitoring using biomarkers a case study

The biomarkers in marine bivalves based on sub-lethal effects of contaminants are ecologically relevant and can be used to give subtle signals of response to contaminants before damage becomes irreversible. The water quality in European coastal sites was classified ranging from class 1 (clean areas) to class 5 (highly polluted areas), based on global biomarker index for

Baltic mussels [93]. The Marine Strategy Framework Directive (Directive 2008/56/EC) since 2008 emphasized on the importance of assessing key biological responses for evaluating the health of organisms and linking the observed changes to potential contaminant effects [94].

The studies conducted prior to 1990s from Puget Sound, Washington, reported high concentrations of toxic metals, polycyclic aromatic hydrocarbons (PAHs) and PCBs in sediments and toxicant-induced, adverse effects in benthic fish samples collected from the urban associated sites [95]. As an example of how biomarker-based indices can be integrated into environmental monitoring of Puget Sound, biomonitoring study using mussels was conducted in 1992 [7]. Blue mussels (*Mytilus edulis*) were collected from their natural beds from nine sites in Puget Sound (**Figure 2**). Sites included the minimally contaminated reference areas of Oak Bay, Coupeville, and Double Bluff, in central and north Puget Sound, and Saltwater Park of south Puget Sound. Urban sites that were sampled for mussels included Eagle Harbor, Seacrest and Four Mile Rock in Elliott Bay, City Waterway in Commencement Bay, and Sinclair Inlet.

Relatively high tissue concentrations of contaminants including toxic trace metals were observed in mussels tissue samples from the urban-associated sites compared to the minimally

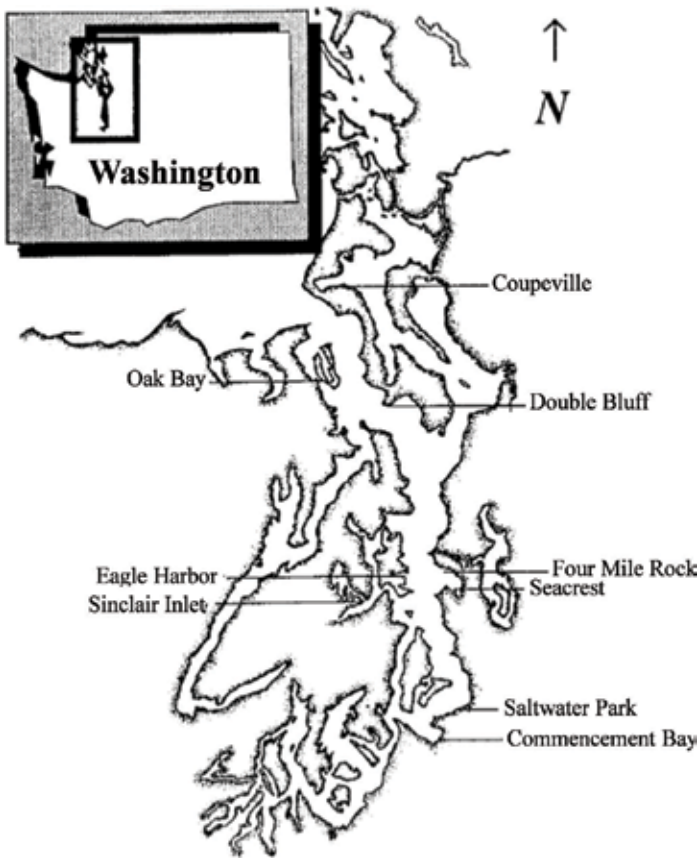

Figure 2. Map showing the mussel sampling sites in Puget Sound, Washington [7].

http://dx.doi.org/10.5772/intechopen.76938

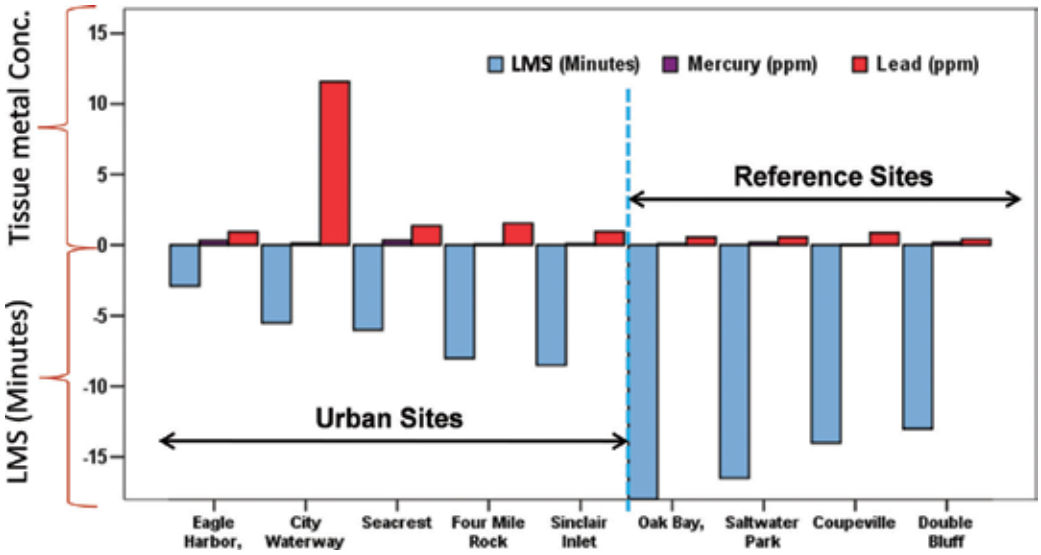

Figure 3. Relationship between lysosomal membrane stability (LMS) and tissue concentration of heavy metals (mercury and lead) of mussels from urban-associated and reference sites in Puget Sound [7].

contaminated (reference) sites (**Figure 3**). Mussels from contaminated sites showed low LMS, enhanced lipofuscin deposition, and increased accumulation of lysosomal and cytoplasmic unsaturated neutral lipids (**Figure 3**). Mussels from the contaminated sites were smaller in size together with lower somatic tissue weight relative to shell length [7]. Highly significant correlations were observed between tissue concentrations of selected toxic elements (measures of anthropogenic exposure) and LMS [7]. The study showed that biomarkers in mussels have the potential to be used as sensitive, accurate, and rapid techniques for assessing the biological impact of environmental contaminants in the coastal waters. The study results were in agreement with the previous study results, which showed an association between metabolites of aromatic compounds in bile and the occurrence of hepatic lesions in English sole (*Parophrys vetulus*) from Puget Sound [96].

7. Conclusion

Commercially and ecologically important marine bivalves (clams, mussels, and oysters) are widely used for monitoring levels of trace metals in the marine environment from several parts of the world. Trace metal monitoring using bivalves has several advantages compared to using seawater or sediment samples for the same purpose. Bivalves such as mussels are having global distribution from the polar to the tropical region and being successfully used for temporal and spatial trend monitoring of trace metals in the coastal waters across the globe. Recently several biomarkers, the biological responses of bivalves to contaminants including trace metals, are being developed and tested to assess the coastal water quality. The biomarkers of stress in bivalves give early warning signal about the presence of toxic trace metals in the marine environment.

Acknowledgements

We thank the Center for Environment and Water, Research Institute, King Fahd University of Petroleum and Minerals, Dhahran, Saudi Arabia, for providing research facilities. We acknowledge the research funding (# T.K. 11-0629) of the King Abdulaziz City for Science and Technology (KACST). We also thank our colleagues and students who helped us to prepare this manuscript.

Author details

Periyadan K. Krishnakumar[1]*, Mohammad A. Qurban[1] and Geetha Sasikumar[2]

*Address all correspondence to: kkumarpk@kfupm.edu.sa

1 Center for Environment and Water, Research Institute, King Fahd University of Petroleum and Minerals, Dhahran, Saudi Arabia

2 Mangalore Research Centre, Central Marine Fisheries Research Institute, Mangalore, Karnataka, India

References

[1] Lee RF, Sauerhaber R, Benson AA. Petroleum hydrocarbons. Uptake and discharge by the marine mussel *Mytilus edulis*. Science. 1972;**177**:344-346

[2] Butler PA. Residues in fish, wildlife, and estuaries. Organochlorine residues in estuarine mollusks, 1965-72—National Pesticide Monitoring Program. Pesticides Monitoring Journal. 1973;**6**:238-246

[3] Goldberg ED, Bowen VT, Farrington JW, Harvey G, Martin JH, Parker PL, Risebrough RW, Robertson W, Schneider W, Gamble E. The mussel watch. Environmental Conservation. 1978;**5**:101-125

[4] Rainbow PS. Heavy metal levels in marine invertebrates. In: Furness RW, Rainbow PS, editors. Heavy metals in marine environment. Boca Raton, Florida: CRC Press; 1990. pp. 67-79

[5] Farrington JW, Tripp BW, Tanabe S, Subramanian A, Sericano JL, Wade TL, Knap AH. Edward D. Goldberg's proposal of "the mussel watch": Reflections after 40 years. Marine Pollution Bulletin. 2016;**110**:501-510

[6] Moore MN, Depledge MH, Readman JW, Leonard P. An integrated biomarker based strategy for ecotoxicological evaluation of risk in environmental management. Mutation Research. 2004;**552**:247-268

[7] Krishnakumar PK, Casillas E, Varanasi U. Effects of environmental contaminants on the health of *Mytilus edulis* from Puget Sound, Washington, USA. I. Cytochemical measures of lysosomal responses in the digestive cells using automatic image analysis. Marine Ecology Progress Series. 1994;**106**:249-261

[8] Krishnakumar PK, Casillas E, Varanasi U. Effects of environmental contaminants on the health of *Mytilus edulis* from Puget Sound, Washington, USA. II. Cytochemical detection of subcellular changes in the digestive cells. Marine Biology. 1995;**124**:251-259

[9] Dare PJ. Settlement, growth, and production of the mussel, *Mytilus edulis* L., in Morecambe Bay, England. Fishery Investigations Series II. 1976;**28**(1):1-25

[10] Jørgensen CB. Bivalve Filter Feeding: Hydrodynamics, Bioenergetics, Physiology and Ecology. Fredensborg, Denmark: Olsen & Olsen; 1990

[11] Famme P, Riisgård H, Jørgensen C. On direct measurement of pumping rates in the mussel *Mytilus edulis*. Marine Biology. 1986;**92**:323-327

[12] Boening DW. An evaluation of bivalves as biomonitors of heavy metals pollution in marine waters. Environmental Monitoring and Assessment. 1999;**55**:459-470

[13] Kimbrough KL, Johnson WE, Lauenstein GG, Christensen JD, Apeti DA. An Assessment of two Decades of Contaminant Monitoring in the nation's Coastal Zone. NOAA Technical Memorandum NOS NCCOS 74. Silver Spring, Maryland, USA: NOAA; 2008. p. 105. https://ccma.nos.noaa.gov/stressors/pollution/nsandt/>)

[14] O'Conner TP. Mussel Watch: Recent Trends in Coastal Environmental Quality. Silver Spring, MD: National Oceanic and Atmospheric Administartion; 1992. p. 46

[15] Sasikumar G, Krishnakumar PK, Bhat GS. Monitoring trace metal contaminants in green mussel, *Perna viridis* from the coastal waters of Karnataka, Southwest Coast of India. Archives of Environmental Contamination and Toxicology. 2006;**51**:206-214

[16] O'Connor TP, Lauenstein GG. Trends in chemical concentrations in mussels and oysters collected along the US coast: Update to 2003. Marine Environmental Research. 2006; **62**:261-285

[17] Casas S, Gonzalez JL, Andral B, Cossa D. Relation between metal concentration in water and metal content in marine mussels (Mytilus galloprovincialis): Impact of physiology. Environmental Toxicology and Chemistry. 2008;**27**:1543-1552

[18] WHO/FAO/IAEA. Trace Elements in Human Nutrition and Health. Switzerland: Geneva: World Health Organization; 1996

[19] Chang LW, Magos L, Suzuki T, editors. Toxicology of Metals. Boca Raton. FL, USA: CRC Press; 1996

[20] Beyer J, Green NW, Brooks S, Allan IJ, Ruus A, Gomes T, Bråte ILN, Schøyen M. Blue mussels (*Mytilus edulis* spp.) as sentinel organisms in coastal pollution monitoring: A review. Marine Environmental Research. 2017;**130**:338-365

[21] Luoma SN, Rainbow PS. Why is metal bioaccumulation so variable? Biodynamics as a unifying concept. Environmental Science & Technology. 2005;**39**:1921-1931

[22] Solaun O, Rodríguez JG, Borja A, Gonzalez M, SaizSalinas JI. Biomonitoring of metals under the water framework directive: Detecting temporal trends and abrupt changes, in relation to the removal of pollution sources. Marine Pollution Bulletin. 2013;**67**:26-35

[23] Rainbow PS. Trace metal concentrations in aquatic invertebrates: Why and so what? Environmental Pollution. 2002;**120**:497-507

[24] Saavedra Y, Gonzalez A, Fernandez P, Blanco J. The effect of size on trace metal concentrations in raft cultivated mussels (*Mytilus galloprovincialis*). Science of the Total Environment. 2004;**318**:115-124

[25] Mubiana VK, Vercauteren K, Blust R. The influence of body size, condition index and tidal exposure on the variability in metal bioaccumulation in *Mytilus edulis*. Environmental Pollution. 2006;**144**:272-279

[26] Krishnakumar PK, Asokan PK, Pillai VK. Physiological and cellular responses to copper and mercury in the green mussel *Perna viridis*. Aquatic Toxicology. 1990;**18**:163-174

[27] Yap CK, Ismail A, Edward FB, Tan SG, Siraj SS. Use of different soft tissues of *Perna viridis* as biomonitors of bioavailability and contamination by heavy metals (cd, cu, Fe, Pb, Ni, and Zn) in semi-enclosed intertidal water, the Johore Straits. Toxicology and Environmental Chemistry. 2006;**88**(1-4):683-695

[28] Viarengo A. Heavy metals in marine invertebrates: Mechanisms of regulation and toxicity at the cellular level. CRC Critical Reviews in Aquatic Sciences. 1989;**1**:295-317

[29] Marigomez I, Soto M, Cajaraville MP, Angulo E, Giamberini L. Cellular and subcellular distribution of metals in molluscs. Microscopy Research and Technique. 2002;**56**:358-392

[30] Beeby A. What do sentinels stand for? Environmental Pollution. 2001;**112**:285-298

[31] Philips DJH. The use of biological indicator organisms to monitor trace metal pollution in marine and estuarine environments–A review. Environmental Pollution. 1977; **13**:281-317

[32] Phillips DJH. Quantitative Aquatic Biological Indicators: Their Use to Monitor Trace Metal and Orgnanochlorine Pollution. London, UK: Elsevier Applied Science; 1980. Rainbow 2002

[33] Zhou Q, Zhang J, Fu J, Shi J, Jiang G. Biomonitoring: An appealing tool assessment of metal pollution in the aquatic ecosystem. Analytica Chimica Acta. 2008;**606**:135-150

[34] Gupta SK, Singh J. Evaluation of mollusc as sensitive indicator of heavy metal pollution in aquatic system: A review. Institute of Integrative Omics and Applied Biotechnology Journal. 2011;**2**:49-57

[35] Waykar B, Deshmukh G. Evaluation of bivalves as bioindicators of metal pollution in freshwater. Bulletin of Environmental Contamination and Toxicology. 2012;**88**:48-53

[36] Melwani AR, Gregorio D, Jin Y, Stephenson M, Ichikawa G, Siegel E, Crane D, Lauenstein G, Davis JA. Mussel watch update: Long-term trends in selected contaminants from coastal California, 1977-2010. Marine Pollution Bulletin. 2014;**81**:291-302

[37] Claisse D. Chemical contamination of French coasts: The results of a ten years mussel watch. Marine Pollution Bulletin. 1989;**20**:523-528

[38] Ramu K, Kajiwara N, Sudaryanto A, Isobe T, Takahashi S, Subramanian A, Ueno D, Zheng GJ, Lam PKS, Takada H, Zakaria MP, Viet PH, Prudente M, Tana TS, Tanabe S. Asian mussel watch program: Contamination status of polybrominated diphenyl ethers and organochlorines in coastal waters of Asian countries. Environmental Science & Technology. 2007;**41**:4580-4586

[39] Zuykov M, Pelletier E, Harper DAT. Bivalve mollusks in metal pollution studies: From bioaccumulation to biomonitoring. Chemosphere. 2013;**93**:201-208

[40] Goldberg E. The mussel watch–a first step in global marine monitoring. Marine Pollution Bulletin. 1975;**6**:111

[41] Goldberg ED. The mussel watch concept. Environmental Monitoring and Assessment. 1986;**7**:91-103

[42] Goldberg E. The International MUSSEL WATCH–Report of a Workshop Sponsored by the Environmental Studies Board, Commission on Natural Resources and the National Research Council. Washington D.C: National Academy of Sciences; 1980. p. 269. Library of Congress Catalog Card Number 80-80896. International Standard Book Number 0-309-03040-4

[43] Farrington JW, Goldberg ED, Risebrough RW, Martin JH, Bowen VT. U.S. "Mussel Watch" 1976-1978. An overview of the trace metal, DDE, PCB, hydrocarbon and artificial radionuclide data. Environmental Science and Technology. 1983;**17**:490-496

[44] Wade TL, Atlas EL, Brooks JM, Kennicutt MC II, Fox RG, Sericano JL, Garcia-Romero B, DeFreitas D. NOAA Gulf of Mexico status and trends program: Trace organic distribution in sediments and oysters. Estuaries. 1988;**11**:171-179

[45] O'Connor TP. Mussel watch results from 1986 to 1996. Marine Pollution Bulletin. 1998; **37**:14-19

[46] Launestei GG, Daskalakis KD. U.S. long-term coastal contaminant temporal trends determined from mollusk monitoring programs 1965-1993. Marine Pollution Bulletin. 1998;**37**:6-13

[47] White H. Mussel madness: Use and misuse of biological monitors of marine pollution. In: White H, editor. Concepts in Marine Pollution Measurements. A Maryland Sea Grant Publication. College Park, MD, USA: University of Maryland; 1984. pp. 325-337 (743 pp.)

[48] Cantillo AY. Comparison of results of mussel watch programs of the United States and France with worldwide mussel watch studies. Marine Pollution Bulletin. 1998;**36**:712-717

[49] Pan K, Wang WX. Trace metal contamination in estuarine and coastal environments in China. Science of the Total Environment. 2012;**421**:3-16

[50] Sparks C, Odendaal J, Snyman R. An analysis of historical Mussel Watch Programme data from the west coast of the cape peninsula, cape town. Marine Pollution Bulletin. 2014; **87**:374-380

[51] Green NW, Schøyen M, Øxnevad S, Ruus A, Allan I, Hjermann D, Severinsen G, Høgåsen T, Beylich B, Håvardstun J, Lund E, Tveiten L, Bæk K. Contaminants in Coastal Waters of Norway–2015. Oslo, Norway: Norwegian Environment Agency Miljødirektoratet & Norwegian Institute for Water Research; 2016. p. 209

[52] Phelps DK, Galloway WB. A report on the coastal environmental assessment stations (CEAS) program. Rapports et procés-verbaux des réunions - Conseil international pour l'exploration de la mer. 1980;**179**:76-81

[53] Anderlini VC, Al-Harmi L, De Lappe BW, Risebrough RW, Walker W III, Simoneit BRT, Newton AS. Distribution of hydrocarbons in the oyster, Pinctada margaratifera, along the coast of Kuwait. Marine Pollution Bulletin. 1981;**12**:57-62

[54] Martin M. State mussel watch: Toxic surveillance in California. Marine Pollution Bulletin. 1985;**16**:140-146

[55] Ramesh A, Tanabe S, Subramanian A, Mohan D, Venugopalan VK, Tatsukawa R. Persistent organochlorine residues in green mussels from coastal waters of South India. Marine Pollution Bulletin. 1990;**21**:587-590

[56] Kan-Atireklap S, Yen TH, Tanabe S, Subramanian A. Butyltin compounds and organochlorine residues in green mussel (*Perna viridis* L.) from India. Environmental Toxicology and Chemistry. 1998;**67**:409-424. Kimbrough et al., 2008

[57] Tsutsumi S, Yamaguchi Y, Nishida I, Aliyama K, Zakaria M, Takada H. Alkylbenzenes in mussels from south and south Asian coasts as a molecular tool to assess sewage impact. Marine Pollution Bulletin. 2002;**45**:325-331

[58] Rouane-Hacene O, Boutiba Z, Belhaouari B, Guibbolini-Sabatier ME, Francour P, Risso-de Faverney C. Seasonal assessment of biological indices, bioaccumulation and bioavailability of heavy metals in mussels *Mytilus galloprovincialis* from Algerian west coast, applied to environmental monitoring. Oceanologia. 2015;**57**:362-374

[59] Bayne BL, Moore MN, Widdows J, Livingstone DR, Salkeld PN. Measurement of the responses of individuals to environmental stress and pollution: Studies with bivalve molluscs. Philosophical Transactions of the Royal Society B: Biological Science. 1979; **286**:563-581

[60] Bayne BL, Brown DA, Burns K, Dixon DR, Ivanovici A, Livingstone DR, Lowe DM, Moore MN, Stebbing ARD, Widdows J, editors. The Effects of Stress and Pollution on Marine Animals. New York: Praeger Press; 1985

[61] Moore MN. Cytochemical responses of the lysosomal system and NADPH-ferrihemoprotein reductase in molluscan digestive cells to environmental and experimental exposure to xenobiotics. Marine Ecology Progress Series. 1988;**46**:81-89

[62] Livingstone DR, Chipman JK, Lowe DM, Minier C, Pipe RK. Development of biomarkers to detect the effects of organic pollution on aquatic invertebrates: Recent molecular, genotoxic, cellular and immunological studies on the common mussel (*Mytilus edulis*). International Journal of Environment and Pollution. 2000;**13**:56-91

[63] Sanchez W, Porcher JM. Fish biomarkers for environmental monitoring within the water framework directive of the European Union. Trends in Analytical Chemistry. 2009;**28**:150-158

[64] Viarengo A, Lowe D, Bolognesi C, Fabbri E, Koehler A. The use of biomarkers in biomonitoring: A 2-tier approach assessing the level of pollutant induced stress syndrome in sentinel organisms. Comparative Biochemistry and Physiology-Part C. 2007;**146**:281-300

[65] ICES. Report of the Joint ICES/OSPAR Study Group on Integrated Monitoring of Contaminants and Bio–Logical Effects (SGIMC) ICES Document CM 2009/ACOM:30 Ref. OSPAR; 2009

[66] Lyons BP, Thain JE, Stentiford GD, Hylland K, Davies IM, Vethaak AD. Using biological effects tools to define good environmental status under the European Union marine strategy framework directive. Marine Pollution Bulletin. 2010;**60**:1647-1651

[67] UNEP/RAMOGE. Manual on the Biomarkers Recommended for the MED POL Biomonitoring Programme. Athens: UNEP; 1999. pp. 1-92

[68] UNEP/MAP. Fact Sheets on Marine Pollution Indicators. Meeting of the MED POL National Coordinators. Barcelona, Spain, 24e27 May 2005. WGUNEP(DEC)/MED/WG.264/Inf.14. UNEP, Athens: 2005

[69] Vethaak AD, Davies IM, Thain JE, Gubbins MJ, Martínez-Gomez C, Robinson CD, Moffat CF, Burgeot T, Maes T, Wosniok W, Giltrap M, Lang T, Hylland K. Integrated indicator framework and methodology for monitoring and assessment of hazardous substances and their effects in the marine environment. Marine Environmental Research. 2017;**124**:11-20. DOI: 10.1016/j.marenvres.2015.09.010

[70] Martínez-Gomez C, Robinson CD, Burgeot T, Gubbins M, Halldorsson HP, Albentosa M, Bignell JP, Hylland K, Vethaak D. Biomarkers of general stress in mussels as common indicators for marine biomonitoring programmes in Europe: The ICON experience. Marine Environmental Research. 2017;**124**:70-80

[71] Viarengo A, Canesi L, Pertica M, Mancinelli G, Accomando R, Smaal AC, Orunesu M. Stress on stress response: A simple monitoring tool in the assessment of a general stress syndrome in mussels. Marine Environmental Research. 1995;**39**:245-248

[72] Benali I, Boutiba Z, Merabet A, Chèvre N. Integrated use of biomarkers and condition indices in mussels (*Mytilus galloprovincialis*) for monitoring pollution and development of biomarker index to assess the potential toxic of coastal sites. Marine Pollution Bulletin. 2015;**95**:385-394

[73] Smolders R, Bervoets L, De Coen W, Blust R. Cellular energy allocation in zebra mussels exposed along a pollution gradient: Linking cellular effects to higher levels of biological organization. Environmental Pollution. 2004;**129**:99-112

[74] Widdows J, Donkin P. Chapter 8: Mussels and environmental contaminants: Bioaccumulation and physiological aspects. In: Gosling E, editor. The Mussel Mytilus. Amsterdam: Elsevier Press; 1992. pp. 383-424

[75] Widdows J, Donkin P, Staff FJ, Matthiessen P, Law RJ, Allen YT, Thain JE, Allchin CR, Jones BR. Measurement of stress effects (scope for growth) and contaminant levels in mussels (*Mytilus edulis*) collected from the Irish Sea. Marine Environmental Research. 2002;**53**(4):327-356

[76] Widdows J, Johnson D. Physiological energetics of *Mytilus edulis*: Scope for growth. Marine Ecology Progress Series. 1988;**46**:113-121

[77] Widdows J, Burns KA, Menon NR, Page DS, Soria S. Measurement of physiological energetics (scope for growth) and chemical contaminants in mussel (*Arca zebra*) transplanted along a contamination gradient in Bermuda. Journal of Experimental Marine Biology and Ecology. 1990;**138**:99-117

[78] Martin M, Ichikawa G, Goetzl J, de los Reyes M, Stephenson MD. Relationships between physiological stress and trace toxic substances in the bay mussel, *Mytilus edulis*, from San Francisco Bay, California. Marine Environmental Research. 1984;**11**:91-110

[79] Salazar MH, Salazar SM. Assessing site-specific effects of TBT contamination with mussel growth-rates. Marine Environmental Research. 1991;**32**:131-150

[80] Livingstone DR. Organic xenobiotic metabolism in marine invertebrates. In: Gilles R, editor. Advances in Comparative and Environmental Physiology. Vol. 7. Berlin: Springer-Verlag; 1991. p. 45 185

[81] Moore MN. Environmental distress signals: Cellular reactions to marine pollution. In: Graumann W, Drukker J, editors. Histo- and Cytochemistry as a Tool in Environmental Toxicology. Progress in Histochemistry and Cytochemistry. Vol. 23. 1991. pp. 2-19

[82] Moore MN. Lysosomal cytochemistry in marine environmental monitoring. Histochemical Journal. 1990;**22**:187-191

[83] Moore MN. Biocomplexity: The post-genome challenge in ecotoxicology. Aquatic Toxicology. 2002;**59**:1-15

[84] Moore MN, Allen JI, McVeigh A, Shaw J. Lysosomal and autophagic reactions as predictive indicators of environmental impact in aquatic animals. Autophagy. 2006;**2**:217-220

[85] OSPAR. JAMP Guidelines for General Biological Effects Monitoring (OSPAR Agreement 1997-7). OSPAR Commission, Monitoring guidelines. Ref. No: 1997-7; 1997. 20 pp

[86] Davies IM, Vethaak AD. Integrated marine environmental monitoring of chemicals and their effects. ICES Cooperative Research Report. 2012;**315**:277

[87] HELCOM. Development of a set of core indicators: Interim report of the HELCOM CORESET project. PART B: Descriptions of the indicators. Baltic Sea Environment Proceedings No. 129 B; 2012

[88] UNEP/MAP. Report of the Correspondence Group on Monitoring, Pollution and Litter (CORMON). Monitoring Guidance on Ecological Objective 9: contaminants. UNEP(DEPI)/MED WG.394/5 and 394/7. Athens (Greece), 8-9 May 2014

[89] Viarengo A, Palmero S, Zanicchi G, Capelli R, Vaissiere R, Orunesu M. Role of metallotbioneins in cu and cd accumulation and elimination in tbe gill and digestive gland cells of Mytilus gaUoprovincialisam. Marine Environmental Research. 1985;**16**:23-36

[90] Viarengo A, Burlando B, Dondero F, Marro A, Fabbri R. Metallothionein as a tool in biomonitoring programmes. Biomarkers. 1999;**4**:455-466

[91] Jha AN. Genotoxicological studies in aquatic organisms: An overview. Mutation Research. 2004;**552**:1-17

[92] Bolognesi C, Cirillo S. Genotoxicity biomarkers in aquatic bioindicators. Current Zoology. 2014;**60**:273-284

[93] Narbonne JF, Daubeze M, Clerandeau C, Garrigues P. Scale of classification based on biochemical markers in mussels: Application to pollution monitoring in European coasts. Biomarkers. 1999;**4**:415-424

[94] Law R, Hanke G, Angelidis M, Batty J, Bignert A, Dachs J, Davies I, Denga A, Duffek B, Herut H, Hylland K, Lepom P, Leonards P, Mehtonen J, Piha M, Roose P, Tronczynski J, Velikova V, Vethaak D. Marine Strategy Framework Directive–Task Group 8 Report Contaminants and Pollution Effects. EUR 24335 EN–Joint Research Centre Scientific and Technical Reports. Vol. 161 pp. Scientific and Technical Research series, ISSN 978-92-79-15648-9. Luxembourg: Office for Official Publications of the European Communities; 2010. DOI: 10.2788/85887

[95] Malins DC, McCain BC, Brown DW, Chan S, Myers MS, Landahl JT, Prohaska PG, Friedman AJ, Rhodes LD, Burrows DG, Gronlund WD, Hodgins H. Chemical pollutants in sediments and diseases of bottom-dwelling fish in Puget Sound, Washington. Environmental Science & Technology. 1984;**18**:705-713

[96] Krahn MM, Rhodes LD, Myers MS, Moore LK, MacLeod WD, Malins DC. Association between metabolites of aromatic compounds in bile and the occurence of hepatic lesions in English sole (*Parophry vetulus*) from Puget Sound, Washington. Archives of Environmental Contamination and Toxicology. 1986;**15**:61-67

[97] Wang W-X, Fisher NS, Luoma SN. Kinetic determinations of trace element bioaccumulation in the mussel, *Mytilus edulis*. Marine Ecology Progress Series. 1996;**140**:91-113

[98] Wang W-X, Griscom SB, Fisher NS. Bioavailability of Cr (III) and Cr (VI) to marine mussels from solute and particulate pathways. Environmental Science & Technology. 1997;**31**:603-611

[99] Nice HE, Fisher SJ. Ecotoxicological and Bioaccumulation Investigations of the Swan Estuary in the Vicinity of Claisebrook, Water Science Technical Series, Report no. 28, Western Australia: Department of Water; 2011

[100] Chandurvelan R, ID Marsden, CN Glover, Gawb S. Assessment of a Mussel as a Metal Bioindicator of Coastal Contamination: Relationships between Metal Bioaccumulation and Multiple Biomarker Responses; 2015

[101] Wang X, Li C, Zhoud L. Metal concentrations in the mussel *Bathymodiolus platifrons* from a cold in the South China Sea. Deep-Sea Research Part I. 2017;**129**(2017):80-88

[102] Fung CN, Lam JCW, Zheng GJ, Connell DW, Monirith I, Tanabe S, Richardson BJ, Lam PKS. Mussel-based monitoring of trace metal and organic contaminants along the east coast of China using *Perna viridis* and *Mytilus edulis*. Environmental Pollution. 2004;**127**(2): 203-216

[103] Orescanin V, Lovrencic I, Mikelic L, Barisic D, Matasin Z, Lulic S, Pezelj D. Biomonitoring of heavy metals and arsenic on the east coast of the middle Adriatic Sea using *Mytilus galloprovincialis*. Nuclear Instruments and Methods in Physics Research Section B. 2006;**245**:495-500

[104] Joksimovic D, Tomic I, Stankovic AR, et al. Trace metal concentrations in Mediterranean blue mussel and surface sediments and evaluation of the mussels quality and possible risks of high human consumption. Food Chemistry. 2011;**127**:632-637

[105] Conti ME, Cecchetti G. A biomonitoring study: Trace metals in algae and molluscs Tyrrhenian coastal areas. Environmental Research. 2003;**93**:99-112

[106] Topcuoglu S, Kirba-soglu C, Yilmaz YZ. Heavy metal levels in biota and sediments in the northern coast of the Marmara Sea. Environmental Monitoring and Assessment. 2004;**96**(1-3):183-189

[107] Kucuksezgin F, Kayatekin BM, Uluturhan E, et al. Preliminary investigation of sensitive biomarkers of trace metal pollution in mussel (Mytilus galloprovincialis) from Izmir Bay (Turkey). Environmental Monitoring and Assessment. 2008;**141**:339-345

[108] Besada V, Andrade JM, Schultze F, et al. Monitoring of heavy metals in wild mussels (*Mytilus galloprovincialis*) from the Spanish North-Atlantic coast. Continental Shelf Research. 2011;**31**:457-465

[109] Brooks S, Harman C, Soto M, et al. Integrated coastal monitoring of a gas processing plant using native and caged mussels. Science of the Total Environment. 2012;**426**:375-386

[110] Bartolome´ L, Navarro P, Raposo JC, Arana G, Zuloaga O, Etxebarria N, Soto M. Occurrence and distribution of metals in mussels from the cantabrian coast. Archives of Environmental Contamination and Toxicology. 2010;**59**:235-243

[111] Yigit M, Celikkol B, Yilmaz S, Bulut M, Ozalp B, Dwyer RL, Maita M, Kizilkaya B, Yigit Ü, Ergün S, Gürses K, Buyukates Y. Bioaccumulation of trace metals in Mediterranean mussels (Mytilus galloprovincialis) from a fish farm with copper-alloy mesh pens and potential risk assessment. Human and Ecological Risk Assessment: An International Journal. 2017:10.1080/10807039.2017.1387476

[112] Astudillo LRD, Yen IC, Agard J, Bekele I, Hubbard R. Heavy metals in green mussel (*Perna viridis*) andoysters (Crassostrea sp.) from Trinidad and Venezuela. Archives of Environmental Contamination and Toxicology. 2002;**42**(2002):410-415

[113] Bakan G, €Ozko¸c HB. An ecological risk assessment of the impact of heavy metals in surface sediments on biota from the mid-Black Sea coast of Turkey. International Journal of Environmental Studies. 2007;**64**(1):45-57

[114] Bilgin M, Uluturhan-Suzer U. Assessment of trace metal concentrations and human health risk in clam (*Tapes decussatus*) and mussel (*Mytilus galloprovincialis*) from the Homa Lagoon (Eastern Aegean Sea). Environmental Science and Pollution Research. 2017;**24**:4174-4184

[115] Nesto N, Romano S, Moschino V, Mauri M, Da Ros L. Bioaccumulation and biomarker responses of trace metals and micro-organic pollutants in mussels and fish from the lagoon of Venice, Italy. Marine Pollution Bulletin. 2007;**55**(10):469-484

[116] de Souza MM, Windmoller CC, Hatje V. Shellfish from Todos os Santos Bay, Bahia, Brazil: Treat or threat? Marine Pollution Bulletin. 2011;**62**(10):2254-2263

[117] Sericano JL, Wade TL, Jackson TJ, Brooks JM, Tripp BW, Farrington JW, Mee L, Readman JW, Villeneuve J-P, Goldberg ED. Trace organic contamination in the Americas: An overview of the US national status and trends and the interna-tional mussel watch programmes. Marine Pollution Bulletin. 1995;**31**:214-225

[118] Tanabe S. International mussel watch in Asia-Pacific phase. Marine Pollution Bulletin. 1994;**28**(9):518

[119] Tanabe S. Asia-Pacific mussel watch progress report. Marine Pollution Bulletin. 2000; **40**:651

[120] Sudaryanto A, Takahashi S, Monirith I, Ismail A, Muchatar M, Zheng J, Richardson BR, Subramanian A, Prudente M, Hue ND, Tanabe S. Asia-Pacific mussel watch: Monitoring of butyltin contamination in coastal waters of Asian developing countries. Environmental Toxicology and Chemistry. 2002;**21**:2119-2130

[121] Monirith I, Ueno D, Takahashi S, Nakata H, Sudaryanto A, Subramanian A, Karuppiah S, Ismail A, Muchtar M, Zheng J, Richardson BJ, Prudente M, Hue ND, Tana TS, Tkalin AV, Tanabe S. Asia-Pacific mussel watch: Monitoring contamination of persistent organochlorine compounds in coastal waters of Asian countries. Marine Pollution Bulletin. 2003;**46**:281-300

[122] Moore MN, Lowe DM, Wade T, Wedderburn RJ, Depledge MH, Balashov G, Büyükgüngör H, Özkoc H, Daurova Y, Denga Y, Kostylev E, Mihnea P, Ciocanu C, Moncheva S, Tabagari S. International Mussel Watch (UNESCO/IOC) in the Black Sea: A Pilot Study for Biological Effects and Contaminant Residues. Environ- Mental Degradation of the Black Sea: Challenges and Remedies. Netherlands: Kluwer Academic Publishers; 1999. pp. 273-289

[123] Scarpato A, Romanelli G, Galgani F, Andral B, Amici M, Giordano P, Caixach J, Calvo M, Campillo JA, Albadalejo JB, Cento A, BenBrahim S, Sammari C, Deudro S, Boulahdid M, Giovanardi F. Western Mediterranean coastal waters—Moni-toring PCBs and pesticides accumulation in Mytilus galloprovincialis by active mussel watching: The Mytilos project. Journal of Environmental Monitoring. 2010;**12**(4):924-935

[124] Andral B, Galgani F, Tomasino C, Bouchoucha M, Blottiere C, Scarpato A, Benedicto J, Deudro S, Calvo M, Centa A, Benbrahim S, Boulahdid M, Sammi C. Chemical contamination baseline in the western Mediterranean Sea based on transplanted mussels. Archives of Environmental Contamination and Toxicology. 2011;**61**:216-271

[125] Galgani F, Martinez-Gomiz C, Giovaranardi F, Romaneli G, Caixach J, Cento A, Scarpato A, BebRahim S, Massaoudi S, Deudro S, Bouladhid M, Benedicto J, Andral B. Assessment of polycyclic aromatic hydrocarbon concentrations in mussels (*Mytilus gallprovincialis*) from the western basin of the Mediterranean Sea. Environmental Monitoring and Assessment. 2011;**172**(1-4):301-317

[126] Sasikumar G, Krishnakumar PK. Aquaculture planning for suspended bivalve farming systems: The integration of physiological response of green mussel with environmental variability in site selection. Ecological Indicators. 2011;**11**:734-740

[127] Jha AN, Dogra Y, Turner A, Millward GE. Impact of low doses of tritium on the marine mussel, *Mytilus edulis*: Genotoxic effects and tissue-specific bioconcentration. Mutation Research. 2005;**586**:47-57

[128] Banni M, Sforzini S, Arlt VM, Barranger A, Dallas LJ, Oliveri C, Aminot Y, Pacchioni B, Millino C, Lanfranchi G, Readman JW, Moore MN, Viarengo A, Jha AN. Assessing the impact of Benzo[a]pyrene on marine mussels: Application of a novel targeted low density microarray complementing classical biomarker responses. PLoS One. 2017;**12**(6):e0178460. DOI: 10.1371/journal.pone.0178460

Edited by Hosam El-Din M. Saleh and Eithar El-Adham

Over the last few years, we have witnessed increasing efforts dedicated to the scientific investigation and characteristics of trace elements. Especially in the field of human and animal nutrition, trace elements display a considerably attractive issue for research because they play an essential role in the nutrition of both animals and humans. Aquatic environments contaminated with trace elements are an emerging research area due to the toxicity, abundance, and environmental persistence of trace elements. Accumulation of heavy metals as a class of trace elements in various environments, and the subsequent transition of these elements into the food and feed chain, severely affects human health.

The determination of type and concentration of trace elements is regarded as the first and most important step to follow the mechanisms controlling the dispersal and accumulation of trace elements. Element speciation in different media (water, soil, food, plants, coal, biological matter, food, and fodder) is pivotal to assess an element's toxicity, bioavailability, environmental mobility, and biogeochemical performance. Recently, new analytical techniques have been developed, which greatly simplified the quantitation of many trace elements and considerably extended their detection range. In this context, the development of reproducible and accurate techniques for trace element analysis in different media using spectroscopic instrumentation is continuously updated.

Published in London, UK

IntechOpen

ISBN 978-1-83881-677-3